Proteomic Investigation of Blood-based Biomarkers for the Diagnosis of HIV-associated Neurocognitive Disorders

Brandon Dean Murugan
(MRGBRA003)

SUBMITTED TO THE UNIVERSITY OF CAPE TOWN
In fulfilment of the requirements for the degree:
MSc (Med) Medical Biochemistry

Faculty of Health Sciences
UNIVERSITY OF CAPE TOWN

June 2015
Supervisor: Professor Jonathan Blackburn
Department of Integrative Biomedical Sciences

Declaration

I, *Brandon Dean Murugan*, hereby declare that the work on which this dissertation/thesis is based is my original work (except where acknowledgements indicate otherwise) and that neither the whole work nor any part of it has been, is being, or is to be submitted for another degree in this or any other university.

I have used the American Chemical Society convention (specifically from The Journal of Proteome Research) for citation and referencing. Each contribution to, and quotation in, this thesis from the work(s) of other people has been attributed, and has been cited and referenced.

I empower the university to reproduce for the purpose of research either the whole or any portion of the contents in any manner whatsoever.

Brandon Dean Murugan

29/06/2015

Date

Acknowledgements

First and foremost I would like to thank my parents, Donovan and Saroj Murugan, for their love and support during all my years of study. Through the good times and the rough times. I love you guys. I would like to thank my supervisor, Professor Jonathan Blackburn, for all of his support; patience; and guidance through this degree that was wrought with difficulties. You have my utmost respect and appreciation, for allowing me the opportunity to grow as a scientist. To the rest of my family, thank you all for your love and understanding. I would especially like to thank Dr Janique Peyper for her invaluable assistance. From proofreading this thesis, to assistance in navigating the treacherous worlds of statistics and Immunology. Not forgetting the much needed moral support, ice cream, and caramel Swiss rolls when times were tough and deadlines loomed. Your contribution, most of all, maintained my sanity. I am greatly indebted to you my friend. I would like to acknowledge Shaun Garnett and Tariq Ganief for establishing and optimising the discovery mass spectrometry platform that I used. To Alexander Giddey, thank you for the stimulating technical discussions when I needed fresh perspective, as well as for the random yet ever-interesting conversations. To Muneerah Smith for the last minute proofreading, and for the much needed moral support. To Naadir Ganief, Dr Andrew Nel, and Dr Leshern Karamchand for the last minute error checks; as well as the awesome daily conversations. To Cashifa Karriem, thank you for all the admin assistance and the ever-entertaining conversations. I would also like to thank Dr Nelson Soares for his support and helpful discussions. To the Blackburn lab as a whole, members past and present: I am immensely grateful to be part of a group where ideas can grow and support is always available. To the Milan family: all my love and appreciation for making me feel at home here in Cape Town. Thank you for making me feel like a part of the family. And last but not least, I thank God for keeping me grounded and faithful during all of the trying times, of which there were many.

I would also like to thank the National Research Foundation (Scarce Skill Scholarship) and The KW Johnstone Scholarship for financial support during this degree.

Abstract

Background: South Africa has the fourth highest prevalence of Human Immunodeficiency Virus (HIV) in the world, with over 340 000 new infections in 2013 alone. Implementation of Highly Active Antiretroviral Treatment (HAART) regimens, has improved the lives of many HIV-infected individuals, and has led to a decrease in the incidence of extreme forms of HIV-associated dementia. However, the extended lifespan afforded by HAART has also resulted in an increase in the prevalence of milder forms of HIV-associated Neurocognitive Disorders (HAND). Clinical diagnosis of such cognitive decline currently relies on neurocognitive assessments, as no definitive biochemical test exists. A point-of-care test designed for use with easily accessible samples (e.g. blood) would be of great utility in both HAND research and clinical diagnosis, prognostication, and provision of timeous therapy. A blood-based biomarker test would also be less subjective than neurocognitive testing, which can be adversely affected by the patient's level of education as well as operator competency. Recently, Professor Simon Lovestone (University of Oxford) developed a panel of blood-based biomarkers for the diagnosis of Alzheimer's disease. Due to pathological similarities between HAND and Alzheimer's disease, it is hypothesised that there may be applicability of this panel to diagnosis of HAND. The differential protein expression profile of patients with and without HAND is thus compared.

Aims and Objectives: The aim of this study was to assess the applicability of a set of Alzheimer's disease biomarkers to the diagnosis of HAND. In order to achieve this, targeted proteomic assays were developed to measure the markers in human serum. This assay was then applied to defined patient cohorts.

Methods: Targeted proteomic assays were developed in order to quantify candidate markers in patient blood serum. Parallel Reaction Monitoring assays were developed on a Thermo Q Exactive Quadrupole-Orbitrap mass spectrometer, for application to defined patient samples collected from Groote Schuur Hospital (Cape Town, South Africa). Patient samples were divided into groups according to HAND severity (based on the HIV Dementia Scale), namely: Normal (HIV+), Minor Neurocognitive Disorders and HIV-associated Dementia. Discovery proteomic analysis was performed on pooled patient samples in order to determine the optimal peptides for identification and quantitation of candidate proteins. Targeted methods were then developed and refined using the same pooled samples. Finally, patient samples (N=81) from the three classes were analysed in a statistically rigorous manner. Data were normalised to correct for possible loading inconsistencies by two independent methods. Quantitative differences were investigated using t-tests and non-parametric statistical tests where appropriate.

Results: Statistical assessment of final data indicated no significant differences in proteins between patient classes.

Discussion & Conclusions: It is likely that the inflammatory nature of HIV itself influences the levels of these markers in HIV-positive patient samples to a greater degree than neurocognitive effects. Alternatively, possible co-infection by TB may have confounded the results. Regardless, it was concluded that the candidate Alzheimer's biomarkers were not applicable to diagnosis of HAND. Further analysis on a larger sample cohort is recommended, utilising the assays optimised herein. Prospective studies to obtain viable biomarkers for definitive diagnosis may lie in proteomic analysis of model infection systems and cerebrospinal fluid.

Table of Contents

Chapter 1 Introduction 1

Chapter 2 Sample Preparation for Mass Spectrometric Analyses 16

2.1. Introduction 16

2.2. Materials and Methods 17

2.2.1. Cohort Collection and Serum Isolation 17

2.2.2. Sample Selection and Stratification 18

2.2.3. Depletion Strategy 18

2.2.4. Sample Loading Determination 18

2.2.5. Sample Preparation for Pilot Analysis 18

2.2.6. Sample Preparation for Mass Spectrometric Analysis 19

Chapter 3 Optimisation A: Identification of Candidate Peptides for Parallel Reaction Monitoring Assays through Shotgun Proteomic Analysis of Pooled Sera 24

3.1. Introduction 24

3.2. Materials and Methods 25

3.2.1. Sample Pooling 25

3.2.2. LC/MS Instrumentation and Parameters 26

3.2.3. Protein/Peptide Identification and Quantitation 28

3.2.4. Preliminary Peptide Selection 28

3.3. Results and Discussion 29

3.3.1. Protein Identification and Quantitation 29

3.3.2. Preliminary Peptide Selection 30

3.4. Conclusion 38

Chapter 4 Optimisation B: Optimisation of Instrument Parameters for Parallel Reaction Monitoring Assays 39

4.1. Introduction 39

4.2. Materials and Methods 40

4.2.1. Identification of Reference Sample Peptides for Method Development 40

4.2.2. Parameter Optimisation.....40

4.3. Results and Discussion.....48

4.3.1. Identification of Reference Sample Peptides for Method Development 48

4.3.2. Parameter Optimisation.....50

4.4. Conclusion.....62

Chapter 5 Optimisation C: Selection of Final Peptides for Final Parallel Reaction Monitoring Assay.....63

5.1. Introduction 63

5.2. Materials and Methods.....64

5.2.1. Sample Selection 64

5.2.2. LC/MS Instrumentation and Parameters 64

5.2.3. Optimal Peptide Selection.....65

5.3. Results and Discussion.....77

5.3.1. Optimal Peptide Selection.....77

5.4. Conclusion.....84

Chapter 6 Optimisation D: Selection of Reference Peptides for Normalisation.....85

6.1. Introduction 85

6.2. Materials and Methods.....86

6.2.1. Normalisation of Shotgun Peptide Data 86

6.2.2. Reference Peptide Selection 88

6.3. Results and Discussion.....90

6.3.1. Normalisation of Shotgun Peptide Data 90

6.3.2. Reference Peptide Selection 92

6.4. Conclusions 97

Chapter 7 High-throughput Parallel Reaction Monitoring Assay of Clinical Samples 98

7.1. Introduction 98

7.2. Materials and Methods....99
7.2.1. Sample Preparation....99
7.2.2. Analytical Parameters....99
7.2.3. LC/MS Instrumentation and Parameters....101
7.2.4. Preliminary Data and Repeat Analyses....102
7.2.5. Data Curation....103
7.2.6. Power Analysis....103
7.2.7. Data Handling and Statistical Analyses....104
7.3. Results and Discussion....105
7.3.1. Analytical Parameters....105
7.3.2. Preliminary Data and Repeat Analyses....107
7.3.3. Data Curation....108
7.3.4. Power Analysis....111
7.3.5. Data Handling and Statistical Analyses....112
7.3.6. Interpretation....119
7.4. Conclusions and Future Prospects....132
Bibliography....134
Chapter 8 Appendix A: Sample Preparation....160
Chapter 9 Appendix B: Optimisation A....164
Chapter 10 Appendix C: Final High Throughput PRM Assay....197

List of Figures

Figure 1.1: Mechanisms of HIV pathogenesis in the CNS. Adapted from González-Scarano and Martín-García[47] 4

Figure 1.2: Example of a shotgun mass spectrometric chromatogram. Upper panel: MS^1 ion chromatogram; Centre panel: MS^2 ion chromatogram; Lower Panel: MS^2 mass spectrum for a 491.76 m/z peptide 8

Figure 1.3: Schematic of a Triple Quadrupole mass analyser. Q1: Quadrupole 1, Q2: Quadrupole 2. Q3: Quadrupole 3. Adapted from Boja et al.[127] 9

Figure 1.4: Schematic of the Q Exactive quadrupole-orbitrap mass spectrometer. Adapted from Michalski et al.[184] 10

Figure 1.5: Schematics of Single- (A) and multi-plexed (B) Parallel Reaction Monitoring on Q-exactive mass spectrometer. Adapted from Gallien et al.[132] 11

Figure 1.6: Data visualisation of a targeted mass spectrometric experiment. A: peptide ions; B: MS^2 spectrum; C: Transition chromatogram of intensity over time 12

Figure 1.7: Quantitation in targeted mass spectrometric experiments. A: Transition chromatogram; B: Peak area bar plot 13

Figure 2.1: Fractionation of gel lane for in-gel digest. Fraction 4 is presumed to be the Albumin band. Molecular weight marker band weights in red. 20

Figure 4.1: Example of a scan diagram outlining scan parameters. Scan time (in seconds) is calculated by multiplying the time between scans (in minutes) by 60 46

Figure 4.2: Representative mass spectrometric chromatogram of a single reference sample. Upper panel: MS^1 ion chromatogram; Lower panel: MS^2 ion chromatogram 48

Figure 4.3: Scan diagrams showing scan times with increasing MSX level. A: MSX=1, B: MSX=2, C: MSX=3, D: MSX=4. Image not to scale, *: AGC prescan 50

Figure 4.4: Scan Diagrams showing scan times with concomitantly adjusted MSX and Max IT. A: single-plex & 110ms, B: duplex & 55ms, C: triplex and 36ms. Image not to scale 52

Figure 4.5: Scan diagrams showing scan times for injection time optimisation. A: Max IT=50ms, B: Max IT=100ms. Image not to scale 55

Figure 4.6: Scan diagrams showing scan times for predicted injection times at varying MSX levels. A: MSX = 2, Max IT = 45ms; B: MSX = 3, Max IT = 27ms 57

Figure 4.7: Skyline chromatograms of single-plex vs duplex analyses of VDSAATSGYEIGNPPDYR. A: single-plex, B: duplex 59

Figure 4.8: Excel-generated chromatograms of single-plex vs duplex analyses of VDSAATSGYEIGNPPDYR. Markers represent mass-spectrometric sampling points. A: single-plex, B: duplex 60
Figure 5.1: Examples of chromatograms of varying quality for optimal peptide selection. 77
Figure 5.2: Transition distribution plot for estimation of overlapping precursors in final scheduled biomarker list 83
Figure 6.1: Intensity plot for all identified peptides across pooled samples. Each line represents individual peptide intensity trends. A: Lower intensities appear flat due to scale of plot, B: Log10 transformed plot for ease of interpretation. 90
Figure 6.2: Normalised Intensity plots for each peptide across pooled samples. Each line represents individual peptide intensity trends. A: Lower intensities appear flat due to scale of plot, B: Log10 transformed plot for ease of interpretation. 91
Figure 6.3: Boxplots of pre- and post-normalisation shotgun proteomic data. A: Raw data, B: Normalised data 92
Figure 6.4: Raw intensity plots of preliminarily selected Ig peptides before and after normalisation. Intensities are Log_2-normalised 93
Figure 6.5: Skyline chromatograms for selected immunoglobulin peptides. Note that axes for each peptide are not at the same scale. Intensity shown on each y-axis, and retention time on each x-axis 95
Figure 7.1: Transition distribution plot for estimation of overlapping precursors in final assay (including internal reference peptides) 106
Figure 7.2: Examples of desirable and poor MS^2-TICs for sample quality assessment. A: desirable chromatogram, B-D: poor chromatograms. 107
Figure 7.3: Examples of peak quality variation. A: satisfactory peak, B: unsatisfactory peak shape with broadening, C: unsatisfactory peak shape with significant retention time drift, D: unsatisfactory peak shape with significant broadening, E: peak with missing transitions, F: no transitions detected 108
Figure 7.4: Peak intensities normalised to total peak area. Before (left) and after (right) removal of inconsistent product ions 109
Figure 7.5: Bar graphs comparing means of alpha-2-macroglobulin representative peptides across disease groups, using both normalisation methods. Error bars represent Standard Error of the Mean. A: IR normalised, B: NanoDrop normalised 120

Figure 7.6: Bar graphs comparing means of clusterin representative peptides across disease groups, using both normalisation methods. Error bars represent Standard Error of the Mean. A: IR normalised, B: NanoDrop normalised.....121
Figure 7.7: Bar graphs comparing means of ceruloplasmin representative peptides across disease groups, using both normalisation methods. Error bars represent Standard Error of the Mean. A: IR normalised, B: NanoDrop normalised 122
Figure 7.8: Bar graphs comparing means of alpha-1-antitrypsin representative peptides across disease groups, using both normalisation methods. Error bars represent Standard Error of the Mean. A: IR normalised, B: NanoDrop normalised 123
Figure 7.9: Bar graphs comparing means of alpha-1-acid glycoprotein representative peptides across disease groups, using both normalisation methods. Error bars represent Standard Error of the Mean. A: IR normalised, B: NanoDrop normalised.....124
Figure 7.10: Bar graphs comparing means of gelsolin representative peptides across disease groups, using both normalisation methods. Error bars represent Standard Error of the Mean. A: IR normalised, B: NanoDrop normalised.....125
Figure 7.11: Bar graphs comparing means of serum amyloid P representative peptides across disease groups, using both normalisation methods. Error bars represent Standard Error of the Mean. A: IR normalised, B: NanoDrop normalised 126
Figure 7.12: Bar graphs comparing means of apolipoprotein E representative peptides across disease groups, using both normalisation methods. Error bars represent Standard Error of the Mean. A: IR normalised, B: NanoDrop normalised 127
Figure 7.13: Bar graphs comparing means of apolipoprotein A-I representative peptides across disease groups, using both normalisation methods. Error bars represent Standard Error of the Mean. A: IR normalised, B: NanoDrop normalised 129
Figure 7.14: Bar graphs comparing means of complement protein representative peptides across disease groups, using both normalisation methods. Error bars represent Standard Error of the Mean. A.1: IR normalised complement C3, A.2: NanoDrop normalised complement C3; B.1: IR normalised complement C4, B.2: NanoDrop normalised complement C4; C.1: IR normalised complement factor H, C.2: NanoDrop normalised complement factor H 130
Figure 8.1: Figure showing images of SDS-PAGE gels stained with zinc-imidazole reversible stain. Gel photographed against a dark background. Clear protein bands appear dark. 163
Figure 8.2: Schematic of Thermo-Pierce Spin column for C18-based sample clean-up 163

List of Tables

Table 3.1: Randomised sample pooling for discovery proteomic analysis 25
Table 3.2: Candidate biomarkers represented in discovery analysis results. 31
Table 3.3: Preliminarily selected peptides for targeted assay method development 32
Table 4.1: Isolation list for unscheduled PRM analysis of reference sample peptides. 42
Table 4.2: Table of base settings for PRM analysis. 43
Table 4.3: Table of Orbitrap scan time parameters based on resolution setting. Adapted from Schroeder et al.[148] 45
Table 4.4: Table of chosen peptides for instrument method development. 49
Table 4.5: Summary of scan time changes associated with change in MSX 51
Table 4.6: Table showing overall scan time. Adapted from Schroeder et al.[148] 51
Table 4.7: Summary of scan times associated with concomitant changes in MSX and Max IT 53
Table 4.8: Table of Adjusted IT values based on multiplex level and additional delay 54
Table 4.9: Summary of scan times for injection time optimisation 55
Table 4.10: Table of optimum injection times for each MSX level at 35 000 resolution 56
Table 4.11: Summary of scan times resulting from predicted injection times in single and duplex modes 57
Table 4.12: Table of injection time estimations for multiplexing up to 6x, and isolation list lengths for a predefined cycle time of 2 s 58
Table 4.13: Final settings for PRM Analyses at 35 000 Resolution. AGC: Automatic gain control, ISO: Isolation, NCE: Normalised collision energy, MSX: Multiplex level, Max IT: Maximum injection time. 62
Table 5.1: Initial settings for optimal peptide selection by PRM assay at 35 000 Resolution. 64
Table 5.2: Isolation list A, Round 1 (Unscheduled) 65
Table 5.3: Isolation list B, Round 1 (Unscheduled) 67
Table 5.4: Isolation list A repeat, Round 2 (Unscheduled) 70
Table 5.5: Isolation list A, Round 3 (Unscheduled) 71
Table 5.6: Isolation list B, Round 3 (Unscheduled) 72
Table 5.7: Isolation List A, Round 4 (Unscheduled) 73
Table 5.8: Isolation List B, Round 4 (Unscheduled) 74
Table 5.9: Scheduled isolation list for final list of PRM target peptides 75

Table 5.10: Tally of peptide performance for Round 1 78
Table 5.11: Tally of peptide performance for round 2 79
Table 5.12: Tally of peptide performance for round 3 80
Table 5.13: Tally of peptide performance for round 4 80
Table 5.14: List of optimal peptides for final PRM assay 81
Table 6.1: Normalisation factor calculation for shotgun proteomic data 87
Table 6.2: Unscheduled isolation list of prospective internal standard peptides 89
Table 6.3: List of internal reference peptide candidates 94
Table 6.4: Final list of internal reference peptides 96
Table 6.5: Scheduled isolation list of selected internal reference peptides 96
Table 7.1: Scheduled Isolation list for final PRM analysis 99
Table 7.2: Final settings for PRM Analyses at 35 000 Resolution. 101
Table 7.3: Sequence of samples for targeted analysis 102
Table 7.4: Selected samples for final statistical analysis 109
Table 7.5: Peptides assigned to each protein for the purposes of protein inference 110
Table 7.6: Sample size estimations for an independent samples *t*-test, where significance = 0.05, and predicted power = 0.8. Adapted from van Belle et al.[198] 111
Table 7.7: Example of Skyline data output 112
Table 7.8: Example of data prepared for statistical analysis 112
Table 7.9: Example of internal reference normalised data 113
Table 7.10: Example of total peptide normalised data 113
Table 7.11: Shapiro-Wilk normality test results on internal reference-normalised data 114
Table 7.12: Results from Welch's *t-test* and Wilcoxon test on internal reference-normalised data 115
Table 7.13: Shapiro-Wilk normality test results on NanoDrop-normalised data 116
Table 7.14: Results from Welch's *t-test* and Wilcoxon test on NanoDrop-normalised data 117
Table 8.1: Table of serum batching and dilutions for mass spectrometry analysis (Final concentration: 1.53 µg/µl) 160
Table 9.1: Maxquant settings for shotgun proteomic analysis of pooled samples 164
Table 9.2: Table of discovery protein IDs from pooled analysis. Leading proteins of each group are shown for simplicity. PEP: Posterior Error Probability 167
Table 9.3: Table of raw peptide data for candidate biomarkers. Leading proteins of each group are used for simplicity. 172

Table 10.1: Raw PRM peptide data averaged to give representative protein values.....197

Abbreviations

A: Solvent A

A1AG: Alpha-1-acid glycoprotein

A1AT: Alpha-1-antitrypsin

A2M: Alpha-2-macroglobulin

ABC: Ammonium Bicarbonate

ACN: Acetonitrile

AD: Alzheimer's disease

ADC: AIDS dementia complex

AGC: Automatic gain control

AIDS: Acquired immune deficiency syndrome

ANI: Asymptomatic neurocognitive impairment

ApoA-I: Apolipoprotein A-I

ApoE: Apolipoprotein E

Aβ: Amyloid beta

B: Solvent B

BBB: Blood-brain barrier

BCA: Bicinchoninic acid

BSA: Bovine serum albumin

C3: Complement C3

C4: Complement C4

C4A: Complement C4-A

C4B: Complement C4-B

CDK5: Cyclin-dependent kinase 5

CE: Collision energy

CERU: Ceruloplasmin

CFH: Complement factor H

CID: Collision induced dissociation

CLU: Clusterin

CNS: Central nervous system

CSF: Cerebrospinal fluid

CSV: Comma separated values

CV: Coefficient of variation

Da: Dalton

DDA: Data dependent acquisition

EDTA: Ethylenediaminetetraacetic acid

ELISA: Enzyme-linked immunosorbent assay

ESI: Electrospray ionisation

FA: Formic acid

FASP: Filter aided sample preparation

FDR: False discovery rate

FGG: Fibrinogen-gamma

Gp120: Glycoprotein 120

GSN: Gelsolin

HAART: Highly active antiretroviral therapy

HAD: HIV-associated dementia

HAND: HIV-associated neurocognitive disorders

HCD: High energy collision dissociation

HDL: High density lipoprotein

HIV: Human immunodeficiency virus

HPLC: High performance liquid chromatography

HPLC-UV: High performance liquid chromatography-ultraviolet

IAA: Iodoacetamide

IDM: Institute of Infectious Diseases and Molecular Medicine

IEF: Isoelectric focusing

Ig: Immunoglobulin

IgG: Immunoglobulin G

IgG_1: Immunoglobulin G subclass 1

IgG_3: Immunoglobulin G subclass 3

IgG_4: Immunoglobulin G subclass 4

IT: Injection time

kDa: Kilodalton

LC/MS: Liquid chromatography-mass spectrometry

LC: Liquid chromatography

LC-MS/MS: Liquid chromatography-tandem mass spectrometry

LFQ: Label-free quantitation

LRP: Low-density lipoprotein receptor-related protein

m/z: Mass-to-charge ratio

MALDI: Matrix-assisted laser desorption ionisation

MARS: Multiple affinity removal system

Max IT: Maximum injection time

MND: Mild neurocognitive disorder

MNI: Mild neurocognitive impairment

MRM: Multiple reaction monitoring

MS: Mass spectrometry

MS^1-TIC: Total MS^1 ion chromatogram

MS^2-TIC: Total MS^2 ion chromatogram

MSX: Multiplex level

NCE: Normalised collision energy

nESI: Nanoelectrospray ionisation

NFκB: Nuclear factor kappa B

nLC: Nano liquid chromatography

NMDA: N-methyl-D-aspartate

PBMC: Peripheral blood mononuclear cells

PEP: Posterior error probability

PI: Principal investigator

PIP_2: Polyphosphoinositide 4,5-bisphosphate

POS: HIV-positive control

ppm: Parts per million

PRM: Parallel reaction monitoring

Q1: Quadrupole 1

Q2: Quadrupole 2

Q3: Quadrupole 3

QIT: Quadrupole ion trap

QTOF: Quadrupole time-of-flight

RPLC: Reversed-phase liquid chromatography

SA: South Africa

SAP: Serum amyloid P

SCX: Strong cation exchange

SDS: Sodium dodecyl sulphate

SDS-PAGE: Sodium dodecyl sulphate-polyacrylamide gel electrophoresis

SEM: Standard error of the mean

SRM: Single reaction monitoring

Tat: Transactivator of transcription

TB: Tuberculosis

TCEP•HCl: Tris(2-carboxyethyl)phospine hydrochloride

TIC: Total ion chromatogram

tMS2: Targeted MS2

TOF: Time-of-flight

TSQ: Triple stage quadrupole

TSV: Tab separated values

TTY: Transthyretin

UV: Ultraviolet

VLDL: Very low density lipoproteins

Vpr: Viral protein R

Chapter 1
Introduction

CLINICAL AND EPIDEMIOLOGICAL OVERVIEW OF HIV ASSOCIATED NEUROCOGNITIVE DISORDERS

Central nervous system (CNS) infection by human immunodeficiency virus (HIV) was first characterised as acquired immune deficiency syndrome (AIDS) dementia complex (ADC), and involved significant neurological pathologies.[1,2] Common clinical features ranged from motor dysfunction, behavioural anomalies, as well as memory and concentration deficits in milder forms of the disease, to partial paralysis, uncontrollable muscle spasms, mutism, full-blown dementia, and death in more advanced forms.[2–4] The median survival for an HIV infected individual with ADC was six months, with an annual ADC incidence of 7% following onset of AIDS.[5]

The implementation of highly active antiretroviral treatment (HAART) regimens have greatly extended the lifespan of HIV infected individuals, while vastly improving their quality of life.[6,7] This includes patients diagnosed with ADC, where there has been a marked improvement in clinical prognosis, and increase in life expectancy.[8,9]

The detrimental neurological effects of HIV are now collectively referred to as HIV-associated neurocognitive disorders (HAND). HAND is classified into three progressively more severe levels of neurocognitive impairment as defined by the HIV Neurobehavioral Research Centre at the University of California, San Diego: asymptomatic neurocognitive impairment (ANI), mild neurocognitive disorder/impairment (MND/MNI), and HIV-associated dementia (HAD).[10] HAART has led to a marked decrease in prevalence of the more severe forms of HAND but, due partly to the positive effect of HAART on survival, a high prevalence of the milder forms of the disease are still observed.[11,12] Even in the HAART era, neurocognitive impairment caused by HIV infection has significant negative effects on adherence to HAART; job performance; employment; execution of simple tasks; and general quality of life.[13–16] These effects may also impact negatively on the economy of countries, taking into account impacts on employment as well as the increased costs of specialised healthcare.[14,17]

MOLECULAR PATHOGENESIS OF HAND

Due to compartmentalisation of the CNS, by virtue of the blood-brain barrier (BBB), it is protected from diffusional entry of deleterious substances from the systemic circulation, and is regarded as immune privileged.[18] Despite this, CNS infection is a common cause of high morbidity and mortality rates in immunocompromised individuals.[1,2] HIV itself is able to infiltrate the CNS with entry occurring early in infection, often prior to serodiagnosis or commencement of HAART, leading to neurological complications.[19–21]

The mechanisms by which HIV gains entry into the CNS are not fully understood. Most evidence supports the 'Trojan Horse' hypothesis, which proposes that lentiviruses such as HIV enter the CNS within infected leukocytes, such as monocytes and T-cells.[22] Indeed, CNS-localised virions preferentially infect macrophages and microglia.[23,24]

The major route by which HIV gains access to the CNS thus appears to be via infected macrophages, and to a lesser extent lymphocytes, from the systemic circulation.[25–30] The CNS contains perivascular macrophages that reside along the endothelial cells of the BBB, whose population can be replenished by monocytes from the systemic circulation.[29,31] These cells, in addition to microglia (macrophage-like glial cells) and astrocytes, are the primary targets for infection and viral replication following CNS infiltration by HIV.[23,24,32–34] Indeed, HIV infection in the CNS upregulates release of chemokines such as monocyte chemotactic protein-1 from monocytes, microglia, and astrocytes; which promotes CNS infiltration by potentially HIV-infected monocytes from the systemic circulation.[25–28,35] Interestingly, a recent study by Louveau et al.[36] has shown evidence of previously unknown lymphatic vessels supplying the CNS, and suggests these as efficient routes via which immune cells may gain access to the CNS and systemic circulation. This, by extension, may provide an optimal route for entry of HIV-infected immune cells into the CNS.

Another proposed but less well-characterised mechanism which may play a minor role in HIV entry into the CNS includes direct infection via BBB endothelial cells.[37,38]

Neurons do not express CD4, the surface protein that facilitates HIV entry.[39,40] Despite this, HIV is able to effect neuronal cell death in the CNS, probably without direct infection of the neurons themselves.[41–44] To date, there is no evidence for productive HIV infection of neurons.[45,46] It has been hypothesised instead that neuronal cell death results from response to various factors released during infection-related processes (Figure 1.1).[47] One hypothesis

proposes that neurons are directly damaged by viral proteins released during infection.[48] The other, more likely, scenario involves indirect neuronal cell death by chemokines released from microglia; macrophages; and astrocytes during the inflammatory response to the virus.[48]

Direct neuronal injury is believed to be effected by HIV proteins such as transactivator of transcription (Tat), viral protein R (Vpr), and glycoprotein (gp)120.[49–59] Vpr has been observed to directly cause apoptosis of neurons and astrocytes *in vitro*, possibly by caspase-8 mediated mechanisms.[49–51] HIV gp120 has also been observed to cause neuronal apoptosis by activation of neuronal N-methyl-D-aspartate (NMDA) receptors on neurons.[52–54] Excessive stimulation of NMDA receptors is believed to cause excessive Ca^{2+} influx as well as mitochondrial membrane depolarisation, both of which lead to apoptotic cell death.[60,61] Studies have also implicated gp120-mediated activation of neuronal CXCR4 receptors, resulting in increased Ca^{2+} influx and subsequent excitotoxic cell death.[55,56] Extracellular Tat has been implicated in neuronal apoptosis by direct stimulation of NMDA receptors.[57,58] Evidence also exists for direct Tat-mediated hyper-activation of neuronal cyclin-dependent kinase 5 (CDK5), as well effecting its accumulation in the cytoplasm, resulting in neuronal cell death due to CDK5-mediated cytoskeletal dysregulation.[59]

Neuronal damage may also be effected indirectly by factors related to HIV-induced inflammatory processes.[48] Release of soluble factors by microglia/macrophages is stimulated by either HIV infection or HIV protein binding, and may cause neuronal cell death directly or via astrocyte involvement.[60–67] Binding of gp120 to CD4 receptors on macrophages results in release of arachidonic acid which inhibits glutamate uptake by astrocytes.[62] Additionally, tumour-necrosis factor alpha (TNF-α) and arachidonic acid released by productively infected microglia/macrophages also causes increased release, and decreased reuptake of glutamate by astrocytes.[63–65] Altogether, the increase in extracellular glutamate results in excessive stimulation of neuronal NMDA receptors, and eventual excitotoxic cell death (*vide supra*).[60,61] Productive macrophage infection by HIV has also been shown to cause direct NDMA receptor-mediated neuronal cell death, by stimulating release of quinolinic acid.[60,61,66,67]

Owing to the complexity of HIV infection and the inflammatory response, it is likely that the combination of both direct and indirect mechanisms are responsible for HIV neuropathogenesis.[48]

Despite releasing factors that are primarily responsible for pathogenic processes in HAND, microglia may also serve a protective role by regulating inflammatory processes in the CNS, possibly in concert with astrocytes and regulatory T lymphocytes.[68–71]

Indeed, there is a complex immunological interplay in the CNS, which appears to be skewed towards neuropathogenic outcomes as evidenced by the prevalence of HAND.

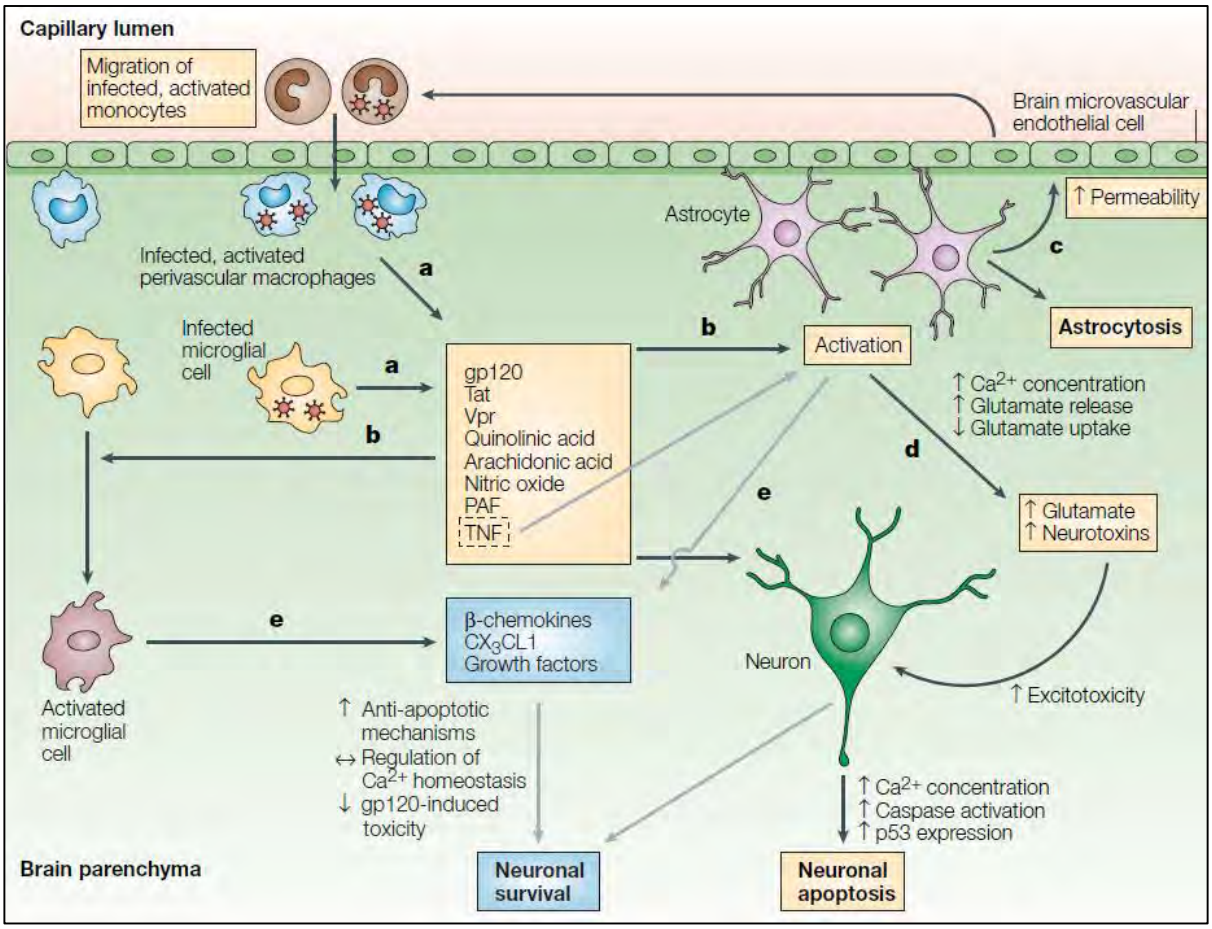

FIGURE 1.1: MECHANISMS OF HIV PATHOGENESIS IN THE CNS. ADAPTED FROM GONZÁLEZ-SCARANO AND MARTÍN-GARCÍA[47]

HAART AND HAND IN THE SOUTH AFRICAN CONTEXT

The impact of HAND in a South African (SA) context is of particular concern, given the high local HIV prevalence. At last count (2013) SA had the fourth highest HIV prevalence in the world, with 19% of the adult population infected, bringing the number of people living with HIV to 6.3 million.[72] In that year alone, 340 000 people were newly infected with the virus.[72] New infections however, have been steadily decreasing since 1999; and the number of AIDS-related deaths have been rapidly decreasing from the highest recorded level of 410 000 in 2010, to 200 000 in 2013.[72]

The HIV burden in SA is still of significant importance, however, even 12 years after the implementation of HAART.[73] The high prevalence of HIV highlights the potential impact of HAND on the SA populace. Indeed, neurocognitive impairment due to HAND has far reaching socio-economic consequences, with negative effects on employment; adherence to HAART; completion of daily tasks; and general quality of life.[13–16] Definitive diagnostics, understanding, and treatment of this disorder is thus a matter of great urgency in an SA context.

DIAGNOSTIC CHALLENGES

Clinical diagnosis of HIV-induced cognitive decline currently relies on neurocognitive assessments as no definitive biochemical test exists.[10,74] A biological marker or 'Biomarker' is defined by the National Institutes of Health as "A characteristic that is objectively measured and evaluated as an indicator of normal biological processes, pathogenic processes, or pharmacologic responses to a therapeutic intervention".[75] Biomarkers exist for a multitude of diseases and influence diagnosis, disease characterisation, and design of appropriate treatment regimens.[75,76] Several studies have attempted to identify HAND biomarkers in body fluids such as blood serum and cerebrospinal fluid (CSF).[77–82] However, none of the markers that have shown promise have been approved, presumably due to complexities inherent in the biomarker development pipeline as well as possible sub-optimal specificity for HAND.[82–84] Indeed, a point-of-care test designed for use with easily accessible biological samples (e.g. blood) would be of great utility in HAND research, clinical diagnosis, prognostication, and provision of timeous and appropriate therapy. A blood-based biomarker test would also be less subjective than neurocognitive testing, which can be adversely affected by the patient's level of education as well as operator competency, and would be ideally suited to diagnosis of HAND in the SA context.[74,85–88] Biochemical confirmation of diagnosis in combination with neurocognitive examination would be ideal.[74]

PROTEOMIC MASS SPECTROMETRY

Mass spectrometry (MS) involves characterisation of ions or charged molecules in gas phase based on their mass, charge and/or structure.[89] The mass spectrometer is able to measure the mass-to-charge ratio (m/z) of a charged molecule, from which the atomic mass (in Dalton) and molecular structure can be determined.[89]

Ionisation is the mechanism by which molecules form charged ions.[90] The two most widely used methods of ionisation used in biological MS analyses are matrix-assisted laser desorption

ionisation (MALDI), and electrospray ionisation (ESI).[91–95] ESI is commonly used in conjunction with high performance liquid chromatography (HPLC) for the analysis of complex mixtures.[96,97] This technique often involves separation of sample analytes on a liquid chromatography (LC) column, thereby reducing complexity and aiding analysis.[98] ESI is pertinent to the present study, and will be discussed briefly. ESI is a complex mechanism that involves formation of gas phase ions, from aerosolisation of ionised molecules in solution.[89] Although not fully understood, a popular model for describing the ESI process is the 'Ion Evaporation Model'.[95,99,100] Briefly, a considerable charge applied across the capillary tip causes the liquid to nebulise due to the Coulomb forces overcoming surface tension (Raleigh limit).[95] The positively charged droplets are drawn toward the entry orifice of the mass spectrometer by the potential difference between the spray needle and the entry capillary.[95] As the droplets desolvate and decrease in size, the protons within them move to the surface of the molecule.[95] These protons aggregate until the Raleigh limit is reached, and the repulsive force causes the droplets to explode into smaller droplets by a process known as 'Coulombic explosion'.[95] This process continues, until the droplet becomes so small that ions are ejected from the droplet due to the field strength at the surface.[95]

The development of nanoelectrospray ionisation (nESI) has led to a significant gain in sensitivity due to vastly improved ionisation efficiency.[101,102] Nanoelectrospray MS is a significantly scaled-down form of classical ESI; wherein flow rates as low as 20 nl/min, as well as spray needles approximately 1-2 µm in diameters are used.[102] The significant decrease in spray size is accompanied by a concomitant decrease in the size of solvent droplets formed.[101,102] This increases ionisation efficiency by several orders of magnitude since the droplets evaporate much more rapidly, allowing for faster transfer of charge to analyte molecules.[101,102]

Determination of a molecule's m/z is made by a mass analyser.[103] The simplest type of mass analyser is the time-of-flight (TOF), which involves measurement of the time taken for a charged molecule to travel the fixed length of an evacuated tube, and enables estimation of its m/z based on linear velocity.[104,105]

Tandem MS involves mass analysis at two levels: the first being the identification, and often quantitation, of the m/z of the 'parent' (entire) molecule; while the second involves controlled fragmentation of the molecule and subsequent measurement of the fragment m/z values.[89,106] Measured m/z values of parent molecules and their fragments are known as a

tandem mass spectrum: where intensity measurements pertaining to the m/z values of parent molecules in the sample are known as the MS^1 spectrum, and those of the fragments form the MS^2 spectrum.[89,107] Predictable fragmentation enables reliable structural elucidation of the analyte.[106] The most common types of fragmentation are collision-induced dissociation (CID) and high-energy collision dissociation (HCD) – a modified form of CID.[108,109] CID involves the fragmentation of molecules by accelerating them into a stream of inert gas (e.g. Argon, Helium) to prevent chemical reactions during collision.[108]

Of particular importance to the current study are Quadrupole and Orbitrap mass analysers. Quadrupoles function as mass filters such that, based on a combination of accurately timed adjustment of both direct current and alternating current potentials across opposing sets of quadrupole pairs, selectively allow molecules within a narrow m/z range through to the detector.[110,111] Quadrupoles are able to discard all masses except those within a narrow range of interest, and are therefore utilised primarily for detection of molecules of known m/z.[110] The high resolution Orbitrap mass analyser is similar to ion cyclotron mass analysers, which determine the m/z of ions based on their rotation within a static magnetic field.[112,113] In an ion cyclotron, the m/z is calculated by taking a Fourier transformation of the signal measured from ion cycling.[112] m/z analysis in the Orbitrap is carried out by measurement of the lateral motion of ions, orbiting around a central spindle-shaped electrode within an electrostatic field.[113] This signal is then converted to mass spectra using Fourier transform.[113] Orbitrap mass analysers can also act as ion detectors.[113]

Proteomic MS is the utilisation of MS technologies in the analysis of peptide and proteins.[97] Shotgun proteomic MS involves analysis of enzymatic digests of complex protein samples, to enable protein identification and quantitation.[96,97] Digestion is commonly performed by trypsin to yield predictable peptide products, although other enzymes may also be used.[96,97] These peptides are separated by online HPLC (*vide supra*), ionised by ESI (*vide supra*), and analysed by tandem MS.[96] Reversed-phase liquid chromatography (RPLC) is generally used as the on-line separation method for shotgun MS analyses.[97] RPLC primarily involves separation of analytes based on their hydrophobicity.[98] During gradient elution, the hydrophobicity of the mobile phase gradually increases, allowing peptides of increasing hydrophobicity to elute off the chromatography column and be analysed by the mass spectrometer.[98] Figure 1.2 below shows the output from a reference shotgun mass spectrometric analysis conducted 'in-house'. The upper panel shows a graphical representation of the total MS^1 ion chromatogram (MS^1-

TIC), depicting all peptide ion intensities over the chromatographic elution; while the centre panel shows the total MS^2 ion chromatogram (MS^2-TIC), or fragment ions. The signal intensity at each time point on either chromatogram contains the summed intensities for all ions in each spectrum (MS^1 or MS^2).[103] For example, the lower panel in Figure 1.2 shows the ions detected at MS^2 level at 25.88 minutes, for the 491.76m/z parent ion.

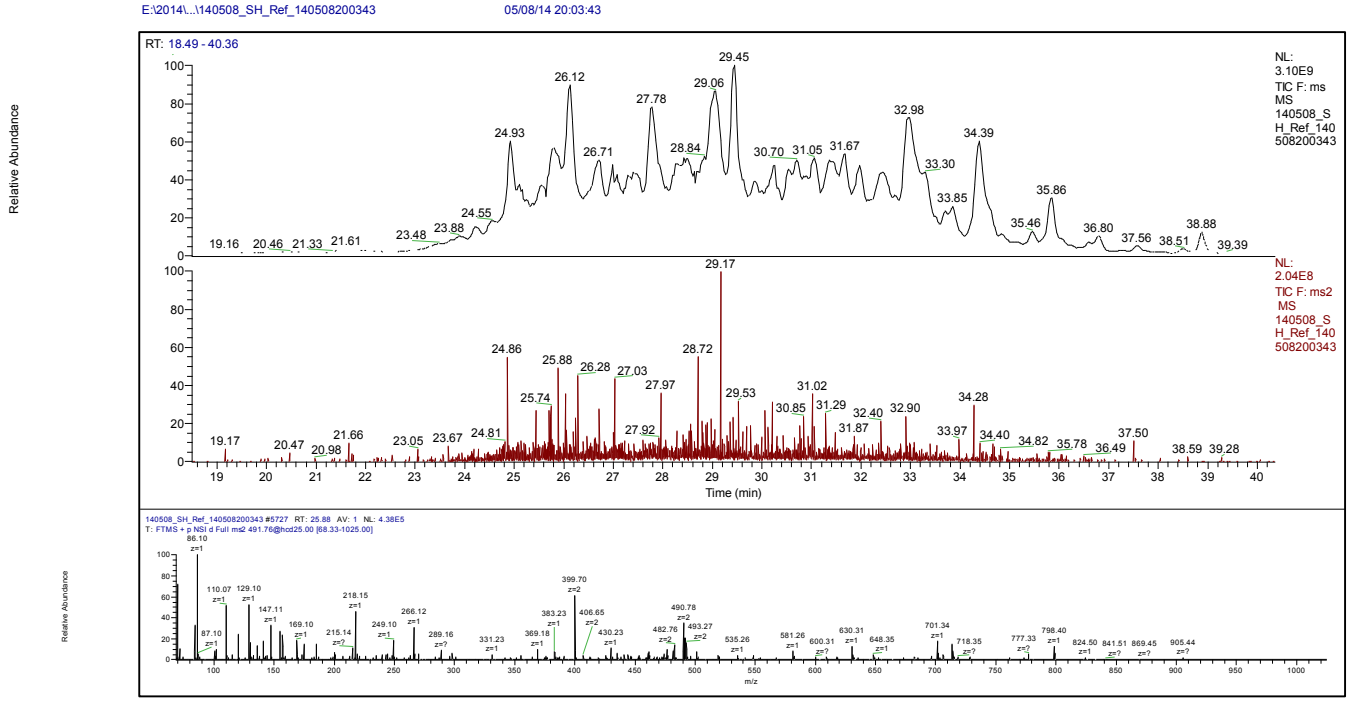

FIGURE 1.2: EXAMPLE OF A SHOTGUN MASS SPECTROMETRIC CHROMATOGRAM. UPPER PANEL: MS^1 ION CHROMATOGRAM; CENTRE PANEL: MS^2 ION CHROMATOGRAM; LOWER PANEL: MS^2 MASS SPECTRUM FOR A 491.76 M/Z PEPTIDE

The measured mass spectral data are then compared to theoretical mass spectra generated from *in silico* digestion of known protein sequences.[114] Theoretical peptide fragmentation outlines possible fragmentation sites of a peptide molecule based on Roepstorff-Fohlman-Biemann nomenclature.[114–116] The most common type of fragments seen with CID and HCD are *y*- and *b*-type ions, which are produced from fragmentation at the peptide bond.[109,115–117] Generally the m/z values of these fragments, including adducts and neutral losses, are used to construct theoretical mass spectra for identification of peptides by MS.[114] Software packages, such as MaxQuant and the Andromeda search engine, used in the present study, are designed to assess experimental mass spectra and compare them to *in silico*-derived versions, thereby identifying peptides in the sample.[114,118,119] Protein identity can then be inferred based on peptide composition.[114] False identifications are detected based on matches to a decoy database, which is usually a reversed version of the reference protein sequence

database.[120] Peptide abundances are calculated based on the signal over time for peptide ions extracted from the MS^1 chromatogram.[118] Protein abundances are then calculated from peptide abundances using established algorithms.[118]

Targeted proteomic analysis involves the detection and quantitation of pre-selected peptides by tandem MS. Specifically, parent ions of predefined m/z are selected and fragmented, prior to selection and quantitation of predefined product ions.[121] This type of analysis is referred to as selected reaction monitoring (SRM), whereas the measurement of multiple product ions per parent is known as multiple reaction monitoring (MRM).[89,121–123] When this analysis is applied to peptides, fragment ions can be predicted based on their theoretical amino acid sequence.[124] Triple quadrupole instruments are specifically designed for targeted analyses, owing to the mass filtering ability of the quadrupoles.[125,126] Triple quadrupole mass spectrometers are comprised of three quadrupole mass filters in series.[125] The basic layout of a triple quadrupole mass spectrometer is illustrated in Figure 1.3.[127]

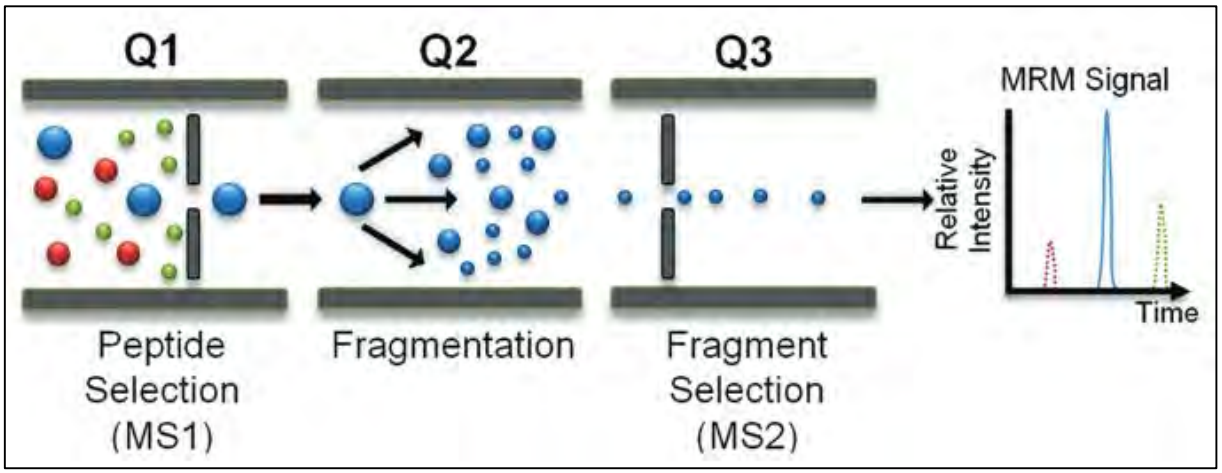

FIGURE 1.3: SCHEMATIC OF A TRIPLE QUADRUPOLE MASS ANALYSER. Q1: QUADRUPOLE 1, Q2: QUADRUPOLE 2. Q3: QUADRUPOLE 3. ADAPTED FROM BOJA ET AL.[127]

In this instrument ionised peptides of a predefined m/z are allowed to pass through the first quadrupole (Q1) while the remaining peptides are filtered out.[125] These selected peptides are then accelerated into a stream of inert gas particles (e.g. Argon) in the second quadrupole (Q2), resulting in fragmentation of the peptides – where the kinetic energy applied to the peptides determine the fragments produced.[125,128] Fragments are transferred to the third quadrupole (Q3) where fragments of a preselected m/z are allowed to pass, while the remaining ions are ejected from the instrument.[125] The selected fragment ions reach a detector, usually an electron multiplier, which amplifies the signal that is recorded by the

instrument control software.[125,129] MRM enables confident identification of peptides – and other – molecules as any ambiguity resulting from measurement of only the precursor mass is eliminated by measurement of several fragments.[121]

Parallel reaction monitoring (PRM) is a similar analytical technique to SRM, except during PRM analysis all detectable product ions are measured for each parent ion.[130] In addition to its full scan capabilities, the Q Exactive Quadrupole-Orbitrap mass spectrometer is also able to perform PRM analyses (Figure 1.4).[131] In this instrument the quadrupole acts as the precursor mass filter, and the Orbitrap provides high resolution detection of product ions.[131] Briefly, selected precursor ions are filtered through by the quadrupole and accumulated in the HCD collision cell – acting as an ion trap.[131,132] Once the ions have accumulated for the pre-set injection time (IT), they are fragmented into product ions.[131,132] These product ions are then injected, via the C-trap, into the Orbitrap for mass determination and quantitation.[131,132]

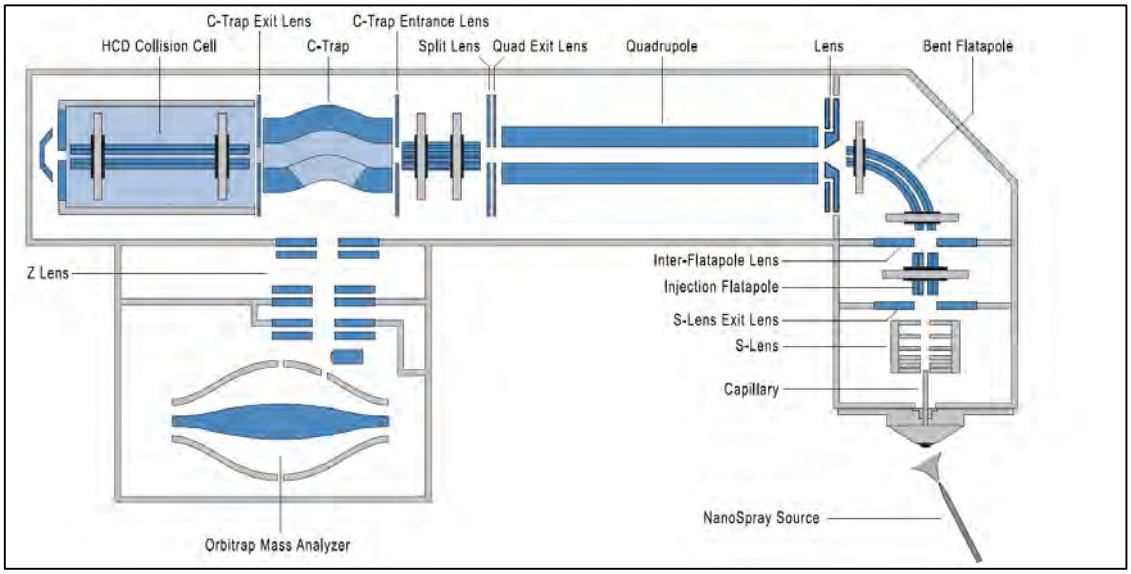

FIGURE 1.4: SCHEMATIC OF THE Q EXACTIVE QUADRUPOLE-ORBITRAP MASS SPECTROMETER. ADAPTED FROM MICHALSKI ET AL.[187]

This process can be applied to single precursors in sequence, as illustrated in Figure 1.5-A, where each precursor is successively selected and its product ions quantified.[131,132] It is also possible to quantify multiple precursors simultaneously to increase analytical throughput as shown in Figure 1.5-B.[131,132] In the latter scenario, each precursor is selected by the quadrupole and successively accumulated in the HCD cell.[131,132] Once the final set of precursor ions have accumulated, all the ions in the cell are fragmented and injected into the Orbitrap for analysis.[131,132] Regarding triple quadrupole instruments, every precursor can be tied back to each product ion as selection at both MS levels occurs in sequence, thus preventing 'crosstalk'.[125] This is not the case with multiplexed PRM analyses, as all product ions are analysed simultaneously.[130] It should be noted that this restricts the product ions that can be multiplexed such that no two precursors may have product ions with the same mass.

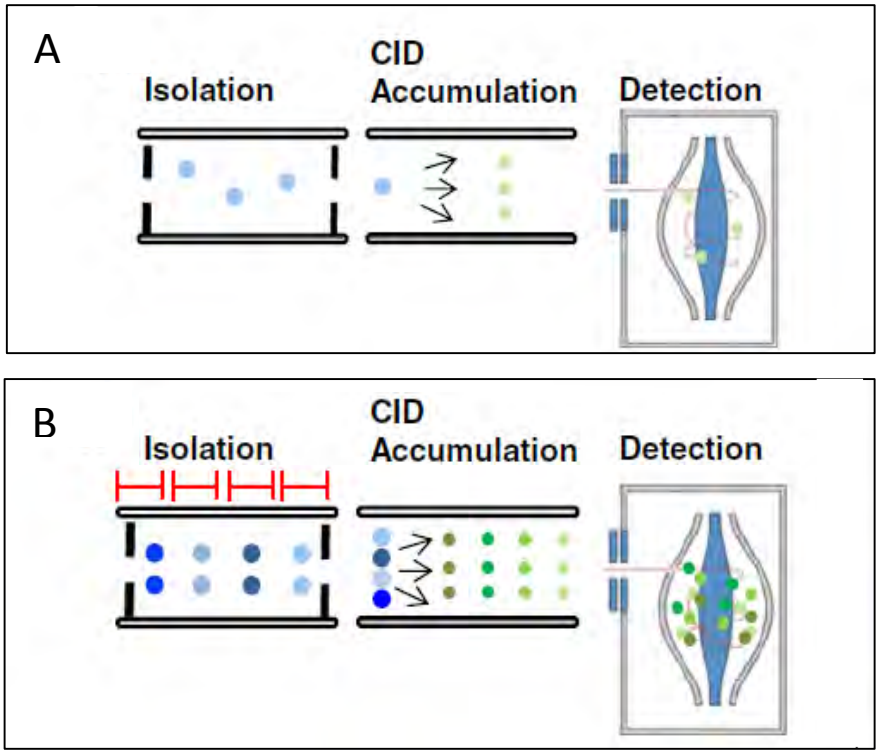

FIGURE 1.5: SCHEMATICS OF SINGLE- (A) AND MULTI-PLEXED (B) PARALLEL REACTION MONITORING ON Q-EXACTIVE MASS SPECTROMETER. ADAPTED FROM GALLIEN ET AL.[132]

The data output from PRM and MRM assays are expressed as product ion signal over the chromatographic elution time (Figure 1.6). Specialised software, such as Skyline, used in the present study, is used to read and display this data in graphical form.[133] The signal of each measured fragment, collectively known as the MS^2 spectrum in tandem MS (Figure 1.6-B), is linked to its parent. This pair or ions is known as a parent to product ion 'transition' (Figure 1.6-C).[134]

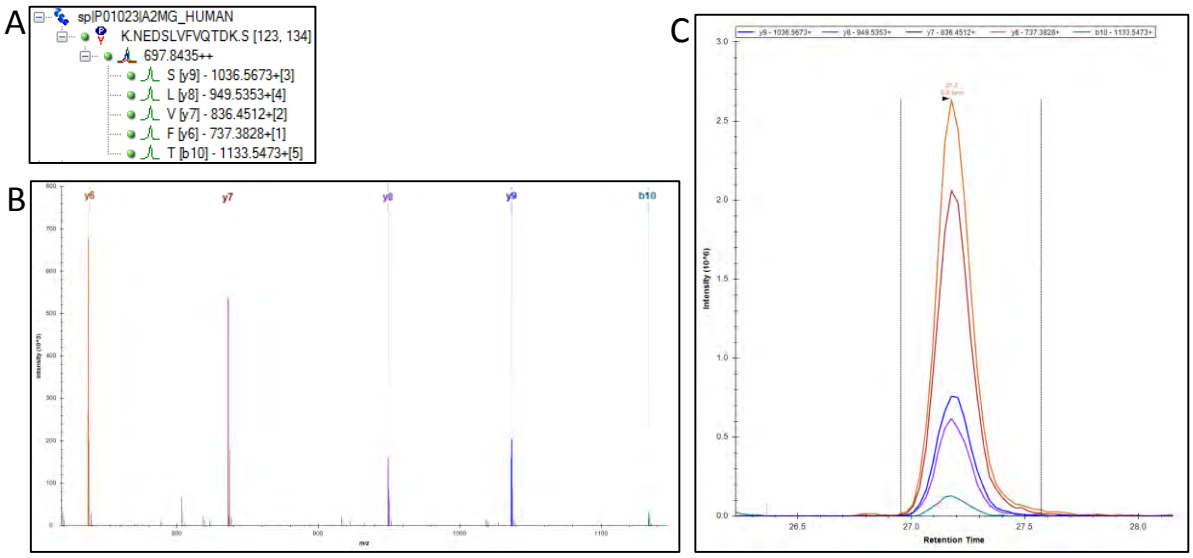

FIGURE 1.6: DATA VISUALISATION OF A TARGETED MASS SPECTROMETRIC EXPERIMENT. A: PEPTIDE IONS; B: MS^2 SPECTRUM; C: TRANSITION CHROMATOGRAM OF INTENSITY OVER TIME

The graphical data output is expressed as quantitative data by calculating the areas under the intensity vs retention time chromatogram for each transition (Figure 1.7).[127,133,135] These areas can then be summed to yield a representative area value for the parent peptide, which can then be used for comparative quantitation.[127]

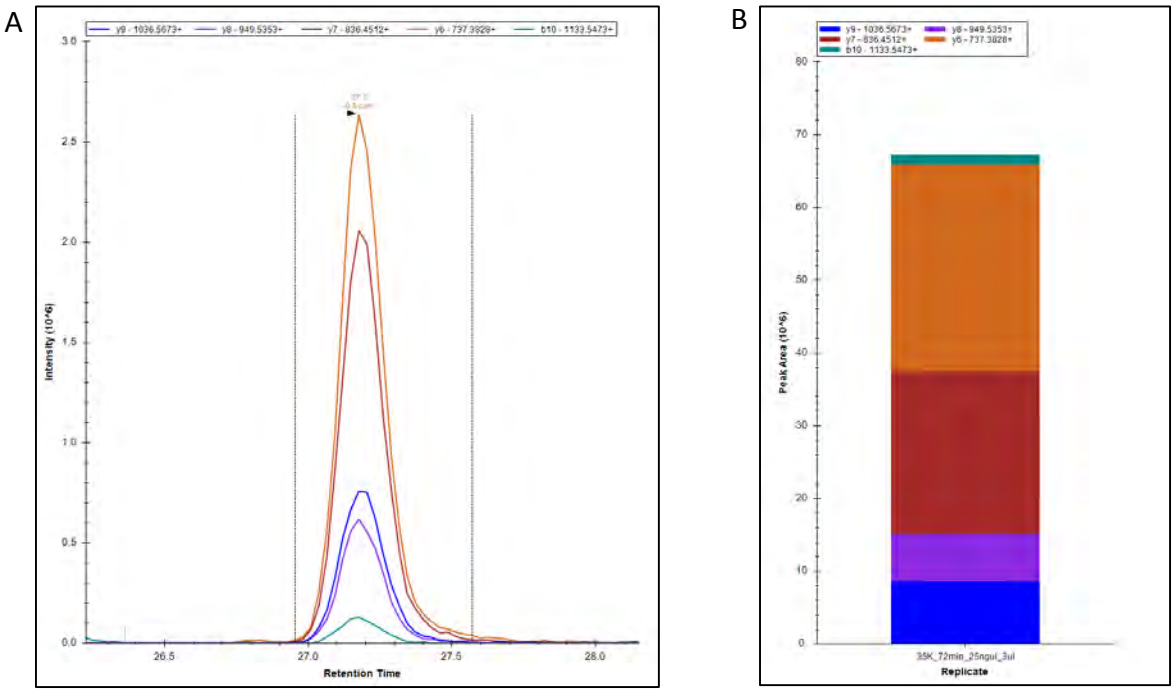

FIGURE 1.7: QUANTITATION IN TARGETED MASS SPECTROMETRIC EXPERIMENTS. A: TRANSITION CHROMATOGRAM; B: PEAK AREA BAR PLOT

MASS SPECTROMETRY BASED BIOMARKER ASSESSMENT

The utilisation of MS for the discovery, and high throughput validation of disease markers in biological fluids is an attractive prospect that has gained significant attention since the advent of proteomic MS.[136] The recent advances in mass spectrometric technologies has led to a burgeoning in the field of MS-based proteomics, and in turn to growth in the field of systems biology.[96] It is now possible to identify and accurately quantify several thousands of proteins in complex biological samples.[96] This provides significant utility for the identification of markers of disease. Targeted analyses allow for accurate quantitation and validation of prospective markers, in a large number of biological replicates at high throughput.[127,137–139]

Targeted proteomic MS possesses major advantages over classical quantitative techniques such as enzyme-linked immunosorbent assays (ELISAs) for biomarker screening, as mass spectrometric assays are high throughput; allow for high multiplexing without extensive optimisation; and are highly automatable.[138–140] Targeted proteomic assays are also less costly to develop, as expensive antibodies are not required.[138,139] Addition of markers to an existing method requires minimal optimisation. Ideally, the endpoint of MS-based screening of potential biomarkers would be an easily administered point-of-care test.[141]

THE 'ALZHEIMER'S DISEASE BIOMARKER IN HAND' HYPOTHESIS

Alzheimer's disease (AD) is a complex neuro-inflammatory disorder characterised by intra-neuronal amyloid beta (Aβ) plaques, extracellular accumulation of soluble Aβ oligomers, and intra-neuronal neurofibrillary tangles composed of hyper-phosphorylated tau protein.[142–146] Although the neuropathogenesis of AD is not completely understood, these protein are believed to be involved in the inflammatory pathology characteristic of AD.[142,144,146]

There appear to be some similarities between the inflammatory mechanisms underlying neuropathogenesis in HAND and AD. Indeed, Inflammatory mechanisms mediated by microglia and CNS macrophages are thought to be responsible for, or at the very least contribute to, inflammation-related neuronal cell death in these disorders.[23,24,33,34,147–151] Aβ plaques have also been found in the brains of HAND patients.[152,153]

We hypothesised that this inflammatory similarity may provide a suitable starting point for the development of molecular diagnostic tests aimed at HAND. A panel of serum-based protein markers would be of significant utility in the diagnosis of HAND, and could perhaps be based on established markers for neurodegenerative disorders with a similar inflammatory basis. Utilisation of markers previously associated with AD was proposed. It should be noted that any biomarker expression profile seen in HAND *must* be compared with that in other neuroinflammatory disorders, especially AD, in order to differentiate between disorders with similar inflammatory pathogeneses. Indeed, utilisation of a panel of markers with an expression signature specific for HAND subtypes would allow for differentiation between other disorders with similar underlying pathologies.

Recently, Professor Simon Lovestone (Department of Psychiatry, University of Oxford) reported a panel of blood-based biomarkers for the diagnosis of AD.[154–159] Accuracy, sensitivity, and specificity of the final panel for conversion from mild neurocognitive dysfunction to AD was estimated at 94.9%, 73.6%, and 94.9% respectively.[154] These diagnostic indicators were assisted by Apolipoprotein E genotype-based prediction of progression to AD.[154] We hypothesised that there may be applicability of this panel to diagnosis of HAND. At the initial stages of the present study, twelve protein candidates were proposed from within the AD biomarker panel, based on suggestions by Professor Lovestone: alpha-1-acid glycoprotein (A1AG), alpha-1-antitrypsin (A1AT), alpha-2-macroglobulin (A2M), apolipoprotein A-I (ApoA-I), apolipoprotein E (ApoE), ceruloplasmin (CERU), clusterin (CLU),

complement C3 (C3), complement C4 (C4), complement factor H (CFH), gelsolin (GSN), serum amyloid P-component (SAP). Differential marker expression profiling between patients with intermediate and severe forms of HAND, as well as without HAND, forms the basis of the present study.

AIMS AND OBJECTIVES OF STUDY

The aim of this study was to assess the applicability of a set of AD biomarkers to the diagnosis of HAND. Objectives included:

1. Shotgun proteomic analyses on pooled samples to identify representative peptides for marker proteins,
2. Development and optimisation of PRM assays for markers and internal reference peptides,
3. Application of PRM assays to clinical samples across representative disease groups.

Chapter 2
Sample Preparation for Mass Spectrometric Analyses

2.1. Introduction

Bottom up proteomic MS is primarily concerned with identification of proteins by inference from identified peptides (see Chapter 3). Sample preparation for this type of analysis involves generation of peptides by a specific protease, usually trypsin, and is equivalent to that required for targeted proteomic analyses.

Modern shotgun analyses that employ full mass range scanning are able to detect analytes up to 10^4 orders of dynamic range.[160] Targeted mass spectrometric assays such as MRM, which utilise non-scanning methods, increase the dynamic range to 4-5 orders of magnitude.[124,134,161] This however, is insufficient in detecting all the constituents of a complex biological matrix exceeding 10^5 orders of dynamic range. Proteomic analysis of blood serum and plasma is therefore difficult, owing to the fact that human plasma proteins span an abundance range of approximately 12 orders of magnitude, with albumin alone comprising up to 55% of total protein.[162] It is for this reason that affinity depletion and extensive fractionation is routinely employed to enable identification of lower abundance plasma proteins in discovery analyses.[163–165]

For the purposes of the present study however, depletion and fractionation were deemed unnecessary, since the proteins of interest belong to the high to medium abundance portion of the plasma proteome.[137,162,166,167] Extensive fractionation and depletion would also negatively impact high throughput analysis of clinical samples[168,169]. Kuzyk et al.[137] provide a list of 45 quantifiable plasma proteins quantifiable by MRM in crude plasma, of which eight of the 13 markers of interest were represented. It was therefore deemed likely that the markers of interest would be quantifiable in serum, due to lack of abundant coagulation related proteins. Additionally, in order to increase the likelihood of detecting and quantifying the markers of interest, depletion of albumin alone was performed by means of gel-based removal of the dominant 67 kDa band. This Chapter outlines albumin depletion and sample preparation for analysis by targeted MS.

2.2. Materials and Methods

2.2.1. Cohort Collection and Serum Isolation

This study was approved by the University of Cape Town Human Research Ethics Committee of the Faculty of Health Sciences as an amendment to approval for the study "Characterisation of HIV Dementia among individuals starting antiretroviral therapy in South Africa".[170] (HREC 023/2008).

Patients who met recruitment criteria, outlined in the primary publication by Dr John Joska[170], and who provided written informed consent were enrolled into the study. Participants were predominantly female (75%), ranging from 18 to 35 years of age. Other recruitment criteria included recent confirmation of HIV status (<6 months prior to study commencement), and at least 7 years of formal education. Ethnicity data was not available. The 170 enrolled patients, including HIV-positive control patients, were subjected to various neuropsychological tests, and HAND statuses were determined based on the American Academy of Neurology criteria.[10,170]

Venous blood samples were collected in Vacutainer serum-separating tubes (SST, BD Biosciences, for serum isolation). Phlebotomy and clinical characterisations were performed by the Department of Psychiatry (Groote Schuur Hospital) for ApoE genotyping as part of the larger project headed by Dr John Joska (PI: Dr Dan Stein), entitled "Characterisation of HIV Dementia among individuals starting antiretroviral therapy in South Africa".[170,171] Groote Schuur hospital is a large tertiary hospital in the Western Cape at which a substantial proportion of patients are HIV-infected.

Samples were transported at room temperature to a biosafety level two facility at the Institute of Infectious Disease and Molecular Medicine (IDM) for processing. Dr Kathryn Wood (Professor Robert Wilkinson's Group, CIDRI. IDM) and Tariq Ganief (Blackburn Group, IDM) were responsible for isolating and storing serum. Serum from a total of 138 patients were isolated. For serum isolation, SST tubes were centrifuged (1500 x g, 10 minutes, room temperature) and serum fractions collected and stored at -80˚C.

2.2.2. Sample Selection and Stratification

Serum samples were selected based on their HAND status. Of the 138 isolated patient samples, 81 were selected for analysis. These comprised of 27 Normal (HIV positive), 27 MNI, and 27 HAD patient samples. These samples were derived from patients ranging from 23-30 years of age. Of the 81 samples selected, 67 (83%) were derived from female participants. Normal, MNI, and HAD groups consisted of 24 (89%), 22 (81%), and 21 (78%) samples from female participants respectively. All selected samples Serum samples were randomised for processing in batches of nine, comprising three samples from each disease group (normal, MNI, HAD) (Appendix A: Table 8.1).

2.2.3. Depletion Strategy

Non-reducing sodium dodecyl sulphate polyacrylamide gel electrophoresis (SDS-PAGE) was utilised to effect the depletion of abundant proteins. Samples were separated on a 4-20% Tris-Glycine pre-cast gradient gel (Mini-PROTEAN TGX Precast Gel, Bio-Rad Laboratories, Cat#: 456-1093) to maximise band resolution and minimise concomitant removal of proteins other than albumin. Albumin (±67 kDa) was the only abundant protein depleted, by band excision.

2.2.4. Sample Loading Determination

Gel loading amounts were determined by trial and error. Maximal loading was preferred, with overlap of protein bands between lanes as the limiting factor. At this stage, serum total protein concentration was estimated at approximately 70 mg/ml. Upon running several serum loads (23 µg, 25 µg and 30 µg) on a 10% SDS-PAGE gel, a final concentration of 1.53 µg/µl in 18 µl (23 µg per well) was chosen as it provided maximal loading without compromising band resolution.

2.2.5. Sample Preparation for Pilot Analysis

Total protein in serum samples was estimated using the Bicinchoninic acid assay (BCA, Thermo-Pierce), according to manufacturer instructions. Briefly, samples were incubated at 60°C for 1 hour to deactivate HIV in plasma. Samples were then diluted 100-fold, to allow the protein concentration to fall within the linear range (20-2000 µg/ml) of the micro-plate BCA assay. Total protein concentration was then estimated by extrapolation from a BSA standard

curve ranging from 0.02 to 2 µg/µl. Crude concentrations were calculated for all samples by multiplying calculated concentrations by the dilution factor.

2.2.6. Sample Preparation for Mass Spectrometric Analysis

2.2.6.1. Sample Normalisation

Raw serum sample randomised batches (as discussed above in Section 2.2.2), were processed independently. Serum samples were normalised based on total protein to a final concentration of 1.53 µg/µl (Appendix A: Table 8.1). Samples were diluted with Milli-Q water (Merck Millipore), on ice.

2.2.6.2. Gel-based Separation

45 µl of sample was dispensed into sterile screw-top polypropylene vials (Greiner Bio-One), and 9 µl of 6x SDS-PAGE sample buffer (4× Tris Cl/SDS [pH 6.8], 3.0 ml glycerol [30% final], 1 g SDS [10% final], 0.93 g DTT [0.6 M final], 1.2 mg bromphenol blue [0.012% final], H_2O to 10 ml)[172] was added. The vials were kept on ice. Once all samples in the batch were dispensed and sample buffer added, vials were vortexed briefly and heated at 95°C for 5 minutes to denature proteins. Samples were left to cool at room temperature, vortexed briefly at low speed, and centrifuged (10000 x g, 2 minutes, room temperature) to ensure no loss of condensate. 18 µl of each sample/sample buffer mixture was loaded onto each gel, which was organised into one molecular weight marker lane containing 5 µl of PageRuler Plus standard (mass range 10-250 kDa, Thermo Scientific) and nine sample lanes (one gel per batch). Gels were run in a BioRad Mini Protean 4 system (Bio-Rad Laboratories) with SDS running buffer (25 mM Tris, 192 mM glycine, 0.1% SDS)[173] prepared in-house. Each gel was run individually, at a constant voltage of 100V until the Bromophenol dye front approached the end of the gel (approximately 1.5hrs).

2.2.6.3. Zinc Reversible Gel Staining

Each gel was rinsed briefly and stained using a zinc-imidazole reversible stain (Thermo-Pierce, Cat#: 24582) as per the manufacturer's protocol. Briefly, the gel was incubated in approximately 25 mL of zinc stain solution (Imidazole-SDS solution[174]) on an orbital shaker at low speed for 10 minutes. The zinc-imidazole stain renders the gel opaque while leaving protein bands unstained. This "negative staining" procedure is advantageous in that unbound proteins facilitate downstream analysis flexibility. This, in contrast to Coomassie-stained gels,

eliminates the need for intensive removal of stain from protein during the in-gel digest procedure. The stain was removed and replaced by 25 mL of zinc developer solution (Zinc sulphate solution[174]), and developed for 30 seconds. The developer was quickly removed and the gel rinsed three times with Milli-Q water for 1 minute on an orbital shaker at low speed. The gel was then photographed on a glass plate with a black background to visualise the clear protein bands (Appendix A: Figure 8.1).

2.2.6.4. In-gel Digest

An in-gel digest protocol for Coomassie-stained gels[175], was modified to extract tryptic peptides from the gel:

GEL DISSECTION

Each lane was dissected from the gel and divided into fractions according to Figure 2.1. Each fraction was cut into smaller blocks (approximately 1 mm x 1 mm) to maximise surface area for tryptic digestion. To prevent cross-contamination, scalpels and forceps were rinsed with

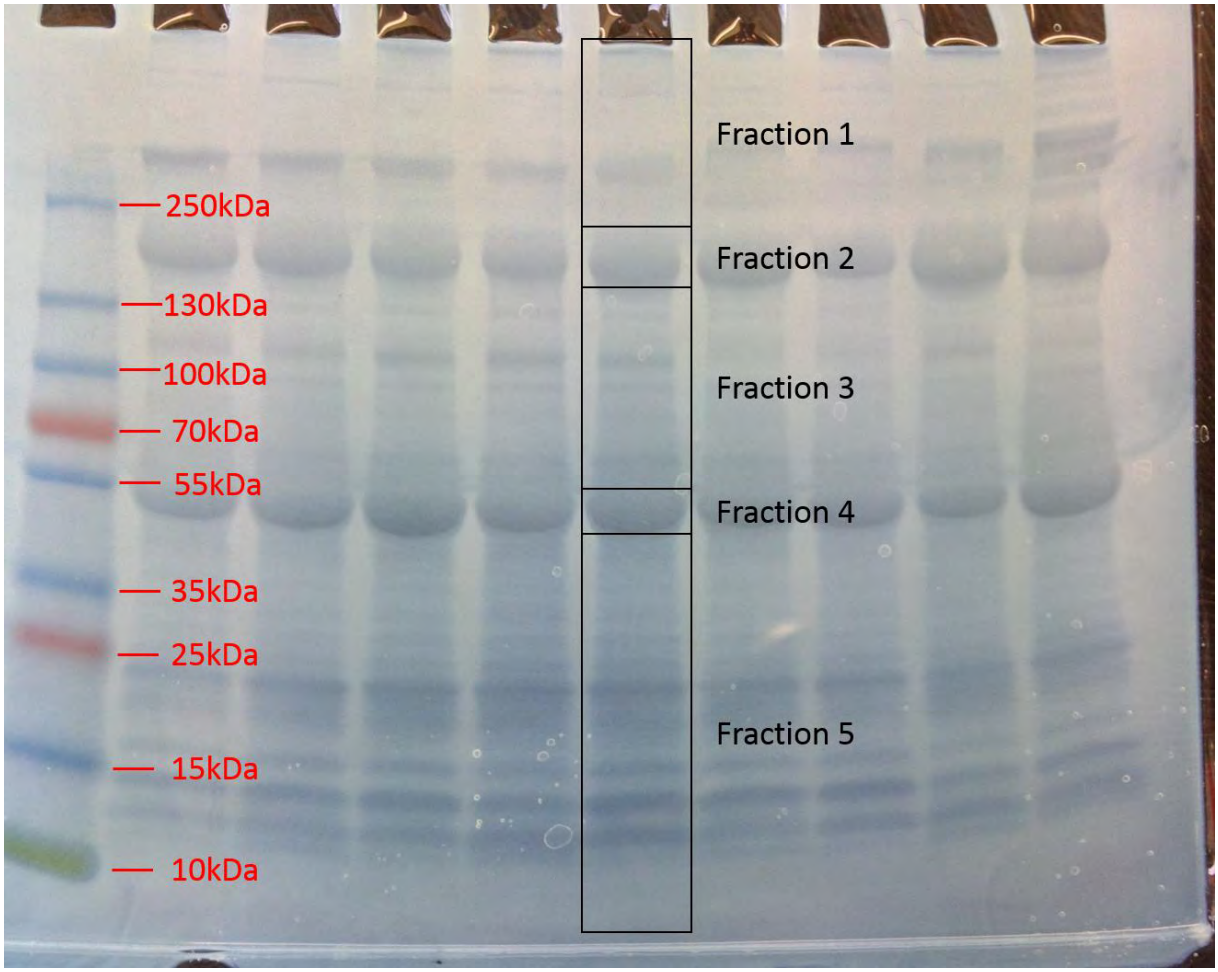

FIGURE 2.1: FRACTIONATION OF GEL LANE FOR IN-GEL DIGEST. FRACTION 4 IS PRESUMED TO BE THE ALBUMIN BAND. MOLECULAR WEIGHT MARKER BAND WEIGHTS IN RED.

50% methanol in water following isolation of each individual fraction. Fractions were then transferred to 1.5 mL flip-top polypropylene vials and submerged in Milli-Q water.

The water was removed using a 200 µl micro-pipette, and 250 µl of Tris-Glycine buffer (50 mM Tris, 192 mM Glycine, in Milli-Q water) was added to all vials (500 µl for Fraction 5, due to the larger gel volume) using a HandyStep (Brand GmbH & Co. KG) liquid dispenser with PD-tips (Brand GmbH & Co. KG) for rapid dispensing across all fraction vials. The vials were then vortexed at low speed for 10 minutes. The Tris-Glycine buffer chelates zinc precipitate from the gel to de-stain it. The buffer was then exchanged for 250 µl (500 µl for Fraction 5) of 50 mM Ammonium Bicarbonate (ABC, Sigma-Aldrich), after which the vials were briefly vortexed at low speed and incubated at room temperature for 10 minutes.

ABC was exchanged for 250 µl 100% Acetonitrile (ACN, Gradient grade, Merck) and vials were incubated while vortexing at low speed for 30 minutes. ACN was replaced with fresh ACN and incubated while vortexing at low speed for 10 minutes, or until gel pieces turned opaque. ACN was removed and gel pieces dehydrated in a SpeedVac (Savant, Thermo Scientific) for 30 minutes (or until completely dry). Vials were stored at -20°C for further processing. Fraction 4 (the presumed albumin fraction) was not taken to the next phase of processing, in the interest of efficiency.

REDUCTION AND ALKYLATION

Gel pieces were equilibrated to reach room temperature before subsequent processing. Disulphide bonds between cysteine residues were reduced by addition of 250 µl 2 mM Tris(2-carboxyethyl)phospine hydrochloride (TCEP•HCl, Sigma-Aldrich). Samples were then incubated at 37°C for 30 minutes, TCEP was removed, and 250 µl 50 mM ABC was added to all vials (500 µl for Fraction 5) for 1 minute. ABC was removed, and 250 µl 50% ACN was added to all vials for 1 minute. ACN was removed, and 200 µl 55 mM Iodoacetamide (IAA, Sigma-Aldrich) was added to all vials (300 µl for Fraction 5) and incubated at room temperature in the dark for 60 minutes in order to block exposed sulfhydryl groups of reduced cysteine residues by addition of a carbamidomethyl group to prevent reformation of disulphide bonds. IAA was removed and 200 µl 50 mM ABC was added to all vials for 10 minutes. ABC was replaced with 250 µl 50% ACN (500 µl for Fraction 5) for 20 minutes. ACN was removed and

samples were completely dehydrated in a SpeedVac (approximately 1 hour) to remove residual ACN.

TRYPTIC DIGEST

During dehydration, sequencing-grade modified porcine trypsin (Promega) was prepared by reconstituting 20 µg lyophilised trypsin in 100 µl 50 mM acetic acid to yield a 0.2 µg/µl solution. Prior to adding trypsin to gel pieces, 900 µl 50 mM ABC was added to the reconstituted trypsin to activate it (optimal pH: 7-9) and yield a final concentration of 20 ng/µl. Trypsin was kept at 4°C prior to addition to gel pieces to minimise enzyme autolysis and maximise activity. Trypsin was added to dehydrated gel pieces until the enzyme solution just covered the pieces (100 µg of trypsin per gel, due to reagent constraints). Generally, the volumes used for each vial were as follows (allowing for "topping up" of vials where necessary): fraction 1 ~125 µl, fraction 2 ~50 µl, fraction 3 ~125 µl, fraction 5 ~250 µl. Vials were incubated for 17 hours at 37°C in a wet box to maintain even heat distribution and minimise evaporation.

PEPTIDE EXTRACTION

Following tryptic digest, 100 µl 70% ACN was added to all vials, which were incubated at room temperature for 30 minutes. Supernatant was transferred to clean vials. This step was repeated and the new supernatant was harvested and added to the original supernatant. The supernatant (peptide extract) was dehydrated in a CentriVap concentrator (LabconCo) at 35°C for ~150 minutes. Peptides were stored at -20°C prior to downstream processing.

PEPTIDE CLEAN-UP

Silica beads with functionalised 18-carbon chains (which bind peptides via hydrophobic interactions) were utilised to remove MS-incompatible buffers, salts, and contaminants from prepared peptides. The peptides were then eluted with a highly hydrophobic solvent, which disrupts the hydrophobic interactions. Samples were 'cleaned' using C18 spin columns packed in-house[102,176]: empty spin columns that fit into 1.5/2.0 mL polypropylene vials (Appendix A: Figure 8.2, 30 µm pore size, Thermo-Pierce) were packed with 8 mg C18 reversed phase beads (Supelco Discovery C18, 50 µm particle size, Sigma-Aldrich) to bind 30 µg of peptide.[177] The samples were cleaned according to the manufacturer's instructions for Thermo-Pierce C18 spin columns.[177]

Stored samples were allowed to reach room temperature before 100 µl 5% ACN/0.5% Formic Acid (FA, MS grade, Sigma-Aldrich) in Milli-Q water was added to each vial. The vials were then vortexed at low speed for 5 minutes to resolubilise peptides, and centrifuged (10000 x g, 2 minutes, room temperature) to collect condensed droplets and sediment gel particulates. Each column was tapped to settle C18 resin and inserted into clean 2 mL flip-top polypropylene vials. This was followed by addition of 200 µl activation solution (50% ACN) using a 200 µl gel-loading pipette tip (Sigma-Aldrich) to prevent air bubble formation and resin disturbance. Columns were centrifuged (1500 x g, 1 minute, room temperature) to activate beads, and flow-through was discarded. These steps were repeated with an additional 200 µl activation solution. Equilibration solution (200 µl 0.5% FA in 5% ACN) was added, columns were centrifuged (1500 x g, 1 minute, room temperature) to equilibrate beads, and flow-through was discarded. These steps were repeated with an additional 200 µl equilibration solution.

Each column was transferred to a clean 2 mL flip-top polypropylene vial. All fractions belonging to each individual sample were loaded on a single column with the aim of recombining them into a single final fraction: for each sample, each fraction was dispensed in a step-wise manner onto the corresponding column after centrifugation (1500 x g, 1 minute, room temperature) with the previous fraction until all fractions had been added and without discarding the flow-through. Each column was then transferred to a clean 2 mL flip-top polypropylene vial. The flow-through was then run through each column again to ensure sample binding: 2 x 200 µl of each sample was centrifuged (1500 x g, 1 minute, room temperature). Flow-through was stored at -20°C for future quality control assessment of sample binding. Each column was transferred to a clean 2 mL flip-top polypropylene vial. Wash solution (200 µl 0.5% FA in 5% ACN) was added to each column prior to centrifugation (1500 x g, 1 minute, room temperature) to remove contaminants, and flow-through was discarded. These steps were repeated with an additional 200 µl of wash solution per column. Each column was transferred to a sterile, un-autoclaved 2 mL screw-cap polypropylene vial. Elution buffer (25 µl 0.1% FA in 70% ACN) was added to each column prior to centrifugation (1500 x g, 1 minute, room temperature) to release and elute bound peptides from the column. These steps were repeated with an additional 25 µl of elution buffer per column. The samples were dehydrated in a CentriVap concentrator at 35°C for ~60 minutes. Vials were stored at -20°C until analysis.

Chapter 3
Optimisation A: Identification of Candidate Peptides for Parallel Reaction Monitoring Assays through Shotgun Proteomic Analysis of Pooled Sera

3.1. Introduction

In order to be useful in biomarker validation, targeted MS analysis of biological samples requires *a priori* identification of ideally-performing (*vide infra*) peptides with which to infer protein quantities. It is feasible to predict all possible tryptic peptides *in silico,* then assess each via multiple rounds of targeted MS. This method, however, is labour intensive and inefficient. As an alternative, SRMatlas (www.srmatlas.org) is an online repository of targeted proteomic data, and includes empirically determined peptide lists for given proteins, as well as associated instrument parameters. However, this route to peptide selection may result in peptides and parameters that are not the most effective, given the in-house instrument configuration. A further route of optimal peptide selection, therefore, is via shotgun proteomic MS of pilot samples which are representative of final analytical samples.

During shotgun MS, tryptic peptides are separated by online liquid chromatography and analysed by tandem mass spectrometry (LC-MS/MS).[97] These peptides are sequenced by matching their masses, as well as the masses of their fragment ions, obtained by MS to a theoretical peptide database which was generated *in silico.*[114] Peptides are then mapped to parent proteins in the original sample and can also be utilised to infer parent protein abundance.[114]

In the present study, sample depletion followed by fractionation were not employed, contrary to the norm for shotgun proteomic analysis of human serum. Instead, gel fractionation was employed to remove albumin, after which fractions were recombined for targeted proteomic analysis. Re-pooling of the fractions after removal of albumin was due to the initial intent of the study, where no shotgun proteomic analysis was planned. MRM assays, based on peptides and parameters provided by Dr Malcolm Ward (Proteome Sciences), were to be applied to

minimally depleted samples without fractionation to increase throughput. Discovery proteomic analysis was subsequently performed due to failure of these initial MRM assays in pilot experiments (data not included).

This Chapter therefore describes MS-based identification of the peptides present in pooled patient samples, and subsequent selection of a set of optimally performing peptides representing candidate biomarkers of neurodegeneration. The ultimate intention is utilisation of this peptide set to develop a PRM assay for these biomarkers.

3.2. Materials and Methods

3.2.1. Sample Pooling

Table 3.1 shows sample selection for discovery analysis, including disease group and batch membership, as well as pooling assignments. Nine samples from each cohort (n=9) were randomly selected for shotgun analysis. One sample was selected from each batch, per disease group (described in Chapter 2 and Appendix A: Table 8.1), to ensure equivalent representation across all batches. Within each disease group, samples were combined into three pools of three. Pooling was employed to minimise initial analysis time, given limited instrument time. Three biological replicates were run per disease group, and all disease groups were represented to ensure that candidate peptides would be detected independently of disease state.

TABLE 3.1: RANDOMISED SAMPLE POOLING FOR DISCOVERY PROTEOMIC ANALYSIS

Pool	Disease Group	Sample	Batch
POS_1	HIV-positive Control	J061	1
		J204	2
		J0231	3
POS_2	HIV-positive Control	J0203	4
		J009	5
		J0260	6
POS_3	HIV-positive Control	J035	7
		J068	8
		J0233	9
MNI_1	MNI	J0179	1

Pool	Disease Group	Sample	Batch
		J0193	2
		J0125	3
MNI_2	MNI	J063	4
		J020	5
		J0167	6
MNI_3	MNI	J079	7
		J074	8
		J0207	9
HAD_1	HAD	J0149	1
		J030	2
		J206	3
HAD_2	HAD	J0148	4
		J097	5
		J0236	6
HAD_3	HAD	J005	7
		J0132	8
		J216	9

HAD: HIV Associated Dementia, MNI: Minor Neurocognitive Impairment, POS: HIV positive control.

Stored samples (Section 2.2.6) were re-suspended in 25 µl 2% ACN/0.1% FA to an estimated concentration of 0.4 µg/µl (assuming no loss during in-gel digests) per stock solution. Stock solutions were pooled, as per Table 3.1, and adjusted to a final concentration of 25 ng/µl by addition of 2% ACN/0.1% FA. Samples were transferred to 2 ml autosampler vials fitted with tapered 100 µl glass inserts (Macherey-Nagal) and stored at 4°C prior to mass spectrometric analysis.

3.2.2. LC/MS Instrumentation and Parameters

Discovery proteomic analysis was performed on a Q Exactive Quadrupole-Orbitrap mass spectrometer (Thermo Scientific), coupled to a Dionex UltiMate 3500 RSLC nano-LC system (Thermo Scientific). A standardised LC gradient, developed in our laboratory for use with mammalian peptide extracts, was used for all MS analyses unless otherwise stated. Approximately 250 ng of pooled sample was introduced by partial loop injection onto a trap

column packed in-house with Luna C18 coated silica beads (75 µm x 2 cm fused silica: New Objective; 5 µm Luna C18 resin: Phenomenex). Separation was performed by reversed phase chromatography on a nanoscale analytical column, also packed in-house (5 µm Luna C18 beads, 75 µm x 50 cm). Ionisation was attained by application of charge over a steel emitter (Thermo Scientific, Cat#: TFES542) affixed to the end of the analytical column.

Solvent A comprised 0.1% FA (LC-MS Ultra, Eluent Additive, Sigma) in UHPLC grade H_2O (LC-MS Ultra, Sigma), while Solvent B – hereafter referred to as B - comprised 0.1% FA (LC-MS Ultra, Eluent Additive) in ACN (LC-MS Ultra, Sigma). Samples were eluted using a linear 177 minute gradient at a constant flow rate of 300 nl/min, as follows: 2% B for 10 minutes, 2-25% B over 115 minutes, 25-35% B over 5 minutes, 35-80% B over 5 minutes, held at 80% B for 20 minutes, before returning to 2% B in 2 minutes, followed by re-equilibration at 2% B for 20 minutes. Each disease group replicate was run successively, with different groups separated by an 80 minute wash. The linear wash gradient was run at a constant flow rate of 300 nl/min, as follows: 2-35% B over 10 minutes, 35-50% B over 5 minutes, 50-80% B over 5 minutes, held at 80% B for 25 minutes, before returning to 2% B in 5 minutes, followed by re-equilibration at 2% B for 20 minutes. Because the intrinsic analytic gradient wash interval (80% B) was sufficient to prevent carry over for up to three consecutive samples, and in order to reduce instrument usage time, extended washes were inserted between disease groups only.

Mass spectrometric analysis was controlled by Xcalibur software (Thermo Scientific; v2.2). Mass spectrometric acquisition parameters were developed in-house and based on initial settings from Pirmoradian *et al*.[178] They are the default for all discovery analyses conducted in our laboratory. Acquisition was performed in 'Top 10', data-dependent, positive ion mode. MS^1 settings included resolution at 70 000, automatic gain control (AGC) target of $3x10^6$, and an ion injection time of 250 ms. At the MS^2 level, resolution was set at 17 500, AGC target of $2x10^5$, ion injection time of 120 ms, isolation window of 4.0 m/z and a normalised collision energy (NCE) of 25. Data dependent settings included an underfill ratio of 1% (which equates to an intensity threshold of $1.7x10^4$ for triggering of MS^2 scan), peptide match set to "preferred", isotopic exclusion, and a dynamic exclusion of 30 s. Charge exclusion was set to all unassigned charges, as well as all charges other than 2 or 3.

3.2.3. Protein/Peptide Identification and Quantitation

Data analysis was performed using MaxQuant version 1.3.0.5, which utilises the Andromeda search engine.[118,119] Masses and intensities for all detected peptide and fragment ions were extracted using default MaxQuant settings (Appendix B: Table 9.1), with the following adjustments. Briefly, multiplicity was set to 1 since no labelling strategy was employed. Peptide and protein false discovery rate (FDR) cut-offs of 0.01 were used for identification. Protein identification was 'lenient', with a minimum of one peptide required for protein identification. Peptides unique to a protein group were not required for protein inference. Label-free quantitation (LFQ) was enabled with a minimum ratio count of 2. Finally, Fast LFQ was enabled. The UniProt complete human proteome .fasta file (downloaded on 9/01/2014) was selected for sequence database searching, with sequence reversal used to construct the decoy database. Each replicate was treated as a separate experiment in the *experimentalDesignTemplate.txt* file.

The Andromeda search engine matched extracted MS^1 and MS^2 masses to an *in silico* digested human proteome sequence file consisting of known human protein sequences. Peptides were identified by matching theoretical peptide masses as well as the masses of resultant MS^2 fragments, to best-fit experimental MS^1 and MS^2 spectra. False identifications were estimated by matching measured masses to a reversed version of the human proteome sequence. Protein identities were inferred based on peptide sequence matching. Confidence in protein identity increased with increasing unique peptide identifications. Unique peptides are defined as peptides that belong to only one protein or protein group, and do not share complete sequence homology with any other protein or protein group.

Data quality and identification statistics were summarised by an R-script kindly provided by Dr Karsten Krug (Proteome Centre, University of Tübingen, Germany).

3.2.4. Preliminary Peptide Selection

The *proteingroups.txt* and *peptides.txt* Maxquant output files were interrogated manually to ascertain the presence of the candidate biomarkers. The *proteingroups.txt* file provided details on sequence coverage of proteins. Data for candidate proteins were assessed for the potential to extract representative peptides.

Data related to detected peptides contributing to the sequence of the candidate proteins were extracted from the *peptides.txt* output file. To obtain a set of representative peptides for downstream targeted analysis, 10 peptides were selected for each protein, or all identified peptides in the case of proteins with fewer than 10 identified peptides. A2M, C3 and CFH were exceptions, with 12, 12 and 15 peptides respectively as an unsatisfactory number of peptides satisfied the selection criteria (*vide infra*). Primary peptide selection criteria included good PEP (posterior error probability) scores (≤0.01) and, as a secondary criteria, the presence of the peptide in all or most of the samples. The PEP score is essentially a *p* value that represents the probability of a false identification[118], where a low score indicates a more reliable identification. Only peptides unique to a protein group were chosen, to ensure definitive protein identification.

Exclusion criteria included: peptides containing amino acid residues susceptible to variable modifications, peptides containing histidine and methionine residues (due to their tendency to become oxidised), cysteine-containing peptides (in the event of incomplete alkylation), and peptides containing missed cleavages (due to the possibility of inter-sample digest inconsistency).

3.3. Results and Discussion

3.3.1. Protein Identification and Quantitation

A total of 175 protein groups were identified by MaxQuant, with 22 of these categorised as contaminants and reverse hits (Appendix B: Table 9.2). A total of 1178 non-redundant peptides were identified, of which 204 were contaminants and reverse hits (Data not shown). Of the 381780 peptide spectra recorded, only 4.75% were assigned.

This number of protein identifications may seem low, when compared to the average identifications of up to 4000 proteins seen in proteomic experiments conducted in our laboratory. Plasma proteomic analysis however, cannot be compared to that of biological samples possessing lower dynamic range (despite albumin-depletion, as other high-abundance plasma proteins remain). Serum and plasma samples routinely require extensive processing prior to mass spectrometric analysis. Depletion of abundant proteins, preferably by antibody affinity chromatography, is required to reduce plasma's broad dynamic range.[163] However, depletion of abundant proteins alone is not adequate, and extensive fractionation

via techniques orthogonal to the reversed phase chromatographic separation online with MS – such as isoelectric focusing (IEF) or strong cation exchange (SCX) chromatography, are also required.[164,165]

The Human Proteome Organisation Plasma Proteome Project identified 3020 proteins in serum and plasma from data acquired in 35 laboratories, employing various depletion and fractionation strategies, as well as analysis by various mass spectrometer types.[179] In a recent study comparing serum analysis between several high resolution mass spectrometers, samples were subjected to two rounds of abundant protein depletion, followed by extensive IEF fractionation into 30 fractions. The highest number of identifications were obtained from a Q Exactive mass spectrometer with 1349 proteins (≥2 peptides per protein, FDR=1%).[180] Extensive fractionation, however, does not guarantee identifications in excess of 1000 protein identifications, as shown by another study employing Multiple Affinity Removal System (MARS) depletion coupled with SCX fractionation and analysis by a relatively low resolution Q-TOF mass spectrometer, which identified 125 proteins (≥2 peptides per protein, peptide FDR=0.6%, protein FDR=0%).[181] The same study also detected 63 proteins in crude plasma.

The rudimentary depletion strategy employed in the present study served to remove only albumin, with remaining fractions recombined thereafter. It would therefore be reasonable to expect that protein identification would not be on par with analyses employing extensive depletion and fractionation strategies.

Despite limited protein coverage, the proteins identified in the shotgun proteomic analysis did indeed identify the candidate biomarkers of interest, with acceptable peptide coverage, and therefore served its purpose in the context of the present study. Assessment of additional protein biomarkers would indeed require more optimised sample preparation in subsequent studies.

3.3.2. Preliminary Peptide Selection

Data output files from MaxQuant analysis were manually interrogated to locate protein biomarkers identified by Professor Simon Lovestone: A1AG, A1AT, A2M, ApoA-I, ApoE, CERU, CLU, C3, C4, CFH, GSN, and SAP. All candidate biomarkers were found to be represented in the total list of 175 identified proteins. These proteins (Table 3.2) were extracted from the *proteingroups.txt* file (Appendix B: Table 9.2). Table 3.2 includes Uniprot IDs, peptides

belonging to the protein identified, as well as percentage sequence coverage. Most of the identified proteins' sequence coverage was adequate, except proteins such as A1AG, for which only two peptides were identified (10.9% coverage). Despite poor protein coverage for proteins such as SAP, CLU, GSN, and the apolipoproteins; there were sufficient peptides from which to obtain candidate peptides for PRM analysis.

TABLE 3.2: CANDIDATE BIOMARKERS REPRESENTED IN DISCOVERY ANALYSIS RESULTS.

	Protein IDs	Protein names	Peptides	Sequence coverage [%]
1	P02763	Alpha-1-acid glycoprotein (A1AG)	2	10.9
2	P01009	Alpha-1-antitrypsin (A1AT)	18	47.8
3	P01023	Alpha-2-macroglobulin (A2M)	58	51.8
4	P02647	Apolipoprotein A-I (ApoA-I)	12	48.3
5	P02649	Apolipoprotein E (ApoE)	7	27.8
6	P00450	Ceruloplasmin (CERU)	22	24.7
7	P10909-2	Clusterin (CLU)	7	19.4
8	P01024	Complement C3 (C3)	75	49.2
9	P0C0L4	Complement C4-A (C4A)	45	32.9
10	P0C0L5	Complement C4-B (C4B)	43	30.4
11	P08603	Complement factor H (CFH)	21	24.1
12	P06396	Gelsolin (GSN)	10	19.1
13	P02743	Serum amyloid P-component (SAP)	5	23.8

PEP: Posterior Error Probability

The set of 106 preliminarily selected peptides, in order of increasing PEP score, are shown in Table 3.3. Missed cleavages, uniqueness between protein groups, as well as charge states and PEP scores are shown. These peptides were selected primarily on the basis of uniqueness to a protein group to ensure that PRM quantitation applies only to the protein of interest. Shared peptides are not representative of a single protein of interest, and therefore would skew quantitation if included in analyses. Selection of peptides possessing good PEP scores increases the likelihood of finding adequately-performing peptides in subsequent PRM-based validation.

TABLE 3.3: PRELIMINARILY SELECTED PEPTIDES FOR TARGETED ASSAY METHOD DEVELOPMENT

Protein name	Sequence	Missed cleavages	Unique (Groups)	Charge States	PEP	Raw Intensity								
						HAD 1	HAD 2	HAD 3	MNI 1	MNI 2	MNI 3	POS 1	POS 2	POS 3
A1AG	TEDTIFLR	0	no	2	4.28E-13	1.73E+07	1.18E+07	0.00E+00	9.07E+06	0.00E+00	0.00E+00	8.90E+06	0.00E+00	0.00E+00
A1AG	EQLGEFYEALDCLR *	0	yes	2	1.31E-02	0.00E+00	5.60E+06	0.00E+00	0.00E+00	0.00E+00	0.00E+00	0.00E+00	0.00E+00	0.00E+00
A1AT	TLNQPDSQLQLTT GNGLFLSEGLK	0	yes	2,3	4.61E-188	4.99E+07	6.70E+07	6.50E+06	5.57E+07	1.37E+07	1.64E+06	2.85E+07	1.28E+07	1.81E+06
A1AT	VFSNGADLSGVTE EAPLK	0	yes	2,3	1.54E-111	2.69E+08	1.73E+08	2.51E+07	2.66E+08	0.00E+00	0.00E+00	2.26E+08	1.17E+08	0.00E+00
A1AT	AVLTIDEK	0	yes	2	1.03E-67	1.93E+08	0.00E+00	0.00E+00	0.00E+00	0.00E+00	7.96E+07	1.49E+08	1.29E+08	0.00E+00
A1AT	LSITGTYDLK	0	yes	2	1.21E-15	2.56E+08	2.49E+08	9.02E+06	2.48E+08	1.93E+07	8.25E+06	1.72E+08	1.29E+08	0.00E+00
A1AT	FLENEDRR*	1	yes	2,3	1.21E-08	9.63E+06	6.08E+06	0.00E+00	2.68E+07	0.00E+00	1.57E+07	2.16E+07	1.43E+07	0.00E+00
A1AT	ITPNLAEFAFSLYR	0	yes	2,3	6.61E-06	1.81E+07	5.58E+06	1.23E+06	6.46E+07	2.57E+06	0.00E+00	2.25E+07	4.46E+06	0.00E+00
A1AT	QINDYVEK	0	yes	2	8.86E-05	1.05E+08	6.60E+07	4.56E+07	9.94E+07	6.00E+07	7.14E+07	8.84E+07	6.98E+07	4.12E+06
A1AT	SVLGQLGITK	0	yes	2	3.59E-04	3.57E+08	2.20E+08	1.77E+07	2.73E+08	2.24E+07	1.76E+07	2.21E+08	1.40E+08	2.75E+07
A1AT	DTVFALVNYIFFK	0	yes	2	6.65E-04	0.00E+00	0.00E+00	0.00E+00	0.00E+00	0.00E+00	0.00E+00	1.75E+06	0.00E+00	0.00E+00
A1AT	FLENEDR	0	yes	2	3.77E-02	2.60E+07	9.73E+06	0.00E+00	0.00E+00	1.23E+07	1.58E+07	1.37E+07	0.00E+00	0.00E+00
A2M	QFSFPLSSEPFQGS YK	0	yes	2,3	1.64E-145	4.06E+07	9.02E+07	2.57E+07	7.58E+07	2.85E+07	1.89E+07	2.83E+06	3.82E+06	1.80E+07
A2M	NEDSLVFVQTDK	0	yes	2	8.08E-124	1.52E+08	1.49E+08	1.92E+07	2.81E+08	2.52E+07	2.02E+07	1.24E+08	1.34E+08	2.43E+07
A2M	AAQVTIQSSGTFSS K	0	yes	2	5.71E-75	2.96E+07	7.15E+06	1.51E+07	7.34E+07	1.07E+07	1.43E+07	3.59E+07	4.94E+07	3.87E+06
A2M	AIGYLNTGYQR	0	yes	2	7.04E-52	1.84E+08	1.77E+08	2.37E+07	3.15E+08	2.08E+07	2.85E+07	1.23E+08	2.05E+08	3.11E+07
A2M	IAQWQSFQLEGGL K	0	yes	2	2.91E-47	7.03E+06	1.02E+08	1.13E+07	7.44E+07	1.70E+07	7.64E+06	2.22E+07	2.24E+07	6.04E+06
A2M	VSVQLEASPAFLAV PVEK	0	yes	2,3	3.59E-41	2.11E+07	1.46E+08	1.70E+07	4.52E+07	1.75E+07	1.45E+07	1.28E+07	1.98E+07	1.13E+07
A2M	ALLAYAFALAGNQ DK	0	yes	2,3	1.90E-36	7.09E+06	1.37E+07	0.00E+00	2.97E+07	2.59E+06	7.72E+05	1.15E+07	4.01E+06	0.00E+00

Protein name	Sequence	Missed cleavages	Unique (Groups)	Charge States	PEP	Raw Intensity								
						HAD 1	HAD 2	HAD 3	MNI 1	MNI 2	MNI 3	POS 1	POS 2	POS 3
A2M	FEVQVTVPK	0	yes	2	4.32E-22	8.18E+07	1.01E+08	1.06E+07	1.77E+08	1.33E+07	6.15E+06	5.96E+07	7.32E+07	7.17E+06
A2M	FQVDNNNR	0	yes	2	1.93E-19	1.56E+07	9.50E+06	1.37E+07	2.66E+07	1.29E+07	1.43E+07	9.87E+06	1.51E+07	0.00E+00
A2M	QTVSWAVTPK	0	yes	2	1.74E-10	9.14E+07	7.26E+07	1.67E+07	1.49E+08	1.42E+07	1.66E+07	5.76E+07	8.78E+07	0.00E+00
A2M	LLIYAVLPTGDVIGDSAK	0	yes	2,3	3.50E-10	1.87E+07	8.60E+07	1.35E+07	6.46E+07	2.19E+07	7.84E+06	1.78E+07	1.51E+07	3.04E+06
A2M	LPPNVVEESAR	0	yes	2	8.16E-06	1.07E+08	8.60E+07	3.32E+07	1.71E+08	2.96E+07	3.29E+07	7.96E+07	1.35E+08	2.49E+07
ApoA-I	DYVSQFEGSALGK	0	yes	2	7.99E-185	1.05E+08	8.32E+07	0.00E+00	1.32E+08	0.00E+00	0.00E+00	1.19E+08	7.47E+07	0.00E+00
ApoA-I	LLDNWDSVTSTFSK	0	yes	2	8.52E-74	2.87E+07	7.32E+07	1.07E+07	4.28E+07	1.09E+07	1.35E+07	3.26E+07	1.57E+07	1.02E+07
ApoA-I	EQLGPVTQEFWDNLEK	0	yes	2	3.04E-68	1.55E+07	0.00E+00	4.42E+06	1.81E+07	6.89E+06	6.61E+06	1.08E+07	5.13E+06	2.73E+06
ApoA-I	VSFLSALEEYTK	0	yes	2	4.38E-47	3.39E+07	7.55E+07	6.93E+06	6.20E+07	1.00E+07	6.29E+06	3.89E+07	1.22E+07	2.55E+06
ApoA-I	DLATVYVDVLK	0	yes	2	2.96E-14	1.68E+07	4.96E+07	8.27E+06	5.74E+07	0.00E+00	6.75E+06	2.51E+07	1.12E+07	2.80E+06
ApoA-I	AKPALEDLR*	1	yes	2,3	1.40E-09	5.03E+07	1.52E+07	0.00E+00	2.29E+07	0.00E+00	0.00E+00	1.83E+07	1.71E+07	0.00E+00
ApoA-I	QGLLPVLESFK	0	yes	2	4.02E-04	2.83E+07	3.74E+07	1.53E+07	4.28E+07	1.69E+07	1.49E+07	2.69E+07	9.27E+06	0.00E+00
ApoA-I	VQPYLDDFQK	0	yes	2	9.66E-04	1.16E+08	8.47E+07	8.08E+06	1.06E+08	0.00E+00	9.30E+06	1.02E+08	6.06E+07	1.83E+07
ApoA-I	VKDLATVYVDVLK*	1	yes	3	5.69E-02	0.00E+00	0.00E+00	0.00E+00	6.07E+06	0.00E+00	0.00E+00	0.00E+00	0.00E+00	0.00E+00
ApoE	LEEQAQQIR	0	yes	2	0.00E+00	0.00E+00	0.00E+00	0.00E+00	0.00E+00	0.00E+00	0.00E+00	0.00E+00	0.00E+00	0.00E+00
ApoE	SELEEQLTPVAEETR	0	yes	2	4.25E-19	1.05E+07	2.83E+06	0.00E+00	7.17E+06	0.00E+00	0.00E+00	5.59E+06	3.98E+06	0.00E+00
ApoE	AATVGSLAGQPLQER	0	yes	2	1.30E-03	1.04E+07	5.92E+06	0.00E+00	6.99E+06	8.87E+05	0.00E+00	6.59E+06	6.45E+06	0.00E+00
ApoE	VEQAVETEPEPELR	0	yes	2	2.02E-02	0.00E+00	0.00E+00	0.00E+00	0.00E+00	0.00E+00	0.00E+00	0.00E+00	0.00E+00	0.00E+00
ApoE	LGPLVEQGR	0	yes	2	2.08E-02	0.00E+00	0.00E+00	0.00E+00	0.00E+00	0.00E+00	0.00E+00	0.00E+00	0.00E+00	0.00E+00
ApoE	LAVYQAGAR	0	yes	2	2.75E-02	4.61E+06	0.00E+00	0.00E+00	0.00E+00	0.00E+00	0.00E+00	0.00E+00	0.00E+00	0.00E+00
CERU	VNKDDEEFIESNK*	1	yes	2,3	2.00E-122	6.21E+07	3.79E+07	0.00E+00	4.70E+07	0.00E+00	0.00E+00	4.45E+07	5.34E+07	0.00E+00
CERU	NNEGTYYSPNYNPQSR	0	yes	2	1.62E-61	2.42E+07	1.39E+07	4.02E+06	1.74E+07	6.17E+06	6.77E+06	2.46E+07	1.60E+07	2.19E+06

Protein name	Sequence	Missed cleavages	Unique (Groups)	Charge States	PEP	Raw Intensity								
						HAD 1	HAD 2	HAD 3	MNI 1	MNI 2	MNI 3	POS 1	POS 2	POS 3
CERU	ALYLQYTDETFR	0	yes	2	2.07E-36	1.45E+07	6.81E+07	2.73E+06	3.47E+07	4.07E+06	2.62E+06	3.38E+07	1.10E+07	0.00E+00
CERU	EYTDASFTNR	0	yes	2	3.12E-29	6.26E+07	4.66E+07	2.20E+07	5.28E+07	2.57E+07	4.17E+07	6.41E+07	5.22E+07	3.30E+06
CERU	GAYPLSIEPIGVR	0	yes	2	3.51E-26	5.08E+07	5.18E+07	9.49E+06	6.05E+07	1.09E+07	1.12E+07	6.92E+07	2.70E+07	1.50E+07
CERU	DDEEFIESNK	0	yes	2	4.86E-11	0.00E+00	0.00E+00	0.00E+00	0.00E+00	1.07E+06	0.00E+00	0.00E+00	0.00E+00	0.00E+00
CERU	QSEDSTFYLGER	0	yes	2	1.97E-05	4.25E+07	3.54E+07	1.59E+06	3.69E+07	2.01E+06	2.05E+06	4.05E+07	3.75E+07	8.92E+05
CERU	QYTDSTFR	0	yes	2	1.09E-02	2.47E+07	1.69E+07	1.36E+07	2.44E+07	1.69E+07	2.48E+07	2.24E+07	2.29E+07	0.00E+00
CERU	GEFYIGSK	0	yes	2	2.49E-02	2.01E+07	0.00E+00	0.00E+00	0.00E+00	0.00E+00	0.00E+00	0.00E+00	0.00E+00	0.00E+00
CERU	PVWLGFLGPIIK	0	yes	2	4.65E-02	0.00E+00	0.00E+00	0.00E+00	1.46E+06	0.00E+00	0.00E+00	0.00E+00	0.00E+00	0.00E+00
CLU	ASSIIDELFQDR	0	yes	2	2.65E-26	5.99E+06	2.16E+07	2.98E+06	1.48E+07	5.04E+06	2.64E+06	6.16E+06	3.43E+06	0.00E+00
CLU	LFDSDPITVTVPVEVSR	0	yes	2	8.44E-12	0.00E+00	1.48E+07	0.00E+00	8.71E+06	1.86E+06	0.00E+00	3.72E+06	0.00E+00	0.00E+00
CLU	EIQNAVNGVK	0	yes	2	2.00E-04	2.72E+06	0.00E+00	0.00E+00	4.74E+06	2.87E+06	2.85E+06	3.03E+06	2.96E+06	0.00E+00
CLU	IDSLLENDR	0	yes	2	1.81E-03	1.52E+07	1.08E+07	4.19E+06	1.95E+07	5.59E+06	7.77E+06	1.51E+07	1.07E+07	0.00E+00
CLU	TLLSNLEEAK	0	yes	2	6.13E-03	1.00E+07	8.72E+06	1.55E+06	0.00E+00	0.00E+00	0.00E+00	0.00E+00	0.00E+00	2.15E+06
C3	APSTWLTAYVVK	0	yes	2	0.00E+00	9.09E+06	6.82E+07	0.00E+00	3.12E+07	0.00E+00	0.00E+00	2.09E+07	2.35E+07	0.00E+00
C3	GVFVLNK	0	no	1,2	0.00E+00	2.39E+07	3.02E+07	7.54E+06	5.33E+07	1.23E+07	7.79E+06	3.46E+07	7.24E+07	0.00E+00
C3	VPVAVQGEDTVQSLTQGDGVAK	0	yes	2,3	1.02E-285	1.88E+07	1.06E+08	0.00E+00	1.06E+08	3.21E+07	0.00E+00	1.12E+08	4.64E+07	4.10E+07
C3	DYAGVFSDAGLTFTSSSGQQTAQR	0	yes	2,3	1.15E-145	1.62E+07	3.98E+07	4.85E+06	2.70E+07	6.73E+06	5.37E+06	1.97E+07	2.58E+07	2.86E+06
C3	AYYENSPQQVFSTEFEVK	0	yes	2	3.44E-94	0.00E+00	3.26E+07	7.74E+06	2.17E+07	1.33E+07	8.60E+06	1.58E+07	2.16E+07	1.01E+07
C3	SGSDEVQVGQQR	0	yes	2	2.07E-89	1.09E+07	1.06E+07	1.21E+07	1.92E+07	2.30E+07	1.92E+07	2.05E+07	2.35E+07	2.21E+06
C3	SNLDEDIIAEENIVSR	0	yes	2,3	5.71E-76	3.43E+07	1.10E+08	1.26E+07	8.53E+07	2.58E+07	3.13E+06	6.94E+07	6.50E+07	1.88E+07
C3	QELSEAEQATR	0	yes	2	3.98E-61	1.68E+07	1.50E+07	1.05E+07	2.22E+07	2.22E+07	1.90E+07	2.62E+07	2.93E+07	0.00E+00
C3	TIYTPGSTVLYR	0	no	2	2.06E-47	1.12E+08	1.54E+08	0.00E+00	1.66E+08	2.16E+07	1.34E+07	1.64E+08	1.87E+08	2.70E+07

Protein name	Sequence	Missed cleavages	Unique (Groups)	Charge States	PEP	Raw Intensity								
						HAD 1	HAD 2	HAD 3	MNI 1	MNI 2	MNI 3	POS 1	POS 2	POS 3
C3	EDIPPADLSDQVPDTESETR	0	yes	2	9.42E-36	4.16E+06	6.76E+06	2.65E+06	6.90E+06	7.88E+06	4.03E+06	5.46E+06	1.11E+07	5.35E+06
C3	IPIEDGSGEVVLSR	0	yes	2,3	1.39E-35	1.01E+08	1.18E+08	1.15E+07	1.56E+08	2.38E+07	1.21E+07	1.46E+08	1.72E+08	2.20E+07
C3	TGLQEVEVK	0	yes	2	1.22E-33	8.35E+07	8.54E+07	4.67E+07	1.21E+08	7.68E+07	7.88E+07	1.23E+08	1.41E+08	8.86E+06
C4A	PVAFSVVPTAAAAVSLK	0	yes	2,3	2.47E-50	1.85E+06	2.08E+07	2.09E+06	5.25E+06	2.66E+06	3.02E+06	4.99E+06	3.11E+06	1.46E+06
C4A	LQETSNWLLSQQQADGSFQDPCPVLDR*	0	yes	3	7.10E-08	0.00E+00	4.85E+06	0.00E+00	0.00E+00	0.00E+00	0.00E+00	0.00E+00	0.00E+00	0.00E+00
C4A	DSSTWLTAFVLK	0	yes	2	2.01E-02	0.00E+00	3.15E+06	0.00E+00	3.50E+06	2.62E+06	0.00E+00	3.66E+06	0.00E+00	0.00E+00
C4B	VLSLAQEQVGGSPEK	0	no	2	6.66E-175	6.75E+07	7.22E+07	1.50E+07	7.51E+07	4.78E+06	1.02E+07	6.58E+07	7.39E+07	0.00E+00
C4B	VTASDPLDTLGSEGALSPGGVASLLR	0	no	2,3	4.29E-106	1.72E+07	4.68E+07	7.58E+06	1.84E+07	4.58E+06	1.16E+07	9.88E+06	1.09E+07	9.75E+06
C4B	TTNIQGINLLFSSR	0	no	2	1.75E-60	2.78E+06	4.51E+07	6.00E+06	1.26E+07	5.29E+06	3.74E+06	8.64E+06	7.81E+06	1.30E+06
C4B	ALEILQEEDLIDEDDIPVR	0	no	2	1.31E-44	0.00E+00	0.00E+00	2.77E+06	0.00E+00	0.00E+00	0.00E+00	0.00E+00	6.79E+06	0.00E+00
C4B	QGSFQGGFR	0	no	2	2.49E-15	1.54E+07	1.16E+07	8.41E+06	1.89E+07	5.55E+06	9.53E+06	1.54E+07	1.61E+07	0.00E+00
C4B	DFALLSLQVPLK	0	no	2	2.64E-13	8.41E+06	2.19E+07	5.30E+06	1.10E+07	6.02E+06	2.12E+06	8.27E+06	4.31E+06	6.71E+05
C4B	VGDTLNLNLR	0	no	2	1.71E-11	0.00E+00	6.24E+07	0.00E+00	8.45E+07	5.08E+06	0.00E+00	4.76E+07	3.43E+07	4.53E+06
C4B	AEFQDALEK	0	no	2	3.09E-06	3.29E+07	3.10E+07	1.42E+07	3.99E+07	9.99E+06	1.62E+07	3.04E+07	3.79E+07	0.00E+00
C4B	PVQGVAYVR	0	no	2	3.35E-06	8.55E+06	1.03E+07	3.37E+06	2.02E+07	3.26E+06	2.94E+06	1.16E+07	1.35E+07	0.00E+00
C4B	GSSTWLTAFVLK	0	yes	2	5.90E-02	0.00E+00	0.00E+00	0.00E+00	0.00E+00	0.00E+00	0.00E+00	4.25E+06	0.00E+00	0.00E+00
CFH	LGYVTADGETSGSITCGK*	0	yes	2	1.66E-40	7.43E+06	1.25E+07	0.00E+00	1.29E+07	3.35E+06	1.69E+06	1.29E+07	1.13E+07	0.00E+00
CFH	AGEQVTYTCATYYK*	0	yes	2	1.33E-26	1.21E+07	2.34E+07	0.00E+00	2.19E+07	2.93E+06	1.12E+06	1.96E+07	2.33E+07	7.34E+05
CFH	VSVLCQENYLIQEGEEITCK*	0	yes	2,3	1.58E-15	2.83E+06	1.33E+07	2.97E+06	1.25E+07	3.05E+06	3.30E+06	9.27E+06	6.16E+06	1.29E+06

Protein name	Sequence	Missed cleavages	Unique (Groups)	Charge States	PEP	Raw Intensity								
						HAD 1	HAD 2	HAD 3	MNI 1	MNI 2	MNI 3	POS 1	POS 2	POS 3
CFH	AVYTCNEGYQLLGEINYR*	0	yes	2	1.49E-06	0.00E+00	1.02E+07	0.00E+00	3.54E+06	2.08E+06	0.00E+00	2.20E+06	2.79E+06	0.00E+00
CFH	SSIDIENGFISESQYTYALK	0	yes	2	1.94E-06	0.00E+00	2.80E+06	0.00E+00	2.88E+06	0.00E+00	0.00E+00	0.00E+00	1.16E+06	0.00E+00
CFH	LSYTCEGGFR*	0	yes	2	9.26E-05	2.20E+07	2.16E+07	0.00E+00	2.48E+07	4.80E+06	0.00E+00	2.34E+07	2.53E+07	2.10E+06
CFH	SSNLIILEEHLK*	0	yes	2,3	6.62E-04	0.00E+00	0.00E+00	0.00E+00	1.58E+07	0.00E+00	0.00E+00	1.65E+07	0.00E+00	0.00E+00
CFH	EQVQSCGPPPELLNGNVK*	0	yes	2	1.72E-03	8.15E+05	7.63E+05	0.00E+00	1.71E+06	0.00E+00	0.00E+00	1.20E+06	1.31E+06	0.00E+00
CFH	WSSPPQCEGLPCK*	0	yes	2	2.18E-03	4.04E+06	6.20E+06	0.00E+00	5.28E+06	0.00E+00	0.00E+00	5.00E+06	7.18E+06	0.00E+00
CFH	CFEGFGIDGPAIAK*	0	yes	2	3.20E-03	4.76E+06	8.66E+06	1.26E+06	2.54E+06	2.98E+06	3.77E+06	9.18E+06	1.56E+06	0.00E+00
CFH	IDVHLVPDR*	0	yes	2	3.64E-03	7.37E+06	8.93E+06	0.00E+00	8.12E+06	0.00E+00	0.00E+00	0.00E+00	0.00E+00	0.00E+00
CFH	NTEILTGSWSDQTYPEGTQAIYK	0	yes	2	4.23E-03	0.00E+00	0.00E+00	0.00E+00	1.76E+06	0.00E+00	0.00E+00	0.00E+00	0.00E+00	0.00E+00
CFH	DTSCVNPPTVQNAYIVSR*	0	yes	2	4.35E-03	0.00E+00	0.00E+00	0.00E+00	1.58E+06	0.00E+00	0.00E+00	0.00E+00	0.00E+00	0.00E+00
CFH	SCDNPYIPNGDYSPLR*	0	yes	2	5.50E-03	2.14E+06	0.00E+00	0.00E+00	2.37E+06	0.00E+00	0.00E+00	2.12E+06	0.00E+00	0.00E+00
CFH	KGEWVALNPLR*	1	yes	3	5.63E-03	0.00E+00	6.66E+06	0.00E+00	0.00E+00	0.00E+00	0.00E+00	0.00E+00	0.00E+00	0.00E+00
GSN	TPSAAYLWVGTGASEAEK	0	yes	2	4.20E-16	0.00E+00	5.43E+06	0.00E+00	5.78E+06	0.00E+00	0.00E+00	5.17E+06	0.00E+00	0.00E+00
GSN	QTQVSVLPEGGETPLFK	0	yes	2	3.62E-08	2.62E+06	6.26E+06	0.00E+00	8.74E+06	2.76E+06	1.48E+06	6.08E+06	1.96E+06	1.99E+06
GSN	EVQGFESATFLGYFK	0	yes	2	7.65E-07	1.50E+06	5.17E+06	0.00E+00	4.19E+06	1.64E+06	0.00E+00	3.03E+06	9.55E+05	0.00E+00
GSN	AQPVQVAEGSEPDGFWEALGGK	0	yes	2	1.78E-06	0.00E+00	1.88E+06	0.00E+00	1.87E+06	0.00E+00	0.00E+00	0.00E+00	0.00E+00	0.00E+00
GSN	AGALNSNDAFVLK	0	yes	2	4.08E-04	0.00E+00	1.11E+07	0.00E+00	1.35E+07	0.00E+00	0.00E+00	1.23E+07	7.21E+06	0.00E+00
GSN	PALPAGTEDTAK	0	yes	2	7.97E-03	0.00E+00	1.03E+06	0.00E+00	3.18E+06	0.00E+00	0.00E+00	3.45E+06	0.00E+00	0.00E+00

Protein name	Sequence	Missed cleavages	Unique (Groups)	Charge States	PEP	Raw Intensity								
						HAD 1	HAD 2	HAD 3	MNI 1	MNI 2	MNI 3	POS 1	POS 2	POS 3
GSN	EPGLQIWR	0	yes	2	3.76E-02	0.00E+00	0.00E+00	0.00E+00	4.82E+06	0.00E+00	0.00E+00	0.00E+00	0.00E+00	0.00E+00
SAP	IVLGQEQDSYGGK	0	yes	2	6.40E-04	0.00E+00	9.38E+06	0.00E+00	7.40E+06	0.00E+00	0.00E+00	0.00E+00	8.68E+06	0.00E+00
SAP	AYSLFSYNTQGR	0	yes	2	1.12E-03	7.95E+06	1.02E+07	0.00E+00	0.00E+00	0.00E+00	0.00E+00	3.48E+06	9.08E+06	0.00E+00
SAP	QGYFVEAQPK	0	yes	2	5.26E-03	8.02E+06	6.10E+06	0.00E+00	5.57E+06	0.00E+00	0.00E+00	2.09E+06	0.00E+00	0.00E+00
SAP	VGEYSLYIGR	0	yes	2	5.26E-03	0.00E+00	0.00E+00	0.00E+00	6.48E+06	0.00E+00	0.00E+00	0.00E+00	4.80E+06	0.00E+00
SAP	DNELLVYK	0	yes	2	1.01E-02	4.69E+06	0.00E+00	0.00E+00	4.09E+06	0.00E+00	0.00E+00	2.25E+06	2.61E+06	0.00E+00

*: Does not adhere to selection criteria

PEP: Posterior Error Probability

3.4. Conclusion

As a means to identify precursor ions suitable for PRM analysis of our candidate biomarkers, discovery proteomic analysis of pooled patient samples yielded an acceptable number of protein identifications, considering the low degree of abundant protein depletion. Analysis successfully identified all candidate biomarker proteins, with varying degrees of peptide coverage. Peptide identifications provided an adequate number of prospective target peptides for almost all candidate biomarkers. Peptides unique to a protein group were selected based on suitability for downstream screening by PRM analysis, and a final set of 106 peptides were chosen for validation by PRM analysis. Screening by PRM analysis would also serve to exclude false hits, regardless of assessment of quality based on discovery proteomic data analysis. The best peptides from this validation can then be used to construct a PRM assay for high throughput analysis of patient serum samples.

Chapter 4
Optimisation B: Optimisation of Instrument Parameters for Parallel Reaction Monitoring Assays

4.1. Introduction

PRM is a targeted mass spectrometric method, that when applied to a Q Exactive quadrupole-Orbitrap mass spectrometer, possesses several advantages over classical SRM assays conducted on triple quadrupole instruments.[130] Both methods entail selection of precursors by the first quadrupole, however, PRM involves high resolution detection of all fragment ions in the Orbitrap detector; while SRM assays entail selection and detection of predefined fragment ions.[125,126,130] The high resolution capability, coupled with the ability to detect all possible fragments, make PRM analysis well suited to high throughput, high resolution targeted analysis.[130]

Previously developed PRM assay parameters have been outlined in the literature, which include suggested ion injection times, AGC target values, and isolation list sizes at various resolution settings.[132,182] Multiplexing considerations such as injection time and isolation list modification have also been outlined.[132] These settings however require verification to ensure their validity, as well as to gain a more practical understanding of PRMs.

This Chapter is thus concerned with determination of optimal mass spectrometer parameters for proteomic PRM assays using our Q Exactive mass spectrometer. Analysis in duplex mode (i.e.: two peptides analysed simultaneously), at a resolution of 35 000, and requisite cycle time of 2 seconds, has been reported to allow a maximum 32 peptides to be measured.[132] In the present study an isolation list of 36 precursors would be analysed with an average of 3 peptides per protein, and a list of 12 proteins – with consideration for at least 5 internal reference peptides. Factoring in retention time scheduling should theoretically improve quantitation.[138] A resolution of 35 000 resolution was therefore selected for optimisation.

In order to further optimise instrument parameters for PRMs, a laboratory reference sample – for which LC and data-dependent acquisition parameters had already been established –

was initially utilised. The reference sample consists of a tryptic digest of total protein extracted from SHSY-5Y neuroblastoma cells, processed according to a modified filter-aided sample preparation (FASP) protocol.[183] Peptides detected in this sample were used as surrogates for determination of optimal instrument parameters for further PRM analyses.

4.2. Materials and Methods

4.2.1. Identification of Reference Sample Peptides for Method Development

Data files from 11 LC-MS/MS analyses were interrogated to identify proteins present in the sample. Discovery proteomic analysis was performed as outlined in Section 3.2.2, with 50 ng of reference sample loaded onto the LC column. Three samples were chromatographically separated using an 85 minute gradient (*vide infra*), while the remaining eight were separated on a 45 minute gradient (*vide infra*). The former was run on the Dionex UltiMate 3500 RSLC nano-LC instrument equipped with a nanoscale analytical column, packed in-house with Luna C18 coated silica beads (75 µm x 50 cm). The gradient comprised a constant flow rate of 300 nl/min over a linear gradient: 2% B for 10 minutes, 2-35% B over 23 minutes, 35-50% B over 5 minutes, 50-80% B over 5 minutes, held at 80% B for 20 minutes, before returning to 2% B in 2 minutes, followed by re-equilibration at 2% B for 20 minutes. The latter was run on a Proxeon Easy nLC (Thermo Scientific) instrument equipped with a nanoscale analytical column, packed in-house with Luna C18 coated silica beads (75 µm x 20 cm). The gradient comprised a constant flow rate of 300 nl/min: 5-35% B over 30 minutes, 35-80% B over 5 minutes, and held at 80% B for 10 minutes. Equilibration at 5% B is conducted pre-run. Data analysis was performed as described in Section 3.2.3.

4.2.2. Parameter Optimisation

4.2.2.1. Baseline Settings

ISOLATION LIST CONSTRUCTION

Skyline (v3.1) – an open source targeted proteomic software tool – was used to prepare methods and to visualise PRM data.[133] It was also subsequently used to process and export data for statistical analysis (Chapter 7).

The software settings used here for analysis of instrument parameter optimisation data were used throughout the present study for all other PRM analyses, as these settings correspond to characteristics of the target peptides used throughout the study. Trypsin was chosen as the enzyme, with one accepted missed cleavage. The UniProt complete human proteome .fasta file (downloaded on 9/01/2014) was used to construct the background proteome. The minimum and maximum allowed peptide lengths were set to 6 and 25 amino acids respectively, while no N-terminal amino acids were excluded. Cysteine, methionine and histidine residues were permitted in peptide sequences. Peptides possessing consensus glycosylation sites (NXT/NXS) were excluded since glycosylated peptides are not easily identified or consistently quantifiable.[184] Proline residues flanking cleavage sites (KP/RP) were also excluded due to their inhibition of tryptic cleavage.[185] Carbamidomethyl cysteine (57m/z) was defined as the only fixed structural modification (www.unimod.org). The default monoisotopic precursor ion charges states were set to 3 and 2, while the product ion (b and y) charge states were set to 1. The mass range was adjusted to reflect Q Exactive instrument capabilities, with a minimum and maximum m/z of 50 and 3000 respectively. Remaining settings were retained as default.

The aforementioned settings may be used at any level of PRM analysis, with the option to disregard them by manually adding or removing precursor or product ions. The Full Scan settings are the most influential in PRM analyses, and required adjustment when exporting and importing isolation lists and data respectively. When exporting isolation lists, the precursor isotope peaks were set to 'Count', with one peak chosen. The Orbitrap was chosen as the MS^1 mass analyser with resolution set to 35 000 at 200m/z. The Targeted MS^2 acquisition method was chosen with the Orbitrap mass analyser resolution also set to 35 000 at 200m/z. When importing data files into Skyline, the precursor mass analyser was set to quadrupole ion trap (QIT) with a resolution of 1m/z (the closest match to the Q Exactive quadrupole mass filter).

Once Skyline settings were adjusted, reference peptides selected from data-dependent analysis (Section 4.3.1) were imported into Skyline by manual sequence entry. The unscheduled isolation list (Table 4.1) was then exported as a .csv file for import into Xcalibur. Empty columns are intentional, as this is the format required by Xcalibur for isolation list import and applies to all isolation lists used hereafter.

TABLE 4.1: ISOLATION LIST FOR UNSCHEDULED PRM ANALYSIS OF REFERENCE SAMPLE PEPTIDES.

Mass [m/z]	Formula [M]	Species	CS [z]	Polarity	Start [min]	End [min]	NCE	Comment
1081.991			2	Positive			27	AENNSEVGASGYGVPGPTWDR (light)
1243.065			2	Positive			27	KAAAPAPEEEMDEC[+57.0]EQ ALAAEPK (light)
1280.628			2	Positive			27	LVQDVANNTNEEAGDGTTTAT VLAR (light)
786.9458			2	Positive			27	TLTDELAALQITGVK (light)
956.4396			2	Positive			27	VDSAATSGYEIGNPPDYR (light)
1189.087			2	Positive			27	QVQSLTC[+57.0]EVDALKGTNE SLER (light)
1257.525			2	Positive			27	NADMSEEMQQDSVEC[+57.0] ATQALEK (light)
652.3099			2	Positive			27	SPEEVDKESQR (light)
1058.994			2	Positive			27	DQQEAALVDMVNDGVEDLR (light)
754.3823			2	Positive			27	VIQC[+57.0]FAETGQVQK (light)
1147.574			2	Positive			27	EAFLNTEDKGDSLDSVEALIK (light)
1179.546			2	Positive			27	MQEAMTQEVSDVFSDTTTPIK (light)
607.3142			2	Positive			27	DSPSVWAAVPGK (light)
931.4423			2	Positive			27	SPSDSSTASTPVAEQIER (light)
922.9493			2	Positive			27	EAFSLFDKDGDGTITTK (light)
980.966			2	Positive			27	DATNVGDEGGFAPNILENK (light)
1246.059			2	Positive			27	LC[+57.0]SLLDSEDYNTC[+57.0]EGAFGALQK (light)
640.3192			2	Positive			27	SVNSSTMVAQQK (light)
448.7366			2	Positive			27	ALTTMGFR (light)
648.807			2	Positive			27	GGELVYTDSEAR (light)

CS: Charge State, NCE: Normalised Collision Energy.
* Isolation list columns left blank intentionally, as this is the required format from Xcalibur.

INSTRUMENT PARAMETERS

In order to develop PRM assays for specific peptides, baseline instrument parameters had to be established. Several publications provided a general outline of the PRM assay parameters applicable to the Q Exactive mass spectrometer.[131,132,182] The major parameters involved in PRM methods – referred to in the software as Targeted MS2 (tMS2) – are: Lock Mass, Chromatographic Peak Width, Resolution, AGC Target, Max Injection Time (Max IT), Multiplex Level (MSX), Isolation Window, and NCE.

Baseline settings (some of which are evident in Table 4.2) were obtained from Schroeder et al.[182] The lock mass function instructs the instrument to begin scanning at a predefined m/z value. Lock masses were set to 'off' during PRM analysis as the start of each scan is instead determined by the inclusion list. Chromatographic peak width was set to 15 s, this being the average width of peaks on the LC gradient in our laboratory. The charge state for each precursor is indicated in the isolation list. A resolution setting of 35 000 (at 200m/z) was chosen. The AGC target limits the amount of ions allowed to enter the Orbitrap – by varying ITs – to avoid space charging effects which adversely affect detection.[186] The highest setting was selected to prevent inconsistent ITs, which could impact quantitation. Max IT is the amount of time that the instrument spends collecting each precursor in the collision cell for subsequent Orbitrap analysis. Higher ITs result in greater sensitivity since more ions are injected into the detector.

MSX indicates the number of precursors that are analysed together after fragmentation in the collision cell. It was not clear from the literature however, whether increasing MSX requires a concomitant reduction of Max IT, assuming IT is assigned to each precursor when multiplexing, and was therefore established experimentally. Isolation Window indicates the 'margin of error' allowed by the quadrupole when selecting precursor masses. A wider window increases the number of different precursor ions that enter the Orbitrap, including isotopes, but also permitting entry of untargeted peptides. An isolation width of 2m/z was therefore used as this permitted relatively high selectivity of the quadrupole, without significantly sacrificing signal intensity, since signal intensity has been found to be comparable when using either a 2 or 4m/z isolation window.[132] The NCE value influences collision energy based on the mass of the precursor. Essentially, increasing the NCE will increase the effective collision energy to a varying extent for precursors of different masses. The Skyline default NCE of 27 was used.

TABLE 4.2: TABLE OF BASE SETTINGS FOR PRM ANALYSIS.

Lock masses	Off
Chrom. peak width	15 s
Charge state	2
Resolution	35000
AGC Target	5.00E+06

Max IT	110 ms
MSX	1
ISO Window	2 m/z
NCE	27

AGC: Automatic Gain Control, MSX: Multiplex level, ISO: Isolation, NCE: Normalised Collision Energy, Max IT: Maximum Injection time.

4.2.2.2. LC/MS Instrumentation and Parameters

Parallel reaction monitoring analysis was performed on the Q Exactive, coupled to the Dionex UltiMate 3500 RSLC nano-LC system. Approximately 100 ng of reference sample was loaded onto the reversed phase chromatography column as outlined in Section 3.2.2. Samples were eluted with an 85 minute gradient as described in Section 4.2.1. A Targeted MS^2 method was constructed starting with the baseline instrument settings as outlined in Table 4.2, using the .csv file in Table 4.1 as an inclusion list. Xcalibur instrument settings were then varied between optimisation steps, with remaining LC/MS parameters remaining constant unless otherwise stated.

4.2.2.3. Injection Time Optimisation

Correct IT is integral to an efficient PRM experiment. A short IT compromises sensitivity by unnecessarily limiting the number of ions entering the mass analyser.[187] On the other hand, excessively long ITs extend cycle time (time taken to cycle though the target list), impeding quantitation by limiting the number of sampling points on the chromatogram.[134] It stands to reason that this may also cause the Orbitrap to idle between injections, if the injection time is too long, thereby wasting analysis time. Ideally, IT should be balanced with the scanning time of the Orbitrap, ensuring minimal time is wasted between scan cycles.

A transient is the time domain signal of an oscillating molecule detected over time, which is converted by Fourier Transform into a mass spectrum in the frequency domain.[113,188] Higher resolution is correlated with higher transient measurement times.[188] Schroeder et al.[148] maintain that IT should not exceed the theoretical transient time of the Orbitrap detector, and provide suggested ITs for each resolution setting (Table 4.3). Gallien et al.[132] predict that the IT should be calculated by dividing the transient time by MSX, therefore assigning an IT of 128 ms at a resolution of 35 000 in single-plex mode. However, they do not adhere to this claim as

their instrument parameters reflect an IT of 120 ms under the previously mentioned conditions.

TABLE 4.3: TABLE OF ORBITRAP SCAN TIME PARAMETERS BASED ON RESOLUTION SETTING. ADAPTED FROM SCHROEDER ET AL.[148]

Resolution at m/z 200	Scan speed (Hz)	Transient length (ms)	*Suggested Max Fill Time (ms)*
17 500	13	64	*50*
35 000	7	128	*110*
70 000	3	256	*240*
140 000	1.5	512	*500*

Determination of optimal injection time was performed due to the lack of consensus on this baseline parameter, as incorrect IT may adversely affect sensitivity and quantitation (*vide supra*). The following experiments served to ascertain the optimal injection time necessary to maximise sensitivity whilst maintaining sufficiently high quantitative ability.

SCAN EVENT ANALYSIS

In order to assess the effect of alterations in IT, scan events were examined in each .RAW file. The total MS^2 chromatogram was set to show scan events as vertical lines (or 'sticks'), each labelled with scan number and retention time (Figure 4.1). The time between scan events indicates scan time and was used to compare different IT settings. Changes in scan time may indicate injection time causing varying delays between successive scans. According to our current knowledge, the application of this method of scan time evaluation to PRM analysis is novel.

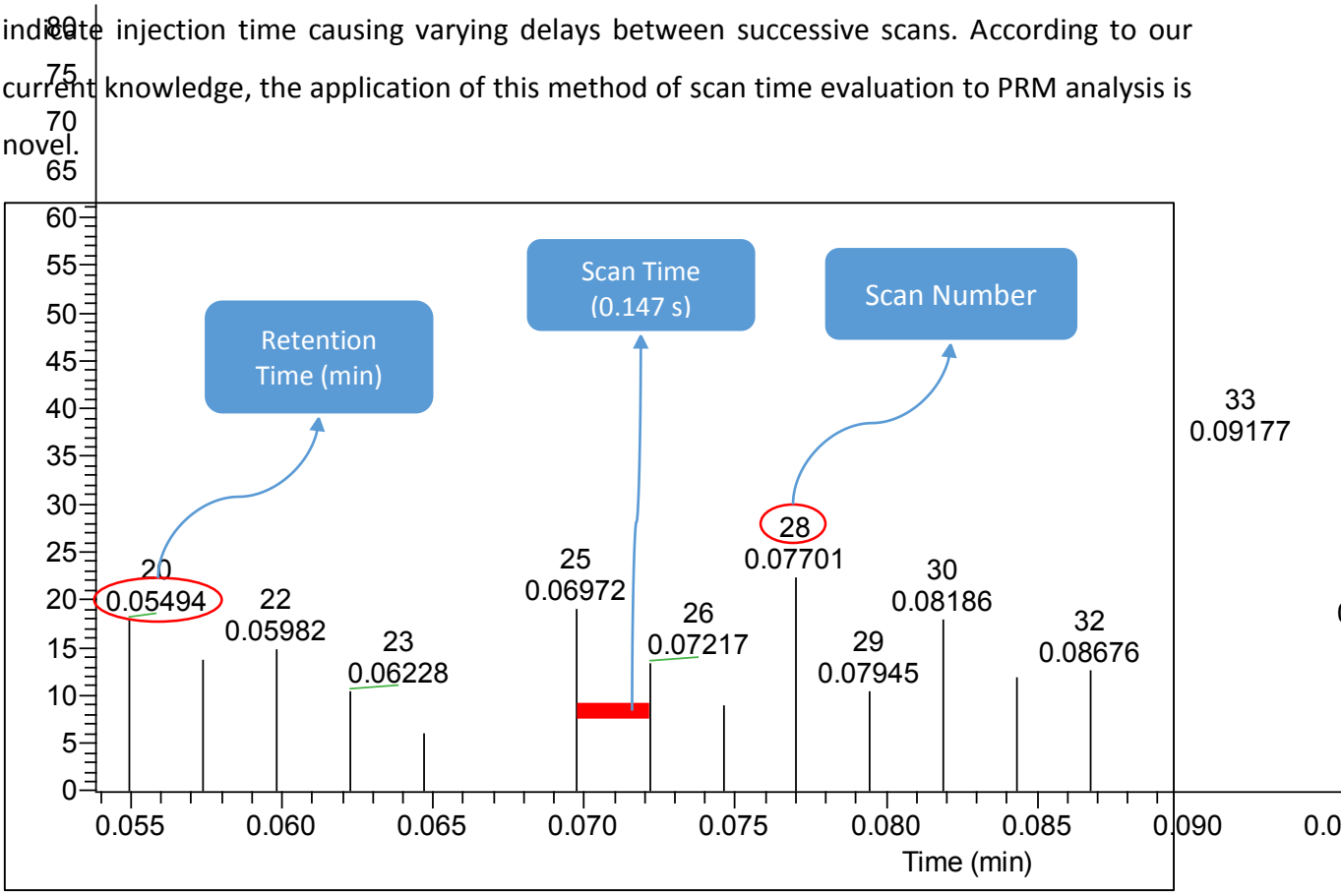

FIGURE 4.1: EXAMPLE OF A SCAN DIAGRAM OUTLINING SCAN PARAMETERS. SCAN TIME (IN SECONDS) IS CALCULATED BY MULTIPLYING THE TIME BETWEEN SCANS (IN MINUTES) BY 60

For all applicable optimisation steps, scans were taken from random retention time points on the chromatogram and average scan time calculated.

ESTABLISHING THE RELATIONSHIP BETWEEN MSX AND INJECTION TIME

It was initially unclear whether increasing MSX required a concomitant reduction of Max IT. It was hypothesised that Max IT was assigned to each precursor independently when multiplexing. To test this hypothesis, all settings (Table 4.2) were kept constant while MSX was varied. For each consecutive analysis, MSX was varied from 1 to 4 inclusive.

ASSESSMENT OF SUGGESTED INJECTION TIME SETTINGS

In order to assess the effect of increasing multiplexing degree on scan times, MSX levels as well as Max IT settings were varied concomitantly (other baseline settings remained constant as in Table 4.2). Multiplex levels were set to 1, 2, and 3; while Max IT was set to 110, 55 and 36 ms respectively (i.e. Max IT at single-plex was divided by MSX level).

DETERMINATION OF OPTIMUM INJECTION TIME

To test the optimal IT (110 ms) suggested by Schroeder et al.[182], and establish the highest permissible IT that would permit *only* the Orbitrap scanning time to influence overall scan time, overall scan time solely dependent on Orbitrap scanning time was established. A short IT and associated delays does not influence total scan time. ITs of 50 ms and 100 ms respectively were evaluated at 35 000 resolution in single-plex mode, with all other settings kept constant (Table 4.2). These ITs were chosen for their proximity to and position below the suggested value.

VALIDATION OF INJECTION TIMES AT OTHER MULTIPLEX LEVELS

The optimal IT for single-plex PRM analysis was confirmed to be 100 ms. This information, together with Equation 1 (p. 54), was used to predict the IT settings for higher multiplex levels, which were then validated for single- and duplex assays, confirming the predictive ability of Equation 1 when optimum single-plex IT is known. ITs of 45 ms and 27 ms were used at MSX levels of 2 and 3 respectively, with all other settings kept constant (Table 4.2).

4.2.2.4. Multiplexing Considerations

Multiplexing in PRM facilitates analysis of multiple precursors in a single scan, significantly increasing the number of peptides that can be measured in a single assay. It also increases the number of sampling scans over the chromatographic peak by shortening the time taken for the mass spectrometer to cycle through the isolation list. One drawback to multiplexing lies in the reduction in IT afforded to each precursor. Data files from the 100 ms single-plex and 45 ms duplex evaluations were used to assess these aspects by comparing peptide VDSAATSGYEIGNPPDYR (Table 4.4) in the two MSX modes. Isolation lists were identical in both analyses. Data were visualised in Skyline, and the chromatogram was reconstructed in Excel to visualise the points on the curve. Data were copied from Skyline, consisting of each data point used to generate the chromatogram, and were pasted into Microsoft Excel. The data

points were used to construct a line graph with multiple markers, each representing an individual scan.

4.3. Results and Discussion

4.3.1. Identification of Reference Sample Peptides for Method Development

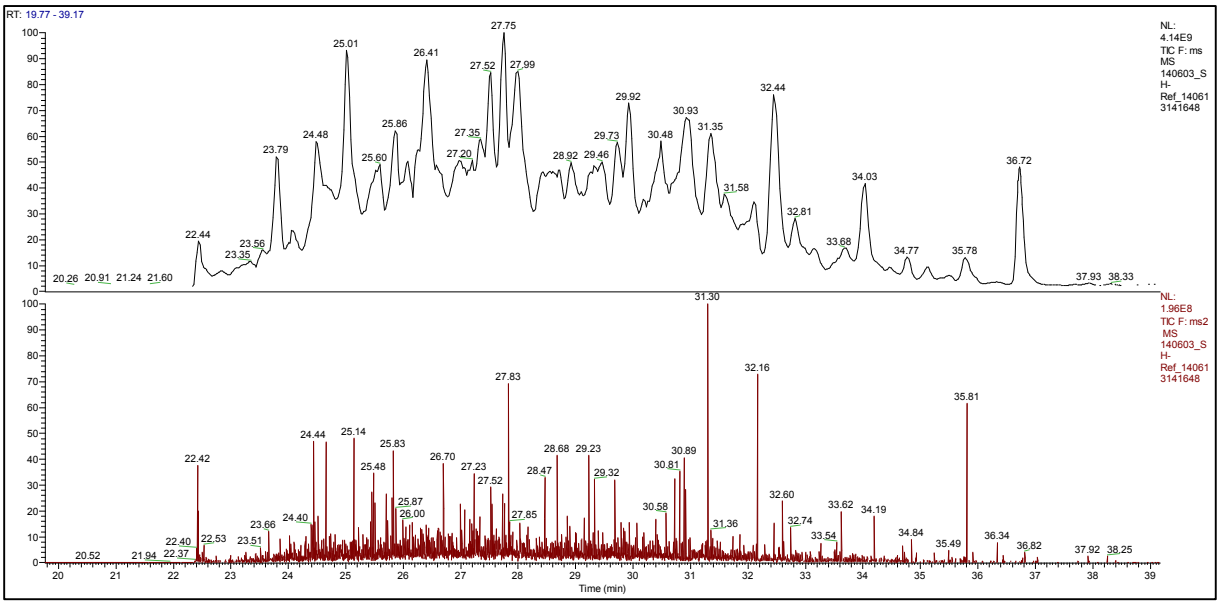

FIGURE 4.2: REPRESENTATIVE MASS SPECTROMETRIC CHROMATOGRAM OF A SINGLE REFERENCE SAMPLE. UPPER PANEL: MS^1 ION CHROMATOGRAM; LOWER PANEL: MS^2 ION CHROMATOGRAM

Following MaxQuant analysis of ideal reference LC-MS/MS data files (Figure 4.2), the output was interrogated to identify ideal peptides for instrument optimisation. The number of protein groups identified, including contaminants and reverse hits, totalled 2499 across 11 data files (Data not shown). Excluding contaminants and reverse hits reduced the total to 2451 protein groups. Of 73643 identified peptides, 20 were selected for instrument method development (Table 4.4). Peptides with good PEP scores were preferred and were randomly selected, with three relatively low-scoring peptides included to avoid bias. Peptides with variable modifications such as oxidation and N-terminal acetylation were excluded, as they may not be reliably detected at high abundance. Additionally, detection of these variants were not necessary for the purposes of instrument optimisation. Peptides containing cysteine and methionine residues, as well as missed cleavages were allowed.

TABLE 4.4: TABLE OF CHOSEN PEPTIDES FOR INSTRUMENT METHOD DEVELOPMENT.

Sequence	Protein Names	PEP
AENNSEVGASGYGVPGPTWDR	ATP-dependent RNA helicase A	0
KAAAPAPEEEMDECEQALAAEPK	Elongation factor 1-gamma	0
LVQDVANNTNEEAGDGTTTATVLAR	60 kDa heat shock protein, mitochondrial	0
TLTDELAALQITGVK	Estradiol 17-beta-dehydrogenase 11	0
VDSAATSGYEIGNPPDYR	Low molecular weight phosphotyrosine protein phosphatase	2.62E-291
QVQSLTCEVDALKGTNESLER	Vimentin	2.37E-279
NADMSEEMQQDSVECATQALEK	Dynein light chain 1, cytoplasmic	7.00E-256
SPEEVDKESQR	Nestin	5.68E-249
DQQEAALVDMVNDGVEDLR	Glutathione S-transferase P	2.50E-150
VIQCFAETGQVQK	Clathrin heavy chain 1	2.61E-144
EAFLNTEDKGDSLDSVEALIK	Spectrin alpha chain, brain	9.45E-144
MQEAMTQEVSDVFSDTTTPIK	Vinculin	2.25E-143
DSPSVWAAVPGK	Profilin-1	1.93E-141
SPSDSSTASTPVAEQIER	Drebrin	1.84E-140
EAFSLFDKDGDGTITTK	Calmodulin	2.11E-139
DATNVGDEGGFAPNILENK	Alpha-enolase	2.08E-133
LCSLLDSEDYNTCEGAFGALQK	Transportin-1	2.89E-96
SVNSSTMVAQQK	Septin-7	0.003154
ALTTMGFR	Sorcin	0.003363
GGELVYTDSEAR	Plectin	0.10254

PEP: Posterior Error Probability

4.3.2. Parameter Optimisation

4.3.2.1. Injection Time Optimisation

ESTABLISHING THE RELATIONSHIP BETWEEN MSX AND INJECTION TIME

IT was kept constant at 110 ms, while MSX level was varied. Samples of scan diagrams (Figure 4.3) show the scan time changes associated with an increase in MSX.

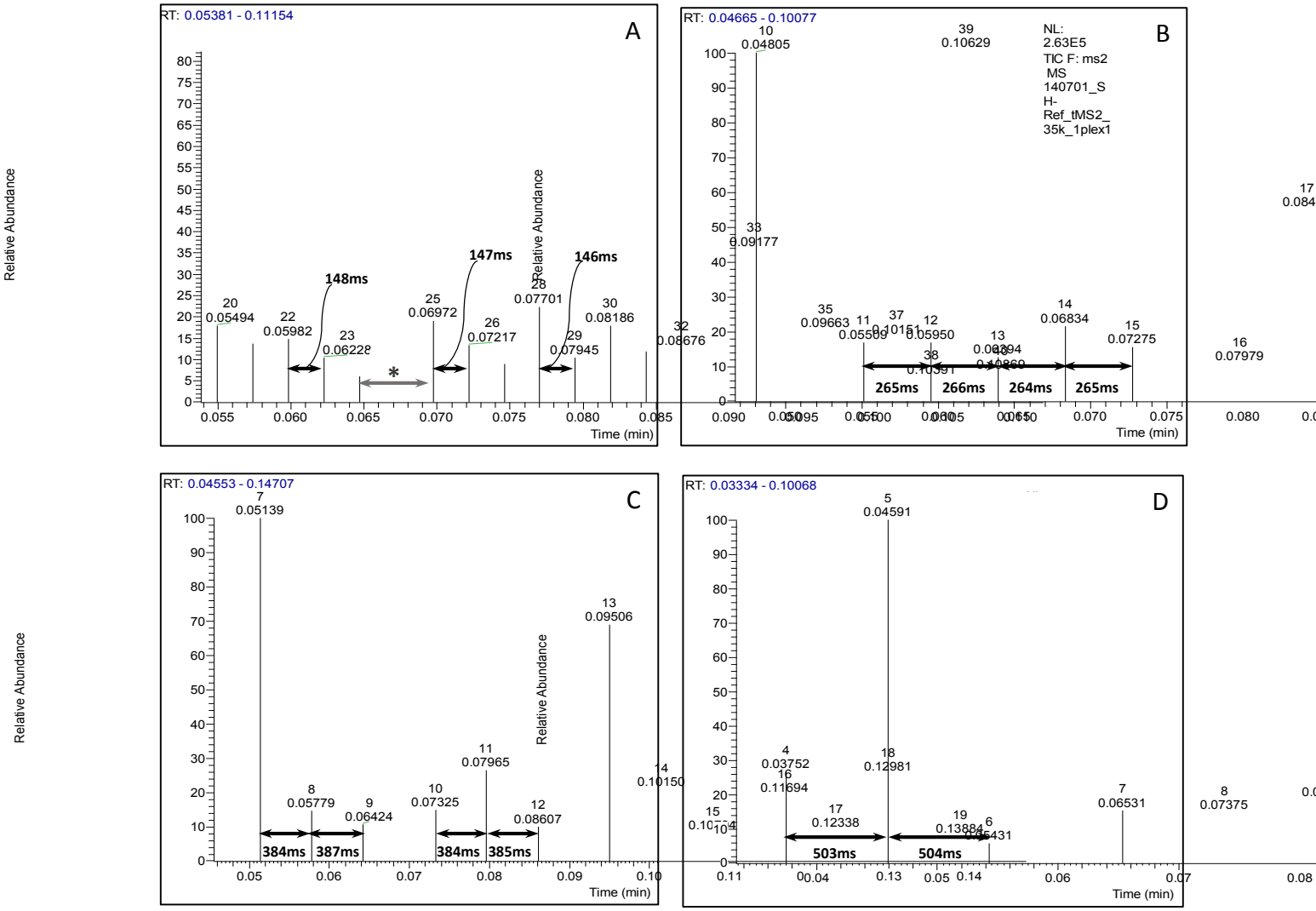

FIGURE 4.3: SCAN DIAGRAMS SHOWING SCAN TIMES WITH INCREASING MSX LEVEL. A: MSX=1, B: MSX=2, C: MSX=3, D: MSX=4. IMAGE NOT TO SCALE, *: AGC PRESCAN

Summarised in Table 4.5 are the scan time changes associated with changes in degree of MSX. The significant scan time increase of 120 ms, as degree of multiplexing increases, indicates that the Max IT value is indeed assigned to each precursor when multiplexing. Therefore, when multiplexing, the IT used during single-plex analysis needs to be adjusted based on the level of multiplexing. For example, a duplex assay would have a Max IT of 55 ms when the

single-plex Max IT is 110 ms. This relationship between IT and MSX was unclear at the outset of PRM analysis, although it had previously been inferred by Gallien et al.[132] It should be noted, for all subsequent scan diagrams, that a scan approximately twice as long as an average scan is periodically observed (*: Figure 4.3). We hypothesised that this additional scan was the AGC prescan, and it is excluded from our calculations as it is a built-in mass spectrometer function.

TABLE 4.5: SUMMARY OF SCAN TIME CHANGES ASSOCIATED WITH CHANGE IN MSX

Parameters			Scan Times		
Resolution	Max IT	MSX	Transient Time	Ave. Scan Time	Δ Scan Time
35 000	110 ms	1	128 ms	145	120
		2		265	120
		3		385	120
		4		505	

This experiment also revealed an unexpected additional change in scan time between consecutive multiplex levels was identified. It would be reasonable to assume that the overall scan time should increase by multiples of the Max IT value. This is clearly not the case however, as the observed change in scan time was calculated to be approximately 120 ms rather than 110 ms (Table 4.5). It would appear that there is an additional 10 ms scan delay – in addition to the expected 110 ms – associated with each increase in multiplex level.

The average scanning time of the Orbitrap at 35 000 resolution was measured at approximately 145 ms (single-plex). Calculating the inverse of scan speed (Hz or cycles/second) results in overall scan time (seconds/cycle) as shown in Table 4.6.[182] The measured scan time very nearly agrees with the predicted overall scan time. However, optimal IT has yet to be determined. An IT that results in a total scan time equal to or lower than the predicted scan time in Table 4.6 would be deemed optimal.

TABLE 4.6: TABLE SHOWING OVERALL SCAN TIME. ADAPTED FROM SCHROEDER ET AL.[148]

Resolution at m/z 200	Scan speed (Hz)	Transient length (ms)	**Scan time (1/scan speed, ms)**
17 500	13	64	**77**
35 000	7	128	**143**
70 000	3	256	**333**

140 000	1.5	512	**667**

ASSESSMENT OF SUGGESTED INJECTION TIME SETTINGS

Having established that Max IT requires adjustment when increasing MSX level, MSX level was therefore increased, while Max IT was adjusted for each level by dividing the single-plex Max IT by its respective MSX level. Scan times were measured for each set of conditions (Figure 4.4).

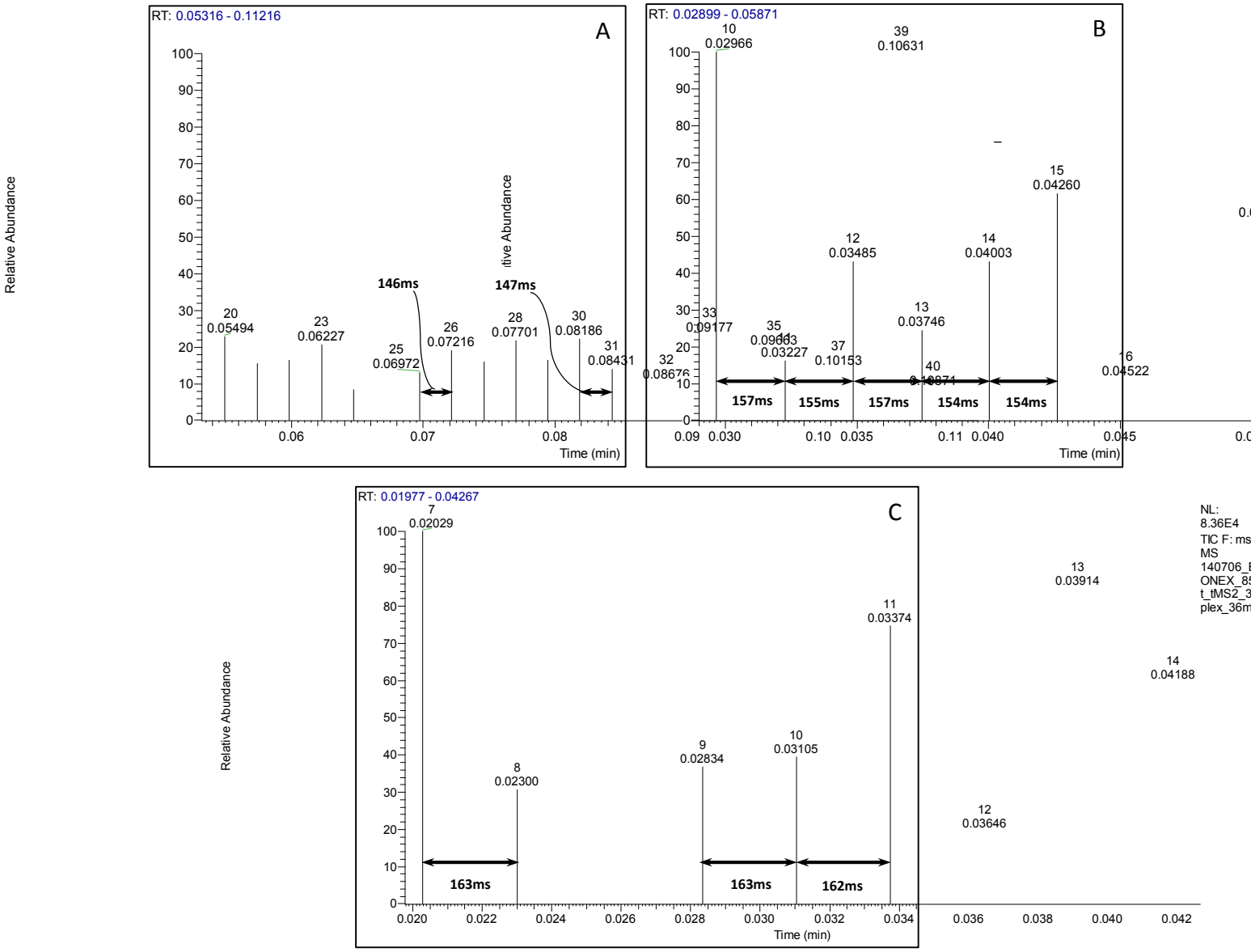

FIGURE 4.4: SCAN DIAGRAMS SHOWING SCAN TIMES WITH CONCOMITANTLY ADJUSTED MSX AND MAX IT. A: SINGLE-PLEX & 110MS, B: DUPLEX & 55MS, C: TRIPLEX AND 36MS. IMAGE NOT TO SCALE

Decreasing Max IT proportionately with increasing MSX was predicted to result in a constant overall scan time. However, with an increase in MSX, an *increase* in overall scan time was

unexpectedly observed (Table 4.7). This can be interpreted as IT-related delays between successive scans, an additional 10 ms delay being observed with each increase in MSX. This observation is contrary to the assertion by Gallien et al.[132] that the Max IT for higher MSX levels simply equates to the transient time divided by MSX.

TABLE 4.7: SUMMARY OF SCAN TIMES ASSOCIATED WITH CONCOMITANT CHANGES IN MSX AND MAX IT

Parameters			Scan Times			
Resolution	Max IT	MSX	Transient Time	Ave. Scan Time	Δ Scan Time	
35 000	110 ms	1	128 ms	145	10	
	55 ms	2		155		8
	36 ms	3		163		

With increasing MSX, there are no additional Orbitrap scans since all multiplexed ions are scanned simultaneously.[132] It can therefore be assumed that the 10 ms delay is independent of Orbitrap scanning and is an artefact of additional injections. A portion of this delay could be attributed to the 6 ms it takes for the quadrupole to switch to the next mass in the isolation list.[187] With the absence of definitive reasoning for this additional delay in the literature, considerations for future assessment is recommended.

If the scan delay is related to ion injection and fragmentation, it is likely that the delay also applies to the IT in single-plex mode. The actual IT (effective IT) for a Max IT setting of 110 ms in single-plex mode would therefore be 120 ms. The effective IT values for MSX greater than one must equal the effective IT at single-plex.

It is apparent that simply dividing the single-plex IT by MSX is not sufficient to eliminate additional scan delays between multiplex levels; this additional delay needs to be taken into account for each level of multiplexing.

In order to maintain a constant effective IT at each multiplex level that is equal to the effective IT at single-plex, the Max IT would need to be adjusted for each MSX level based on the effective IT at single-plex, cumulative delay, and multiplex level. A general equation can be expressed as:

EQUATION 1: EQUATION TO CALCULATE INJECTION TIME SETTINGS FOR A GIVEN MULTIPLEX LEVEL

$$Max\ IT = \frac{\left((Effective\ IT\ @\ single\ plex) - (10ms\ \times multiplex\ level)\right)}{multiplex\ level}$$

Table 4.8 illustrates application of Equation 1 to predict IT values for higher MSX based on an effective single-plex IT of 120 ms

TABLE 4.8: TABLE OF ADJUSTED IT VALUES BASED ON MULTIPLEX LEVEL AND ADDITIONAL DELAY

MSX	Effective IT	Adjustment	Adjusted Max IT
1	120 ms	N/A	110 ms
2	120 ms*	(120-20)/2	50 ms
3	120 ms*	(120-30)/3	30 ms

*Effective IT of single-plex injection is the target of the adjustment

These assumptions only hold assuming the single-plex IT of 110 ms is optimal, which can be easily verified.

DETERMINATION OF OPTIMAL INJECTION TIME

To establish the total scan time when Orbitrap scanning time was the limiting factor, a significantly shorter IT was evaluated, as well as one 10 ms lower than that suggested by Schroeder *et al.*[182] (Figure 4.5).

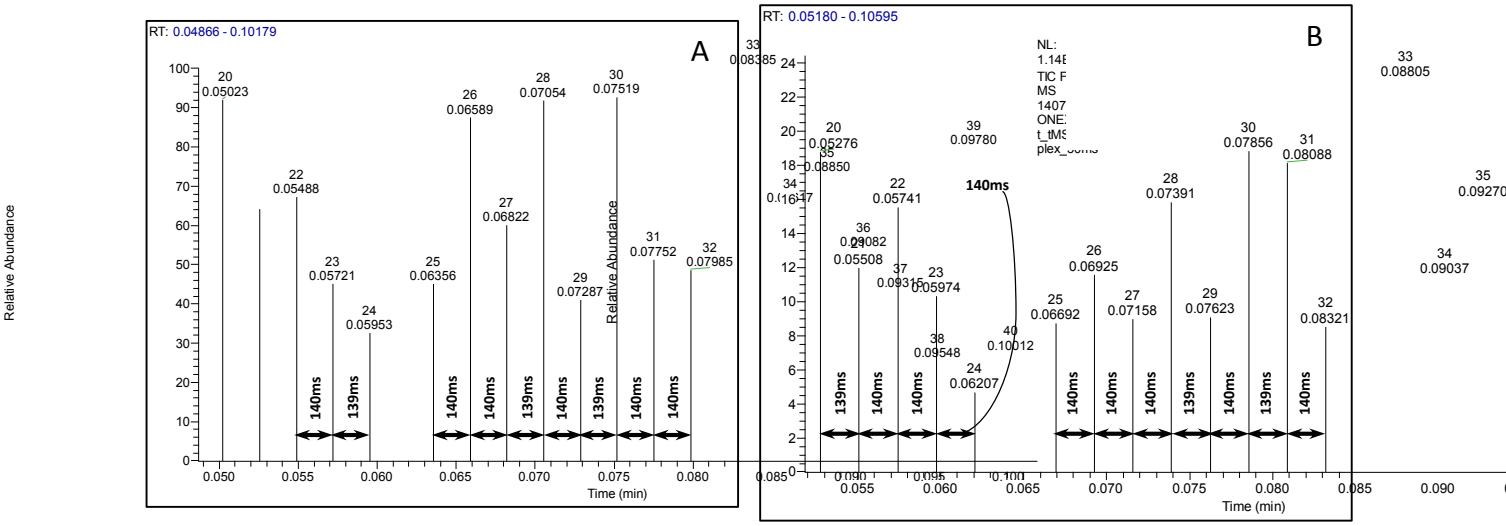

FIGURE 4.5: SCAN DIAGRAMS SHOWING SCAN TIMES FOR INJECTION TIME OPTIMISATION. A: MAX IT=50MS, B: MAX IT=100MS. IMAGE NOT TO SCALE

In the event that the suggested IT was in fact correct, the average scan time would remain the same as previously measured (Table 4.7). As can be seen in Table 4.9 below, the overall scan time for the 50 ms IT is approximately 140 ms. This suggests that the recommended IT of 110 ms was not optimal. When an IT of 100 ms was assessed, the overall scan time was the same as that for 50 ms. It can therefore be concluded that an IT of 100 ms is optimal.

The determination of optimal IT at 35 000 resolution of 110 ms here differs from IT parameters reported by Gallien et al.[132] (120 ms) and Schroeder et al.[182] (110 ms). Considering IT parameters used in those studies were determined by theoretical transient times of the Orbitrap analyser, the empirically determined IT parameter in the present study can be regarded as more reliable.

TABLE 4.9: SUMMARY OF SCAN TIMES FOR INJECTION TIME OPTIMISATION

Parameters			Scan Times			
Resolution	Max IT	MSX	Transient Time	Ave. Scan Time	Δ Scan Time	
35 000	50 ms	1	128 ms	139-140	0	
	100 ms			139-140		~5

Parameters			Scan Times		
Resolution	Max IT	MSX	Transient Time	Ave. Scan Time	Δ Scan Time
	110 ms			145	

Utilising the scan delay equation above, together with the optimum single-plex, Max IT settings for higher multiplex levels could now be calculated. The Max IT settings can be seen in Table 4.10 below, where effective IT was maintained across increasing multiplex levels by using Equation 1. Injection times for duplex and triplex assays were calculated at 45- and 27 ms respectively.

TABLE 4.10: TABLE OF OPTIMUM INJECTION TIMES FOR EACH MSX LEVEL AT 35 000 RESOLUTION

MSX	Effective IT	Calculation	**Max IT Setting**
1	110	(110-10)/1	**100 ms**
2	110	(110-20)/2	**45 ms**
3	110	(110-30)/3	**27 ms**

The IT for a single-plex assay was thus established, but predicted injection times for other multiplex levels require validation.

VALIDATION OF INJECTION TIMES AT OTHER MULTIPLEX LEVELS

The hypothesised ITs for single and duplex assays were verified to confirm IT settings for these multiplex levels and assess the predictive ability of Equation 1. Sample scans were assessed

and scan times measured for multiplex levels 2 and 3, with ITs of 45- and 27 ms respectively (Figure 4.6).

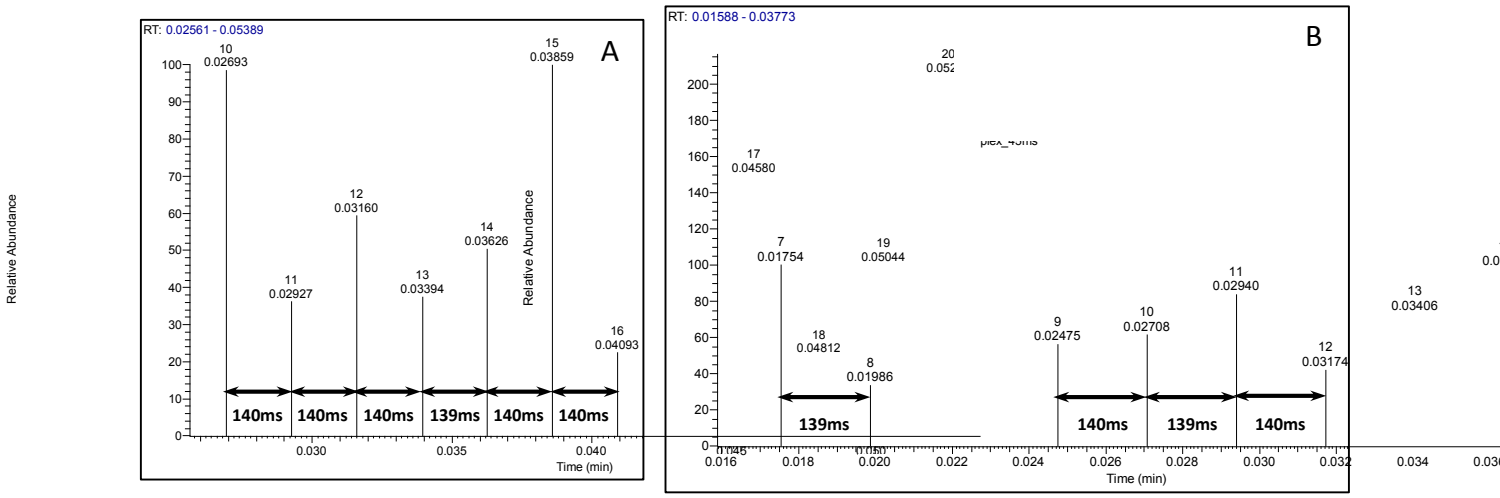

FIGURE 4.6: SCAN DIAGRAMS SHOWING SCAN TIMES FOR PREDICTED INJECTION TIMES AT VARYING MSX LEVELS. A: MSX = 2, MAX IT = 45MS; B: MSX = 3, MAX IT = 27MS

It was observed that overall scan times are equivalent between duplex and triplex scans with predicted ITs (Table 4.11). The scan times are equivalent to the minimum scan time previously established, so predicted ITs can therefore be accepted as optimal.

TABLE 4.11: SUMMARY OF SCAN TIMES RESULTING FROM PREDICTED INJECTION TIMES IN SINGLE AND DUPLEX MODES

Parameters			Scan Times		
Resolution	Max IT	MSX	Transient Time	Ave. Scan Time	Δ Scan Time
35 000	45 ms	2	128 ms	139-140	0
	27 ms	3		139-140	

As an extension of the predictive ability of the IT equation (Equation 1), Max IT settings for multiplex levels four to six can be calculated (Table 4.12). However, 4-plex was selected as the highest feasible multiplex level as markedly short ITs result in a significant loss in sensitivity.[132] Isolation list size allowance was calculated based on a requisite cycle time of 2 s, as this translates to at least six sampling points on a 12-second chromatographic peak. The assumption, based on previous experiments in our laboratory, is that peaks elute in 12-18 seconds on average. The calculation for number of precursors is as follows:

EQUATION 2: EQUATION TO ESTIMATE MAXIMUM NUMBER OF PRECURSORS IN A GIVEN PRM ASSAY

$$Number\ of\ Precursors = \left(\frac{Requisite\ Cycle\ Time}{Scan\ Time}\right) \times MSX\ Level$$

Table 4.12 shows the calculated isolation list size based on Equation 2. Gallien et al.[132] conducted sensitivity assessments on a concentration range of peptide standards spiked into a biological matrix, at varying injection times (70 000 resolution, in single-plex mode). They found that decreasing IT resulted in a marked decrease in the number of reliably quantifiable product ions, and this decrease was exacerbated by decrease in the amount of spiked in peptide. It can be inferred that to maintain a reasonable level of quantitative ability, IT should be kept as high as possible. Limits on IT should therefore be decided on a per-experiment basis, taking into account the inherent aims as well as sample type. Extensive multiplexing can also be avoided by implementation of retention time scheduling, which essentially decreases the isolation list size by segregating it according to the retention times of the analytes.[138]

TABLE 4.12: TABLE OF INJECTION TIME ESTIMATIONS FOR MULTIPLEXING UP TO 6X, AND ISOLATION LIST LENGTHS FOR A PREDEFINED CYCLE TIME OF 2 S

Requisite Cycle Time	Resolution	MSX	Max IT	Scan Time (Total)	Precursors	*Actual* Cycle Time
2000 ms	35 000	1	100 ms	140 ms	14	2002 ms
		2	45 ms		28	
		3	27 ms		42	
		4	18 ms		56	
		5	12 ms		70	
		6	8 ms		84	

In conclusion, optimal Max ITs were determined for analysis at 35 000 resolution, at multiple MSX levels. Isolation list sizes were also calculated for an ideal cycle time of 2 seconds. These parameters may be utilised in any proteomic PRM assay, and were applied to detection of the candidate serum biomarkers in subsequent stages of the present study.

4.3.2.2. Multiplexing Considerations

The effects of multiplexing were assessed by comparing single-plex and duplex scans in Skyline (Figure 4.7(A) and Figure 4.7(B) respectively). The effective ITs for the VDSAATSGYEIGNPPDYR peptide in single-plex and duplex modes were 100- and 45 ms respectively.

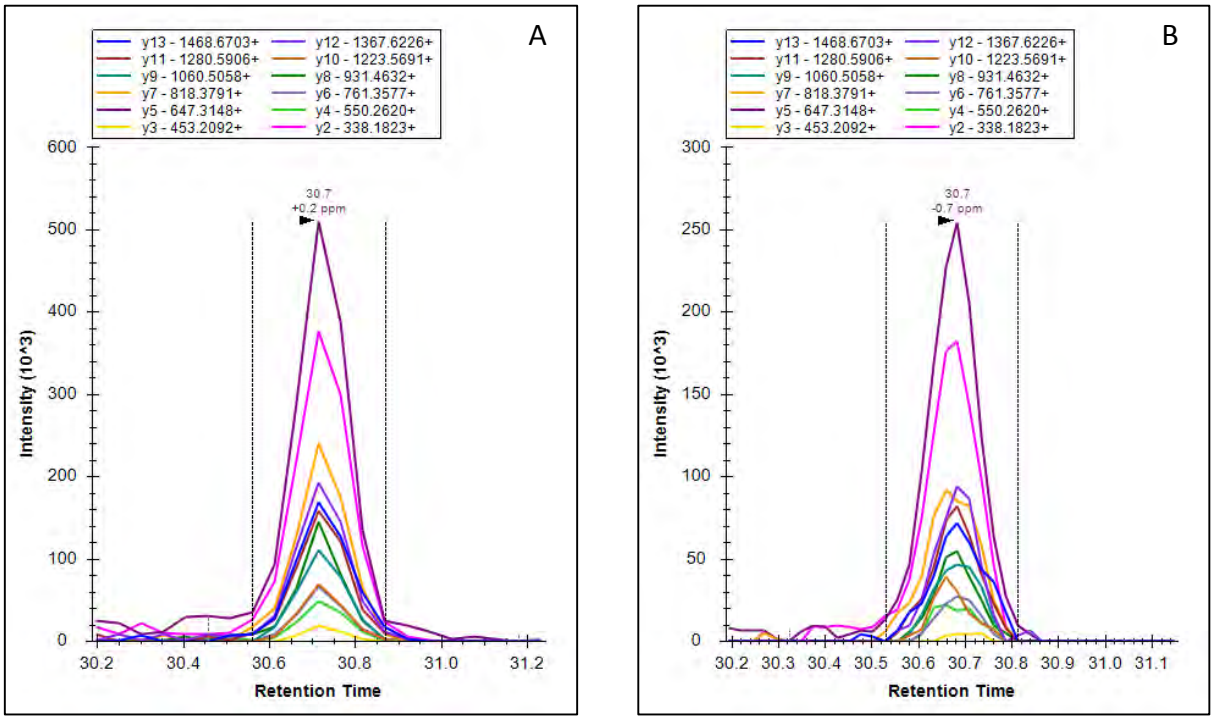

FIGURE 4.7: SKYLINE CHROMATOGRAMS OF SINGLE-PLEX VS DUPLEX ANALYSES OF VDSAATSGYEIGNPPDYR. A: SINGLE-PLEX, B: DUPLEX

It is observed that the duplex chromatogram appears smoother than the single-plex counterpart, suggesting fewer sampling points on the latter curve. Peak intensity for the single-plex experiment appears to be approximately twice that of the duplex experiment. For example, the y5 ion appears to have a peak height of approximately $510x10^3$ at single-plex, compared to $260x10^3$ at duplex. This observation supports the assumption that multiplexing results in decreased sensitivity; this can be attributed to the lower IT associated with multiplexing, which results in fewer ions being collected for detection.

Sampling rate was assessed by visualising the chromatogram in Microsoft Excel. Line markers in Figure 4.8 represent individual data sampling points taken over the chromatographic peak.

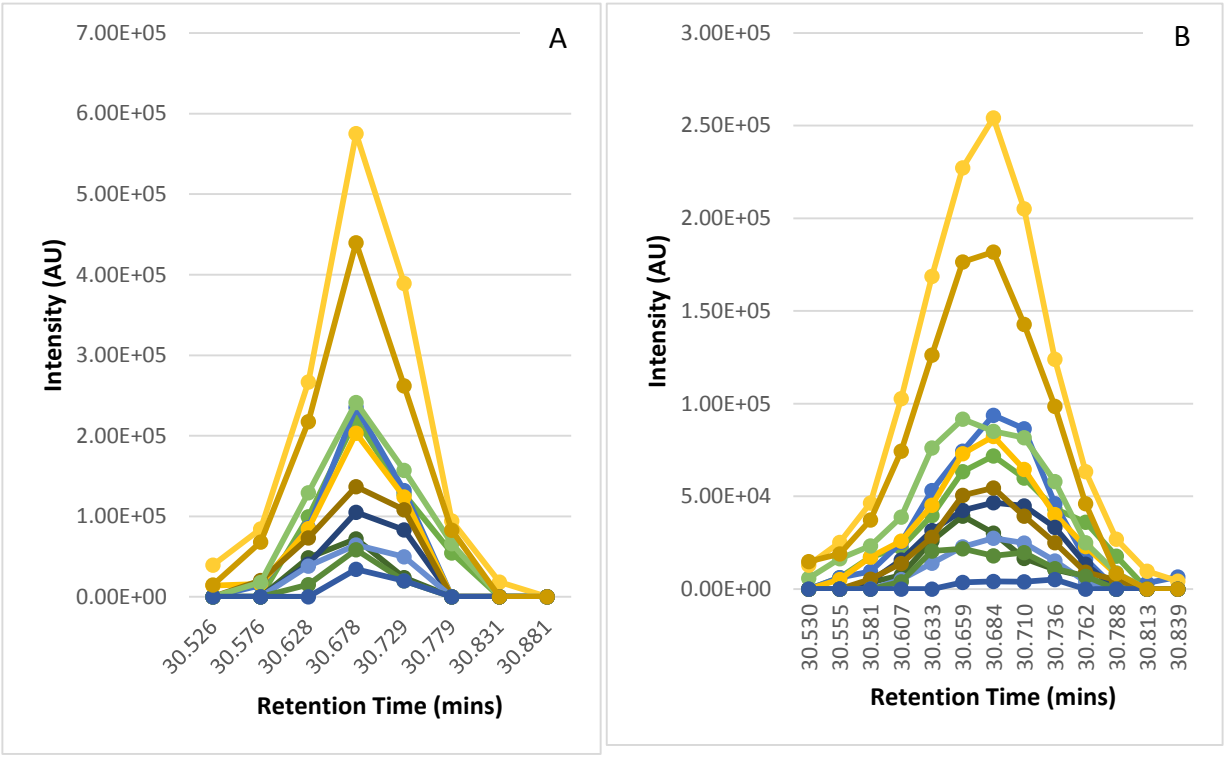

FIGURE 4.8: EXCEL-GENERATED CHROMATOGRAMS OF SINGLE-PLEX VS DUPLEX ANALYSES OF VDSAATSGYEIGNPPDYR. MARKERS REPRESENT MASS-SPECTROMETRIC SAMPLING POINTS. A: SINGLE-PLEX, B: DUPLEX

The single-plex experiment yielded an average of five points on the curve, whereas its duplex counterpart had approximately ten. This suggests that multiplexing increases the sampling points on a chromatographic peak, due to the isolation list being essentially halved by measuring two precursors per scan, resulting in approximately twice as many sampling points on the precursor elution curve. The higher number of sampling points on the curve allow for a more accurate representation of analyte elution – illustrated by a more smoothly defined curve, which increases quantitative accuracy.[124]

It is important to note that isolation list order should be carefully assessed when multiplexing peptides. Owing to the mechanism by which the Q Exactive performs multiplexing, it should be ensured that peptides which are multiplexed together do not have fragment ions with identical m/z values. Each precursor ion is selected by the quadrupole and consecutively accumulated in the HCD cell.[131,132] Once all precursors have been accumulated, they are fragmented and transferred to the Orbitrap for analysis.[131,132] It can be inferred that this mechanism renders it impossible for the mass spectrometer to relate each fragment ion back to its parent. In the event that precursors being multiplexed together have fragment ions of

the same m/z, the total signal for that ion would be incorrectly attributed to both parent ions, as was observed in our pilot PRM analyses (data not shown). Additionally, when assessing different charge states of a given peptide, the precursors should not be multiplexed if the product ions are both presumed to be singly charged. Indeed, it is difficult to avoid multiplexing peptides containing either arginine or lysine residues, since all tryptic peptides will end in either one of these amino acids. It is for this reason that product ions of arginine or lysine should be excluded from analyses.

In conclusion, multiplexing has definitive advantages for high throughput PRM analysis, as well as improving quantitative accuracy. These advantages come though at the price of significant loss in sensitivity at higher multiplex levels. Therefore, multiplexing must be balanced against isolation list and quantitative requirements, carefully considering the loss of sensitivity at high multiplexing levels. Isolation list order must also be carefully considered to avoid ambiguity in identification of detected product ions, which could have a detrimental effect on the PRM assay as a whole.

4.4. Conclusion

Instrument parameters were successfully optimised for PRM analysis at 35 000 resolution, and are summarised in Table 4.13 below. Lock masses, Chromatographic peak width, Charge state, AGC Target, ISO Window, and NCE values remained at baseline. Max IT settings optimised for each MSX level are shown, together with the recommended maximum number of precursors per analysis.

TABLE 4.13: FINAL SETTINGS FOR PRM ANALYSES AT 35 000 RESOLUTION. AGC: AUTOMATIC GAIN CONTROL, ISO: ISOLATION, NCE: NORMALISED COLLISION ENERGY, MSX: MULTIPLEX LEVEL, MAX IT: MAXIMUM INJECTION TIME.

Resolution	35000			
Lock masses	Off			
Chrom peak width	15 s			
Charge state	2			
AGC Target	5.00E+06			
ISO Window	2 m/z			
NCE	27			
MSX	1	2	3	4
Max IT	100 ms	45 ms	27 ms	18 ms
Precursors	14	28	42	56

These final instrument settings should be used for selection of optimal representative peptides, internal reference peptides, and final PRM analysis. They may also be applied to PRM assays in general, as they improve on the currently accepted IT and MSX settings.[132,182] These improvements may significantly affect sensitivity and quantitation in currently accepted proteomic PRM assays. Although IT and MSX parameters for other resolutions may be inferred based on the optimal values determined in the present study, it is recommended that empirical determination of optimal parameters be performed.

Chapter 5
Optimisation C: Selection of Final Peptides for Final Parallel Reaction Monitoring Assay

5.1. Introduction

Targeted proteomic MS is up to two orders of magnitude more sensitive than shotgun methods, given that particular masses are targeted rather than scanning the entire mass range.[134] As such, it is ideally suited to selection of the best peptides for inclusion in the final PRM assay. It is generally accepted that at least three peptides – with three to five transitions each – are required for confident protein inference in the development of MRM assays (*vide infra*) using triple quadrupole instruments.[124,189]

PRM assays differ from MRM analyses in that the former detect all MS^2 spectra, whereas the latter target predefined MS^2 ions.[125,126,130] Therefore, confirmation of peptide identity is more reliable in PRM analyses, since full MS^2 spectra is stronger evidence than several MS^2 ions. This also simplifies selection of ideal peptides and product ions: MRM product ion selection entails extensive optimisation of collision energies to obtain the strongest product ion signal.[189] The best PRM product ions are immediately apparent following initial analysis.

This Chapter focuses on PRM-based evaluation of peptides identified by shotgun proteomic analysis, with the aim of selecting the three best peptides per protein for inclusion in the final PRM assay. PRM analysis is able to facilitate highly-sensitive verification of discovery peptide identification. Evaluation of preliminarily selected peptides is conducted on pooled samples, analysed previously by discovery MS and using previously-optimised PRM instrument parameters (Chapter 4).

5.2. Materials and Methods

5.2.1. Sample Selection

Prospective peptides identified during discovery proteomic analysis of pooled samples (Table 3.3) were selected for verification by PRM analysis. Analyses were conducted on pooled samples used previously for discovery analysis (Table 3.1). Samples were chosen based on the most comprehensive membership of the preliminarily selected peptides (Table 3.3): POS_1, POS_2, MNI_1, MNI_2, MNI_3, HAD_1, and HAD_2.

5.2.2. LC/MS Instrumentation and Parameters

Targeted proteomic analysis was performed on a Q Exactive Quadrupole-Orbitrap Mass Spectrometer, coupled to a Dionex UltiMate 3500 RSLC nano-LC system. Approximately 125 ng of pooled sample peptides were injected onto the same LC setup described in Section 3.2.2, with the exception of the analytical column dimensions which were 75 µm x 15 cm. A shortened 72 minute linear gradient, developed for rapid targeted analysis, ran at a constant flow rate of 300 nl/min as follows: 2% B for 5 minutes, 2-35% B over 35 minutes, 35-80% B over 5 minutes, held at 80% B for 15 minutes, before returning to 2% B in 2 minutes, followed by re-equilibration at 2% B for 10 minutes.

Previously-developed baseline instrument parameter settings (Table 5.1) were utilised (Chapter 4), with appropriate modifications as isolation list size decreased. Multiplex level and injection time were varied with each round of optimisation. Skyline software settings for analysis and data input are described in Section 4.2.2.1.

TABLE 5.1: INITIAL SETTINGS FOR OPTIMAL PEPTIDE SELECTION BY PRM ASSAY AT 35 000 RESOLUTION.

Lock masses	Off
Chrom. peak width	15 s
Charge state	2
Resolution	35000
AGC Target	5.00E+06
ISO Window	2 m/z
NCE	27

AGC: Automatic Gain Control, ISO: Isolation, NCE: Normalised Collision Energy

5.2.3. Optimal Peptide Selection

A total of 106 prospective peptides were selected from the discovery analysis. Due to the multiple charge states assessed for certain peptides, the final isolation list consisted of 124 precursor ions. Peptides were pasted manually into Skyline, with detection of the source protein facilitated by automated comparison of imported sequences to a human proteome database. To maintain an overall cycle time of 2 seconds for each individual unscheduled analysis, isolation list sizes must obey the constraints outlined in Table 4.12 for a resolution setting of 35 000. After each round of optimisation, results were assessed via manual chromatogram inspection in Skyline according to several exclusion criteria (see Section 5.3.1). For example: poor peak shape, significant transition misalignment, low number of transitions, low signal-to-noise ratio, and missing peaks. Mass accuracy of identified peaks, as calculated by Skyline, was also taken into account.

5.2.3.1. Round 1

The master Skyline file was divided into two unscheduled isolation lists due to the large number of precursors, and these were exported for initial analyses. List A (Table 5.2) consisted of 72 precursors belonging to A2M, ApoE, CLU, C3, CFH, GSN, and SAP. List B (Table 5.3) comprised of 52 precursors belonging to A1AG, A1AT, CERU, C4A, and C4B. The numerical disparity was not realised until after initial analyses were conducted. Certain isolation list columns were left blank intentionally, as this is the required format from Xcalibur.

TABLE 5.2: ISOLATION LIST A, ROUND 1 (UNSCHEDULED)

Mass [m/z]	Formula [M]	Species	CS [z]	Polarity	Start [min]	End [min]	NCE	Comment
388.7369			2	Positive			27	GVFVLNK (light)
465.9329			3	Positive			27	SSNLIILEEHLK (light)
474.7667			2	Positive			27	LAVYQAGAR (light)
484.7798			2	Positive			27	LGPLVEQGR (light)
490.9315			3	Positive			27	IPIEDGSGEVVLSR (light)
497.2662			2	Positive			27	DNELLVYK (light)
499.7745			2	Positive			27	EPGLQIWR (light)
501.7769			2	Positive			27	TGLQEVEVK (light)
503.7387			2	Positive			27	FQVDNNNR (light)
522.6156			3	Positive			27	ALLAYAFALAGNQDK (light)
523.7977			2	Positive			27	FEVQVTVPK (light)
532.2984			2	Positive			27	IDVHLVPDR (light)
536.2933			2	Positive			27	EIQNAVNGVK (light)
537.7749			2	Positive			27	IDSLLENDR (light)

Mass [m/z]	Formula [M]	Species	CS [z]	Polarity	Start [min]	End [min]	NCE	Comment
557.7962			2	Positive			27	LEEQAQQIR (light)
558.806			2	Positive			27	QTVSWAVTPK (light)
559.3086			2	Positive			27	TLLSNLEEAK (light)
578.8035			2	Positive			27	VGEYSLYIGR (light)
583.7957			2	Positive			27	QGYFVEAQPK (light)
585.8037			2	Positive			27	PALPAGTEDTAK (light)
595.269			2	Positive			27	LSYTC[+57.0]EGGFR (light)
605.825			2	Positive			27	LPPNVVEESAR (light)
606.3023			3	Positive			27	SNLDEDIIAEENIVSR (light)
615.6838			3	Positive			27	LLIYAVLPTGDVIGDSAK (light)
616.9649			3	Positive			27	QFSFPLSSEPFQGSYK (light)
628.3251			2	Positive			27	AIGYLNTGYQR (light)
628.6874			3	Positive			27	VSVQLEASPAFLAVPVEK (light)
631.3046			2	Positive			27	QELSEAEQATR (light)
641.867			2	Positive			27	KGEWVALNPLR (light)
645.3077			2	Positive			27	SGSDEVQVGQQR (light)
660.3513			2	Positive			27	AGALNSNDAFVLK (light)
668.369			2	Positive			27	APSTWLTAYVVK (light)
685.8694			2	Positive			27	TIYTPGSTVLYR (light)
697.3515			2	Positive			27	ASSIIDELFQDR (light)
697.3515			2	Positive			27	IVLGQEQDSYGGK (light)
697.8435			2	Positive			27	NEDSLVFVQTDK (light)
698.3957			2	Positive			27	SSNLIILEEHLK (light)
703.8386			2	Positive			27	AYSLFSYNTQGR (light)
733.3815			3	Positive			27	VPVAVQGEDTVQSLTQGDGVAK (light)
735.8936			2	Positive			27	IPIEDGSGEVVLSR (light)
741.3583			2	Positive			27	C[+57.0]FEGFGIDGPAIAK (light)
749.4046			2	Positive			27	AATVGSLAGQPLQER (light)
756.3886			2	Positive			27	AAQVTIQSSGTFSSK (light)
773.3449			2	Positive			27	WSSPPQC[+57.0]EGLPC[+57.0]K (light)
783.4197			2	Positive			27	ALLAYAFALAGNQDK (light)
802.9252			2	Positive			27	IAQWQSFQLEGGLK (light)
804.7189			3	Positive			27	VSVLC[+57.0]QENYLIQEGEEITC[+57.0]K (light)
813.4045			2	Positive			27	VEQAVETEPEPELR (light)
827.8745			2	Positive			27	AGEQVTYTC[+57.0]ATYYK (light)
832.0542			3	Positive			27	DYAGVFSDAGLTFTSSSGQQTAQR (light)
861.9223			2	Positive			27	EVQGFESATFLGYFK (light)
865.9258			2	Positive			27	SELEEQLTPVAEETR (light)
908.4251			2	Positive			27	LGYVTADGETSGSITC[+57.0]GK (light)

Mass [m/z]	Formula [M]	Species	CS [z]	Polarity	Start [min]	End [min]	NCE	Comment
908.9498			2	Positive			27	SNLDEDIIAEENIVSR (light)
915.4858			2	Positive			27	QTQVSVLPEGGETPLFK (light)
919.452			2	Positive			27	TPSAAYLWVGTGASEAEK (light)
923.022			2	Positive			27	LLIYAVLPTGDVIGDSAK (light)
924.9438			2	Positive			27	QFSFPLSSEPFQGSYK (light)
934.4176			2	Positive			27	SC[+57.0]DNPYIPNGDYSPLR (light)
937.4989			2	Positive			27	LFDSDPITVTVPVEVSR (light)
942.5275			2	Positive			27	VSVQLEASPAFLAVPVEK (light)
983.4886			2	Positive			27	EQVQSC[+57.0]GPPPELLNGNVK (light)
1010.991			2	Positive			27	DTSC[+57.0]VNPPTVQNAYIVSR (light)
1082.012			2	Positive			27	AVYTC[+57.0]NEGYQLLGEINYR (light)
1083.505			2	Positive			27	AYYENSPQQVFSTEFEVK (light)
1099.569			2	Positive			27	VPVAVQGEDTVQSLTQGDGVAK (light)
1107.506			2	Positive			27	EDIPPADLSDQVPDTESETR (light)
1133.05			2	Positive			27	SSIDIENGFISESQYTYALK (light)
1136.548			2	Positive			27	AQPVQVAEGSEPDGFWEALGGK (light)
1206.575			2	Positive			27	VSVLC[+57.0]QENYLIQEGEEITC[+57.0]K (light)
1247.578			2	Positive			27	DYAGVFSDAGLTFTSSSGQQTAQR (light)
1301.619			2	Positive			27	NTEILTGSWSDQTYPEGTQAIYK (light)

CS: Charge State, NCE: Normalised Collision Energy.

* Isolation list columns left blank intentionally, as this is the required format from Xcalibur.

TABLE 5.3: ISOLATION LIST B, ROUND 1 (UNSCHEDULED)

Mass [m/z]	Formula [M]	Species	CS [z]	Polarity	Start [min]	End [min]	NCE	Comment
338.1977			3	Positive			27	AKPALEDLR (light)
360.1807			3	Positive			27	FLENEDRR (light)
444.7555			2	Positive			27	AVLTIDEK (light)
450.7267			2	Positive			27	GEFYIGSK (light)
461.7169			2	Positive			27	FLENEDR (light)
488.2887			3	Positive			27	VKDLATVYVDVLK (light)
492.2383			2	Positive			27	QGSFQGGFR (light)
494.7824			2	Positive			27	PVQGVAYVR (light)

Mass [m/z]	Formula [M]	Species	CS [z]	Polarity	Start [min]	End [min]	NCE	Comment
497.7638			2	Positive			27	TEDTIFLR (light)
504.7535			2	Positive			27	QINDYVEK (light)
506.7929			2	Positive			27	AKPALEDLR (light)
508.3109			2	Positive			27	SVLGQLGITK (light)
509.2354			2	Positive			27	QYTDSTFR (light)
522.9143			3	Positive			27	VNKDDEEFIESNK (light)
525.7587			2	Positive			27	AEFQDALEK (light)
539.7674			2	Positive			27	FLENEDRR (light)
543.3188			3	Positive			27	PVAFSVVPTAAAAVSLK (light)
547.9594			3	Positive			27	ITPNLAEFAFSLYR (light)
555.8057			2	Positive			27	LSITGTYDLK (light)
557.8144			2	Positive			27	VGDTLNLNLR (light)
602.2675			2	Positive			27	EYTDASFTNR (light)
611.9791			3	Positive			27	VFSNGADLSGVTEEAPLK (light)
613.2646			2	Positive			27	DDEEFIESNK (light)
615.8583			2	Positive			27	QGLLPVLESFK (light)
618.3477			2	Positive			27	DLATVYVDVLK (light)
626.8141			2	Positive			27	VQPYLDDFQK (light)
655.3612			2	Positive			27	GSSTWLTAFVLK (light)
670.4105			2	Positive			27	PVWLGFLGPIIK (light)
672.4003			2	Positive			27	DFALLSLQVPLK (light)
684.3639			2	Positive			27	DSSTWLTAFVLK (light)
686.3852			2	Positive			27	GAYPLSIEPIGVR (light)
693.8612			2	Positive			27	VSFLSALEEYTK (light)
700.8383			2	Positive			27	DYVSQFEGSALGK (light)
716.323			2	Positive			27	QSEDSTFYLGER (light)
760.375			2	Positive			27	ALYLQYTDETFR (light)
771.4121			2	Positive			27	VLSLAQEQVGGSPEK (light)
782.4281			2	Positive			27	TTNIQGINLLFSSR (light)
783.8677			2	Positive			27	VNKDDEEFIESNK (light)
788.9241			2	Positive			27	DTVFALVNYIFFK (light)
806.8963			2	Positive			27	LLDNWDSVTSTFSK (light)
814.4745			2	Positive			27	PVAFSVVPTAAAAVSLK (light)
821.4354			2	Positive			27	ITPNLAEFAFSLYR (light)
828.4378			3	Positive			27	VTASDPLDTLGSEGALSPGG VASLLR (light)
858.7852			3	Positive			27	TLNQPDSQLQLTTGNGLFLS EGLK (light)
871.9063			2	Positive			27	EQLGEFYEALDC[+57.0]LR (light)
917.4651			2	Positive			27	VFSNGADLSGVTEEAPLK (light)
952.4139			2	Positive			27	NNEGTYYSPNYNPQSR (light)

Mass [m/z]	Formula [M]	Species	CS [z]	Polarity	Start [min]	End [min]	NCE	Comment
966.9705			2	Positive			27	EQLGPVTQEFWDNLEK (light)
1044.828			3	Positive			27	LQETSNWLLSQQQADGSFQ DPC[+57.0]PVLDR (light)
1113.063			2	Positive			27	ALEILQEEDLIDEDDIPVR (light)
1242.153			2	Positive			27	VTASDPLDTLGSEGALSPGG VASLLR (light)
1287.674			2	Positive			27	TLNQPDSQLQLTTGNGLFLS EGLK (light)

CS: Charge State, NCE: Normalised Collision Energy.
* Isolation list columns left blank intentionally, as this is the required format from Xcalibur.

During the first round of optimisation the cycle time was allowed to exceed 2 seconds in the interests of maintaining sensitivity, with a concomitant insignificant decrease in quantitative ability. Lists A and B were imported into Xcalibur with settings as described in Table 5.1, an MSX of 4, and a Max IT of 18 ms. This equated to an effective cycle time of 2.5 and 2 seconds for lists A and B respectively. Sample MNI_1 was used to assess list A, while list B was evaluated by analysing sample POS_1.

Following PRM analysis, data files were imported into Skyline according to settings outlined in Section 4.2.2.1. Chromatograms were assessed for elimination of low-quality peptides.

5.2.3.2. Round 2

To rule out the hypothesis that lower sensitivity at a high multiplex level (4-plex) was responsible for the low quality of some peptides from the analysis of List A, these were re-analysed at a lower MSX, and higher per-precursor ITs to further increase sensitivity. An unscheduled isolation list of 23 precursors (Table 5.4) was assayed with settings as described in Table 5.1, in duplex mode, and with a Max IT of 45 ms. This resulted in an effective cycle time of 1.61 seconds. Sample HAD_2 was re-analysed, while MNI_1 was also analysed in the event that the low-quality peptide signal was sample-related.

TABLE 5.4: ISOLATION LIST A REPEAT, ROUND 2 (UNSCHEDULED)

Mass [m/z]	Formula [M]	Species	CS [z]	Polarity	Start [min]	End [min]	NCE	Comment
813.4045			2	Positive			27	VEQAVETEPEPELR (light)
865.9258			2	Positive			27	SELEEQLTPVAEETR (light)
474.7667			2	Positive			27	LAVYQAGAR (light)
484.7798			2	Positive			27	LGPLVEQGR (light)
749.4046			2	Positive			27	AATVGSLAGQPLQER (light)
557.7962			2	Positive			27	LEEQAQQIR (light)
536.2933			2	Positive			27	EIQNAVNGVK (light)
559.3086			2	Positive			27	TLLSNLEEAK (light)
537.7749			2	Positive			27	IDSLLENDR (light)
697.3515			2	Positive			27	ASSIIDELFQDR (light)
937.4989			2	Positive			27	LFDSDPITVTVPVEVSR (light)
585.8037			2	Positive			27	PALPAGTEDTAK (light)
499.7745			2	Positive			27	EPGLQIWR (light)
861.9223			2	Positive			27	EVQGFESATFLGYFK (light)
915.4858			2	Positive			27	QTQVSVLPEGGETPLFK (light)
660.3513			2	Positive			27	AGALNSNDAFVLK (light)
919.452			2	Positive			27	TPSAAYLWVGTGASEAEK (light)
1136.548			2	Positive			27	AQPVQVAEGSEPDGFWEALGGK (light)
703.8386			2	Positive			27	AYSLFSYNTQGR (light)
497.2662			2	Positive			27	DNELLVYK (light)
578.8035			2	Positive			27	VGEYSLYIGR (light)
583.7957			2	Positive			27	QGYFVEAQPK (light)
697.3515			2	Positive			27	IVLGQEQDSYGGK (light)

CS: Charge State, NCE: Normalised Collision Energy.
* Isolation list columns left blank intentionally, as this is the required format from Xcalibur.

Following PRM analysis, data files were imported into Skyline. Chromatograms were assessed for elimination of low-quality peptides.

5.2.3.3. Round 3

High-quality peptides resulting from round 2 were recombined with their counterparts from Round 1, to yield adjusted lists A and B, consisting of 39 and 26 precursors respectively. In order to equalise the number of precursors in each list, seven C3 peptides were transferred from list A to list B, resulting in final list sizes of 32 and 33 precursors respectively (Table 5.5 and Table 5.6). Disparate list sizes were equalised to maintain consistency and prevent the results from the analysis with the shorter isolation list from appearing misleadingly superior.

TABLE 5.5: ISOLATION LIST A, ROUND 3 (UNSCHEDULED)

Mass [m/z]	Formula [M]	Species	CS [z]	Polarity	Start [min]	End [min]	NCE	Comment
697.8435			2	Positive			27	NEDSLVFVQTDK (light)
802.9252			2	Positive			27	IAQWQSFQLEGGLK (light)
523.7977			2	Positive			27	FEVQVTVPK (light)
923.022			2	Positive			27	LLIYAVLPTGDVIGDSAK (light)
558.806			2	Positive			27	QTVSWAVTPK (light)
605.825			2	Positive			27	LPPNVVEESAR (light)
628.3251			2	Positive			27	AIGYLNTGYQR (light)
756.3886			2	Positive			27	AAQVTIQSSGTFSSK (light)
865.9258			2	Positive			27	SELEEQLTPVAEETR (light)
474.7667			2	Positive			27	LAVYQAGAR (light)
484.7798			2	Positive			27	LGPLVEQGR (light)
749.4046			2	Positive			27	AATVGSLAGQPLQER (light)
559.3086			2	Positive			27	TLLSNLEEAK (light)
537.7749			2	Positive			27	IDSLLENDR (light)
697.3515			2	Positive			27	ASSIIDELFQDR (light)
937.4989			2	Positive			27	LFDSDPITVTVPVEVSR (light)
908.4251			2	Positive			27	LGYVTADGETSGSITC[+57.0]GK (light)
532.2984			2	Positive			27	IDVHLVPDR (light)
698.3957			2	Positive			27	SSNLIILEEHLK (light)
804.7189			3	Positive			27	VSVLC[+57.0]QENYLIQEGEEITC[+57.0]K (light)
595.269			2	Positive			27	LSYTC[+57.0]EGGFR (light)
741.3583			2	Positive			27	C[+57.0]FEGFGIDGPAIAK (light)
827.8745			2	Positive			27	AGEQVTYTC[+57.0]ATYYK (light)
499.7745			2	Positive			27	EPGLQIWR (light)
861.9223			2	Positive			27	EVQGFESATFLGYFK (light)
915.4858			2	Positive			27	QTQVSVLPEGGETPLFK (light)
660.3513			2	Positive			27	AGALNSNDAFVLK (light)
919.452			2	Positive			27	TPSAAYLWVGTGASEAEK (light)
703.8386			2	Positive			27	AYSLFSYNTQGR (light)
497.2662			2	Positive			27	DNELLVYK (light)
578.8035			2	Positive			27	VGEYSLYIGR (light)
697.3515			2	Positive			27	IVLGQEQDSYGGK (light)

CS: Charge State, NCE: Normalised Collision Energy.

* Isolation list columns left blank intentionally, as this is the required format from Xcalibur.

TABLE 5.6: ISOLATION LIST B, ROUND 3 (UNSCHEDULED)

Mass [m/z]	Formula [M]	Species	CS [z]	Polarity	Start [min]	End [min]	NCE	Comment
497.7638			2	Positive			27	TEDTIFLR (light)
504.7535			2	Positive			27	QINDYVEK (light)
461.7169			2	Positive			27	FLENEDR (light)
555.8057			2	Positive			27	LSITGTYDLK (light)
508.3109			2	Positive			27	SVLGQLGITK (light)
917.4651			2	Positive			27	VFSNGADLSGVTEEAPLK (light)
611.9791			3	Positive			27	VFSNGADLSGVTEEAPLK (light)
444.7555			2	Positive			27	AVLTIDEK (light)
618.3477			2	Positive			27	DLATVYVDVLK (light)
700.8383			2	Positive			27	DYVSQFEGSALGK (light)
806.8963			2	Positive			27	LLDNWDSVTSTFSK (light)
626.8141			2	Positive			27	VQPYLDDFQK (light)
615.8583			2	Positive			27	QGLLPVLESFK (light)
693.8612			2	Positive			27	VSFLSALEEYTK (light)
760.375			2	Positive			27	ALYLQYTDETFR (light)
602.2675			2	Positive			27	EYTDASFTNR (light)
686.3852			2	Positive			27	GAYPLSIEPIGVR (light)
952.4139			2	Positive			27	NNEGTYYSPNYNPQSR (light)
716.323			2	Positive			27	QSEDSTFYLGER (light)
509.2354			2	Positive			27	QYTDSTFR (light)
782.4281			2	Positive			27	TTNIQGINLLFSSR (light)
525.7587			2	Positive			27	AEFQDALEK (light)
557.8144			2	Positive			27	VGDTLNLNLR (light)
655.3612			2	Positive			27	GSSTWLTAFVLK (light)
492.2383			2	Positive			27	QGSFQGGFR (light)
494.7824			2	Positive			27	PVQGVAYVR (light)
685.8694			2	Positive			27	TIYTPGSTVLYR (light)
735.8936			2	Positive			27	IPIEDGSGEVVLSR (light)
733.3815			3	Positive			27	VPVAVQGEDTVQSLTQGDG VAK (light)
908.9498			2	Positive			27	SNLDEDIIAEENIVSR (light)
501.7769			2	Positive			27	TGLQEVEVK (light)
668.369			2	Positive			27	APSTWLTAYVVK (light)
645.3077			2	Positive			27	SGSDEVQVGQQR (light)

CS: Charge State, NCE: Normalised Collision Energy.
* Isolation list columns left blank intentionally, as this is the required format from Xcalibur.

Each isolation list was assayed with settings as described in Table 5.1, in triplex mode, and with a Max IT of 27 ms. List A was assessed using HAD_1 and POS_1, while HAD_2 and POS_2 were analysed with precursors from list B. The cycle time for each analysis amounted to

approximately 1.5 seconds. Following PRM analysis, data files were imported into Skyline. Chromatograms were assessed for elimination of low-quality peptides.

5.2.3.4. Round 4

Optimally-performing precursors were brought to the next round of selection. A total of 53 precursors were assessed in this round: 27 in List A (Table 5.7), and 26 in List B.

TABLE 5.7: ISOLATION LIST A, ROUND 4 (UNSCHEDULED)

Mass [m/z]	Formula [M]	Species	CS [z]	Polarity	Start [min]	End [min]	NCE	Comment
697.8435			2	Positive			27	NEDSLVFVQTDK (light)
523.7977			2	Positive			27	FEVQVTVPK (light)
558.806			2	Positive			27	QTVSWAVTPK (light)
605.825			2	Positive			27	LPPNVVEESAR (light)
628.3251			2	Positive			27	AIGYLNTGYQR (light)
865.9258			2	Positive			27	SELEEQLTPVAEETR (light)
474.7667			2	Positive			27	LAVYQAGAR (light)
484.7798			2	Positive			27	LGPLVEQGR (light)
749.4046			2	Positive			27	AATVGSLAGQPLQER (light)
559.3086			2	Positive			27	TLLSNLEEAK (light)
537.7749			2	Positive			27	IDSLLENDR (light)
697.3515			2	Positive			27	ASSIIDELFQDR (light)
937.4989			2	Positive			27	LFDSDPITVTVPVEVSR (light)
908.4251			2	Positive			27	LGYVTADGETSGSITC[+57.0] GK (light)
532.2984			2	Positive			27	IDVHLVPDR (light)
698.3957			2	Positive			27	SSNLIILEEHLK (light)
595.269			2	Positive			27	LSYTC[+57.0]EGGFR (light)
741.3583			2	Positive			27	C[+57.0]FEGFGIDGPAIAK (light)
827.8745			2	Positive			27	AGEQVTYTC[+57.0]ATYYK (light)
499.7745			2	Positive			27	EPGLQIWR (light)
861.9223			2	Positive			27	EVQGFESATFLGYFK (light)
915.4858			2	Positive			27	QTQVSVLPEGGETPLFK (light)
660.3513			2	Positive			27	AGALNSNDAFVLK (light)
703.8386			2	Positive			27	AYSLFSYNTQGR (light)
497.2662			2	Positive			27	DNELLVYK (light)
578.8035			2	Positive			27	VGEYSLYIGR (light)
697.3515			2	Positive			27	IVLGQEQDSYGGK (light)
697.8435			2	Positive			27	NEDSLVFVQTDK (light)
523.7977			2	Positive			27	FEVQVTVPK (light)
558.806			2	Positive			27	QTVSWAVTPK (light)
605.825			2	Positive			27	LPPNVVEESAR (light)

Mass [m/z]	Formula [M]	Species	CS [z]	Polarity	Start [min]	End [min]	NCE	Comment
628.3251			2	Positive			27	AIGYLNTGYQR (light)
865.9258			2	Positive			27	SELEEQLTPVAEETR (light)

CS: Charge State, NCE: Normalised Collision Energy.
* Isolation list columns left blank intentionally, as this is the required format from Xcalibur.

TABLE 5.8: ISOLATION LIST B, ROUND 4 (UNSCHEDULED)

Mass [m/z]	Formula [M]	Species	CS [z]	Polarity	Start [min]	End [min]	NCE	Comment
497.7638			2	Positive			27	TEDTIFLR (light)
504.7535			2	Positive			27	QINDYVEK (light)
461.7169			2	Positive			27	FLENEDR (light)
508.3109			2	Positive			27	SVLGQLGITK (light)
618.3477			2	Positive			27	DLATVYVDVLK (light)
700.8383			2	Positive			27	DYVSQFEGSALGK (light)
806.8963			2	Positive			27	LLDNWDSVTSTFSK (light)
626.8141			2	Positive			27	VQPYLDDFQK (light)
615.8583			2	Positive			27	QGLLPVLESFK (light)
693.8612			2	Positive			27	VSFLSALEEYTK (light)
602.2675			2	Positive			27	EYTDASFTNR (light)
686.3852			2	Positive			27	GAYPLSIEPIGVR (light)
952.4139			2	Positive			27	NNEGTYYSPNYNPQSR (light)
716.323			2	Positive			27	QSEDSTFYLGER (light)
509.2354			2	Positive			27	QYTDSTFR (light)
525.7587			2	Positive			27	AEFQDALEK (light)
557.8144			2	Positive			27	VGDTLNLNLR (light)
444.7578			2	Positive			27	KRLSC[+57.0]PK (light)
492.2383			2	Positive			27	QGSFQGGFR (light)
494.7824			2	Positive			27	PVQGVAYVR (light)
685.8694			2	Positive			27	TIYTPGSTVLYR (light)
735.8936			2	Positive			27	IPIEDGSGEVVLSR (light)
490.9315			3	Positive			27	IPIEDGSGEVVLSR (light)
908.9498			2	Positive			27	SNLDEDIIAEENIVSR (light)
501.7769			2	Positive			27	TGLQEVEVK (light)
645.3077			2	Positive			27	SGSDEVQVGQQR (light)
497.7638			2	Positive			27	TEDTIFLR (light)

CS: Charge State, NCE: Normalised Collision Energy.
* Isolation list columns left blank intentionally, as this is the required format from Xcalibur.

Each isolation list was assayed with settings as described in Table 5.1, in duplex mode, and with a Max IT of 45 ms. Due to diminished sample volume at this stage of optimisation, samples HAD_1, HAD_2, MNI_1, POS_1 and POS_2 were combined into a single sample for

the remainder of optimisation. Both lists were assessed using the pooled sample. The cycle time for each analysis amounted to approximately 1.9 seconds.

Following PRM analysis, data files were imported into Skyline. Chromatograms were assessed for elimination of low-quality peptides. Only high-quality precursors for inclusion in the final PRM assay now remain.

5.2.3.5. Retention Time Scheduling

In order to maximise the number of sampling points on the chromatogram, retention time scheduling windows of peptides were introduced. Skyline settings were modified such that a window of 5 minutes on either side of previously-established peak retention times would be integrated into the method. The isolation list was exported with this retention time scheduling (Table 5.9). Analysis was performed on the pooled sample with settings as described in Table 5.1, in duplex mode, and with a Max IT of 45 ms.

TABLE 5.9: SCHEDULED ISOLATION LIST FOR FINAL LIST OF PRM TARGET PEPTIDES

Mass [m/z]	Formula [M]	Species	CS [z]	Polarity	Start [min]	End [min]	NCE	Comment
697.8435			2	Positive	24.87	29.87	27	NEDSLVFVQTDK (light)
523.7977			2	Positive	24.61	29.61	27	FEVQVTVPK (light)
628.3251			2	Positive	22.78	27.78	27	AIGYLNTGYQR (light)
532.2984			2	Positive	22.06	27.06	27	IDVHLVPDR (light)
595.269			2	Positive	22.1	27.1	27	LSYTC[+57.0]EGGFR (light)
827.8745			2	Positive	21.5	26.5	27	AGEQVTYTC[+57.0]ATYYK (light)
474.7667			2	Positive	18.42	23.42	27	LAVYQAGAR (light)
484.7798			2	Positive	20.42	25.42	27	LGPLVEQGR (light)
749.4046			2	Positive	22.37	27.37	27	AATVGSLAGQPLQER (light)
559.3086			2	Positive	26.96	31.96	27	TLLSNLEEAK (light)
537.7749			2	Positive	22.08	27.08	27	IDSLLENDR (light)
697.3515			2	Positive	33.91	38.91	27	ASSIIDELFQDR (light)
499.7745			2	Positive	26.74	31.74	27	EPGLQIWR (light)
915.4858			2	Positive	28.74	33.74	27	QTQVSVLPEGGETPLFK (light)
660.3513			2	Positive	25.47	30.47	27	AGALNSNDAFVLK (light)
703.8386			2	Positive	26.9	31.9	27	AYSLFSYNTQGR (light)
497.2662			2	Positive	24.19	29.19	27	DNELLVYK (light)
578.8035			2	Positive	25.55	30.55	27	VGEYSLYIGR (light)
497.7638			2	Positive	25.06	30.06	27	TEDTIFLR (light)
461.7169			2	Positive	17.17	22.17	27	FLENEDR (light)
508.3109			2	Positive	27.1	32.1	27	SVLGQLGITK (light)
444.7555			2	Positive	20.48	25.48	27	AVLTIDEK (light)
700.8383			2	Positive	28.19	33.19	27	DYVSQFEGSALGK (light)

Mass [m/z]	Formula [M]	Species	CS [z]	Polarity	Start [min]	End [min]	NCE	Comment
806.8963			2	Positive	30.67	35.67	27	LLDNWDSVTSTFSK (light)
626.8141			2	Positive	24.55	29.55	27	VQPYLDDFQK (light)
602.2675			2	Positive	19.62	24.62	27	EYTDASFTNR (light)
686.3852			2	Positive	28.57	33.57	27	GAYPLSIEPIGVR (light)

CS: Charge State, NCE: Normalised Collision Energy.
* Isolation list columns left blank intentionally, as this is the required format from Xcalibur.

Following PRM analysis, data files were imported into Skyline. Chromatograms were assessed for correct application of retention time windows. Precursor measurement overlap was calculated to estimate average cycle time in the scheduled assay.

5.3. Results and Discussion

5.3.1. Optimal Peptide Selection

Optimal peptide selection during all rounds of optimisation was based on chromatogram quality. Examples of selection criteria are included in Figure 5.1. Favourable peak shape was a basic requirement (A). Peptides with poor peak shape (B), significant transition misalignment (C), low number of transitions (D), low signal-to-noise ratio (E), and missing peaks (F) were eliminated. Peptides exhibiting low mass-accuracy (high parts per million [ppm] values, based on calculations by Skyline), were excluded. These selection criteria were applied at every stage of optimisation.

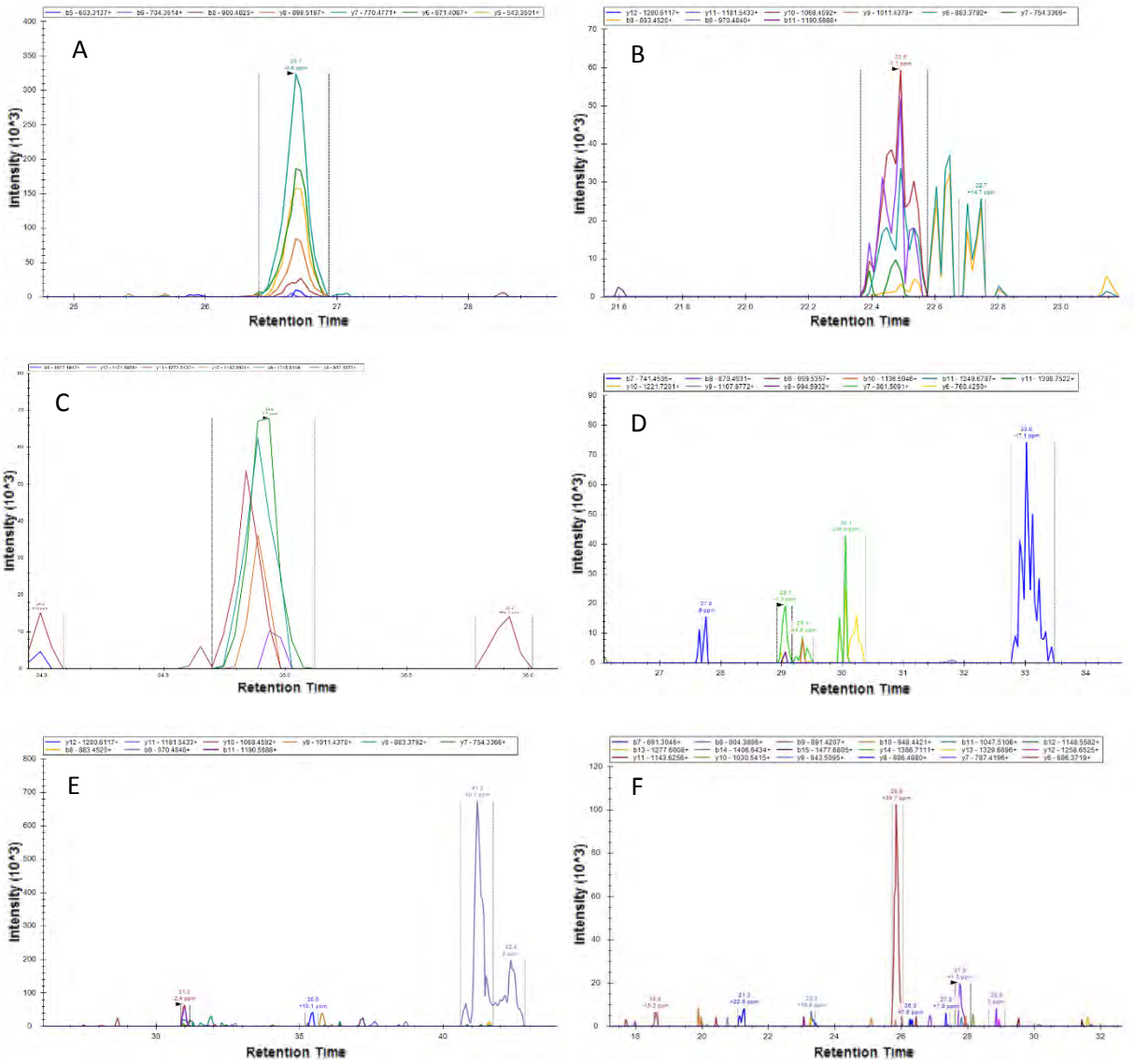

FIGURE 5.1: EXAMPLES OF CHROMATOGRAMS OF VARYING QUALITY FOR OPTIMAL PEPTIDE SELECTION.
A: Favourable chromatogram, B: Poor peak shape, C: Misaligned transitions, D: Few transitions, E: Low signal-to-noise ratio, F: Missing peak.

5.3.1.1. Round 1

During data importation into Skyline, certain preselected peptides were excluded, probably due to automatic filtering of targets according to the predefined settings (the 'automatically filter selected peptides' option was selected in the settings dialog box). Due to the rapid nature of precursor selection and data quality analysis, this was recognised only after final peptide selection, contributing to disparity in transition numbers.

The initial round of selection yielded mixed results, with 22 of 70 precursors from List A, and 16 of 45 precursors from list B performing inadequately (Table 5.10). Low IT may have been responsible for the poor quality of peptides, or the analysed sample may have negatively impacted peptide detection. Thus, repeat analysis of low-quality peptides from List A (Table 5.10: underlined entries) was conducted at a lowed multiplex level prior to continuing optimisation.

TABLE 5.10: TALLY OF PEPTIDE PERFORMANCE FOR ROUND 1

List	Protein	Precursors Analysed	Precursors Accepted	Precursors Rejected
A	A2M	15	15	0
	ApoE	6	0	6
	CLU	5	0	5
	C3	15	15	0
	CFH	17	17	0
	GSN	7	0	7
	SAP	5	0	5
	Subtotal	**70**	**47**	**23**
B	A1AG	2	1	1
	A1AT	13	6	7
	ApoA-I	8	7	0
	CERU	10	8	2
	C4A/B	12	6	6
	Subtotal	**45**	**28**	**16**
TOTAL		**115**	**75**	**39**

A2M: Alpha-2-macroglobulin, ApoE: Apolipoprotein E, CLU: Clusterin, C3: Complement Component C, CFH: Complement Factor H, GSN: Gelsolin, SAP: Serum Amyloid P, A1AG: Alpha-1-acid Glycoprotein 1, A1AT: Alpha-1-antitrypsin, ApoA-I: Apolipoprotein A1, CERU: Ceruloplasmin, C4A/B: Complement Component 4A/B

5.3.1.2. Round 2

Repeat analysis of sample HAD_2 and verification with sample MNI_1 yielded largely favourable results. Both samples exhibited peptide peaks of comparable quality, precluding poor quality of the HAD_2 sample.

A total of 23 precursors were assessed in Skyline, and six were eliminated (Table 5.11), including VEQAVETEPEPELR (ApoE), LEEQAQQIR (ApoE), EIQNAVNGVK (CLU), AQPVQVAEGSEPDGFWEALGGK (GSN), PALPAGTEDTAK (GSN), and QGYFVEAQPK (SAP). The remaining peptides were carried through to the next round of optimisation.

TABLE 5.11: TALLY OF PEPTIDE PERFORMANCE FOR ROUND 2

List	Protein	Precursors Analysed	Precursors Accepted	Precursors Rejected
A	ApoE	6	4	2
	CLU	5	4	1
	GSN	7	5	2
	SAP	5	4	1
TOTAL		**23**	**17**	**6**

5.3.1.3. Round 3

Analysis of recombined lists yielded favourable results. Most of the precursors analysed performed well in all samples assessed. Of the 65 precursors considered, 53 were selected for the next phase of optimisation while 12 were eliminated (Table 5.12). The eliminated peptides included: IAQWQSFQLEGGLK (A2M), LLIYAVLPTGDVIGDSAK (A2M), AAQVTIQSSGTFSSK (A2M), VSVL**C**QENYLIQEGEEIT**C**K (CFH), TPSAAYLWVGTGASEAEK (GSN), LSITGTYDLK (A1AT), VFSNGADLSGVTEEAPLK^{2+} (A1AT), VFSNGADLSGVTEEAPLK^{3+} (A1AT), TTNIQGINLLFSSR (C4), GSSTWLTAFVLK (C4), VPVAVQGEDTVQSLTQGDGVAK (C3), and APSTWLTAYVVK (C3). The 54 peptides chosen for further optimisation were carried over to the next round.

Peptide AVLTIDEK, derived from GSN, had been included in Round 2, but was not considered by Skyline for this list and was thus ignored at this stage of optimisation.

TABLE 5.12: TALLY OF PEPTIDE PERFORMANCE FOR ROUND 3

List	Protein	Precursors Analysed	Precursors Accepted	Precursors Rejected
A	A2M	8	5	3
	ApoE	4	4	0
	CLU	4	4	0
	CFH	7	6	1
	GSN	5	4	1
	SAP	4	4	0
	Subtotal	**32**	**27**	**5**
B	A1AG	1	1	0
	A1AT	6	3	3
	ApoA-I	6	6	0
	CERU	6	6	0
	C4A/B	7	5	2
	C3	7	5	2
	Subtotal	**33**	**26**	**7**
TOTAL		**65**	**53**	**12**

5.3.1.4. Round 4

Of the 53 considered precursors, 20 were eliminated (Table 5.13) based on the criteria outlined in Section 5.3.1. For inclusion in the final PRM assay (patient sample analysis), a total of 33 precursors were selected - three per protein – except in the case of A1AG where only one peptide was of acceptable quality. In the case of GSN, two precursors were selected instead of the required three. It was decided to reincorporate the previously-overlooked AVLTIDEK peptide, given its favourable performance during the initial phase of optimisation, resulting in a total precursor count of 34. Mass accuracy measurements in ppm contributed to final peptide selection: acceptable ppm values for peak identifications did not exceed 6.1ppm (average -0.26 ppm).

TABLE 5.13: TALLY OF PEPTIDE PERFORMANCE FOR ROUND 4

List	Protein	Precursors Analysed	Precursors Accepted	Precursors Rejected
A	A2M	5	3	2

List	Protein	Precursors Analysed	Precursors Accepted	Precursors Rejected
	ApoE	4	3	1
	CLU	4	3	1
	CFH	6	3	3
	GSN	4	3	1
	SAP	4	3	1
	Subtotal	**27**	**18**	**9**
B	A1AG	1	1	0
	A1AT	3	2	1
	ApoA-I	6	3	3
	CERU	6	3	3
	C4A/B	5	3	2
	C3	5	3	2
	Subtotal	**26**	**15**	**11**
TOTAL		**53**	**33**	**20**

The list of precursors for the final PRM assay to be conducted on patient samples is summarised in Table 5.13. The isolation list equated to approximately 4.7 seconds in single-plex PRM mode at 35 000 resolution. In duplex mode, the overall cycle time was reduced to 2.4 seconds. A higher MSX would not be acceptable for the purposes of patient sample analysis, due to the need for a sufficiently high sensitivity to detect low abundance analytes. Multiplexing may therefore not exceed a level of 2 (duplex), introducing the requirement for an excessively high cycle time. In order to maintain quantitative accuracy, cycle time should be less than 2 seconds to allow for at least six sampling points on the chromatographic curve. The cycle time of 2.4 seconds is thus acceptable, but not ideal. Sampling points on analyte chromatograms were, however, improved by the integration of retention time scheduling.

TABLE 5.14: LIST OF OPTIMAL PEPTIDES FOR FINAL PRM ASSAY

Protein	Sequence	m/z	Charge	Mass Accuracy (ppm)
A2M	NEDSLVFVQTDK (light)	697.8435	2	0.0
	FEVQVTVPK (light)	523.7977	2	0.0
	AIGYLNTGYQR (light)	628.3251	2	-0.6

Protein	Sequence	m/z	Charge	Mass Accuracy (ppm)
CFH	IDVHLVPDR (light)	532.2984	2	-0.2
	LSYTC[+57.0]EGGFR (light)	595.269	2	0.7
	AGEQVTYTC[+57.0]ATYYK (light)	827.8745	2	-1.7
ApoE	LAVYQAGAR (light)	474.7667	2	-0.1
	LGPLVEQGR (light)	484.7798	2	-0.7
	AATVGSLAGQPLQER (light)	749.4046	2	-0.9
CLU	TLLSNLEEAK (light)	559.3086	2	-0.4
	IDSLLENDR (light)	537.7749	2	0.2
	ASSIIDELFQDR (light)	697.3515	2	-1.4
GSN	EPGLQIWR (light)	499.7745	2	6.1
	QTQVSVLPEGGETPLFK (light)	915.4858	2	-0.3
	AGALNSNDAFVLK (light)	660.3513	2	-0.8
SAP	AYSLFSYNTQGR (light)	703.8386	2	-0.9
	DNELLVYK (light)	497.2662	2	-0.2
	VGEYSLYIGR (light)	578.8035	2	-3.2
A1AG	TEDTIFLR (light)	497.7638	2	-0.6
A1AT	FLENEDR (light)	461.7169	2	-0.1
	SVLGQLGITK (light)	508.3109	2	-0.4
	AVLTIDEK (light)	444.7555	2	-0.2
ApoA-I	DYVSQFEGSALGK (light)	700.8383	2	-0.6
	LLDNWDSVTSTFSK (light)	806.8963	2	-1.0
	VQPYLDDFQK (light)	626.8141	2	-0.4
CERU	EYTDASFTNR (light)	602.2675	2	0.0
	GAYPLSIEPIGVR (light)	686.3852	2	-0.1
	NNEGTYYSPNYNPQSR (light)	952.4139	2	-0.9
C3	AEFQDALEK (light)	525.7587	2	0.0
	VGDTLNLNLR (light)	557.8144	2	-0.1
	QGSFQGGFR (light)	492.2383	2	0.0
C4	TIYTPGSTVLYR (light)	685.8694	2	-0.5
	IPIEDGSGEVVLSR (light)	735.8936	2	0.0
	TGLQEVEVK (light)	501.7769	2	0.4

m/z: Mass-to-charge ratio, ppm: Parts per Million

5.3.1.5. Retention Time Scheduling

As discussed, retention time scheduling was applied, and results assessed for retention time drift outside the specified window. The Skyline-generated transition distribution plot (Figure 5.2) predicts that at most ~17 precursors can scanned concurrently when the 5-minute retention time window is used (as indicated in the figure legend). This equates to an overall cycle time of 2.4 seconds, in single-plex mode at 35 000 resolution. In duplex mode, cycle time equates to 1.2 seconds. This results in 18 points on a 15-second peptide elution curve, which

is significantly higher that the eight recommended points.[134] Since scheduling directs the instrument to scan for particular peptides in a window around their retention times, this minimises the number of peptides selected in each window.[138] This is in contrast to non-scheduled assays, which scan the entirety of the isolation list continually, leading to a waste of scanning time since all peptides are not present at all retention times. Scheduling restricts the size of the isolation list to the number of peptides eluting at that chromatographic retention time, allowing each peptide to be sampled more frequently during its elution and by extension, increases the total number of precursors that can be monitored in a single run.[138] A higher number of points on each peptide's chromatogram results in greater quantitative accuracy, since the peak shape would be a more accurate representation of the actual peptide elution.[134]

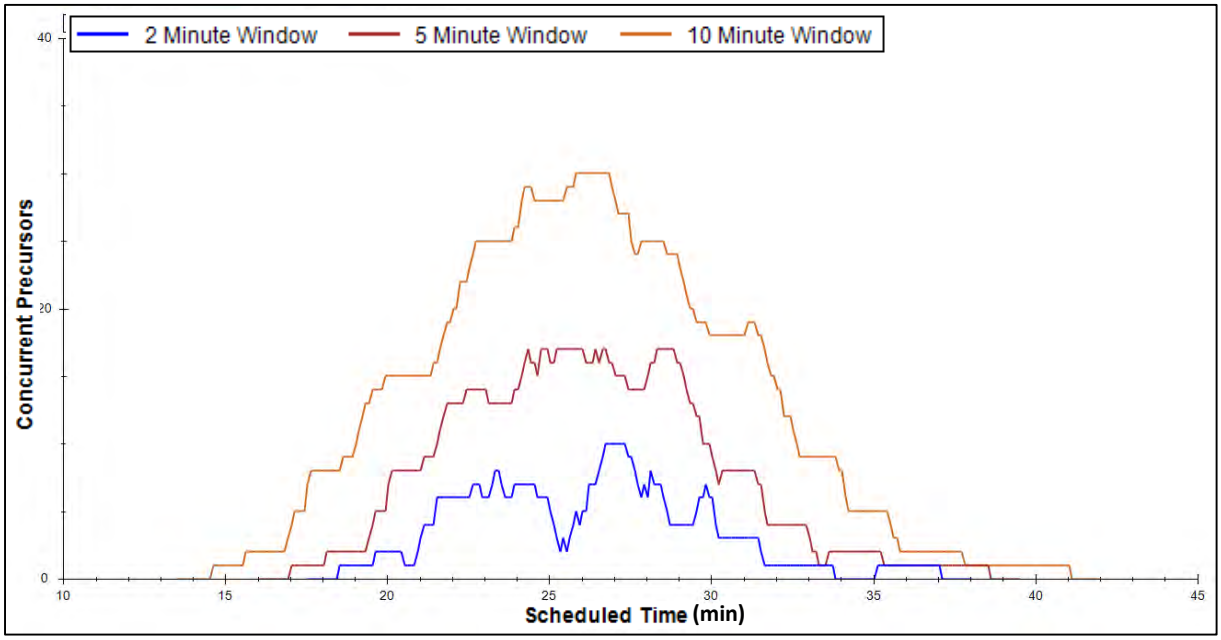

FIGURE 5.2: TRANSITION DISTRIBUTION PLOT FOR ESTIMATION OF OVERLAPPING PRECURSORS IN FINAL SCHEDULED BIOMARKER LIST

5.4. Conclusion

The list of 106 prospective peptides, derived from shotgun analysis of pooled samples, was assessed to select optimal peptides for inclusion in the final high-throughput PRM assay of patient samples. Highly-sensitive PRM assays facilitated identification of 33 optimal peptides for identification and quantitation of candidate biomarkers in patient samples (Table 5.14). As per established standards regarding representative peptides for proteomic MRM assays, three peptides were chosen as representatives of each protein.[124] An exception was made in the case of A1AG: where there were only two prospective peptides, one of which performed optimally. Retention time scheduling in the final isolation list (Table 5.9) minimised cycle time to maximise quantitative capacity. The final isolation list was utilised in a targeted assay of patient samples.

Chapter 6
Optimisation D: Selection of Reference Peptides for Normalisation

6.1. Introduction

A potential problem inherent in all sample preparation methods for MS-based quantitative proteomics is variability in peptide recovery.[190] Differential peptide recovery could lead for example, to inconsistent sample loading between replicates, and in turn to inaccurate quantitation. During in-house shotgun proteomic analyses, peptide loading quantity is determined by MS^1-TIC-based normalisation using short, data-dependent pilot analyses of all samples. The highest peptide peak of the MS^1-TIC, representing summed ion intensity for all peptides eluting during that window, is used as a relative measure of the total peptide content of each sample. Sample loading volumes are then normalised based on differential MS^1-TIC intensities. Another strategy employed is normalisation of individual peptide intensities by the ratio of total peptide intensities between samples. These methods of normalisation are, however, not feasible for targeted analyses as the total signal from all ions in the sample is not detected during typical targeted workflows.[134] Additionally, the total ion chromatogram-based method of normalisation was not feasible given the high number of samples as each sample would have to be analysed twice, first by shotgun and then by targeted analysis, in order to achieve normalisation by this means.

Quantitation of recovered peptides by alternative means could be performed, followed by adjustment of the mass of loaded peptide prior to mass spectrometric analysis. Difficulties arise, however, due to lack of availability of rapid and accurate peptide quantitation techniques. Peptide quantitation using the Bradford or BCA protein assay is not suitable due to the limited mass of peptide sample available. Additionally, dye binding assays such as the Bradford assay lack the ability to detect small peptides (<3000 Da).[191] Quantitation by HPLC-UV (high performance liquid chromatography-ultraviolet) spectroscopy and amino acid analysis are time consuming, highly-specialised techniques, and were therefore not considered.[98,192]

The ideal method by which to assess variability in peptide recovery due to sample preparation involves addition of a known quantity of heavy-labelled protein (or a protein foreign to the organism) to samples, pre-normalised to total protein, prior to downstream processing.[193] Peptides belonging to this protein can later be quantified by the targeted assay, and used to normalise the signal of the remaining analytes. This method is analogous to protein standard absolute quantification (PSAQ), where a heavy-labelled version of the target protein is spiked into the unprocessed sample to attain absolute quantitation.[194]

In the present study, addition of a protein standard to serum samples was not considered prior to commencement of sample processing. Here, we therefore opted to utilise a peptide derived from an endogenous protein as a reference to facilitate quantitative correction. Ideally, this peptide should be selected based on minimal variation across all samples, analogous to the common use of 'housekeeping' genes/proteins in DNA microarray and Western blot analyses.[195]

This chapter focuses on application of the discovery proteomic data in selecting potential reference peptides for PRM assay construction. Peptides exhibiting the least variation *during discovery analysis* are considered as reference peptide candidates for PRM assay quantitation normalisation. This includes normalisation of shotgun peptide data, assessment of the quality of these peptides by PRM analysis, and concludes with selection of the best candidates to be included in the final PRM assay.

6.2. Materials and Methods

6.2.1. Normalisation of Shotgun Peptide Data

6.2.1.1. Assessment of Peptide Raw Intensity Trends

Intensity values for all peptides identified during discovery analysis (Section 3.3.1) were extracted from the peptides.txt MaxQuant output file (data not shown), and intensities were plotted (Section 6.3.1.1) across pooled samples. A line graph was constructed in Microsoft Excel and the y-axis was $\log_{10}$-transformed to aid in interpretation. Visualisation of intensity values for each peptide facilitated determination of loading irregularities.

6.2.1.2. Normalisation

To correct for inconsistent sample loading during shotgun proteomic analysis, individual peptide intensities were normalised by the ratios of total peptide intensities across pooled samples. This strategy is analogous to MS^1-TIC-based normalisation (*vide supra*); the difference being that the MS^1-TIC constitutes all observed masses, at the MS^1 level, and is not restricted to peptides exclusively. Briefly, the raw intensities for all peptides within each sample were summed; and the totals across all samples were averaged (See Table 6.1). This average was then divided by each sum to yield a normalisation factor for each sample. Finally, normalised values were calculated by multiplying each individual peptide's intensity value by the factor for that particular sample. This normalisation method was performed to shift the data distributions of each sample relative to one another to bring them within comparable range. The intended result of this normalisation strategy was to emulate equal sample loading.

TABLE 6.1: NORMALISATION FACTOR CALCULATION FOR SHOTGUN PROTEOMIC DATA

Sample	Sum of Peptide Intensities	Average of Sums	Normalisation factor
HAD 1	49029730900	29239527311	0.596363202
HAD 2	50709959600		0.576603246
HAD 3	6439995100		4.540302726
MNI 1	52986660200		0.551828087
MNI 2	12747293200		2.293783225
MNI 3	9951835900		2.938103844
POS 1	40710368400		0.718232933
POS 2	31754061700		0.920812197
POS 3	8825840800		3.312945245

The transformed peptide intensity values were plotted across pooled samples. A line graph was constructed in Microsoft Excel, and the y-axis was $\log_{10}$-transformed to aid in interpretation (Section 6.3.1.2). Boxplots were also constructed in the R programming language to confirm success of normalisation by comparing the shotgun proteomic data distribution before and after normalisation.[196]

6.2.2. Reference Peptide Selection

The above normalisation method, however effective, was not applicable to PRM analyses. Where only a small portion of the total peptide component was measured, meaning that normalisation would have been highly subjective and would likely have suppressed true biological differences. Suitable internal reference peptides were thus identified from within the discovery analysis for inclusion in the final PRM method. Abundant peptides unlikely to fluctuate significantly between samples were deemed most suitable.

Due to the relatively low number of proteins identified during the discovery analysis (due to the complexity of plasma, as discussed in Chapter 3), there were few candidate housekeeping proteins available to choose from (Appendix B: Table 9.2). It was hypothesised that immunoglobulin G subclass 4 (IgG_4) would not fluctuate significantly between samples, given that all participants were HIV-positive, as well as the lack of IgG_4 involvement in the immune response against HIV.[197,198] Other IgG subclass peptides that did not fluctuate greatly across pooled samples following normalisation were additionally assessed in preparation for the possibility that IgG_4 peptides proved suboptimal as a basis of normalisation.

6.2.2.1. Preliminary Selection

To determine the most suitable reference peptides, raw and normalised plots for each immunoglobulin (Ig) peptide were extracted from Figure 6.1 and Figure 6.2 respectively. Peptides were selected based on visual inspection of variation in their normalised intensity plots only. Peptides were rejected if they showed visually marked differences in intensity across samples after normalisation.

6.2.2.2. Assessment and Final Selections

The 18 preliminarily selected peptides were subjected to PRM analysis on the MNI_1 pooled sample to assess quality. A total of 28 precursors (Table 6.2) were analysed by unscheduled PRM at 35 000 resolution in duplex mode, with an IT of 45 ms. Remaining settings are outlined in Table 4.13. The LC gradient used was the default 72 minute gradient designed for PRM analyses, as described in Section 5.2.2.

TABLE 6.2: UNSCHEDULED ISOLATION LIST OF PROSPECTIVE IMMUNOGLOBULIN INTERNAL STANDARD PEPTIDES

Mass [m/z]	Formula [M]	Species	CS [z]	Polarity	Start [min]	End [min]	NCE	Comment
607.3198			2	Positive			27	WLQGSQELPR (light)
644.3293			2	Positive			27	GPSVFPLAPC[+57.0]SR (light)
678.3223			2	Positive			27	TPLGDTTHTC[+57.0]PR (light)
452.5506			3	Positive			27	TPLGDTTHTC[+57.0]PR (light)
708.849			2	Positive			27	WYVDGVEVHNAK (light)
472.9017			3	Positive			27	WYVDGVEVHNAK (light)
643.8406			2	Positive			27	EPQVYTLPPSR (light)
429.5628			3	Positive			27	EPQVYTLPPSR (light)
581.3184			2	Positive			27	NQVSLTC[+57.0]LVK (light)
712.3585			2	Positive			27	STSESTAALGC[+57.0]LVK (light)
475.2414			3	Positive			27	STSESTAALGC[+57.0]LVK (light)
981.8239			3	Positive			27	YGPPC[+57.0]PSC[+57.0]PAPEFL GGPSVFLFPPKPK (light)
951.4676			2	Positive			27	TTPPVLDSDGSFFLYSR (light)
942.5073			2	Positive			27	EIVLTQSPGTLSLSPGER (light)
628.6739			3	Positive			27	EIVLTQSPGTLSLSPGER (light)
610.3357			2	Positive			27	SGTSASLAISGLR (light)
1002.505			2	Positive			27	SYELTQPPSVSVSPGQTAR (light)
668.6726			3	Positive			27	SYELTQPPSVSVSPGQTAR (light)
856.3832			2	Positive			27	SYSC[+57.0]QVTHEGSTVEK (light)
571.2579			3	Positive			27	SYSC[+57.0]QVTHEGSTVEK (light)
809.4076			2	Positive			27	QVGSGVTTDQVQAEAK (light)
539.9408			3	Positive			27	QVGSGVTTDQVQAEAK (light)
450.7687			2	Positive			27	VSVFVPPR (light)
455.2143			2	Positive			27	DGFFGNPR (light)
625.3215			2	Positive			27	LIC[+57.0]QATGFSPR (light)
417.2168			3	Positive			27	LIC[+57.0]QATGFSPR (light)
809.4076			2	Positive			27	QVGSGVTTDQVQAEAK (light)
695.3101			2	Positive			27	SSEDPNEDIVER (light)

CS: Charge State, NCE: Normalised Collision Energy.
* Isolation list columns left blank intentionally, as this is the required format from Xcalibur.

Following PRM analysis of preliminary Ig peptides, data was imported into Skyline with settings identical to those outlined in Section 4.2.2.1. A consensus set of peptides was selected for inclusion in final clinical sample analysis, by qualitative assessment of variation in intensity across samples, as well as assessment of peak quality (desirable shape, high intensity, low background, and large number of product ions) from PRM results.

6.3. Results and Discussion

6.3.1. Normalisation of Shotgun Peptide Data

6.3.1.1. Assessment of Peptide Intensity Trends

Loading consistency of shotgun proteomic analysis of pooled samples was evaluated by plotting raw peptide intensity values against pooled samples as shown in Figure 6.1(A) below, with an additional plot of log_{10}-transformed intensity values (Figure 6.1(B)) for ease of interpretation.

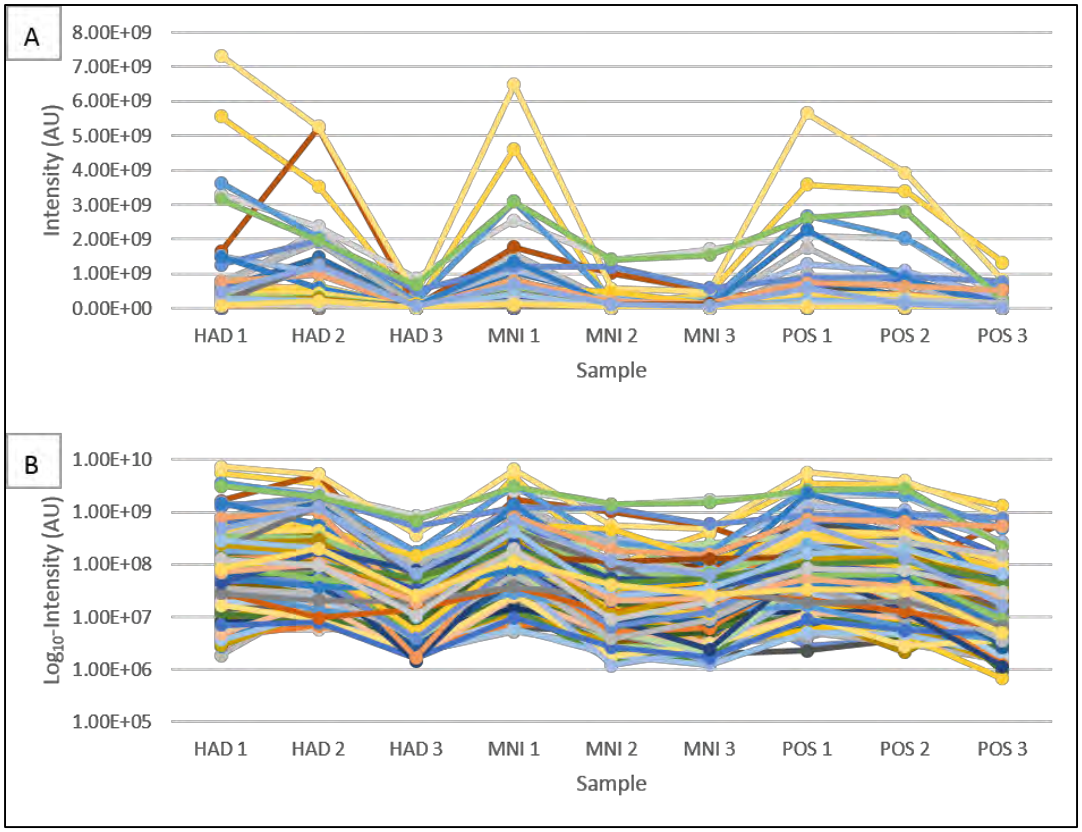

FIGURE 6.1: INTENSITY PLOT FOR ALL IDENTIFIED PEPTIDES ACROSS POOLED SAMPLES. EACH LINE REPRESENTS INDIVIDUAL PEPTIDE INTENSITY TRENDS. A: LOWER INTENSITIES APPEAR FLAT DUE TO SCALE OF PLOT, B: LOG10 TRANSFORMED PLOT FOR EASE OF INTERPRETATION.
HAD: HIV Associated Dementia, MNI: Minor Neurocognitive Impairment, POS: HIV positive control.

Peptide intensities appear to exhibit a sample-dependent trend, which implies inconsistent loading prior to mass spectrometric analysis. This suggests that inconsistent sample loading – rather than biological variation - is influencing the intensities of peptides across samples. Normalisation of these data to account for loading bias should reveal true quantitative trends.

6.3.1.2. Normalisation

Following normalisation (based on pooled shotgun data; Table 6.1), peptide intensities were re-plotted across pooled samples as shown in Figure 6.2(A) below, with an additional plot of log10-transformed intensity values (Figure 6.2(B)) for ease of interpretation.

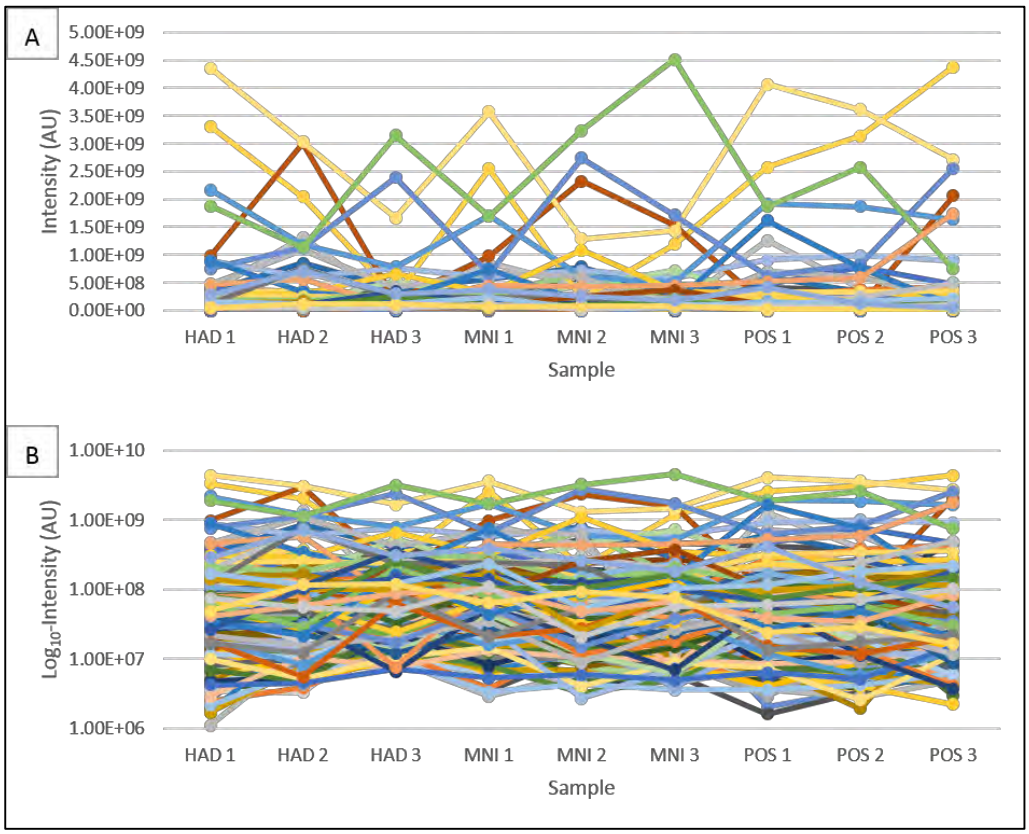

FIGURE 6.2: NORMALISED INTENSITY PLOTS FOR EACH PEPTIDE ACROSS POOLED SAMPLES. EACH LINE REPRESENTS INDIVIDUAL PEPTIDE INTENSITY TRENDS. A: LOWER INTENSITIES APPEAR FLAT DUE TO SCALE OF PLOT, B: LOG10 TRANSFORMED PLOT FOR EASE OF INTERPRETATION.
HAD: HIV Associated Dementia, MNI: Minor Neurocognitive Impairment, POS: HIV positive control.

Peptide intensities do not follow the same trends on a replicate-dependent basis, as is evident in non-normalised (raw) data. Boxplots of pre- and post-normalisation shotgun proteomic data (Figure 6.3) show the within-sample data distributions were not altered, and all sample distributions were shifted within range of one another. This normalisation strategy was deemed successful in emulating equal sample loading. These plots confirmed success of the normalisation strategy in alleviating loading bias effects; thus revealing true relative peptide levels on a 'per µg total peptide' basis, and facilitating selection of an internal reference peptide that remains relatively constant across biological replicates.

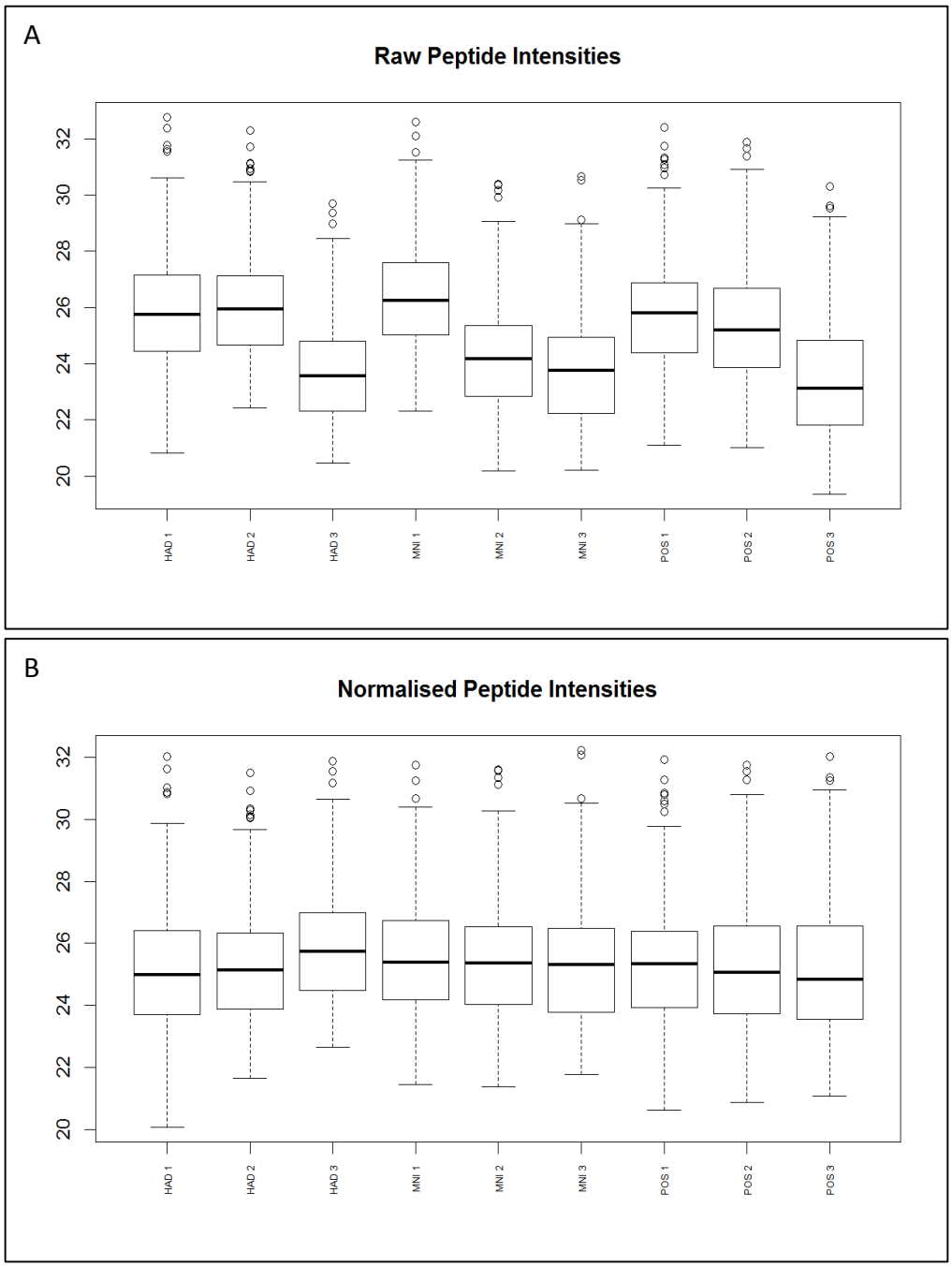

FIGURE 6.3: BOXPLOTS OF PRE- AND POST-NORMALISATION SHOTGUN PROTEOMIC DATA. A: RAW DATA, B: NORMALISED DATA

6.3.2. Reference Peptide Selection

6.3.2.1. Preliminary Selection

Ig peptides were assessed for suitability as internal reference peptides based on their intensity profiles before and after normalisation. Of the total identified Ig peptides, 18 were chosen as prospective standards (Figure 6.4).

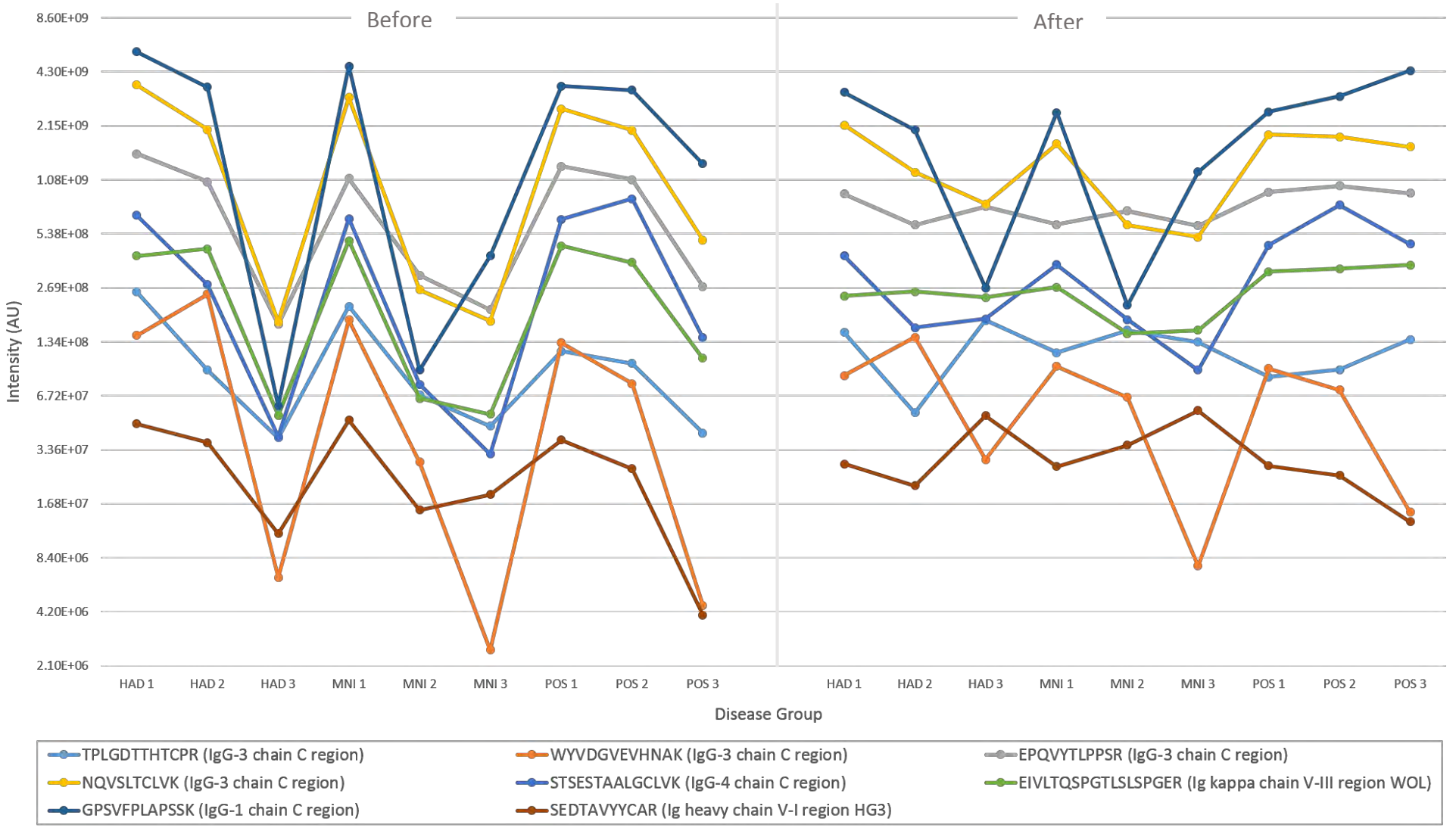

FIGURE 6.4: RAW INTENSITY PLOTS OF PRELIMINARILY SELECTED IG PEPTIDES BEFORE AND AFTER NORMALISATION. INTENSITIES ARE LOG_2-NORMALISED

These peptides were chosen based on visual assessment of decrease in variation across samples following normalisation. As can be seen in the left panel of Figure 6.4, most peptides exhibited intensity profiles similar to the overall trend seen in Figure 6.1. Following normalisation, these profiles appeared to flatten suggesting that the concentrations of these peptides were actually consistent across samples (peptides GPSVFPLAPSSK and WYVDGEVHNAK being obvious exceptions). Peptide EPQVYTLPPSR in particular appeared to exhibit low variation following normalisation, and represented a likely candidate for use as the final internal reference peptide.

The final list of prospective peptides is shown in Table 6.3 including charge states as identified by MaxQuant analysis. These peptides required verification by PRM analysis to be considered for use as internal references in the final PRM assay.

TABLE 6.3: LIST OF INTERNAL REFERENCE PEPTIDE CANDIDATES

Sequence	Protein	Charge
DGFFGNPR	Ig mu chain C region	2
EIVLTQSPGTLSLSPGER	Ig kappa chain V-III region WOL	2, 3
EPQVYTLPPSR	Ig gamma-3 chain C region	2, 3
GPSVFPLAPC[+57.0]SR	Ig gamma-1 chain C region	2
LIC[+57.0]QATGFSPR	Ig mu chain C region	2, 3
NQVSLTC[+57.0]LVK	Ig gamma-3 chain C region	2
QVGSGVTTDQVQAEAK	Ig mu chain C region	2, 3
SGTSASLAISGLR	Ig kappa chain C region	2
SSEDPNEDIVER	Immunoglobulin J chain	2
STSESTAALGC[+57.0]LVK	Ig gamma-4 chain C region	2, 3
SYELTQPPSVSVSPGQTAR	Ig lambda chain V-IV region Hil	2, 3
SYSC[+57.0]QVTHEGSTVEK	Ig lambda-2 chain C regions	2, 3
TPLGDTTHTC[+57.0]PR	Ig gamma-3 chain C region	2, 3
TTPPVLDSDGSFFLYSR	Ig gamma-4 chain C region	2
VSVFVPPR	Ig mu chain C region	2
WLQGSQELPR	Ig alpha-2 chain C region	2
WYVDGVEVHNAK	Ig gamma-3 chain C region	2, 3
YGPPC[+57.0]PSC[+57.0]PAPEFLGGPSVFLFPPKPK	Ig gamma-4 chain C region	3

6.3.2.2. Assessment and Final Selections

Following PRM analysis of the set of preliminary Ig peptides, a final set of six were chosen to be included in the final analytical runs. The list of selected peptides included TPLGDTTHTC[+57.0]PR, WYVDGVEVHNAK, EPQVYTLPPSR, NQVSLTC[+57.0]LVK, STSESTAALGC[+57.0]LVK, and EIVLTQSPGTLSLSPGER. Figure 6.5 shows transition chromatograms extracted from Skyline for the selected peptides. This selection was based on optimal peak characteristics (using exclusion criteria previously defined in Chapter 5, Section 5.3.1), as well as ideal post-normalisation profiles.

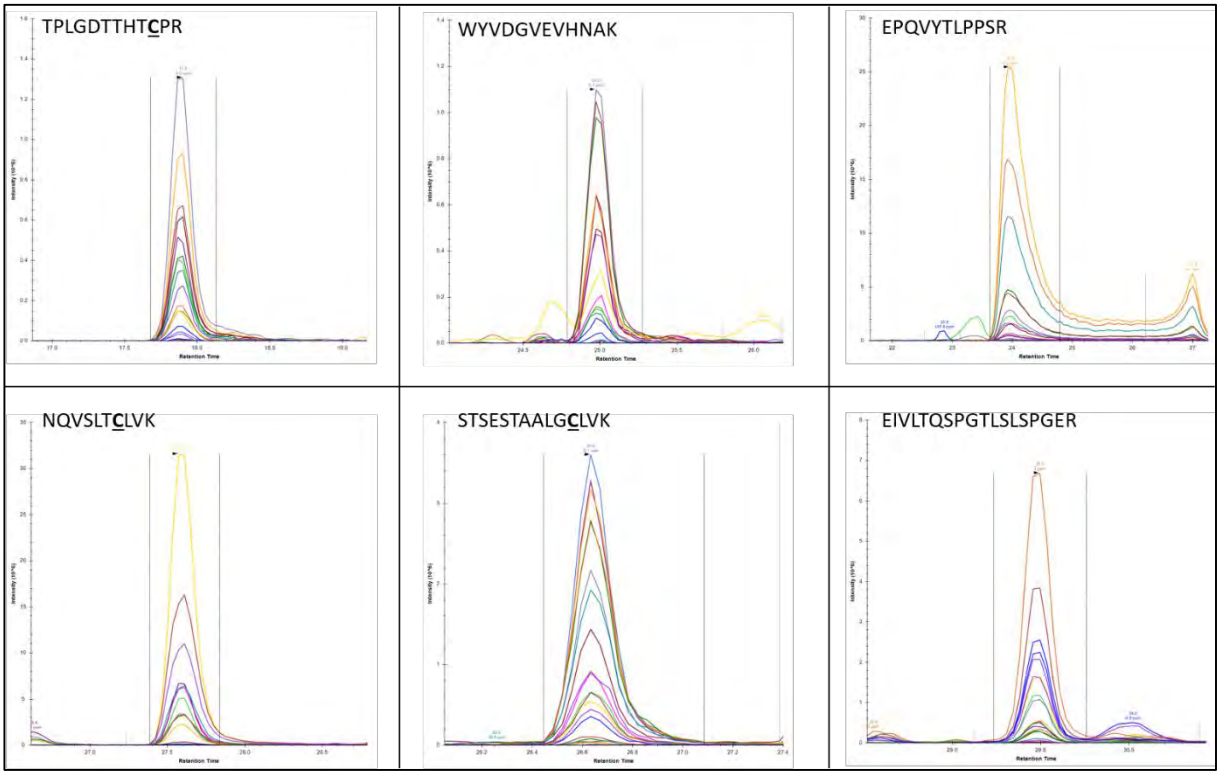

FIGURE 6.5: SKYLINE CHROMATOGRAMS FOR SELECTED IMMUNOGLOBULIN PEPTIDES. NOTE THAT AXES FOR EACH PEPTIDE ARE NOT AT THE SAME SCALE. INTENSITY SHOWN ON EACH Y-AXIS, AND RETENTION TIME (IN MINUTES) ON EACH X-AXIS

Precursor charge states of 2+ and 3+ were used for all peptides chosen for integration into the final PRM method, except NQVSLTC[+57.0]LVK (Table 6.4). Only one of the six peptides originated from IgG_4, four were IgG_3 peptides, and one belonged to the Ig kappa chain.

TABLE 6.4: FINAL LIST OF INTERNAL REFERENCE PEPTIDES

Sequence	Protein	m/z	Charge
EIVLTQSPGTLSLSPGER	Ig kappa chain V-III region WOL	942.5073	2+
EIVLTQSPGTLSLSPGER	Ig kappa chain V-III region WOL	628.6739	3+
EPQVYTLPPSR	Ig gamma-3 chain C region	643.8406	2+
EPQVYTLPPSR	Ig gamma-3 chain C region	429.5628	3+
NQVSLTC[+57.0]LVK	Ig gamma-3 chain C region	581.3184	2+
STSESTAALGC[+57.0]LVK	Ig gamma-4 chain C region	712.3585	2+
STSESTAALGC[+57.0]LVK	Ig gamma-4 chain C region	475.2414	3+
TPLGDTTHTC[+57.0]PR	Ig gamma-3 chain C region	678.3223	2+
TPLGDTTHTC[+57.0]PR	Ig gamma-3 chain C region	452.5506	3+
WYVDGVEVHNAK	Ig gamma-3 chain C region	708.849	2+
WYVDGVEVHNAK	Ig gamma-3 chain C region	472.9017	3+

m/z: Mass-to-charge ratio

The Skyline chromatograms shown in Figure 6.5 indicate high peak intensities for the selected peptides, with NQVSLTCLVK and EPQVYTLPPSR significantly dominating. Of the chosen peptides, EPQVYTLPPSR; NQVSLTCLVK; and TPLGDTTHTCPR appeared to be best suited for use as internal standards, based on their apparently low variation across samples following normalisation. The IgG_4 peptide STSESTAALGC[+57.0]LVK was deemed the optimal internal reference, consistent with our original hypothesis.

It was deemed prudent to include several potential reference peptides during clinical sample assays, however, in the case of sub-optimal performance of the single chosen peptide across all sample analysis runs. The final Scheduled IgG isolation list, including a final set of six peptides (11 precursors, Table 6.5), was generated for integration into the final analytical PRM method. Five minute retention time scheduling windows were used, based on analysis of the MNI_1 sample.

TABLE 6.5: SCHEDULED ISOLATION LIST OF SELECTED INTERNAL REFERENCE PEPTIDES

Mass [m/z]	Formula [M]	Species	CS [z]	Polarity	Start [min]	End [min]	NCE	Comment
678.3223			2	Positive	15.4	20.4	27	TPLGDTTHTC[+57.0]PR (light)
452.5506			3	Positive	15.4	20.4	27	TPLGDTTHTC[+57.0]PR (light)
708.849			2	Positive	22.47	27.47	27	WYVDGVEVHNAK (light)
472.9017			3	Positive	22.47	27.47	27	WYVDGVEVHNAK (light)
643.8406			2	Positive	21.46	26.46	27	EPQVYTLPPSR (light)
429.5628			3	Positive	21.46	26.46	27	EPQVYTLPPSR (light)
581.3184			2	Positive	25.07	30.07	27	NQVSLTC[+57.0]LVK (light)

Mass [m/z]	Formula [M]	Species	CS [z]	Polarity	Start [min]	End [min]	NCE	Comment
712.3585			2	Positive	24.13	29.13	27	STSESTAALGC[+57.0]LVK (light)
475.2414			3	Positive	24.13	29.13	27	STSESTAALGC[+57.0]LVK (light)
942.5073			2	Positive	27	32	27	EIVLTQSPGTLSLSPGER (light)
628.6739			3	Positive	27	32	27	EIVLTQSPGTLSLSPGER (light)

CS: Charge State, NCE: Normalised Collision Energy.
* Isolation list columns left blank intentionally, as this is the required format from Xcalibur.

6.4. Conclusions

Internal reference peptides were required to control for variance in inter-replicate peptide abundances due to unavoidable sample preparation – and therefore peptide loading – inconsistencies. Prospective reference peptides were selected based on qualitative evaluation of their intensities across pooled samples analysed by discovery MS. Final peptide selection was based on qualitative assessment of inter-replicate variation following normalisation, as well as membership to IgG subclasses that do not vary greatly in HIV. Selection of the final list of reference peptides was also based on satisfactory performance in preliminary PRM analysis. For redundancy, six peptides were selected for use in the final assay, with a view to selecting the ultimate normalisation peptide once all samples had been analysed.

Chapter 7
High-throughput Parallel Reaction Monitoring Assay of Clinical Samples

7.1. Introduction

Comprehensive development steps were required to build a PRM assay, *de novo*, for quantitative analysis of candidate Alzheimer's protein biomarkers in blood serum. Development required extensive optimisation of instrument settings, as well as selection of representative peptides that would enable selective and sensitive quantitation of markers. Prospective representative peptides were selected based on shotgun proteomic analysis of patient serum pooled to enable unbiased detection of peptides (Chapter 3). Instrument parameters were optimised for PRM analysis on the Q Exactive Quadrupole-Orbitrap mass spectrometer as literature in this area was incomplete at the time of developing the assay (Chapter 4). Candidate peptides identified during the previous step were assessed by PRM analysis with optimised settings, to identify those optimal for identification and quantitation of parent proteins in the final analytical PRM assay utilising clinical samples (Chapter 5). Internal reference peptides were chosen from shotgun analysis and optimised by PRM analysis to correct for sample recovery inconsistencies evident during discovery analysis (Chapter 6).

Regarding the applicability of Ig peptides as internal reference peptides (Chapter 3): As all patients were HIV positive, it was hypothesised that IgG levels may not fluctuate excessively within disease groups, and could thus be utilised post-hoc to correct for loading differences between samples within a group. Assessment of PRM data largely supports this hypothesis, although the literature suggests that HIV-positive patient total IgG levels do vary.[197] IgG_4 was considered the most likely candidate since its levels are not affected by HIV-infection.[197] On these bases, it was decided to utilise IgG_4 for normalisation of raw data, and to compare analysis outcomes with those from data normalised by total peptide quantitation (*vide infra*).

Extensive assay development has culminated in a finalised PRM assay applicable to clinical samples. Indeed the optimised assay may be utilised to analyse the identified markers of interest in any sample set. This chapter discusses application of the final PRM assay to 81 clinical samples in a high throughput manner to assess the major study hypothesis; that a

panel of AD biomarkers may also be applicable to the diagnosis of HAND, given the underlying molecular similarities between these two disease states.

7.2. Materials and Methods

7.2.1. Sample Preparation

Stored serum peptide samples (preparation described in Chapter 2) were reconstituted in 25 µl 2%ACN/0.1% FA to yield a stock solution with an estimated concentration of 0.4 µg/µl (assuming no loss during in-gel digest). A 25 ng/µl solution was prepared by 16-fold dilution of the stock solution. Samples were loaded into 2 ml autosampler vials with tapered 100 µl glass inserts (Macherey-Nagal), and stored at 4°C until mass spectrometric analysis using instruments and parameters described below.

7.2.2. Analytical Parameters

7.2.2.1. Isolation List Considerations

The PRM assay isolation list was constructed by combining the final isolation lists from sample and internal standard method development (Table 7.1), and included RT scheduling. Analytical parameters such as MSX and Max IT were selected based on the consideration that a minimum cycle time of 2 seconds was required. All parameter changes are for a resolution setting of 35 000.

TABLE 7.1: SCHEDULED ISOLATION LIST FOR FINAL PRM ANALYSIS

Mass [m/z]	Formula [M]	Species	CS [z]	Polarity	Start [min]	End [min]	NCE	Comment
697.8435			2	Positive	24.5	29.5	27	NEDSLVFVQTDK (light)
523.7977			2	Positive	24.19	29.19	27	FEVQVTVPK (light)
628.3251			2	Positive	22.41	27.41	27	AIGYLNTGYQR (light)
532.2984			2	Positive	21.63	26.63	27	IDVHLVPDR (light)
595.269			2	Positive	21.81	26.81	27	LSYTC[+57.0]EGGFR (light)
827.8745			2	Positive	21.13	26.13	27	AGEQVTYTC[+57.0]ATYYK (light)
474.7667			2	Positive	18.08	23.08	27	LAVYQAGAR (light)
484.7798			2	Positive	19.98	24.98	27	LGPLVEQGR (light)
749.4046			2	Positive	21.96	26.96	27	AATVGSLAGQPLQER (light)
559.3086			2	Positive	26.58	31.58	27	TLLSNLEEAK (light)
537.7749			2	Positive	21.67	26.67	27	IDSLLENDR (light)
697.3515			2	Positive	33.58	38.58	27	ASSIIDELFQDR (light)

Mass [m/z]	Formula [M]	Species	CS [z]	Polarity	Start [min]	End [min]	NCE	Comment
499.7745			2	Positive	26.41	31.41	27	EPGLQIWR (light)
915.4858			2	Positive	28.3	33.3	27	QTQVSVLPEGGETPLFK (light)
660.3513			2	Positive	25.07	30.07	27	AGALNSNDAFVLK (light)
703.8386			2	Positive	26.58	31.58	27	AYSLFSYNTQGR (light)
497.2662			2	Positive	23.84	28.84	27	DNELLVYK (light)
578.8035			2	Positive	25.22	30.22	27	VGEYSLYIGR (light)
497.7638			2	Positive	24.68	29.68	27	TEDTIFLR (light)
461.7169			2	Positive	17.04	22.04	27	FLENEDR (light)
508.3109			2	Positive	26.72	31.72	27	SVLGQLGITK (light)
444.7555			2	Positive	20.13	25.13	27	AVLTIDEK (light)
700.8383			2	Positive	27.95	32.95	27	DYVSQFEGSALGK (light)
806.8963			2	Positive	30.3	35.3	27	LLDNWDSVTSTFSK (light)
626.8141			2	Positive	24.24	29.24	27	VQPYLDDFQK (light)
602.2675			2	Positive	19.51	24.51	27	EYTDASFTNR (light)
686.3852			2	Positive	28.11	33.11	27	GAYPLSIEPIGVR (light)
952.4139			2	Positive	20	25	27	NNEGTYYSPNYNPQSR (light)
525.7587			2	Positive	21.44	26.44	27	AEFQDALEK (light)
557.8144			2	Positive	24.94	29.94	27	VGDTLNLNLR (light)
492.2383			2	Positive	19.36	24.36	27	QGSFQGGFR (light)
685.8694			2	Positive	24.66	29.66	27	TIYTPGSTVLYR (light)
735.8936			2	Positive	24.13	29.13	27	IPIEDGSGEVVLSR (light)
501.7769			2	Positive	19.61	24.61	27	TGLQEVEVK (light)
678.3223			2	Positive	15.4	20.4	27	TPLGDTTHTC[+57.0]PR (light)
452.5506			3	Positive	15.4	20.4	27	TPLGDTTHTC[+57.0]PR (light)
708.849			2	Positive	22.47	27.47	27	WYVDGVEVHNAK (light)
472.9017			3	Positive	22.47	27.47	27	WYVDGVEVHNAK (light)
643.8406			2	Positive	21.46	26.46	27	EPQVYTLPPSR (light)
429.5628			3	Positive	21.46	26.46	27	EPQVYTLPPSR (light)
581.3184			2	Positive	25.07	30.07	27	NQVSLTC[+57.0]LVK (light)
712.3585			2	Positive	24.13	29.13	27	STSESTAALGC[+57.0]LVK (light)
475.2414			3	Positive	24.13	29.13	27	STSESTAALGC[+57.0]LVK (light)
942.5073			2	Positive	27	32	27	EIVLTQSPGTLSLSPGER (light)
628.6739			3	Positive	27	32	27	EIVLTQSPGTLSLSPGER (light)

CS: Charge State, NCE: Normalised Collision Energy.
* Isolation list columns left blank intentionally, as this is the required format from Xcalibur.

7.2.2.2. Instrument Parameters

Optimised instrument parameters developed in Chapter 4 were applied to the final PRM analysis at 35 000 resolution in duplex mode (Table 7.2).

TABLE 7.2: FINAL SETTINGS FOR PRM ANALYSES AT 35 000 RESOLUTION.

Resolution	35000
Lock masses	Off
Chrom peak width	15 s
Charge state	2
AGC Target	5.00E+06
ISO Window	2 m/z
NCE	27
MSX	2
Max IT	45 ms
Precursors	45

AGC: Automatic Gain Control, ISO: Isolation, NCE: Normalised Collision Energy, MSX: Multiplex level, Max IT: Maximum Injection time.

7.2.3. LC/MS Instrumentation and Parameters

Targeted proteomic analysis was performed on a Q Exactive Quadrupole-Orbitrap Mass Spectrometer, coupled to a Dionex UltiMate 3500 RSLC nano-LC system. Approximately 125 ng of pooled peptide digest was injected by partial loop injection onto a trap column packed in-house with Luna C18 coated silica beads (75 µm x 2 cm, 5 µm). Separation was performed by reversed phase chromatography on a nanoscale analytical column, also packed in-house with Luna C18 resin (75 µm x 20 cm). Ionisation was attained by application of charge across a steel emitter tip fixed to the end of the analytical column. Solvent A was composed of 0.1% FA in UHPLC-grade H_2O, while Solvent B (B) consisted of 0.1% FA in UHPLC-grade ACN. A shortened 72 minute linear gradient, developed for rapid targeted analysis, was applied at a constant flow rate of 300 nl/min as follows: 2% B for 5 minutes, 2-35% B over 35 minutes, 35-80% B over 5 minutes, held at 80% B for 15 minutes, before returning to 2% B in 2 minutes, followed by re-equilibration at 2% B for 10 minutes.

Samples were analysed in batches equivalent to those used during sample preparation (Appendix A: Table 8.1). Samples from within the same disease groups were analysed consecutively, followed by a blank, to prevent carryover (if any) between different sample types. An additional blank was added between batches. No technical replicates were analysed due to limitations on sample preparation time and mass spectrometric analysis time. The order of analysed samples is shown in Table 7.3. The discrepancies evident in batches five and

nine are due to sample mislabelling and subsequent correction, leading to disproportionate disease group distributions. This is not expected to negatively affect the analysis.

TABLE 7.3: SEQUENCE OF SAMPLES FOR TARGETED ANALYSIS

B3_32N	B4_180N	B8_68N	B6_224N	B7_26N
B3_213N	B4_203N	B8_237N	B6_142N	B7_135N
B3_231N	B4_67N	B8_215N	B6_260N	B7_35N
Blank_Batch3_P1	Blank_Batch4_P1	Blank_Batch8_P1	Blank_Batch6_P1	Blank_Batch7_P1
B3_156M	B4_137M	B8_183M	B6_43M	B7_152M
B3_40M	B4_214M	B8_47M	B6_167M	B7_79M
B3_125M	B4_63M	B8_74M	B6_003M	B7_201M
Blank_Batch3_P2	Blank_Batch4_P2	Blank_Batch8_P2	Blank_Batch6_P2	Blank_Batch7_P2
B3_25H	B4_148H	B8_16H	B6_147H	B7_005H
B3_206H	B4_38H	B8_132H	B6_50H	B7_225H
B3_126H	B4_130H	B8_24H	B6_236H	B7_198H
Blank_Batch3_P3	Blank_Batch4_P3	Blank_Batch8_P3	Blank_Batch6_P3	Blank_Batch7_P3
Wash_Batch3	Wash_Batch4	Wash_Batch8	Wash_Batch6	Wash_Batch7

B9_207M	B2_87N	B5_09N	B1_61N
B9_36M	B2_204N	B5_81N	B1_200N
Blank_Batch9_P1-MID	B2_31N	Blank_Batch5_P1-MID	B1_223N
B9_239N	Blank_Batch2_P1	B5_59M	Blank_Batch1_P1
Blank_Batch9_P1	B2_56M	Blank_Batch5_P1	B1_179M
B9_207M	B2_193M	B5_20M	B1_27M
B9_36M	B2_146M	B5_136M	B1_209M
Blank_Batch9_P2-MID	Blank_Batch2_P2	B5_29M	Blank_Batch1_P2
B9_239N	B2_229H	Blank_Batch5_P2	B1_10H
Blank_Batch9_P2	B2_166H	B5_04H	B1_149H
B9_106H	B2_30H	B5_97H	B1_104H
B9_202H	Blank_Batch2_P3	B5_172H	Blank_Batch1_P3
B9_216H	Wash_Batch2	Blank_Batch5_P3	Wash_Batch1
Blank_Batch9_P3		Wash_Batch5	
Wash_Batch9			

7.2.4. Preliminary Data and Repeat Analyses

Following the first round of analyses, each data file was assessed for quality by viewing Thermo .raw files in Xcalibur Qual Browser (version 3.0, Thermo Scientific). Samples with irregular MS^2-TIC profiles were marked for repeat analysis (Section 7.3.2). In the event that repeat analyses did not yield improved results, injection volumes were doubled and samples re-analysed. In cases where the MS^2-TIC displayed unusually low intensity (in the original analysis), those samples were reanalysed with doubled injection volumes from the outset.

7.2.5. Data Curation

All data files, including those with irregular MS^2-TICs, were imported into Skyline (Section 4.2.2.1) for evaluation. Annotations were set up in Skyline to categorise the samples based on disease status and patient identifier. The disease state ('Condition') consisted of CTRL, MNI, or HAD. Patient identifier ('BioReplicate') was populated with numerical patient identifiers linked to each sample. Each sample, once imported, was designated as belonging to one of the three disease groups, and numerical patient identifiers were entered.

Skyline analysis, being more thorough than the initial MS^2-TIC assessment (*vide supra)*, was utilised to exclude sub-standard samples in order to prevent skewing of data. Chromatographic exclusion criteria included peak broadening and excessive drift, significantly misaligned transitions for the majority of peptides, and missing peaks for the majority of assessed peptides. Product ions were excluded from further analysis based on detection and signal consistency: regarding the former, ions not detected in all samples were excluded; regarding the latter, ions for which peak areas normalised to total signal still yielded unequal transition intensities across samples were excluded.[199] Exceptions were made in cases where the varying ions were the only ions present in particular samples.

Of the three peptides targeted per protein, two were used for quantitation, while the remaining peptide was employed for confirmation of identity.[134] Quantitative peptides were selected based on similar average intensity trends across disease states, as well as ideal peak properties outlined in the exclusion criteria above.[134] Measurement of three peptides also increased the likelihood that two peptides would be available for quantitation in the event that one performed sub-optimally. Five product ions per peptide were selected for quantitation purposes.[134,189,199]

7.2.6. Power Analysis

Sample size estimations for PRM analyses were based on coefficient of variation (CV) of the analytical method, and expected fold-change of the mean.[200,201] Sample size estimations, developed by van Belle et al.[201], were obtained from tabulated values corresponding to CV and fold changes. This calculation assumes a significance level (α) of 0.05, predicted power ($1-\beta$) of 0.80, and applies to independent samples *t*-tests with unknown biological variance.[201] Data obtained from PRM analysis of repeated injection replicates using the final method

(Table 7.1), was used to calculate the average CV applicable to the PRM assay. Four replicate PRM analyses of sample 142N were performed, followed by selection of optimal product ions for each peptide as outlined in Section 7.2.5. All prospective internal reference peptides were removed except for STSESTAALGC[+57.0]LVK. Skyline-calculated CVs for each peptide were exported and the average CV calculated. This value was used to estimate the sample size required for a power of 0.8.

7.2.7. Data Handling and Statistical Analyses

7.2.7.1. Data Export and Manipulation

Data was exported from Skyline in the form of a .csv report file, such that the total peak area for each peptide was calculated from the areas of their constituent ions. Data was then manually rearranged in Microsoft Excel, where the total peak area for the two peptides belonging to each protein were averaged to yield a final area value. Protein names were represented by UniProt identifiers, sample names were removed, and patient identifiers replaced by sequential numbering. The data were then split into separate .csv files according to disease group for downstream statistical analysis.

7.2.7.2. Data Normalisation

INTERNAL REFERENCE PEPTIDE NORMALISATION

Protein intensities were normalised relative to the internal reference peptide (STSESTAALGC[+57.0]LVK) derived from the parent protein IgG_4. Protein intensities in a given replicate were divided by the intensity of the reference peptide present in the same replicate, after which the quotient was multiplied by the average intensity of the internal reference peptide across all replicates, as described in Teleman et al.[140]

NANODROP NORMALISATION

In the event of substandard performance of the internal reference-based normalisation, total peptide-based normalisation was also conducted. Stock peptide samples (0.4 µg/µl) were measured using a NanoDrop 1000 Spectrophotometer (Thermo Scientific) at 214nm wavelength for quantitation of peptide bonds.[98] Eight absorbance measurements were taken for each of the 55 samples selected for final analysis, and the average absorbance value calculated. Each sample absorbance was then divided by the average absorbance across all samples, to yield a normalisation factor for each sample (data not shown). Finally, each

protein intensity value was multiplied by the normalisation factor for its respective sample. (Appendix C: Table 11.2).

7.2.7.3. Statistical Assessment

An R-script, generously provided by Dr Janique Peyper (IDM, University of Cape Town), was used for normality assessment and statistical tests.[196,202,203] All data were log_2-transformed prior to visualisation and statistical analysis. Data were assessed for normality by visual inspection of histograms constructed for each peptide across all samples within each respective disease group.[204] A Shapiro-Wilk test for normality was also conducted to confirm visual findings by evaluating normality of the data in an unbiased fashion.[205]

Statistical tests comparing each protein between groups (Control vs MNI, MNI vs HAD, and Control vs HAD) were conducted on data normalised by the aforementioned methods, in the R statistical computing language.[196] Samples were not stratified based on age, as analysed patient samples fell within a narrow age range (23-30 years). Additionally, sample stratification based on gender was not conducted as 83% of analysed samples were derived from female patients. Welch's unequal variances *t*-tests were conducted on all proteins, but were most effective when applied to proteins that were normally distributed in all three patient groups.[206,207] Welch's *t*-test was used to account for potential heteroscedasticity, and unequal sample sizes.[206,208] For peptides whose distributions were non-normal, a non-parametric Wilcoxon rank sum test was appropriate to assess statistical significance of differences.[209] Group comparisons were initially conducted without applying multiple testing correction in order to assess the data in a less stringent manner. In the event of proteins showing significant differences between disease groups, multiple testing correction using Bonferroni correction would be applied.[210,211] Bar graphs plotting group means, with standard error of the mean (SEM) error bars were constructed to visually assess *t*-test data.[204]

7.3. Results and Discussion

7.3.1. Analytical Parameters

7.3.1.1. Isolation List Considerations

The final scheduled list included 45 peptides, 11 of which were considered internal reference peptides (Table 7.1). These 45 peptides represented a parent protein panel consisting of the

12 candidate AD biomarkers being evaluated here: A2M, CLU, C3, C4, CH, ApoE, SAP, ApoA-I, GSN, A1AG, A1AT, and CERU. This list size would result in an overall cycle time of 6.3 seconds, which is too long for acceptable quantitation as this would equate to two sampling points on an average 15 second chromatogram. With application of 5 minute scheduling windows, the overall cycle time would vary across different precursors within a sample. This is not detrimental, however, as consistent quantitation is only necessary between each precursor across samples. It can be observed from the transition distribution plot generated in Skyline (Figure 7.1), that during the 5 minute retention time window (blue graph) at most 25 precursors are scanned concurrently. This equates to an overall maximum cycle time of 3.5 seconds, which is still too high. Analysis in duplex mode would essentially halve the list length, yielding an overall cycle time of 1.75 seconds at the retention time where most precursors overlap. A cycle time of 1.75 seconds results in an average of 9 points on a 15 second chromatographic curve. This is acceptable, considering that peptides which do not have overlapping retention times with others will result in superior quantitation. Duplex mode was therefore employed during the final analysis.

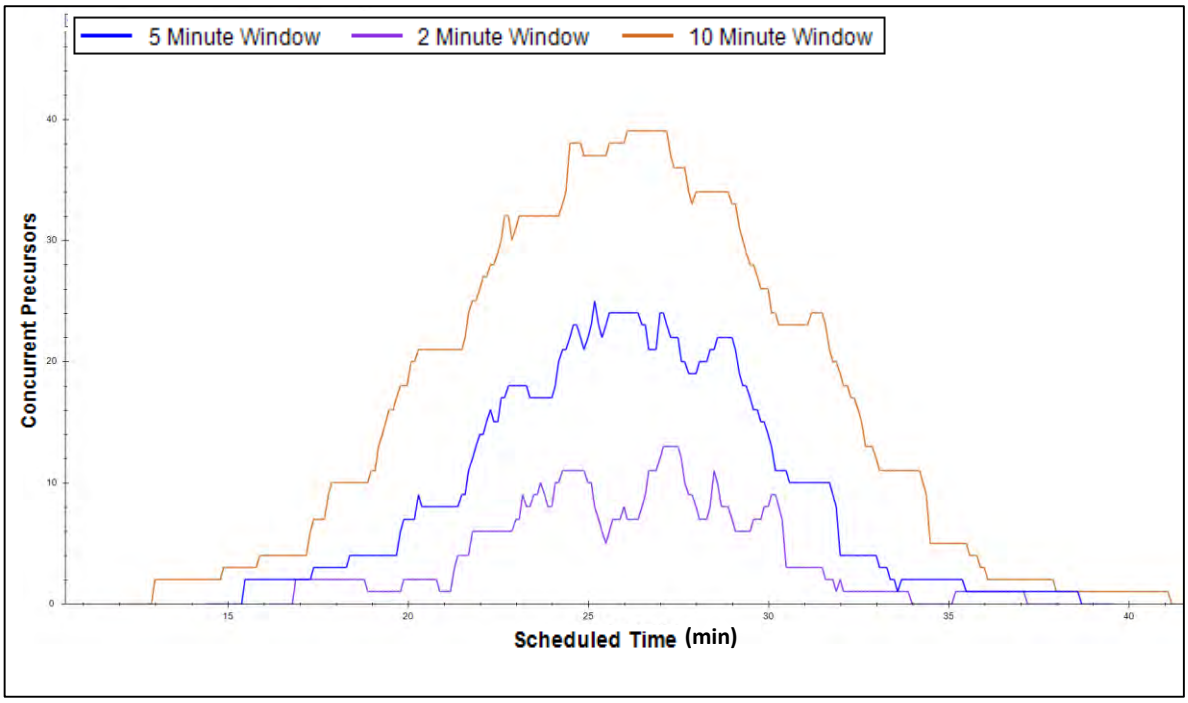

FIGURE 7.1: TRANSITION DISTRIBUTION PLOT FOR ESTIMATION OF OVERLAPPING PRECURSORS IN FINAL ASSAY (INCLUDING INTERNAL REFERENCE PEPTIDES)

7.3.2. Preliminary Data and Repeat Analyses

As outlined above, samples were selected for repeat analysis by assessment of MS^2-TICs. Examples of samples exhibiting desirable MS^2-TIC profiles are shown in Figure 7.2-A. Samples exhibiting poor MS^2-TIC profiles (Figure 7.2-B-D) were reanalysed.

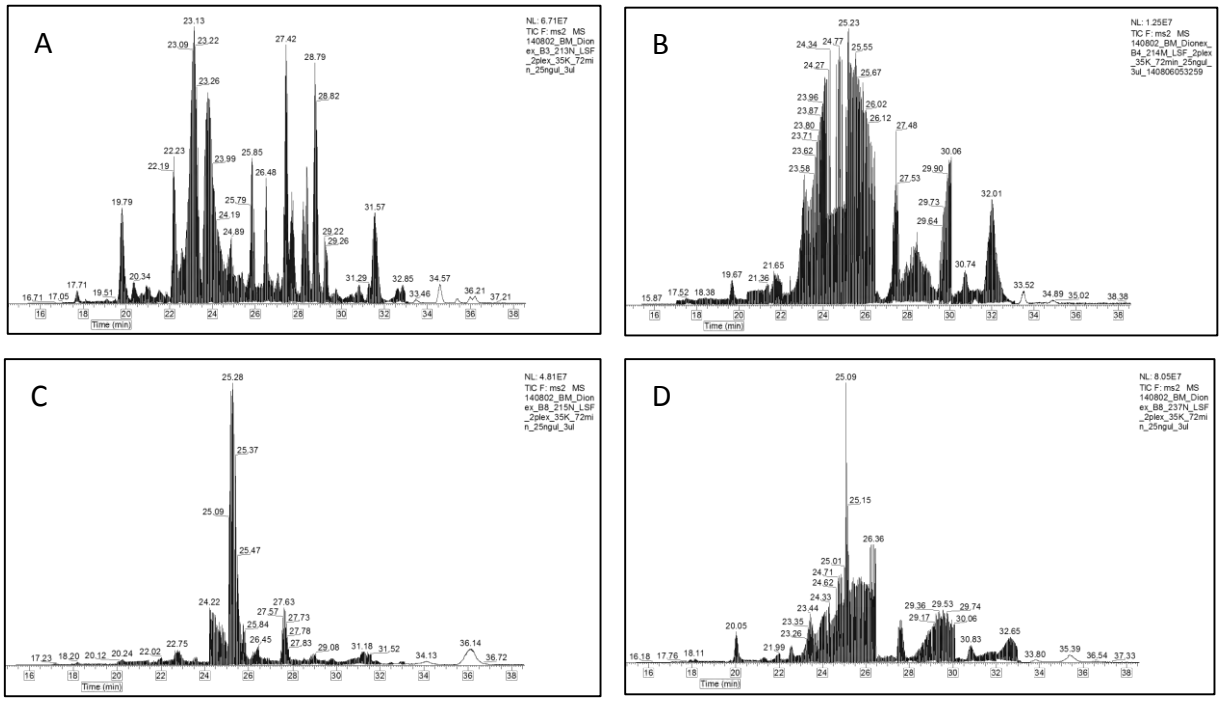

FIGURE 7.2: EXAMPLES OF DESIRABLE AND POOR MS^2-TICS FOR SAMPLE QUALITY ASSESSMENT. A: DESIRABLE CHROMATOGRAM, B-D: POOR CHROMATOGRAMS.

7.3.3. Data Curation

Data quality was assessed based on criteria outlined in Section 7.2.5. Examples of samples possessing mostly good peaks are shown in Figure 7.3-A. Samples were excluded if a substantial number of their peptides were of poor quality based on: unsatisfactory peak shape (Figure 7.3-B), significant peak broadening (Figure 7.3-B and D), retention time drift (Figure 7.3-C), missing transitions (Figure 7.3-E), or no peak detection (Figure 7.3-F).

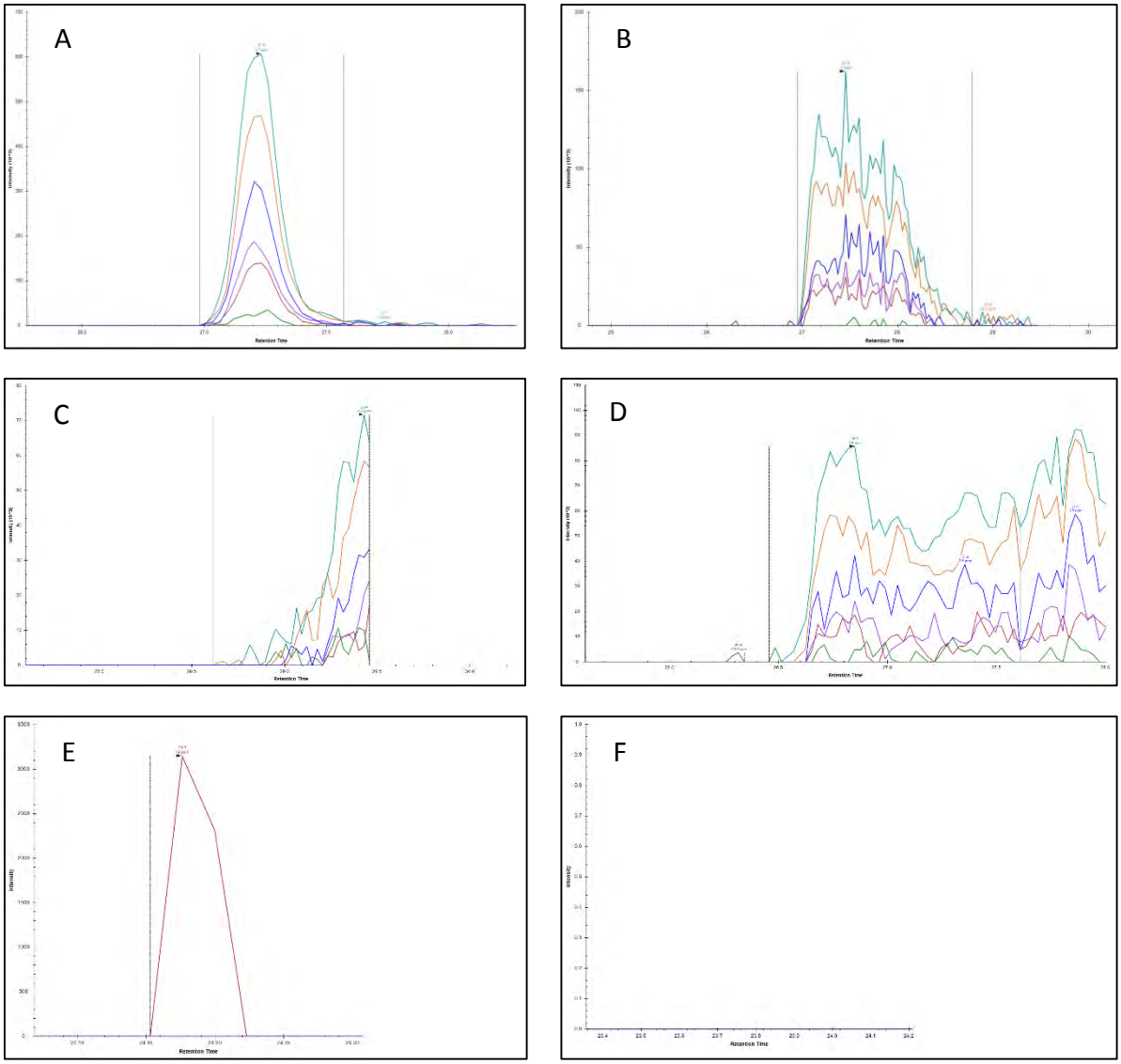

FIGURE 7.3: EXAMPLES OF PEAK QUALITY VARIATION. A: SATISFACTORY PEAK, B: UNSATISFACTORY PEAK SHAPE WITH BROADENING, C: UNSATISFACTORY PEAK SHAPE WITH SIGNIFICANT RETENTION TIME DRIFT, D: UNSATISFACTORY PEAK SHAPE WITH SIGNIFICANT BROADENING, E: PEAK WITH MISSING TRANSITIONS, F: NO TRANSITIONS DETECTED

Determining satisfactory product ions for the remaining peptides was primarily based on consistency of relative product ion abundances across biological replicates. Ions exhibiting

good consistency were retained, while product ions varying significantly between samples were excluded. Consistency of product ion abundances relative to total signal across samples confirm that there is no contribution to ion intensity by interfering species.[212] For example, Figure 7.4 shows consistent peak area consistency following removal of ions y8, b10, and b11. The five most consistent ions were thus chosen for use in downstream quantitation.

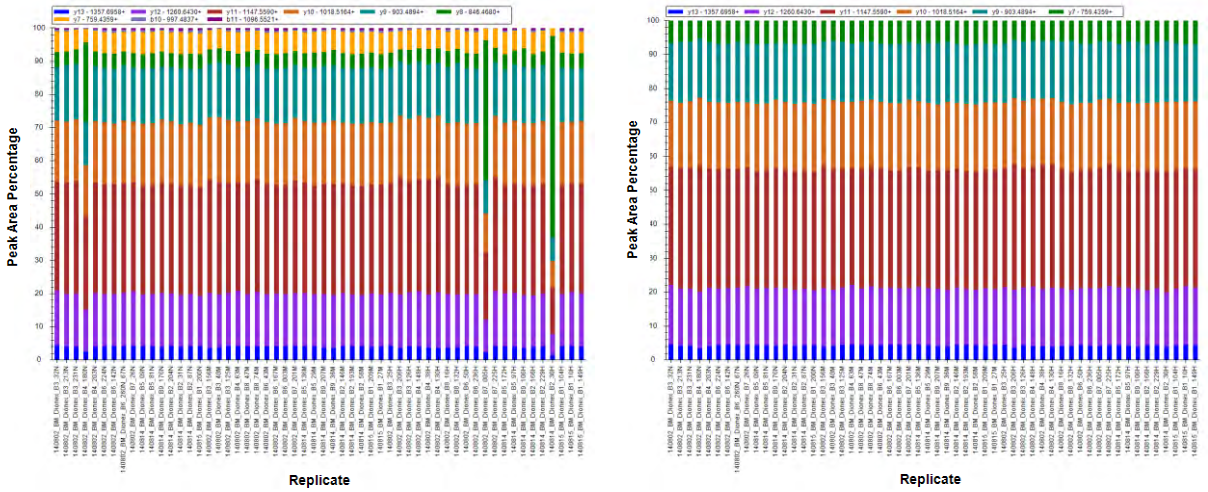

FIGURE 7.4: PEAK INTENSITIES NORMALISED TO TOTAL PEAK AREA. BEFORE (LEFT) AND AFTER (RIGHT) REMOVAL OF INCONSISTENT PRODUCT IONS

Samples chosen based on the above criteria are listed in Table 7.4, with 15; 19; and 21 samples in Control; MNI; and HAD groups, respectively. Of the 81 samples analysed, 26 were excluded (32%); with 12, 8, and 6 samples discarded from Control, MNI, and HAD groups, respectively.

TABLE 7.4: SELECTED SAMPLES FOR FINAL STATISTICAL ANALYSIS

Batch	Group	Patient	Batch	Group	Patient	Batch	Group	Patient
1	Control	200	1	MNI	27	1	HAD	10
2	Control	31	1	MNI	209	1	HAD	104
2	Control	87	2	MNI	56	1	HAD	149
2	Control	204	2	MNI	146	2	HAD	30
3	Control	32	2	MNI	193	2	HAD	166
3	Control	213	3	MNI	40	2	HAD	229
3	Control	231	3	MNI	125	3	HAD	25
4	Control	203	3	MNI	156	3	HAD	126
5	Control	9	4	MNI	63	3	HAD	206
5	Control	81	5	MNI	29	4	HAD	38
6	Control	142	5	MNI	136	4	HAD	130
6	Control	224	6	MNI	3	4	HAD	148
6	Control	260	6	MNI	43	5	HAD	97
7	Control	26	6	MNI	167	5	HAD	172

Batch	Group	Patient	Batch	Group	Patient	Batch	Group	Patient
9	Control	176	7	MNI	201	6	HAD	50
			8	MNI	47	6	HAD	236
			8	MNI	74	7	HAD	5
			9	MNI	36	7	HAD	225
			9	MNI	207	8	HAD	16
						8	HAD	132
						9	HAD	106

Peptides selected for quantitation of their parent protein are shown in Table 7.5 below. Exceptions were made for sp|P02763|A1AG1 and sp|P01861|IGHG4, for which only one peptide was analysed per protein (*vide supra*).

TABLE 7.5: PEPTIDES ASSIGNED TO EACH PROTEIN FOR THE PURPOSES OF PROTEIN INFERENCE

Protein Name	Peptide Sequence
sp|P01023|A2MG	NEDSLVFVQTDK
	AIGYLNTGYQR
sp|P08603|CFAH	IDVHLVPDR
	LSYTCEGGFR
sp|P02649|APOE	LGPLVEQGR
	AATVGSLAGQPLQER
sp|P10909|CLUS	TLLSNLEEAK
	IDSLLENDR
sp|P06396|GELS	QTQVSVLPEGGETPLFK
	AGALNSNDAFVLK
sp|P02743|SAMP	AYSLFSYNTQGR
	DNELLVYK
sp|P02763|A1AG1	TEDTIFLR
sp|P01009|A1AT	SVLGQLGITK
	AVLTIDEK
sp|P02647|APOA1	DYVSQFEGSALGK
	VQPYLDDFQK
sp|P00450|CERU	EYTDASFTNR
	NNEGTYYSPNYNPQSR
sp|P0C0L5|CO4	AEFQDALEK
	QGSFQGGFR
sp|P01024|CO3	IPIEDGSGEVVLSR
	TGLQEVEVK
sp|P01861|IGHG4	STSESTAALGCLVK

7.3.4. Power Analysis

The average CV for the final PRM assay was found to be approximately 13.92% (±0.1411%, data not shown). This value was compared to Table 7.6 adapted from van Belle et al.[201] This table shows sample number estimations according to measurement CV and fold change, for independent samples *t*-tests with unknown biological variance, assuming a significance level (α) of 0.05 and predicted power (1-β) of 0.80. A minimum power of 0.8, and α of 0.05 are conventionally used for statistical analyses.[213] Following sample number reduction, Control; MNI; and HAD disease groups comprised 15; 19; and 21 samples, respectively. Detectable fold changes can be estimated based on these sample numbers. With a conservative CV estimate of 20%, despite the calculated CV being 13.92%, the lowest detectable mean difference would be 1.25-fold with 14 samples per group. Higher minimum fold changes can be detected with 3-5 samples at this CV. Assuming a CV of 80% at worst case, the assay would be able to detect a mean difference of at least 2.5-fold using 11 samples per group. It can be concluded that, despite reduction in sample numbers, *t*-tests of PRM-quantified proteins would nevertheless be able to detect mean differences as low as 1.25-fold.

TABLE 7.6: SAMPLE SIZE ESTIMATIONS FOR AN INDEPENDENT SAMPLES *T*-TEST, WHERE SIGNIFICANCE = 0.05, AND PREDICTED POWER = 0.8. ADAPTED FROM VAN BELLE ET AL.[201]

	Fold change						
CV (%)	1.10	1.25	1.50	1.75	2.00	2.50	3.00
10	19	5	3	3	3	3	4
20	69	14	5	4	3	3	3
30	150	29	10	6	4	3	3
40	258	48	16	9	6	34	4
50	387	72	23	13	9	6	5
60	533	98	31	17	12	7	6
70	691	127	40	22	15	9	7
80	856	157	49	26	18	11	8
90	>1000	189	58	31	21	13	9
100	>1000	220	68	36	24	14	11
200	>1000	509	155	82	54	32	22

Shaded area shows applicable sample numbers for reduced samples assuming a CV of 20%

7.3.5. Data Handling and Statistical Analyses

7.3.5.1. Data Export and Manipulation

The data report exported from Skyline consisted of columns for Protein Name, Peptide Sequence, Replicate filename, Condition, BioReplicate, and total area calculated from the sum of ion peak areas (Table 7.7, All raw data: Appendix C: Table 10.1).

TABLE 7.7: EXAMPLE OF SKYLINE DATA OUTPUT

Protein Name	Peptide Sequence	Replicate	Condition	BioReplicate	Total Area
sp|P01023|A2MG	NEDSLVFVQTDK	140802_BM_Dionex_B3_32N_LSF_2plex_35K_72min_25ngul_3ul	Control	32	16947226
sp|P01023|A2MG	NEDSLVFVQTDK	140802_BM_Dionex_B3_213N_LSF_2plex_35K_72min_25ngul_3ul	Control	213	37269700
sp|P01023|A2MG	NEDSLVFVQTDK	140802_BM_Dionex_B3_231N_LSF_2plex_35K_72min_25ngul_3ul	Control	231	13608301
sp|P01023|A2MG	NEDSLVFVQTDK	140802_BM_Dionex_B3_156M_LSF_2plex_35K_72min_25ngul_3ul	MNI	156	20031696
sp|P01023|A2MG	NEDSLVFVQTDK	140802_BM_Dionex_B3_40M_LSF_2plex_35K_72min_25ngul_3ul	MNI	40	14586175
sp|P01023|A2MG	NEDSLVFVQTDK	140802_BM_Dionex_B3_125M_LSF_2plex_35K_72min_25ngul_3ul	MNI	125	32799076

For full raw data table see Appendix C: Table 10.1

Data rearrangement yielded a result file formatted for downstream statistical analysis, with patient identifiers running down the rows and proteins across the columns (Table 7.8).

TABLE 7.8: EXAMPLE OF DATA PREPARED FOR STATISTICAL ANALYSIS

Patient	Group	sp_P01023_A2MG	sp_P08603_CFAH	sp_P02649_APOE	sp_P10909_CLUS
1	Control	71415240	7782003.5	3005355.5	28342590
2	Control	52129109	4385080	2571627	11731742.5

Patient	Group	sp_P01023_A2MG	sp_P08603_CFAH	sp_P02649_APOE	sp_P10909_CLUS
3	Control	127857096	28001535.5	4515216.5	34542406
4	Control	31038437	4951136.5	2378897.5	16315096

7.3.5.2. Data Normalisation

INTERNAL REFERENCE PEPTIDE NORMALISATION

The first of two normalisation methods utilised in the present study was based on normalisation to the internal reference peptide. An example of the result of normalisation is depicted in Table 7.9 below, which includes the calculated average internal reference peptide intensity as well as the internal reference intensity for each respective sample.

TABLE 7.9: EXAMPLE OF INTERNAL REFERENCE NORMALISED DATA

Patient	Group	Average reference peptide intensity	Sample reference peptide intensity	sp|P01023|A2MG	
				Pre-normalisation	Post-normalisation
1	Control	186617596	364794112	71415240	36533869
2	Control		125390672	52129109	77583195
3	Control		69829224	127857096	341696248
4	Control		107740912	31038437	53761550

NANODROP NORMALISATION

The second normalisation method was based on total peptide quantitation measured by UV spectrophotometry. An example of the result of normalisation is depicted in Table 7.10 below, which includes the normalisation factors for each respective sample.

TABLE 7.10: EXAMPLE OF TOTAL PEPTIDE NORMALISED DATA

Patient	Group	Normalisation factor	sp|P01023|A2MG	
			Pre-normalisation	Post-normalisation
1	Control	0.785853	71415240	56121866.67
2	Control	0.940387	52129109	49021535.74
3	Control	0.965005	127857096	123382698.5
4	Control	1.391285	31038437	43183325.26

7.3.5.3. Statistical Assessment

INTERNAL REFERENCE NORMALISED DATA

The Shapiro-Wilk test for normality, as well as visual inspection of histograms (data not shown) confirmed normal distributions for several peptides in various samples (Table 7.11). Normality is inferred from Shapiro-Wilk output when W approaches 1, and *p* is large (in this case, p>0.2). The results of this test directed use of either the r test or non-parametric Wilcoxon rank-sum test. Only proteins exhibiting normal distributions in all disease groups were considered for analysis by *t*-test. Three of the 12 proteins exhibited normal distributions in all disease groups, and are indicated in bold in Table 7.11.

TABLE 7.11: SHAPIRO-WILK NORMALITY TEST RESULTS ON INTERNAL REFERENCE-NORMALISED DATA

Protein	CTRL		MNI		HAD	
	p	*W*	*p*	*W*	*p*	*W*
sp|P01023|A2MG	0.1125	0.9047	0.0286	0.8871	0.7556	0.9710
sp|P08603|CFAH	0.1463	0.9122	0.8268	0.9726	0.5428	0.9613
sp|P02649|APOE	0.1264	0.9080	0.4268	0.9520	0.0014	0.8208
sp|P10909|CLUS	0.6704	0.9587	0.8580	0.9743	0.6002	0.9640
sp|P06396|GELS	0.6906	0.9599	0.0846	0.9132	0.1515	0.9321
sp|P02743|SAMP	0.6996	0.9604	0.2319	0.9369	0.8062	0.9734
sp|P02763|A1AG1	0.7404	0.9628	0.0542	0.9026	0.4973	0.9591
sp|P01009|A1AT	0.0583	0.8860	0.8047	0.9714	0.0907	0.9210
sp|P02647|APOA1	0.3106	0.9338	0.1241	0.9222	0.0553	0.9102
sp|P00450|CERU	0.0262	0.8624	0.0138	0.8688	0.0772	0.9175
sp|P0C0L5|CO4	0.4670	0.9462	0.6185	0.9623	0.2964	0.9468
sp|P01024|CO3	0.0858	0.8970	0.6924	0.9659	0.9870	0.9864

Proteins with normally distributed values across all disease groups are indicated in **bold.**
Normally distributed values highlighted in grey.

These results facilitated use of the parametric Welch's *t*-test (for unequal variances) to determine statistical significance of quantitative differences between disease groups for peptides with normally distributed values. Only those peptides exhibiting normal distributions across all disease groups may be assessed in this way. For remaining peptides with non-normally distributed values, a non-parametric test of significance – the Wilcoxon rank-sum test – is appropriate. Results for both tests are shown, despite the *t*-test lacking power when

applied to non-normally distributed data (Table 7.12). Each between-group comparison was conducted: Control vs MNI, MNI vs HAD, and Control vs HAD. Upon implementation of both *t*-tests and Wilcoxon rank-sum tests no proteins were found to exhibit significant differences in quantity between disease groups ($p > 0.05$, Table 7.12). Considering this, it was deemed unnecessary for multiple testing correction to be applied to the results of these tests.

TABLE 7.12: RESULTS FROM WELCH'S *T-TEST* AND WILCOXON TEST ON INTERNAL REFERENCE-NORMALISED DATA

Protein	MNI vs CTRL		HAD vs MNI		HAD vs CTRL	
	p	*W/t*	*p*	*W/t*	*p*	*W/t*
Welch's *t-test*						
sp|P01023|A2MG	0.7302	-0.3481	0.8691	-0.1659	0.6294	-0.4871
sp|P08603|CFAH	0.2705	-1.1245	0.7892	-0.2692	0.1815	-1.3710
sp|P02649|APOE	0.8947	0.1338	0.7454	0.3271	0.7015	0.3871
sp|P10909|CLUS	0.4843	-0.7079	0.4883	-0.6999	0.1710	-1.4024
sp|P06396|GELS	0.8707	-0.1642	0.4593	-0.7477	0.3053	-1.0419
sp|P02743|SAMP	0.2439	-1.1876	0.9566	-0.0548	0.2711	-1.1187
sp|P02763|A1AG1	0.6480	-0.4614	0.1989	1.3077	0.5057	0.6740
sp|P01009|A1AT	0.4126	-0.8302	0.9912	0.0111	0.4021	-0.8489
sp|P02647|APOA1	0.7638	-0.3032	0.9886	-0.0144	0.7642	-0.3025
sp|P00450|CERU	0.4048	-0.8454	0.4080	0.8371	0.8864	-0.1442
sp|P0C0L4/5|CO4	0.3305	-0.9881	0.1815	1.3613	0.6483	0.4602
sp|P01024|CO3	0.2697	-1.1263	0.8417	-0.2012	0.2084	-1.2867
Wilcoxon Rank Sum Test						
sp|P01023|A2MG	0.9727	144	0.9147	195	0.6804	144
sp|P08603|CFAH	0.4505	120	0.8935	194	0.4089	131
sp|P02649|APOE	0.6074	158	0.3471	235	0.2385	195
sp|P10909|CLUS	0.6074	127	0.4207	169	0.1698	114
sp|P06396|GELS	0.8373	149	0.4053	168	0.4461	133
sp|P02743|SAMP	0.3024	112	0.8935	194	0.3242	126
sp|P02763|A1AG1	0.8107	135	0.2363	244	0.4461	182
sp|P01009|A1AT	0.5373	124	0.9147	204	0.6573	143
sp|P02647|APOA1	0.9183	146	0.6681	216	0.7756	167
sp|P00450|CERU	0.3538	115	0.0693	267	0.5468	177
sp|P0C0L4/5|CO4	0.5602	125	0.1607	252	0.4273	183

Protein	MNI vs CTRL		HAD vs MNI		HAD vs CTRL	
	p	*W/t*	*p*	*W/t*	*p*	*W/t*
sp|P01024|CO3	0.5373	124	0.9786	198	0.4273	132

Proteins with normally distributed values across all disease groups are indicated in **bold.**

NANODROP NORMALISED DATA

Statistical analysis of Nanodrop-normalised data progressed in much the same fashion as that for the internal reference-normalised data (*vide supra*). Results of the Shapiro-Wilk test for normality are shown in Table 7.13. Normality was assessed as previously discussed. The results of this test also directed use of either the *t*-test or non-parametric Wilcoxon rank-sum test. Only proteins exhibiting normal distributions in all disease groups were considered for analysis by *t*-test. Four of the 12 proteins exhibited normal distributions in all disease groups, and are indicated in bold in Table 7.13

TABLE 7.13: SHAPIRO-WILK NORMALITY TEST RESULTS ON NANODROP-NORMALISED DATA

Protein	CTRL		MNI		HAD	
	p	*W*	*p*	*W*	*p*	*W*
sp|P01023|A2MG	0.9863	0.9831	0.4405	0.9528	0.5437	0.9613
sp|P08603|CFAH	0.1049	0.9028	0.7409	0.9682	0.7565	0.9711
sp|P02649|APOE	0.1880	0.9193	0.1239	0.9221	0.0453	0.9058
sp|P10909|CLUS	0.9213	0.9748	0.9901	0.9863	0.1293	0.9286
sp|P06396|GELS	0.6215	0.9559	0.0309	0.8890	0.0395	0.9027
sp|P02743|SAMP	0.9757	0.9810	0.7550	0.9689	0.0546	0.9099
sp|P02763|A1AG1	0.2183	0.9236	0.7557	0.9690	0.6719	0.9673
sp|P01009|A1AT	0.1197	0.9065	0.9036	0.9771	0.9779	0.9849
sp|P02647|APOA1	0.4590	0.9457	0.6921	0.9659	0.0632	0.9131
sp|P00450|CERU	0.2109	0.9226	0.1410	0.9252	0.1309	0.9289
sp|P0C0L5|CO4	0.8809	0.9716	0.5064	0.9565	0.2783	0.9454
sp|P01024|CO3	0.5964	0.9544	0.6729	0.9650	0.3199	0.9486

Proteins with normally distributed values across all disease groups are indicated in **bold.**
Normally distributed values highlighted in grey.

Welch's *t*-test was used to measure statistically significant differences between disease groups for proteins with normally distributed values, while Wilcoxon rank-sum tests were conducted for proteins that do not satisfy the normality criteria in all disease group samples.

Results for both tests are shown, despite the *t*-test lacking power when applied to non-normally distributed data (Table 7.14). Each between-group comparison was conducted: Control vs MNI, MNI vs HAD, and Control vs HAD. Upon implementation of both *t*-tests and Wilcoxon rank-sum tests, no proteins were found to exhibit significant differences in quantity between disease groups ($p > 0.05$, Table 7.14). Considering this, it was deemed unnecessary for multiple testing correction to be applied to the results of these tests.

TABLE 7.14: RESULTS FROM WELCH'S *T-TEST* AND WILCOXON TEST ON NANODROP-NORMALISED DATA

Protein	MNI vs CTRL		HAD vs MNI		HAD vs CTRL	
	p	*W/t*	*p*	*W/t*	*p*	*W/t*
Welch's *t-test*						
sp|P01023|A2MG	0.7375	-0.3382	0.6587	-0.4453	0.4658	-0.7378
sp|P08603|CFAH	0.2885	-1.0817	0.5731	-0.5685	0.1187	-1.6116
sp|P02649|APOE	0.9060	0.1191	0.9667	0.0421	0.8790	0.1536
sp|P10909|CLUS	0.4821	-0.7124	0.3142	-1.0200	0.1199	-1.6025
sp|P06396|GELS	0.8642	-0.1724	0.2490	-1.1736	0.1497	-1.4795
sp|P02743|SAMP	0.2964	-1.0622	0.7889	-0.2697	0.2278	-1.2282
sp|P02763|A1AG1	0.6465	-0.4633	0.3515	0.9437	0.7016	0.3871
sp|P01009|A1AT	0.4234	-0.8112	0.8107	-0.2413	0.2871	-1.0831
sp|P02647|APOA1	0.7363	-0.3398	0.7672	-0.2983	0.5156	-0.6577
sp|P00450|CERU	0.3427	-0.9644	0.6121	0.5114	0.6643	-0.4380
sp|P0C0L4/5|CO4	0.3920	-0.8679	0.3244	0.9985	0.8962	0.1315
sp|P01024|CO3	0.2985	-1.0579	0.6498	-0.4577	0.1677	-1.4105
Wilcoxon Rank Sum Test						
sp|P01023|A2MG	0.6562	129	0.4688	172	0.4654	134
sp|P08603|CFAH	0.6074	127	0.4053	168	0.1599	113
sp|P02649|APOE	0.7065	154	0.8513	192	0.4273	183
sp|P10909|CLUS	0.4505	120	0.2363	155	0.0955	105
sp|P06396|GELS	0.6316	157	0.0830	135	0.1414	111
sp|P02743|SAMP	0.3361	114	0.8724	206	0.3567	128
sp|P02763|A1AG1	0.7321	132	0.5735	221	0.7038	170
sp|P01009|A1AT	0.4102	118	0.9573	197	0.3087	125
sp|P02647|APOA1	1.0000	143	0.7479	187	0.7038	145
sp|P00450|CERU	0.5149	123	0.7888	210	0.6120	141

Protein	MNI vs CTRL		HAD vs MNI		HAD vs CTRL	
	p	*W/t*	*p*	*W/t*	*p*	*W/t*
sp|P0C0L4/5|CO4	0.5836	126	0.5025	225	0.8992	162
sp|P01024|CO3	0.4505	120	0.5374	176	0.1908	116

Proteins with normally distributed values across all disease groups are indicated in **bold.**

7.3.6. Interpretation

Most mean comparisons (Figure 7.5 - Figure 7.12) - apart from CERU (Figure 7.7), ApoA-I (Figure 7.13), GSN (Figure 7.10), and SAP (Figure 7.11) - exhibited similar trends across disease groups for both NanoDrop- and internal reference-normalised data. The similar trends observed using both normalisation approaches suggests that both methods perform equally well and yield similar results.

Indeed, no significant differences were observed between the biomarker means of any groups compared. No significant quantitative difference – as assessed by representative peptide intensity - existed between HIV positive-control, MNI, and HAD groups for any of the 12 biomarkers investigated. This suggests that levels of these serum proteins – individually or in combination - are not able to discriminate between HIV positivity and development of HIV-related neurocognitive decline. Thus, the use of these Alzheimer's biomarkers cannot be extended to identifying MNI or HAD.

It is possible that systemic HIV infection and resulting systemic inflammatory changes are masking any smaller changes in levels of these non-specific inflammatory markers due to HAND-related processes. This could only be confirmed by inclusion of matched HIV-negative controls, which were not available during the present study.

Interestingly, the lack of correlation between the present study and previous reports in the literature may also reflect the likely very different nature of the cohort studied here. For example: Tuberculosis (TB) is endemic to SA with a prevalence of 1.3% in 2013.[214] As of 2013, an estimated 62% of TB-infected individuals have been found to be HIV-positive.[214] Thus, analysis of markers that are primarily abundant acute phase proteins may be confounded by other co-infections such as TB, further supporting our conclusion that the set of 12 AD markers are not applicable to the diagnosis of HAND, particularly in developing countries such as SA.

Given the satisfactory performance of normalisation and the likely-true observation of no significant differences in biomarker levels between disease groups, results for each biomarker are placed in biological context below.

7.3.6.1. Alpha-2-macroglobulin

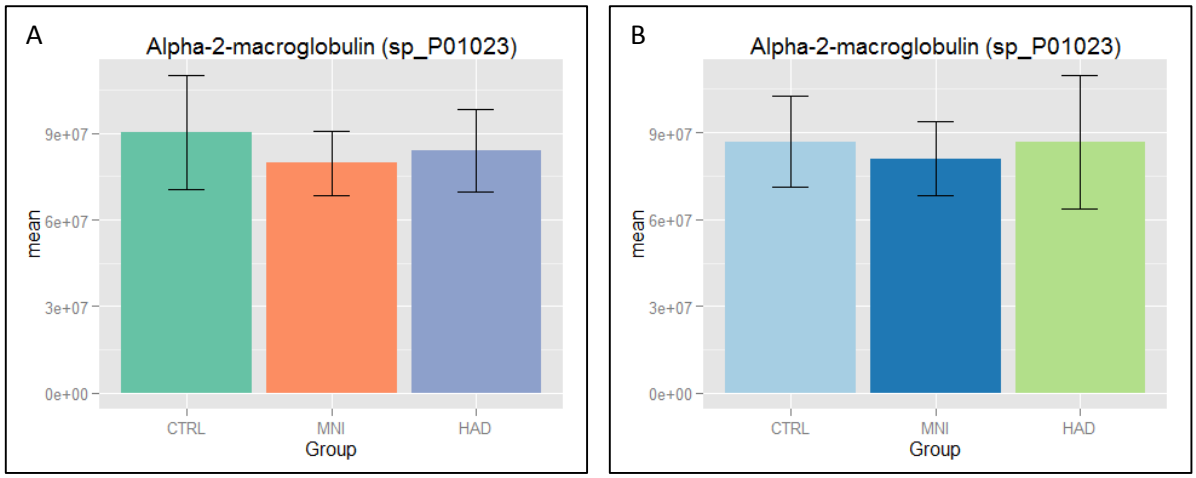

FIGURE 7.5: BAR GRAPHS COMPARING MEANS OF ALPHA-2-MACROGLOBULIN REPRESENTATIVE PEPTIDES ACROSS DISEASE GROUPS, USING BOTH NORMALISATION METHODS. ERROR BARS REPRESENT STANDARD ERROR OF THE MEAN. A: IR NORMALISED, B: NANODROP NORMALISED

A2M functions primarily as an inhibitor of all four protease classes.[215] It is able to inhibit such a wide array of proteases by irreversibly trapping them, following proteolytic attack of its 'bait' region, thereby sterically halting their activity.[215] The complex is then cleared by binding to low-density lipoprotein receptor-related protein (LRP) on Kupffer cells and hepatocytes.[216,217]

The study by Simon Lovestone, identifying A2M as a serum marker for AD, showed that its levels increase with increasing disease severity.[157] Previous studies have implicated A2M in reduction of Aβ aggregates via LRP receptor-mediated clearance in the CNS.[218–221]

A study by Liu et al.[222] suggests that, during CNS HIV infection, extracellular levels of A2M are increased due to competition by HIV-encoded Tat protein for LRP on the neuronal surface. Whether this increase in CNS levels of A2M is detectible in the serum compartment was not addressed by Liu et al.[222] The present study found no statistically significant correlation between serum A2M levels and neurocognitive impairment (Table 7.12, Table 7.14, and Figure 7.5).

7.3.6.2. Clusterin

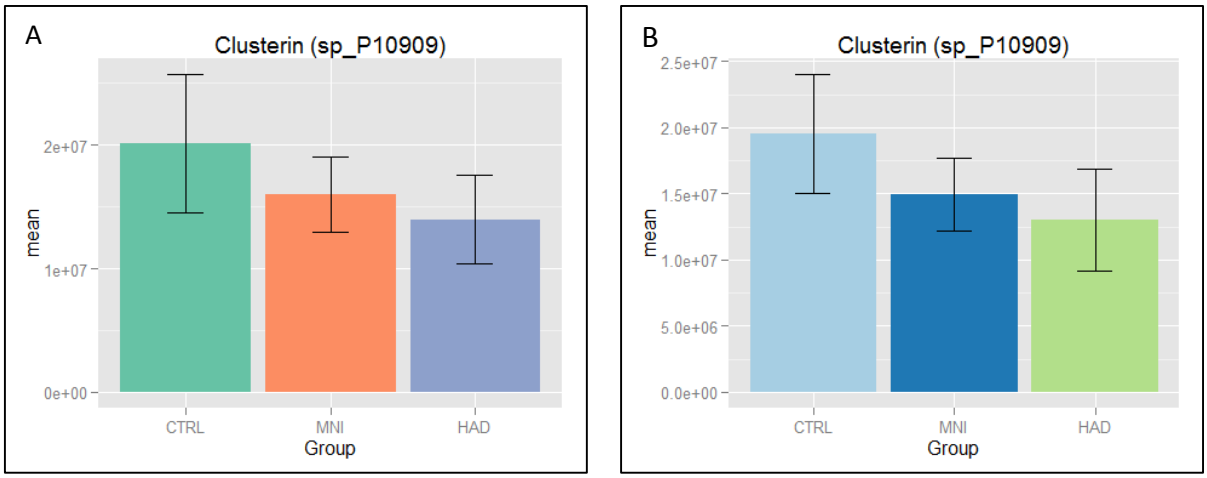

FIGURE 7.6: BAR GRAPHS COMPARING MEANS OF CLUSTERIN REPRESENTATIVE PEPTIDES ACROSS DISEASE GROUPS, USING BOTH NORMALISATION METHODS. ERROR BARS REPRESENT STANDARD ERROR OF THE MEAN. A: IR NORMALISED, B: NANODROP NORMALISED

CLU is a ubiquitously expressed mammalian glycoprotein found in a diverse array of tissues and biological fluids, including blood plasma.[223] Although its main function has not been definitively identified, a crucial function is its ability to act as a chaperone that binds misfolded or stressed proteins for presentation to other proteins able to resolve misfolding, such as heat shock proteins.[224,225]

This hypothesis is consistent with studies by Simon Lovestone which identify CLU as a serum marker for AD, showing an increase in levels of this protein with increasing cognitive decline and brain atrophy.[154,155]

Increased levels of CLU have been found post-mortem in brains of HIV-positive patients, and in this setting it was hypothesised to serve a role in astrocyte protection.[226] Rozek et al.[78], however, observed a decrease in levels of CSF-localised CLU with increasing HAND severity. This apparent contradiction could be attributable to localisation of CLU at sites of astrocyte stress. The present study was unable to find any statistically significant correlation between serum CLU levels and neurocognitive impairment (Table 7.12, Table 7.14, and Figure 7.6); although there appears to be a reduction in serum CLU concentration as HAND severity increases (Figure 7.6), in line with Rozek et al.[78], and in contrast to findings in AD.

7.3.6.3. Ceruloplasmin

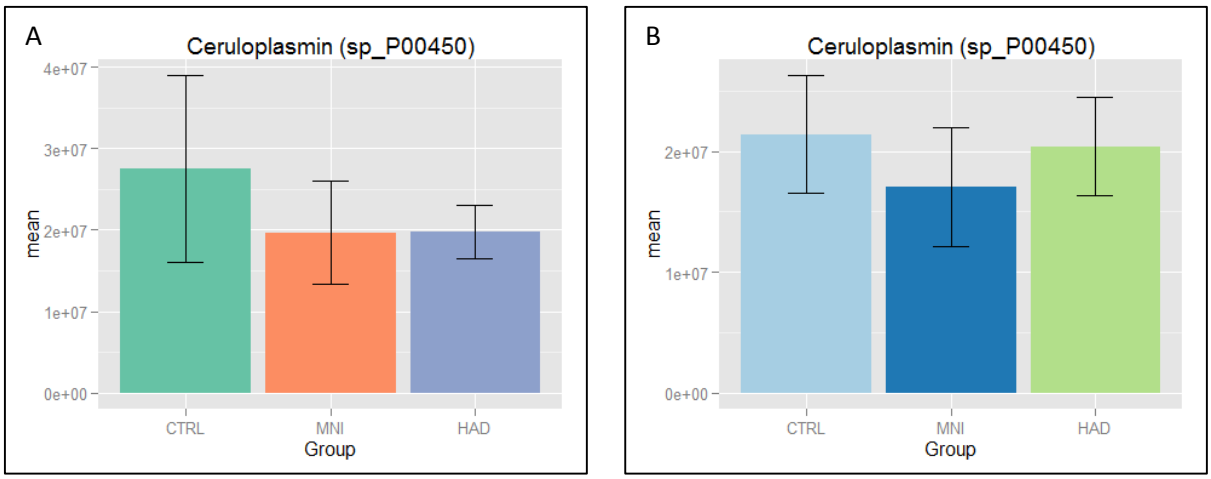

FIGURE 7.7: BAR GRAPHS COMPARING MEANS OF CERULOPLASMIN REPRESENTATIVE PEPTIDES ACROSS DISEASE GROUPS, USING BOTH NORMALISATION METHODS. ERROR BARS REPRESENT STANDARD ERROR OF THE MEAN. A: IR NORMALISED, B: NANODROP NORMALISED

CERU is a copper-containing protein that functions primarily in oxidation of Fe^{2+} to Fe^{3+}, without concomitant release of reactive oxygen species, in order to facilitate Fe^{3+} binding to plasma transferrin.[227–229] CERU is also able to facilitate iron efflux from cells as a result of cross-membrane Fe^{2+} gradient modification when extracellular Fe^{2+} is oxidised and bound to transferrin.[230] Of particular interest in the context of inflammatory disorders, CERU has also exhibited antioxidant abilities, and is regarded as an acute phase protein due to increase in serum levels during infection.[231–233]

Simon Lovestone identified a decrease in plasma CERU as a marker of AD.[157] Kessler et al.[234] confirmed these findings, measuring a significant decrease in CERU and copper levels between control and AD patients in both plasma and CSF.

Rozek et al.[79] detected a significant increase in serum CERU in HAD patients when compared to HIV-positive controls. Identification of differentially expressed proteins were conducted by LC-MS/MS, following abundant protein depletion and separation by 2-dimensional gel electrophoresis.[79] Differential expression of CERU was validated by Western blot analysis. The present study, however, was unable to detect any significant differences in CERU levels across disease groups (Table 7.12, Table 7.14, and Figure 7.7); although the trend appears to be lower levels in HAND compared to controls, consistent with findings in AD and in contrast to Rozek et al.[79]

7.3.6.4. Alpha-1-antitrypsin

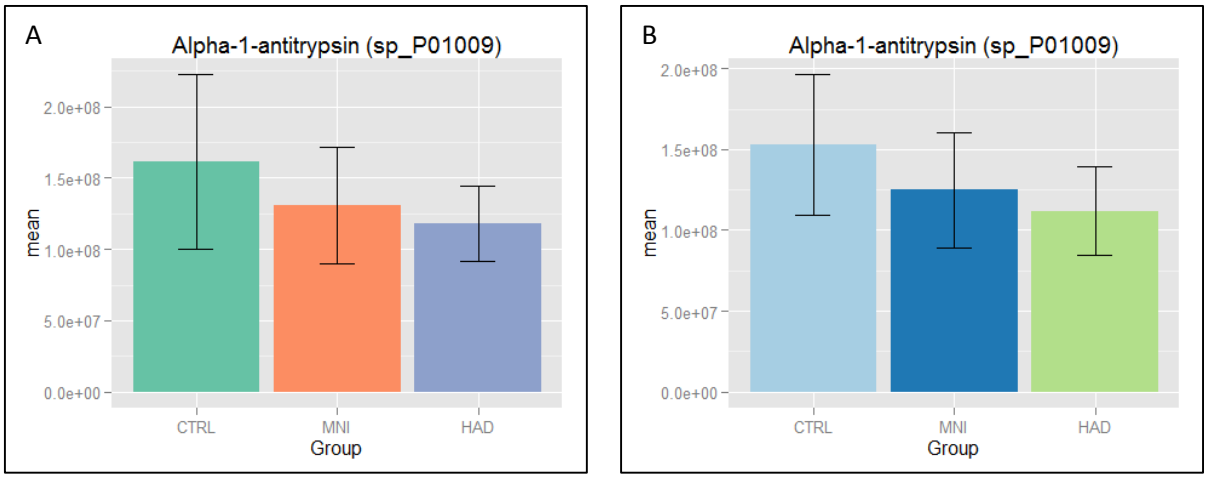

FIGURE 7.8: BAR GRAPHS COMPARING MEANS OF ALPHA-1-ANTITRYPSIN REPRESENTATIVE PEPTIDES ACROSS DISEASE GROUPS, USING BOTH NORMALISATION METHODS. ERROR BARS REPRESENT STANDARD ERROR OF THE MEAN. A: IR NORMALISED, B: NANODROP NORMALISED

A1AT is the most abundant plasma protease inhibitor in human serum.[235] Its primary substrate is neutrophil elastase, although it does possess minor specificity for trypsin and neutrophil Cathepsin G.[235,236] Being an acute phase reactant, it is primarily involved in control of neutrophil-mediated tissue damage in acute inflammation.[233,237] A1AT is unable to completely disrupt neutrophil-mediated tissue damage at inflammatory foci, since reactive oxygen species released by neutrophils and other innate inflammatory cells oxidise the methionine residue at the A1AT active site, and thereby render the protease inhibitor less active.[236,238,239] This interplay allows for controlled inflammatory processes at the site of infection, but prevents widespread tissue damage.

Simon Lovestone identified an increase in plasma A1AT as a marker of AD severity.[154] Studies by Nielson et al.[240] and Sun et al.[241] support this finding.

A1AT has been implicated in the inhibition of both initial HIV entry and viral replication.[242,243] A study by Bryan et al.[244] found a significant decrease in plasma A1AT in HIV positive patients when compared to uninfected controls. Ferreira et al.[245] recently assessed the incidence of genetic A1AT deficiency in HIV positive and negative subjects, where it was observed that deleterious A1AT mutations were correlated with HIV positive status, and may in fact serve to increase susceptibility to HIV infection. This may explain the low levels of plasma A1AT previously found in HIV positive subjects.[244]

The present study was unable to assess the effect of HIV on serum levels of A1AT due to lack of uninfected controls. There was no detectible correlation between serum A1AT levels and neurocognitive impairment (Table 7.12, Table 7.14, and Figure 7.8), although there does appear to be a trend of decreasing A1AT with increase in HAND severity.

7.3.6.5. Alpha-1-acid glycoprotein

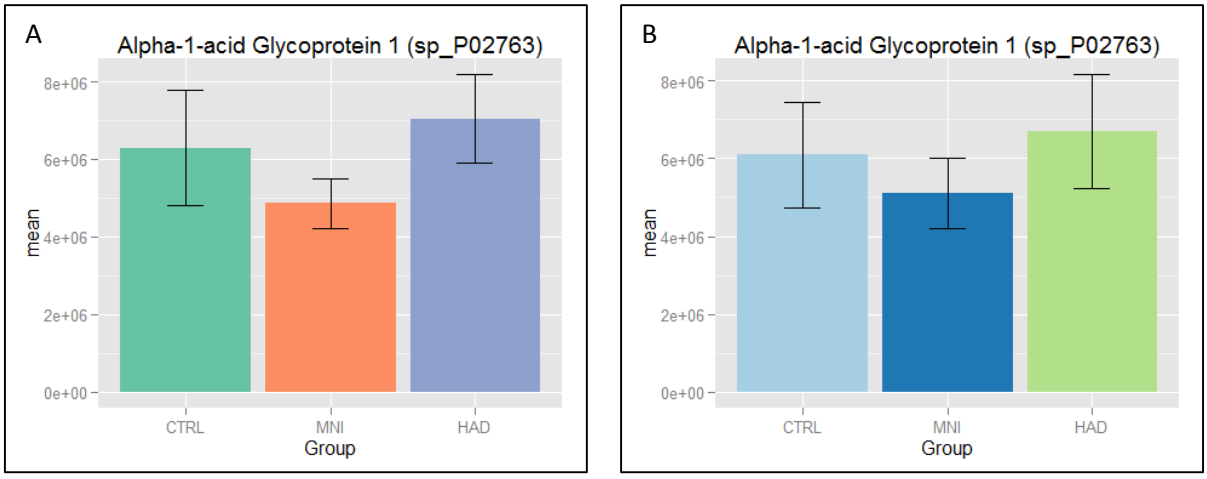

FIGURE 7.9: BAR GRAPHS COMPARING MEANS OF ALPHA-1-ACID GLYCOPROTEIN REPRESENTATIVE PEPTIDES ACROSS DISEASE GROUPS, USING BOTH NORMALISATION METHODS. ERROR BARS REPRESENT STANDARD ERROR OF THE MEAN. A: IR NORMALISED, B: NANODROP NORMALISED

A1AG, also known as Orosomucoid, is a plasma transport protein, primarily responsible for transport of basic and neutral drugs.[246,247] It is also a positive acute phase protein, with increased plasma levels observed during inflammation.[233,246]

Simon Lovestone observed a decrease in plasma A1AG in AD, which both predicted progression to dementia, as well indicated the degree of cognitive decline.[154]

As a result of its acute phase induction, serum levels of A1AG are elevated in HIV positive individuals.[248] No experimental evidence of A1AG differential regulation in relation to severity of HAND was found in the literature. Results of the present study showed no change in serum A1AG levels with increasing HAND severity (Table 7.12, Table 7.14, and Figure 7.9). Indeed, this agrees with the biological role of A1AG in context of HIV, wherein serum levels of this protein may have changed in relation to systemic infection.

7.3.6.6. Gelsolin

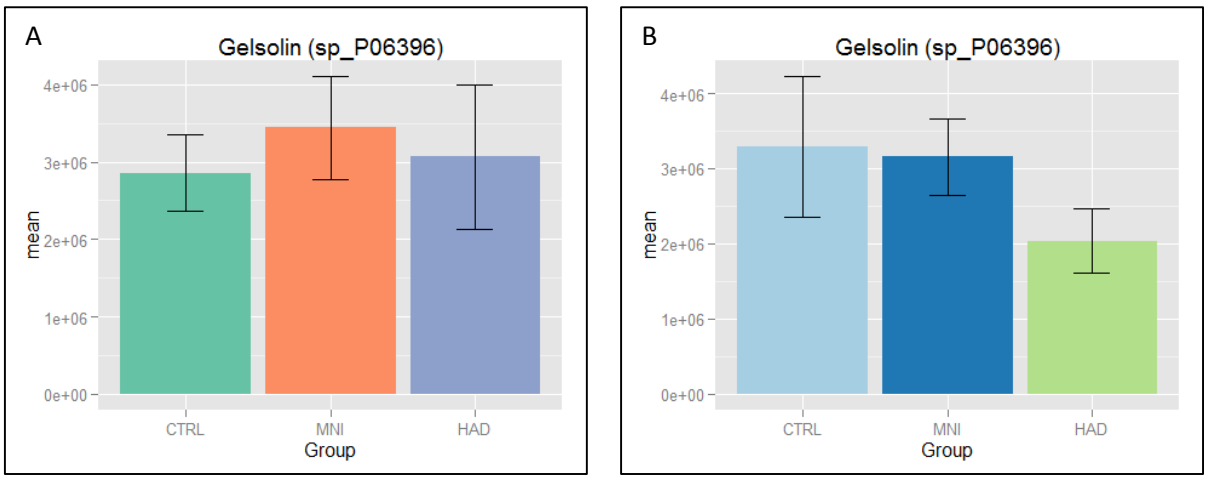

FIGURE 7.10: BAR GRAPHS COMPARING MEANS OF GELSOLIN REPRESENTATIVE PEPTIDES ACROSS DISEASE GROUPS, USING BOTH NORMALISATION METHODS. ERROR BARS REPRESENT STANDARD ERROR OF THE MEAN. A: IR NORMALISED, B: NANODROP NORMALISED

GSN functions primarily as a regulator of actin remodelling.[249,250] It is involved in cell motility, apoptosis, and regulation of structural aspects of the cell.[250–252] GSN functions to sever actin polymers, cap them to prevent polymerisation, as well as control nucleation of actin assembly.[250,253–255] It is positively regulated by calcium ion binding, and inhibited by polyphosphoinositide 4,5-bisphosphate (PIP_2).[249,250,256–258] The plasma variant of GSN acts as an actin scavenger, collecting actin fragments generated from damaged tissue before they can damage blood capillaries and cause unwanted clot formation.[259–262]

Simon Lovestone observed a decrease in plasma GSN correlating with progression of cognitive decline to AD.[158] Studies have suggested a protective role by GSN in AD by inhibition of Aβ fibril formation and protection against apoptosis.[263–266]

Studies have suggested a protective effect of GSN against excitotoxic damage in neurons, by means of actin depolymerisation and Ca^{2+} stabilisation.[267,268] Indeed, excitotoxic damage by excessive extracellular CNS glutamate levels is a proposed mechanism by which HIV causes neuronal apoptosis.[269] Liu et al.[270] also proposed a mechanism of GSN-mediated inhibition of neuronal apoptosis that involved modulation of K^+ exit from K^+ channels in response to gp120-mediated upregulation.

Rozek et al.[78] reported a decrease in CSF levels of GSN in patients with HAND. This is consistent with studies showing reduction in circulating gelsolin in individuals presenting with systemic

and CNS inflammatory pathologies.[271,272] The NanoDrop-normalised data (Figure 7.10-B) does show a trend of decreasing GSN with increasing HAND severity, despite this trend not being mirrored by the IR-normalised data (Figure 7.10-A). It is possible that CNS-inflammation may cause a decrease in circulating GSN as seen in AD, HAND, and CNS inflammation. This trend would have to be confirmed due to the disparity between differentially-normalised data, as well as the lack of statistical significance. Despite any perceivable trend, the present study was unable to detect a significant change in GSN levels with increasing HAND severity (Table 7.12, Table 7.14, and Figure 7.10).

7.3.6.7. Serum amyloid P

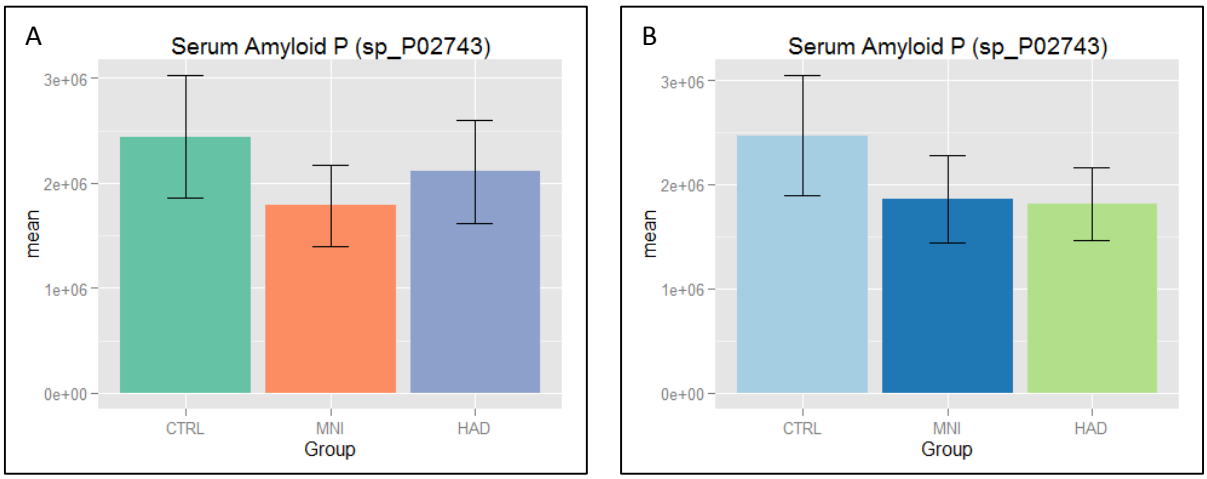

FIGURE 7.11: BAR GRAPHS COMPARING MEANS OF SERUM AMYLOID P REPRESENTATIVE PEPTIDES ACROSS DISEASE GROUPS, USING BOTH NORMALISATION METHODS. ERROR BARS REPRESENT STANDARD ERROR OF THE MEAN. A: IR NORMALISED, B: NANODROP NORMALISED

SAP is a calcium-dependent DNA-binding protein found in human blood serum.[273] It is primarily responsible for regulation of DNA degradation, and thereby prevents production of antibodies against 'self' DNA.[274,275] It has been implicated in amyloidosis, the aggregation of insoluble plaques in systemic tissues, where it may impart resistance to degradation.[276–278] AD, being a form of amyloidosis, is the result of accumulation of Aβ proteins that form insoluble plaques.[279] It has been found that SAP does in fact constitute a portion of AD plaques and neurofibrillary tangles, and is also responsible for resistance to degradation in this setting.[278,280,281] Not surprisingly, Simon Lovestone observed an increase in circulating SAP correlating with increase in AD-related brain atrophy.[159]

Studies have detected the presence of Aβ plaques in brains of HIV patients, alluding to possible similarities between HAND and AD pathogeneses.[152,153,282] From the presence of SAP in Aβ

plaques found in AD, it would be reasonable to assume that SAP levels would indeed increase in HAND. The present study, however, did not detect a significant change in SAP level with increasing HAND severity (Table 7.12, Table 7.14, and Figure 7.11). Despite the lack of statistical significance, there appeared to be a decrease in SAP in HAND compared with the control (Figure 7.11), in contrast with the expected trend.

7.3.6.8. Apolipoprotein E

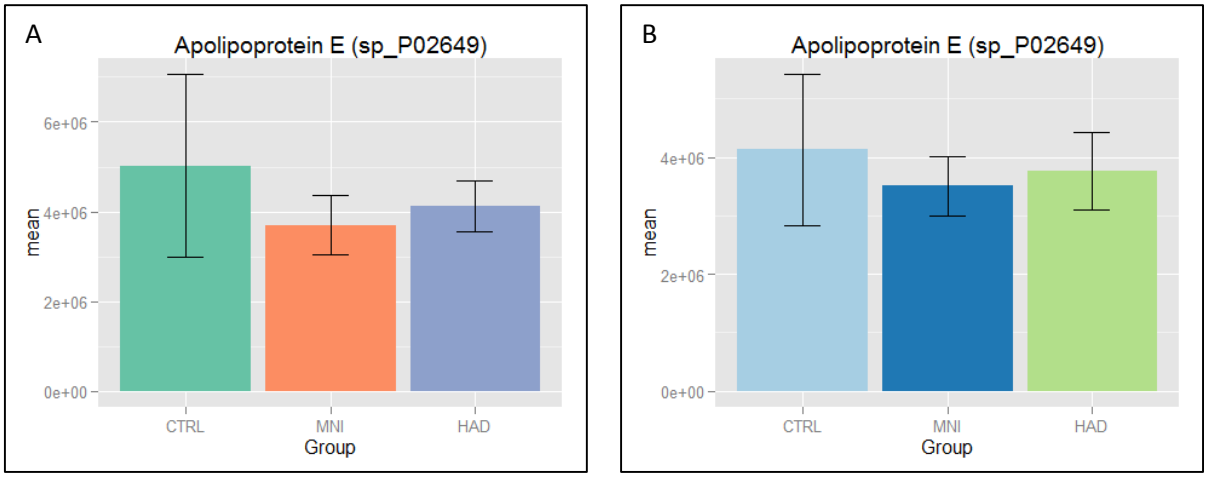

FIGURE 7.12: BAR GRAPHS COMPARING MEANS OF APOLIPOPROTEIN E REPRESENTATIVE PEPTIDES ACROSS DISEASE GROUPS, USING BOTH NORMALISATION METHODS. ERROR BARS REPRESENT STANDARD ERROR OF THE MEAN. A: IR NORMALISED, B: NANODROP NORMALISED

ApoE is a multifunctional variant of the apolipoprotein family, which comprise integral protein constituents of lipoproteins.[283] Lipoproteins are integral to lipid transport and metabolism.[283,284] ApoE has many functions, including: maintaining the structural integrity and solubility of very low density lipoproteins (VLDL), chylomicrons, and ApoE-containing high density lipoproteins (HDL_c) in human blood plasma, and acting as a ligand for low density lipoprotein receptor-mediated tissue internalisation of HDL_c and VLDL.[284,285] ApoE has several variants: E2, E3, and E4; which are expressed by their respective alleles: ε2, ε3, and ε4.[286,287] Expression of different ApoE variants results in variable dietary lipid clearance, with E4 being the most efficient and E2 being the least.[288] This variability has a direct effect on lipid levels in blood plasma.[288]

In studies by Simon Lovestone, there were observed increases in plasma ApoE correlating with both increases in AD-related brain atrophy, as well as higher amounts of brain-localised Aβ in non-demented persons.[154,156] Additionally, an increase in plasma levels of ApoE was observed to predict cognitive decline to AD.[154]

The ApoE ε4 allele is believed to heavily influence severity of AD, whereas studies conflict as to the effect of this mutation on severity of HAND.[289–292] The study by Joska et al.[171], from which the samples in the present study originate, shows no correlation between ApoE allele status and HAND severity in this South African cohort.

In contrast to the ApoE allele, levels of plasma ApoE protein have not been widely assessed in the literature. Generally, the ApoE ε4 allele results in decreased circulating ApoE, whereas the converse is true for ApoE ε2.[293] Regardless, the present study was not able to detect a significant correlation between serum ApoE protein levels and HAND disease severity (Table 7.12, Table 7.14, and Figure 7.12). This may be explained by the lack of ApoE allele correlation with HAND-severity in this cohort.[171]

7.3.6.9. Apolipoprotein A-I

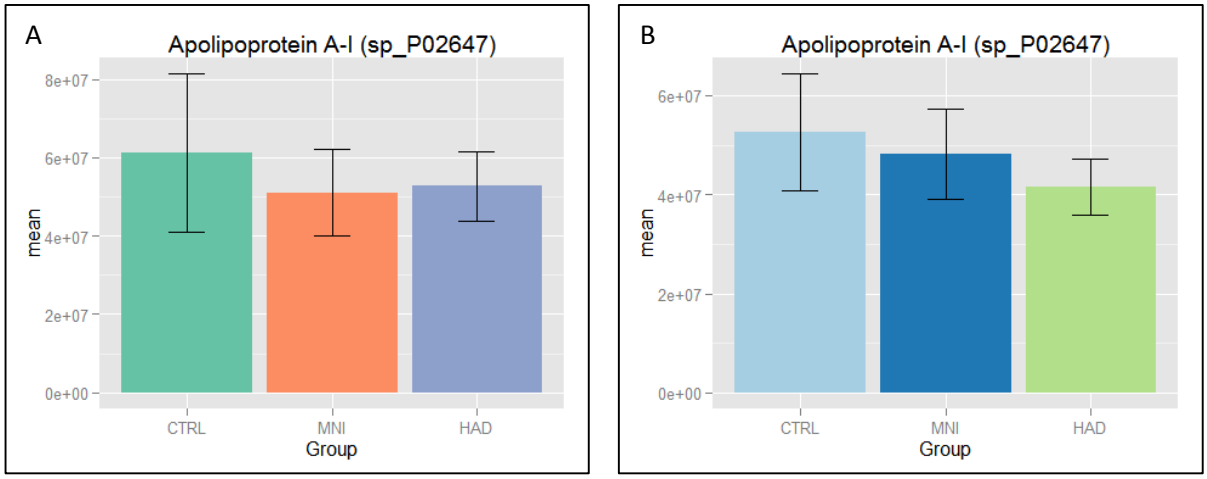

FIGURE 7.13: BAR GRAPHS COMPARING MEANS OF APOLIPOPROTEIN A-I REPRESENTATIVE PEPTIDES ACROSS DISEASE GROUPS, USING BOTH NORMALISATION METHODS. ERROR BARS REPRESENT STANDARD ERROR OF THE MEAN. A: IR NORMALISED, B: NANODROP NORMALISED

ApoA-I is also a member of the apolipoprotein family, and is a structural element in HDL and chylomicrons.[284] It is also a cofactor for the enzyme lecithin:cholesterol acyltransferase, which catalyses the conversion of HDL-localised cholesterol and lecithin to cholesteryl ester and lysolecithin.[294–296]

Simon Lovestone observed increases in plasma ApoA-I correlating with an increase in AD-related brain atrophy.[154]

Decreased plasma ApoA-I levels have been observed in HIV-positive patients independent of HAART status.[297–299] The antiretroviral drug nevirapine has been found to increase ApoA-I levels in HIV-infected individuals, whereas protease inhibitors decrease levels of this protein.[297–302] This, however, is not applicable to the cohort used in the present study, as it consists of HAART-naïve patients.[170] To the best of our knowledge, there are no studies assessing the levels of plasma ApoA-I in HAND. The present study was not able to detect a significant correlation between serum ApoA-I protein levels and HAND disease severity (Table 7.12, Table 7.14, and Figure 7.13); although the trend appears to be lower levels in HAND compared to controls, in contrast to findings in AD.

7.3.6.10. Complement components 3, 4, and Factor H

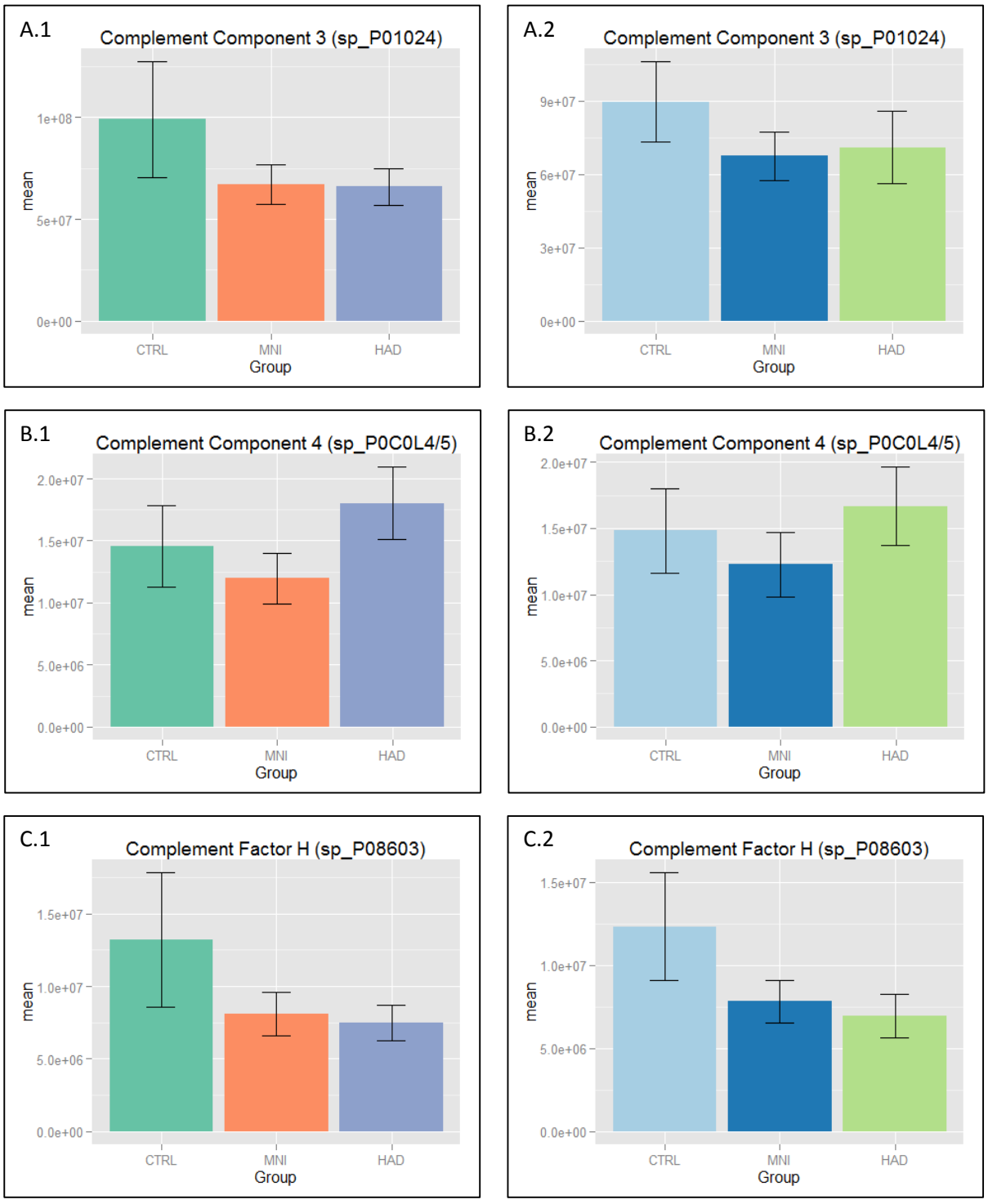

FIGURE 7.14: BAR GRAPHS COMPARING MEANS OF COMPLEMENT PROTEIN REPRESENTATIVE PEPTIDES ACROSS DISEASE GROUPS, USING BOTH NORMALISATION METHODS. ERROR BARS REPRESENT STANDARD ERROR OF THE MEAN. A.1: IR NORMALISED COMPLEMENT C3, A.2: NANODROP NORMALISED COMPLEMENT C3; B.1: IR NORMALISED COMPLEMENT C4, B.2: NANODROP NORMALISED COMPLEMENT C4; C.1: IR NORMALISED COMPLEMENT FACTOR H, C.2: NANODROP NORMALISED COMPLEMENT FACTOR H

The complement system is a cascade-driven innate immunological response which results in pathogen and abnormal cell clearance.[303] It may be activated via three pathways: the classical pathway is initiated by C-reactive protein or antigen-antibody complexes, the alternative pathway is activated by microbial surface macromolecules (e.g. lipopolysaccharides), and the lectin pathway is activated by lectins binding to carbohydrates on pathogen surfaces.[303,304] These pathways converge on activation of C3 convertase, which in turn cleaves C3 to C3a and the opsonin C3b, the main complement effectors.[303]

Amplification cascades produce a large number of complement proteins, which ultimately result in four possible effects: opsonisation of pathogens for phagocytic engulfment, antibody production, chemotactic attraction of immune effector cells, and the formation of a lytic membrane attack complex in target cells or pathogens.[303,304] C3 is central to the cascade originating from all pathways, but is also constitutively cleaved in plasma to produce low levels of C3b in order to *initiate* the alternative pathway under the correct circumstances.[303] Component C4 is involved in the early activation of the classical and lectin pathways, as well as in chemotactic attraction.[303] CFH is a major regulatory protein which protects host cells from complement activation, by binding preferentially to C3b on the host cell membrane.[303] This affinity for C3b is not applicable when it (C3b) is bound to bacterial cells.[303]

A recent study suggests a role for C3 activation by NFκB in dendrite degeneration in the CNS, and therefore to cognitive decline during AD.[305] Classical complement proteins, including C3d and C4d, were also found in senile plaques, suggesting a role for the innate immune response in AD-related neuropathy.[306,307] Studies by Simon Lovestone, identifying C4 as a serum marker for AD, suggest a predictive role based on reduced levels of this protein in minor neurocognitive impairment.[154,157] Increase in C3 and factor H have also been correlated with increasing disease severity.[157,159]

HIV is able to subvert complement-mediated lysis, both by expression of surface proteins that regulate complement activity, and binding of CFH.[308–310] Interestingly, HIV has also been observed to utilise complement to gain entry into target cells via complement receptor binding.[311,312] Indeed, levels of C3 and C4 would be expected to increase in HIV infection considering their roles as positive acute phase proteins.[233] In the CNS, HIV is able to upregulate expression of complement proteins, and thus potentiate infection.[313,314] Thus, an inflammatory or HIV-related increase in complement proteins may be expected, both in the

CNS and in systemic circulation. Indeed, upregulation of complement proteins in the CNS of HAND patients has been observed in analysis of CSF levels of C3 and C4.[315]

Rozek et al.[78], however, observed significantly decreased C3 levels in CSF of individuals with HAD relative to non-demented individuals. Levels of C3 in serum were also observed to be lower in sera of HAD patients.[79] These conflicting observations highlight the need for a comprehensive study on the effect of HAND on serum and CSF levels of complement factors. The present study was not able to detect a significant correlation between serum levels of C3, C4, or CFH and HAND disease severity (Table 7.12, Table 7.14, and Figure 7.14). Despite the lack of statistical significance, there appear to be potential decreases in CFH and C3 in HAND when compared with the controls (i.e.: Control vs MNI, Control vs HAD), in contrast to the trend observed in AD. Indeed, the observed decrease in C3 is in agreement with Rozek et al.[79] Regardless, lack of statistical significance renders these observations invalid. Further study is required to confirm changes in serum and CSF levels of these proteins in HAND.

7.4. Conclusions and Future Prospects

The present study has shown no significant effect of HAND on serum levels of the assessed markers. The possible lack of sufficient distinction between disease groupings, due to possible opportunistic infections or influence of systemic HIV infection, may have reduced the ability to discern applicable molecular differences. Regardless, results of the present study indicate that the primary hypothesis, that a candidate panel of AD biomarkers may also be applicable to the diagnosis of HAND, should be rejected.

It is recommended that a repeat study be conducted to confirm the findings, and address identified shortcomings of the present study. Modifications to future protocols should include: an appropriate internal reference protein spiked into all samples prior to processing, a more consistent method of abundant protein depletion such as MARS, and a higher starting amount of protein which would yield sufficient sample for peptide quantitation and normalisation prior to mass spectrometric analysis. Analysis of post-translational modifications, such as phosphorylation and acetylation, should also be considered to assess changes in protein pathway dynamics that cannot be inferred directly from protein expression. This approach would require enrichment strategies at the peptide level to allow for reliable quantitation. Stratification by TB status, and exclusion of patients with other

opportunistic infections, should also be conducted to control for confounding effects on serum markers. Analysis of patient-matched cerebrospinal fluid samples would also lend credence to conclusions drawn from the serum analysis.

Bibliography

(1) Shaw, G. M.; Harper, M. E.; Hahn, B. H.; Epstein, L. G.; Gajdusek, D. C.; Price, R. W.; Navia, B. A.; Petito, C. K.; O'Hara, C. J.; Groopman, J. E. HTLV-III infection in brains of children and adults with AIDS encephalopathy. *Science (New York, N.Y.)* **1985**, *227* (4683), 177–182.

(2) Navia, B. A.; Jordan, B. D.; Price, R. W. The AIDS dementia complex: I. Clinical features. *Annals of Neurology* **1986**, *19* (6), 517–524.

(3) Price, R.; Brew, B.; Sidtis, J.; Rosenblum, M.; Scheck, A.; Cleary, P. The brain in AIDS: Central nervous system HIV-1 infection and AIDS dementia complex. *Science* **1988**, *239* (4840), 586–592.

(4) Price, R. W.; Brew, B. J. The AIDS Dementia Complex. *Journal of Infectious Diseases* **1988**, *158* (5), 1079–1083.

(5) McArthur, J. C.; Hoover, D. R.; Bacellar, H.; Miller, E. N.; Cohen, B. A.; Becker, J. T.; Graham, N. M.; McArthur, J. H.; Selnes, O. A.; Jacobson, L. P. Dementia in AIDS patients: Incidence and risk factors. *Neurology* **1993**, *43* (11), 2245–2252.

(6) Burgoyne, R. W.; Rourke, S. B.; Behrens, D. M.; Salit, I. E. Long-term quality-of-life outcomes among adults living with HIV in the HAART era: The interplay of changes in clinical factors and symptom profile. *AIDS and Behavior* **2004**, *8* (2), 151–163.

(7) Lima, V. D.; Hogg, R. S.; Harrigan, P. R.; Moore, D.; Yip, B.; Wood, E.; Montaner, J. S. G. Continued improvement in survival among HIV-infected individuals with newer forms of highly active antiretroviral therapy. *AIDS* **2007**, *21* (6), 685–692.

(8) McArthur, J. C. HIV dementia: An evolving disease. *Journal of Neuroimmunology* **2004**, *157* (1-2 SPEC. ISS.), 3–10.

(9) Dore, G. J.; McDonald, A.; Li, Y.; Kaldor, J. M.; Brew, B. J. Marked improvement in survival following AIDS dementia complex in the era of highly active antiretroviral therapy. *AIDS* **2003**, *17* (10), 1539–1545.

(10) Antinori, A.; Arendt, G.; Becker, J. T.; Brew, B. J.; Byrd, D. A.; Cherner, M.; Clifford, D. B.; Cinque, P.; Epstein, L. G.; Goodkin, K.; et al. Updated research nosology for HIV-associated neurocognitive disorders. *Neurology* **2007**, *69* (18), 1789–1799.

(11) Heaton, R. K.; Clifford, D. B.; Franklin, D. R.; Woods, S. P.; Ake, C.; Vaida, F.; Ellis, R. J.; Letendre, S. L.; Marcotte, T. D.; Atkinson, J. H.; et al. HIV-associated neurocognitive disorders persist in the era of potent antiretroviral therapy. *Neurology* **2010**, *75* (23), 2087–2096.

(12) Simioni, S.; Cavassini, M.; Annoni, J.-M.; Rimbault Abraham, A.; Bourquin, I.; Schiffer, V.; Calmy, A.; Chave, J.-P.; Giacobini, E.; Hirschel, B.; et al. Cognitive dysfunction in HIV patients despite long-standing suppression of viremia. *AIDS* **2010**, *24* (9), 1243–1250.

(13) Hinkin, C. H.; Castellon, S. A.; Durvasula, R. S.; Hardy, D. J.; Lam, M. N.; Mason, K. I.; Thrasher, D.; Goetz, M. B.; Stefaniak, M. Medication adherence among HIV+ adults: Effects of cognitive dysfunction and regimen complexity. *Neurology* **2002**, *59* (12), 1944–1950.

(14) Heaton, R. K.; Velin, R. A.; McCutchan, J. A.; Gulevich, S. J.; Atkinson, J. H.; Wallace, M. R.; Godfrey, H. P.; Kirson, D. A.; Grant, I. Neuropsychological impairment in human immunodeficiency virus-infection: Implications for employment. *Psychosomatic Medicine* **1994**, *56* (1), 8–17.

(15) Benedict, R. H. B.; Mezhir, J. J.; Walsh, K.; Hewitt, R. G. Impact of human immunodeficiency virus type-1-associated cognitive dysfunction on activities of daily living and quality of life. *Archives of Clinical Neuropsychology* **2000**, *15* (6), 535–544.

(16) Albert, S. M.; Weber, C. M.; Todak, G.; Polanco, C.; Clouse, R.; McElhiney, M.; Rabkin, J.; Stern, Y.; Marder, K. An Observed Performance Test of Medication Management Ability in HIV: Relation to Neuropsychological Status and Medication Adherence Outcomes. *AIDS and Behavior* **1999**, *3* (2), 121–128.

(17) Yeung, H.; Krentz, H. B.; Gill, M. J.; Power, C. Neuropsychiatric disorders in HIV infection: Impact of diagnosis on economic costs of care. *AIDS* **2006**, *20* (16), 2005–2009.

(18) Abbott, N. J.; Patabendige, A. A. K.; Dolman, D. E. M.; Yusof, S. R.; Begley, D. J. Structure and function of the blood-brain barrier. *Neurobiology of Disease* **2010**, *37* (1), 13–25.

(19) Valcour, V.; Chalermchai, T.; Sailasuta, N.; Marovich, M.; Lerdlum, S.; Suttichom, D.; Suwanwela, N. C.; Jagodzinski, L.; Michael, N.; Spudich, S.; et al. Central nervous system viral invasion and inflammation during acute HIV infection. *Journal of Infectious Diseases* **2012**, *206* (2), 275–282.

(20) Zink, M. C.; Brice, A. K.; Kelly, K. M.; Queen, S. E.; Gama, L.; Li, M.; Adams, R. J.; Bartizal, C.; Varrone, J.; Rabi, S. A.; et al. Simian immunodeficiency virus-infected macaques treated with highly active antiretroviral therapy have reduced central nervous system viral replication and inflammation but persistence of viral DNA. *Journal of Infectious Diseases* **2010**, *202* (1), 161–170.

(21) Resnick, L.; Berger, J. R.; Shapshak, P.; Tourtellotte, W. W. Early penetration of the blood-brain-barrier by HIV. *Neurology* **1988**, *38* (1), 9–14.

(22) Peluso, R.; Haase, A.; Stowring, L.; Edwards, M.; Ventura, P. A Trojan Horse mechanism for the spread of visna virus in monocytes. *Virology* **1985**, *147* (1), 231–236.

(23) Watkins, B. A.; Dorn, H. H.; Kelly, W. B.; Armstrong, R. C.; Potts, B. J.; Michaels, F.; Kufta, C. V; Dubois-Dalcq, M. Specific tropism of HIV-1 for microglial cells in primary human brain cultures. *Science* **1990**, *249* (4968), 549–553.

(24) Koenig, S.; Gendelman, H. E.; Orenstein, J. M.; Dal Canto, M. C.; Pezeshkpour, G. H.; Yungbluth, M.; Janotta, F.; Aksamit, A.; Martin, M. A.; Fauci, A. S. Detection of AIDS virus

in macrophages in brain tissue from AIDS patients with encephalopathy. *Science* **1986**, *233* (4768), 1089–1093.

(25) Persidsky, Y.; Ghorpade, A.; Rasmussen, J.; Limoges, J.; Liu, X. J.; Stins, M.; Fiala, M.; Way, D.; Kim, K. S.; Witte, M. H.; et al. Microglial and astrocyte chemokines regulate monocyte migration through the blood-brain barrier in human immunodeficiency virus-1 encephalitis. *The American Journal of Pathology* **1999**, *155* (5), 1599–1611.

(26) Conant, K.; Garzino-Demo, A.; Nath, A.; McArthur, J. C.; Halliday, W.; Power, C.; Gallo, R. C.; Major, E. O. Induction of monocyte chemoattractant protein-1 in HIV-1 Tat-stimulated astrocytes and elevation in AIDS dementia. *Proceedings of the National Academy of Sciences* **1998**, *95* (6), 3117–3121.

(27) Cinque, P.; Vago, L.; Mengozzi, M.; Torri, V.; Ceresa, D.; Vicenzi, E.; Transidico, P.; Vagani, A.; Sozzani, S.; Mantovani, A.; et al. Elevated cerebrospinal fluid levels of monocyte chemotactic protein-1 correlate with HIV-1 encephalitis and local viral replication. *AIDS* **1998**, *12* (11), 1327–1332.

(28) Mengozzi, M.; De Filippi, C.; Transidico, P.; Biswas, P.; Cota, M.; Ghezzi, S.; Vicenzi, E.; Mantovani, A.; Sozzani, S.; Poli, G. Human immunodeficiency virus replication induces monocyte chemotactic protein-1 in human macrophages and U937 promonocytic cells. *Blood* **1999**, *93* (6), 1851–1857.

(29) Hickey, W.; Kimura, H. Perivascular microglial cells of the CNS are bone marrow-derived and present antigen in vivo. *Science* **1988**, *239* (4837), 290–292.

(30) Pryce, G.; Santos, W.; Male, D. An assay for the analysis of lymphocyte migration across cerebral endothelium in vitro. *Journal of Immunological Methods* **1994**, *167* (1-2), 55–63.

(31) Lassmann, H.; Schmied, M.; Vass, K.; Hickey, W. F. Bone marrow derived elements and resident microglia in brain inflammation. *Glia* **1993**, *7* (1), 19–24.

(32) Del Rio-Hortega, P. *Cytology and Cellular Pathology of the Nervous System*, Vol 2.; Penfield, W., Ed.; PB Hoeber, Inc.: New York, 1932.

(33) Kure, K.; Weidenheim, K. M.; Lyman, W. D.; Dickson, D. W. Morphology and distribution of HIV-1 gp41-positive microglia in subacute AIDS encephalitis. *Acta Neuropathologica* **1990**, *80* (4), 393–400.

(34) An, S. F.; Groves, M.; Gray, F.; Scaravilli, F. Early entry and widespread cellular involvement of HIV-1 DNA in brains of HIV-1 positive asymptomatic individuals. *Journal of Neuropathology and Experimental Neurology* **1999**, *58* (11), 1156–1162.

(35) Weiss, J. M.; Nath, A.; Major, E. O.; Berman, J. W. HIV-1 Tat induces monocyte chemoattractant protein-1-mediated monocyte transmigration across a model of the human blood-brain barrier and up-regulates CCR5 expression on human monocytes. *Journal of Immunology* **1999**, *163* (5), 2953–2959.

(36) Louveau, A.; Smirnov, I.; Keyes, T. J.; Eccles, J. D.; Rouhani, S. J.; Peske, J. D.; Derecki, N. C.; Castle, D.; Mandell, J. W.; Lee, K. S.; et al. Structural and functional features of central nervous system lymphatic vessels. *Nature* **2015**.

(37) Liu, N. Q.; Lossinsky, A. S.; Popik, W.; Li, X.; Gujuluva, C.; Kriederman, B.; Roberts, J.; Pushkarsky, T.; Bukrinsky, M.; Witte, M.; et al. Human immunodeficiency virus type 1 enters brain microvascular endothelia by macropinocytosis dependent on lipid rafts and the mitogen-activated protein kinase signaling pathway. *Journal of Virology* **2002**, *76* (13), 6689–6700.

(38) Bomsel, M. Transcytosis of infectious human immunodeficiency virus across a tight human epithelial cell line barrier. *Nature Medicine* **1997**, *3* (1), 42–47.

(39) Peudenier, S.; Héry, C.; Ng, K. H.; Tardieu, M. HIV receptors within the brain: A study of CD4 and MHC-II on human neurons, astrocytes and microglial cells. *Research in Virology* **1991**, *142* (2-3), 145–149.

(40) Dalgleish, A. G.; Beverley, P. C.; Clapham, P. R.; Crawford, D. H.; Greaves, M. F.; Weiss, R. A. The CD4 (T4) antigen is an essential component of the receptor for the AIDS retrovirus. *Nature* **1984**, *312* (5996), 763–767.

(41) Gelbard, H. A.; James, H. J.; Sharer, L. R.; Perry, S. W.; Saito, Y.; Kazee, A. M.; Blumberg, S. M.; Epstein, L. G. Apoptotic neurons in brains from paediatric patients with HIV-I encephalitis and progressive encephalopathy. *Neuropathology and Applied Neurobiology* **1995**, *21* (3), 208–217.

(42) Petito, C. K.; Roberts, B. Evidence of apoptotic cell death in HIV encephalitis. *The American Journal of Pathology* **1995**, *146* (5), 1121–1130.

(43) Everall, I. .; Luthert, P. .; Lantos, P. . Neuronal loss in the frontal cortex in HIV infection. *The Lancet* **1991**, *337* (8750), 1119–1121.

(44) Wiley, C. A.; Achim, C. L.; Christopherson, C.; Kidane, Y.; Kwok, S.; Masliah, E.; Mellors, J.; Radhakrishnan, L.; Wang, G.; Soontornniyomkij, V. HIV mediates a productive infection of the brain. *AIDS* **1999**, *13* (15), 2055–2059.

(45) Wiley, C. A.; Schrier, R. D.; Nelson, J. A.; Lampert, P. W.; Oldstone, M. B. Cellular localization of human immunodeficiency virus infection within the brains of acquired immune deficiency syndrome patients. *Proceedings of the National Academy of Sciences of the United States of America* **1986**, *83* (18), 7089–7093.

(46) Takahashi, K.; Wesselingh, S. L.; Griffin, D. E.; McArthur, J. C.; Johnson, R. T.; Glass, J. D. Localization of HIV-1 in human brain using polymerase chain reaction/in situ hybridization and immunocytochemistry. *Annals of Neurology* **1996**, *39* (6), 705–711.

(47) González-Scarano, F.; Martín-García, J. The neuropathogenesis of AIDS. *Nature Reviews Immunology* **2005**, *5* (1), 69–81.

(48) Kaul, M.; Garden, G. A.; Lipton, S. A. Pathways to neuronal injury and apoptosis in HIV-associated dementia. *Nature* **2001**, *410* (6831), 988–994.

(49) Patel, C. A.; Mukhtar, M.; Pomerantz, R. J. Human Immunodeficiency Virus Type 1 Vpr Induces Apoptosis in Human Neuronal Cells. *Journal of Virology* **2000**, *74* (20), 9717–9726.

(50) Patel, C. A.; Mukhtar, M.; Harley, S.; Kulkosky, J.; Pomerantz, R. J. Lentiviral expression of HIV-1 Vpr induces apoptosis in human neurons. *Journal of Neurovirology* **2002**, *8* (2), 86–99.

(51) Piller, S. C.; Jans, P.; Gage, P. W.; Jans, D. A. Extracellular HIV-1 virus protein R causes a large inward current and cell death in cultured hippocampal neurons: Implications for AIDS pathology. *Proceedings of the National Academy of Sciences* **1998**, *95* (8), 4595–4600.

(52) Xin, K. Q.; Hamajima, K.; Hattori, S.; Cao, X. R.; Kawamoto, S.; Okuda, K. Evidence of HIV type 1 glycoprotein 120 binding to recombinant N-methyl-D-aspartate receptor subunits expressed in a baculovirus system. *AIDS Research and Human Retroviruses* **1999**, *15* (16), 1461–1467.

(53) Toggas, S. M.; Masliah, E.; Mucke, L. Prevention of HIV-1 gp120-induced neuronal damage in the central nervous system of transgenic mice by the NMDA receptor antagonist memantine. *Brain Research* **1996**, *706* (2), 303–307.

(54) Toggas, S. M.; Masliah, E.; Rockenstein, E. M.; Rall, G. F.; Abraham, C. R.; Mucke, L. Central nervous system damage produced by expression of the HIV-1 coat protein gp120 in transgenic mice. *Nature* **1994**, *367* (6459), 188–193.

(55) Zheng, J.; Ghorpade, A.; Niemann, D.; Cotter, R. L.; Thylin, M. R.; Epstein, L.; Swartz, J. M.; Shepard, R. B.; Liu, X.; Nukuna, A.; et al. Lymphotropic Virions Affect Chemokine Receptor-Mediated Neural Signaling and Apoptosis: Implications for Human Immunodeficiency Virus Type 1-Associated Dementia. *Journal of Virology* **1999**, *73* (10), 8256–8267.

(56) Pandey, V.; Bolsover, S. R. Immediate and neurotoxic effects of HIV protein gp120 act through CXCR4 receptor. *Biochemical and Biophysical Research Communications* **2000**, *274* (1), 212–215.

(57) Li, W.; Huang, Y.; Reid, R.; Steiner, J.; Malpica-Llanos, T.; Darden, T. A.; Shankar, S. K.; Mahadevan, A.; Satishchandra, P.; Nath, A. NMDA receptor activation by HIV-Tat protein is clade dependent. *The Journal of Neuroscience* **2008**, *28* (47), 12190–12198.

(58) Song, L.; Nath, A.; Geiger, J. D.; Moore, A.; Hochman, S. Human immunodeficiency virus type 1 Tat protein directly activates neuronal N-methyl-D-aspartate receptors at an allosteric zinc-sensitive site. *Journal of Neurovirology* **2003**, *9* (3), 399–403.

(59) Fields, J. A.; Dumaop, W.; Crews, L.; Adame, A.; Spencer, B.; Metcalf, J.; He, J.; Rockenstein, E.; Masliah, E. Mechanisms of HIV-1 Tat neurotoxicity via CDK5

translocation and hyper-activation: Role in HIV-associated neurocognitive disorders. *Current HIV Research* **2015**, *13* (1), 43–54.

(60) Choi, D. W. Calcium-mediated neurotoxicity: relationship to specific channel types and role in ischemic damage. *Trends in Neurosciences* **1988**, *11* (10), 465–469.

(61) Garthwaite, G.; Garthwaite, J. Receptor-linked ionic channels mediate neurotoxicity in rat cerebellar slices. *Neuroscience Letters* **1987**, *83* (3), 241–246.

(62) Dreyer, E. B.; Lipton, S. A. The Coat Protein gp120 of HIV-1 Inhibits Astrocyte Uptake of Excitatory Amino Acids via Macrophage Arachidonic Acid. *European Journal of Neuroscience* **1995**, *7* (12), 2502–2507.

(63) Chao, C. C.; Hu, S. Tumor Necrosis Factor-Alpha Potentiates Glutamate Neurotoxicity in Human Fetal Brain Cell Cultures. *Developmental Neuroscience* **1994**, *16* (3-4), 172–179.

(64) Fine, S. M.; Angel, R. A.; Perry, S. W.; Epstein, L. G.; Rothstein, J. D.; Dewhurst, S.; Gelbard, H. A. Tumor necrosis factor alpha inhibits glutamate uptake by primary human astrocytes. Implications for pathogenesis of HIV-1 dementia. *The Journal of Biological Chemistry* **1996**, *271* (26), 15303–15306.

(65) Genis, P.; Jett, M.; Bernton, E. W.; Boyle, T.; Gelbard, H. A.; Dzenko, K.; Keane, R. W.; Resnick, L.; Mizrachi, Y.; Volsky, D. J. Cytokines and arachidonic metabolites produced during human immunodeficiency virus (HIV)-infected macrophage-astroglia interactions: Implications for the neuropathogenesis of HIV disease. *The Journal of Experimental Medicine* **1992**, *176* (6), 1703–1718.

(66) Brew, B. J.; Corbeil, J.; Pemberton, L.; Evans, L.; Saito, K.; Penny, R.; Cooper, D. A.; Heyes, M. P. Quinolinic acid production is related to macrophage tropic isolates of HIV-1. *Journal of Neurovirology* **1995**, *1* (5-6), 369–374.

(67) Kim, J. P.; Choi, D. W. Quinolinate neurotoxicity in cortical cell culture. *Neuroscience* **1987**, *23* (2), 423–432.

(68) Yoshida, H.; Imaizumi, T.; Fujimoto, K.; Matsuo, N.; Kimura, K.; Cui, X.-F.; Matsumiya, T.; Tanji, K.; Shibata, T.; Tamo, W.; et al. Synergistic stimulation, by tumor necrosis factor-α and interferon-γ, of fractalkine expression in human astrocytes. *Neuroscience Letters* **2001**, *303* (2), 132–136.

(69) Meucci, O.; Fatatis, A.; Simen, A. A.; Miller, R. J. Expression of CX3CR1 chemokine receptors on neurons and their role in neuronal survival. *Proceedings of the National Academy of Sciences* **2000**, *97* (14), 8075–8080.

(70) Kipnis, J.; Avidan, H.; Caspi, R. R.; Schwartz, M. Dual effect of CD4+CD25+ regulatory T cells in neurodegeneration: A dialogue with microglia. *Proceedings of the National Academy of Sciences* **2004**, *101* (Supplement 2), 14663–14669.

(71) Shaked, I.; Porat, Z.; Gersner, R.; Kipnis, J.; Schwartz, M. Early activation of microglia as antigen-presenting cells correlates with T cell-mediated protection and repair of the injured central nervous system. *Journal of Neuroimmunology* **2004**, *146* (1-2), 84–93.

(72) UNAIDS. AIDSinfo Epidemiological Status: South Africa. http://www.unaids.org/en/dataanalysis/datatools/aidsinfo (accessed Jun 16, 2015).

(73) Butler, A. South Africa's HIV/AIDS policy, 1994-2004: How can it be explained? *African Affairs* **2005**, *104* (417), 591–614.

(74) Clifford, D. B.; Ances, B. M. HIV-associated neurocognitive disorder. *The Lancet Infectious Diseases* **2013**, *13* (11), 976–986.

(75) Atkinson A.J., J.; Colburn, W. A.; DeGruttola, V. G.; DeMets, D. L.; Downing, G. J.; Hoth, D. F.; Oates, J. A.; Peck, C. C.; Schooley, R. T.; Spilker, B. A.; et al. Biomarkers and surrogate endpoints: Preferred definitions and conceptual framework. *Clinical Pharmacology and Therapeutics* **2001**, *69* (3), 89–95.

(76) Strimbu, K.; Tavel, J. A. What are biomarkers? *Current Opinion in HIV and AIDS* **2010**, *5* (6), 463–466.

(77) Ragin, A. B.; Wu, Y.; Ochs, R.; Scheidegger, R.; Cohen, B. A.; Edelman, R. R.; Epstein, L. G.; McArthur, J. Biomarkers of neurological status in HIV infection: A 3-year study. *Proteomics - Clinical Applications* **2010**, *4* (3), 295–303.

(78) Rozek, W.; Ricardo-Dukelow, M.; Holloway, S.; Gendelman, H. E.; Wojna, V.; Melendez, L. M.; Ciborowski, P. Cerebrospinal fluid proteomic profiling of HIV-1-infected patients with cognitive impairment. *Journal of proteome research* **2007**, *6* (11), 4189–4199.

(79) Rozek, W.; Horning, J.; Anderson, J.; Ciborowski, P. Sera proteomic biomarker profiling in HIV-1 infected subjects with cognitive impairment. *Proteomics - Clinical Applications* **2008**, *2* (10-11), 1498–1507.

(80) Burdo, T. H.; Weiffenbach, A.; Woods, S. P.; Letendre, S.; Ellis, R. J.; Williams, K. C. Elevated sCD163 in plasma but not cerebrospinal fluid is a marker of neurocognitive impairment in HIV infection. *AIDS* **2013**, *27* (9), 1387–1395.

(81) Lyons, J. L.; Uno, H.; Ancuta, P.; Kamat, A.; Moore, D. J.; Singer, E. J.; Morgello, S.; Gabuzda, D. Plasma sCD14 Is a Biomarker Associated With Impaired Neurocognitive Test Performance in Attention and Learning Domains in HIV Infection. *Journal of Acquired Immune Deficiency Syndromes* **2011**, *57* (5), 371–379.

(82) Brew, B. J.; Letendre, S. Biomarkers of HIV-Related Central Nervous System Disease. In *HIV and the Brain: New Challenges in the Modern Era*; Paul, R. H., Sacktor, N. C., Valcour, V., Tashima, K. T., Eds.; Humana Press: New York, 2009; pp 49–73.

(83) McArthur, J. C.; Steiner, J.; Sacktor, N.; Nath, A. Human immunodeficiency virus-associated neurocognitive disorders mind the gap. *Annals of Neurology* **2010**, *67* (6), 699–714.

(84) Rifai, N.; Gillette, M. A.; Carr, S. A. Protein biomarker discovery and validation: the long and uncertain path to clinical utility. *Nature Biotechnology* **2006**, *24* (8), 971–983.

(85) Gisslén, M.; Price, R. W.; Nilsson, S. The definition of HIV-associated neurocognitive disorders: are we overestimating the real prevalence? *BMC Infectious Diseases* **2011**, *11* (1), 356.

(86) Haddow, L. J.; Floyd, S.; Copas, A.; Gilson, R. J. C. A Systematic Review of the Screening Accuracy of the HIV Dementia Scale and International HIV Dementia Scale. *PLoS ONE* **2013**, *8* (4).

(87) Gisslen, M.; Hagberg, L.; Rosengren, L.; Brew, B. J.; Cinque, P.; Spudich, S.; Price, R. W. Defining and evaluating HIV-related neurodegenerative disease and its treatment targets: a combinatorial approach to use of cerebrospinal fluid molecular biomarkers. *Journal of Neuroimmune Pharmacology* **2007**, *2* (1), 112–119.

(88) Joska, J. A.; Westgarth-Taylor, J.; Hoare, J.; Thomas, K. G. F.; Paul, R.; Myer, L.; Stein, D. J. Validity of the International HIV Dementia Scale in South Africa. *AIDS Patient Care and STDs* **2011**, *25* (2), 95–101.

(89) Murray, K. K.; Boyd, R. K.; Eberlin, M. N.; Langley, G. J.; Li, L.; Naito, Y. Definitions of terms relating to mass spectrometry (IUPAC Recommendations 2013). *Pure and Applied Chemistry* **2013**, *85* (7), 1515–1609.

(90) Muller, P. Glossary of terms used in physical organic chemistry (IUPAC Recommendations 1994). *Pure and Applied Chemistry* **1994**, *66* (5), 1077–1184.

(91) Karas, M.; Bachmann, D.; Bahr, U.; Hillenkamp, F. Matrix-assisted ultraviolet laser desorption of non-volatile compounds. *International Journal of Mass Spectrometry and Ion Processes* **1987**, *78*, 53–68.

(92) Yamashita, M.; Fenn, J. B. Electrospray ion source. Another variation on the free-jet theme. *The Journal of Physical Chemistry* **1984**, *88* (20), 4451–4459.

(93) Dole, M. Molecular Beams of Macroions. *The Journal of Chemical Physics* **1968**, *49* (5), 2240–2249.

(94) Karas, M.; Bachmann, D.; Hillenkamp, F. Influence of the wavelength in high-irradiance ultraviolet laser desorption mass spectrometry of organic molecules. *Analytical Chemistry* **1985**, *57* (14), 2935–2939.

(95) Fenn, J. B.; Mann, M.; Meng, C. K.; Wong, S. F.; Whitehouse, C. M. Electrospray ionization for mass spectrometry of large biomolecules. *Science* **1989**, *246* (4926), 64–71.

(96) Aebersold, R.; Mann, M. Mass spectrometry-based proteomics. *Nature* **2003**, *422* (6928), 198–207.

(97) Yates, J. R. Mass spectrometry and the age of the proteome. *Journal of Mass Spectrometry* **1998**, *33*, 1–19.

(98) Aguilar, M. I. *HPLC of Peptides and Proteins: Methods and Protocols*, 1st ed.; Aguilar, M. I., Ed.; Humana Press: Totowa, NJ, 2004; Vol. 251.

(99) Thomson, B. A.; Iribarne, J. V. Field induced ion evaporation from liquid surfaces at atmospheric pressure. *The Journal of Chemical Physics* **1979**, *71* (11), 4451–4463.

(100) Iribarne, J. V. On the evaporation of small ions from charged droplets. *The Journal of Chemical Physics* **1976**, *64* (6), 2287–2294.

(101) Wilm, M. S.; Mann, M. Electrospray and Taylor-Cone theory, Dole's beam of macromolecules at last? *International Journal of Mass Spectrometry and Ion Processes* **1994**, *136* (2-3), 167–180.

(102) Wilm, M.; Mann, M. Analytical properties of the nanoelectrospray ion source. *Analytical Chemistry* **1996**, *68* (1), 1–8.

(103) Hoffmann, E. de; Stroobant, V. *Mass Spectrometry: Principles and Applications*, 3rd ed.; John Wiley & Sons: Chichester, 2007.

(104) Guilhaus, M. Principles and instrumentation in time-of-flight mass spectrometry. *Journal of Mass Spectrometry* **1995**, *30* (11), 1519–1532.

(105) Stephens, W. A pulsed mass spectrometer with time dispersion. *Physical Review* **1946**, *69*, 691.

(106) McLafferty, F. Tandem mass spectrometry. *Science* **1981**, *214* (4518), 280–287.

(107) Dayon, L.; Pasquarello, C.; Hoogland, C.; Sanchez, J. C.; Scherl, A. Combining low- and high-energy tandem mass spectra for optimized peptide quantification with isobaric tags. *Journal of Proteomics* **2010**, *73* (4), 769–777.

(108) Yost, R. A.; Enke, C. G.; McGilvery, D. C.; Smith, D.; Morrison, J. D. High efficiency collision-induced dissociation in an RF-only quadrupole. *International Journal of Mass Spectrometry and Ion Physics* **1979**, *30* (2), 127–136.

(109) Olsen, J. V; Macek, B.; Lange, O.; Makarov, A.; Horning, S.; Mann, M. Higher-energy C-trap dissociation for peptide modification analysis. *Nature Methods* **2007**, *4* (9), 709–712.

(110) Miller, P. E.; Denton, M. B. The quadrupole mass filter: Basic operating concepts. *Journal of Chemical Education* **1986**, *63* (7), 617–622.

(111) Paul, W and Steinwedel, H. Quadrupole mass filter. *Z. Naturforsch. A* **1953**, *8*, 448.

(112) Marshall, A. G.; Hendrickson, C. L.; Jackson, G. S. Fourier transform ion cyclotron resonance mass spectrometry: a primer. *Mass Spectrometry Reviews* **1998**, *17* (1), 1–35.

(113) Makarov, A. Electrostatic axially harmonic orbital trapping: A high-performance technique of mass analysis. *Analytical Chemistry* **2000**, *72* (6), 1156–1162.

(114) Eng, J. K.; McCormack, A. L.; Yates, J. R. An approach to correlate tandem mass spectral data of peptides with amino acid sequences in a protein database. *Journal of the American Society for Mass Spectrometry* **1994**, *5*, 976–989.

(115) Roepstorff, P.; Fohlman, J. Proposal for a Common Nomenclature for Sequence Ions in Mass Spectra of Peptides. *Biomedical Mass Spectrometry* **1985**, *12* (10), 631–631.

(116) Biemann, K. Appendix 5. Nomenclature for peptide fragment ions (positive ions). *Methods in Enzymology* **1990**, *193*, 886–887.

(117) Tang, X. J.; Thibault, P.; Boyd, R. K. Fragmentation reactions of multiply-protonated peptides and implications for sequencing by tandem mass spectrometry with low-energy collision-induced dissociation. *Analytical Chemistry* **1993**, *65* (20), 2824–2834.

(118) Cox, J.; Mann, M. MaxQuant enables high peptide identification rates, individualized p.p.b.-range mass accuracies and proteome-wide protein quantification. *Nature Biotechnology* **2008**, *26* (12), 1367–1372.

(119) Cox, J.; Neuhauser, N.; Michalski, A.; Scheltema, R. a.; Olsen, J. V.; Mann, M. Andromeda: A peptide search engine integrated into the MaxQuant environment. *Journal of Proteome Research* **2011**, *10*, 1794–1805.

(120) Elias, J. E.; Gygi, S. P. Target-decoy search strategy for increased confidence in large-scale protein identifications by mass spectrometry. *Nature Methods* **2007**, *4* (3), 207–214.

(121) Kondrat, R. W.; McClusky, G. A.; Cooks, R. G. Multiple reaction monitoring in mass spectrometry/mass spectrometry for direct analysis of complex mixtures. *Analytical Chemistry* **1978**, *50* (14), 2017–2021.

(122) Baty, J. D.; Robinson, P. R. Single and multiple ion recording techniques for the analysis of diphenylhydantoin and its major metabolite in plasma. *Biomedical mass spectrometry* **1977**, *4* (1), 36–41.

(123) Zakett, D.; Zakett, D.; Flynn, R. G. A.; Flynn, R. G. A.; Cooks, R. G.; Cooks, R. G. Chlorine isotope effects in mass spectrometry by multiple reaction monitoring. *The Journal of Physical Chemistry* **1978**, *82* (22), 2359–2362.

(124) Gallien, S.; Duriez, E.; Domon, B. Selected reaction monitoring applied to proteomics. *Journal of Mass Spectrometry* **2011**, *46*, 298–312.

(125) Yost, R. A.; Enke, C. G. Triple quadrupole mass spectrometry for direct mixture analysis and structure elucidation. *Analytical Chemistry* **1979**, *51*, 1251–1264.

(126) Yost, R. A.; Enke, C. G. Selected Ion Fragmentation with a Tandem Quadrupole Mass Spectrometer. *Journal of the American Chemical Society* **1978**.

(127) Boja, E. S.; Rodriguez, H. The path to clinical proteomics research: Integration of proteomics, genomics, clinical laboratory and regulatory science. *Korean Journal of Laboratory Medicine* **2011**, *31* (2), 61–71.

(128) Cody, R. B.; Burnier, R. C.; Freiser, B. S. Collision-Induced Dissociation with Fourier Transform Mass Spectrometry. *Analytical Chemistry* **1982**, *54* (24), 96–101.

(129) Farnsworth, P. Electron multiplier. US Patent 1,969,399, 1934.

(130) Peterson, A. C.; Russell, J. D.; Bailey, D. J.; Westphall, M. S.; Coon, J. J. Parallel reaction monitoring for high resolution and high mass accuracy quantitative, targeted proteomics. *Molecular & Cellular Proteomics* **2012**, *11* (11), 1475–1488.

(131) Gallien, S.; Duriez, E.; Crone, C.; Kellmann, M.; Moehring, T.; Domon, B. Targeted Proteomic Quantification on Quadrupole-Orbitrap Mass Spectrometer. *Molecular & Cellular Proteomics* **2012**, *11*, 1709–1723.

(132) Gallien, S.; Bourmaud, A.; Kim, S. Y.; Domon, B. Technical considerations for large-scale parallel reaction monitoring analysis. *Journal of Proteomics* **2014**, *100*, 147–159.

(133) MacLean, B.; Tomazela, D. M.; Shulman, N.; Chambers, M.; Finney, G. L.; Frewen, B.; Kern, R.; Tabb, D. L.; Liebler, D. C.; MacCoss, M. J. Skyline: An open source document editor for creating and analyzing targeted proteomics experiments. *Bioinformatics* **2010**, *26* (7), 966–968.

(134) Lange, V.; Picotti, P.; Domon, B.; Aebersold, R. Selected reaction monitoring for quantitative proteomics: A tutorial. *Molecular Systems Biology* **2008**, *4* (1), 222.

(135) Stergachis, A. B.; MacLean, B.; Lee, K.; Stamatoyannopoulos, J. A.; MacCoss, M. J. Rapid empirical discovery of optimal peptides for targeted proteomics. *Nature Methods* **2011**, *8* (12), 1041–1043.

(136) Parker, C. E.; Borchers, C. H. Mass spectrometry based biomarker discovery, verification, and validation - Quality assurance and control of protein biomarker assays. *Molecular Oncology* **2014**, *8* (4), 840–858.

(137) Kuzyk, M. A.; Smith, D.; Yang, J.; Cross, T. J.; Jackson, A. M.; Hardie, D. B.; Anderson, N. L.; Borchers, C. H. Multiple reaction monitoring-based, multiplexed, absolute quantitation of 45 proteins in human plasma. *Molecular & Cellular Proteomics* **2009**, *8* (8), 1860–1877.

(138) Stahl-Zeng, J.; Lange, V.; Ossola, R.; Eckhardt, K.; Krek, W.; Aebersold, R.; Domon, B. High sensitivity detection of plasma proteins by multiple reaction monitoring of N-glycosites. *Molecular & Cellular Proteomics* **2007**, *6* (10), 1809–1817.

(139) Berna, M.; Ackermann, B. Increased throughput for low-abundance protein biomarker verification by liquid chromatography/tandem mass spectrometry. *Analytical Chemistry* **2009**, *81* (10), 3950–3956.

(140) Teleman, J.; Karlsson, C.; Waldemarson, S.; Hansson, K.; James, P.; Malmström, J.; Levander, F. Automated selected reaction monitoring software for accurate label-free protein quantification. *Journal of Proteome Research* **2012**, *11*, 3766–3773.

(141) Gubala, V.; Harris, L. F.; Ricco, A. J.; Tan, M. X.; Williams, D. E. Point of care diagnostics: Status and future. *Analytical Chemistry* **2012**, *84* (2), 487–515.

(142) Lambert, M. P.; Barlow, A. K.; Chromy, B. A.; Edwards, C.; Freed, R.; Liosatos, M.; Morgan, T. E.; Rozovsky, I.; Trommer, B.; Viola, K. L.; et al. Diffusible, nonfibrillar ligands derived from Abeta1-42 are potent central nervous system neurotoxins. *Proceedings of the National Academy of Sciences of the United States of America* **1998**, *95* (11), 6448–6453.

(143) Glenner, G. G.; Wong, C. W. Alzheimer's disease: initial report of the purification and characterization of a novel cerebrovascular amyloid protein. *Biochemical and biophysical research communications* **1984**, *120* (3), 885–890.

(144) Masters, C. L.; Simms, G.; Weinman, N. A.; Multhaup, G.; McDonald, B. L.; Beyreuther, K. Amyloid plaque core protein in Alzheimer disease and Down syndrome. *Proceedings of the National Academy of Sciences of the United States of America* **1985**, *82* (12), 4245–4249.

(145) Delacourte, A.; Defossez, A. Alzheimer's disease: Tau proteins, the promoting factors of microtubule assembly, are major components of paired helical filaments. *Journal of the Neurological Sciences* **1986**, *76* (2-3), 173–186.

(146) Kosik, K. S.; Joachim, C. L.; Selkoe, D. J. Microtubule-associated protein tau (tau) is a major antigenic component of paired helical filaments in Alzheimer disease. *Proceedings of the National Academy of Sciences* **1986**, *83* (11), 4044–4048.

(147) Giulian, D.; Haverkamp, L. J.; Yu, J. H.; Karshin, W.; Tom, D.; Li, J.; Kirkpatrick, J.; Kuo, L. M.; Roher, A. E. Specific domains of beta-amyloid from Alzheimer plaque elicit neuron killing in human microglia. *The Journal of Neuroscience* **1996**, *16* (19), 6021–6037.

(148) Rozemuller, J. M.; Eikelenboom, P.; Stam, F. C. Role of microglia in plaque formation in senile dementia of the Alzheimer type. *Virchows Archiv B Cell Pathology Including Molecular Pathology* **1986**, *51* (1), 247–254.

(149) Giulian, D.; Haverkamp, L. J.; Li, J.; Karshin, W. L.; Yu, J.; Tom, D.; Li, X.; Kirkpatrick, J. B. Senile plaques stimulate microglia to release a neurotoxin found in Alzheimer brain. *Neurochemistry International* **1995**, *27* (1), 119–137.

(150) Meda, L.; Cassatella, M. A.; Szendrei, G. I.; Otvos, L.; Baron, P.; Villalba, M.; Ferrari, D.; Rossi, F. Activation of microglial cells by beta-amyloid protein and interferon-gamma. *Nature* **1995**, *374* (6523), 647–650.

(151) Barger, S. W.; Harmon, A. D. Microglial activation by Alzheimer amyloid precursor protein and modulation by apolipoprotein E. *Nature* **1997**, *388* (6645), 878–881.

(152) Esiri, M. M.; Biddolph, S. C.; Morris, C. S. Prevalence of Alzheimer plaques in AIDS. *Journal of Neurology, Neurosurgery, and Psychiatry* **1998**, *65* (1), 29–33.

(153) Green, D. A.; Masliah, E.; Vinters, H. V; Beizai, P.; Moore, D. J.; Achim, C. L. Brain deposition of beta-amyloid is a common pathologic feature in HIV positive patients. *AIDS* **2005**, *19* (4), 407–411.

(154) Hye, A.; Riddoch-Contreras, J.; Baird, A. L.; Ashton, N. J.; Bazenet, C.; Leung, R.; Westman, E.; Simmons, A.; Dobson, R.; Sattlecker, M.; et al. Plasma proteins predict conversion to dementia from prodromal disease. *Alzheimer's and Dementia* **2014**, *44*, 1–9.

(155) Thambisetty, M.; Simmons, A.; Velayudhan, L.; Hye, A.; Campbell, J.; Zhang, Y.; Wahlund, L.-O.; Westman, E.; Kinsey, A.; Güntert, A.; et al. Association of plasma clusterin concentration with severity, pathology, and progression in Alzheimer disease. *Archives of General Psychiatry* **2010**, *67* (7), 739–748.

(156) Thambisetty, M.; Tripaldi, R.; Riddoch-Contreras, J.; Hye, A.; An, Y.; Campbell, J.; Sojkova, J.; Kinsey, A.; Lynham, S.; Zhou, Y.; et al. Proteome-based plasma markers of brain amyloid-β deposition in non-demented older individuals. *Journal of Alzheimer's disease* **2010**, *22* (4), 1099–1109.

(157) Hye, A.; Lynham, S.; Thambisetty, M.; Causevic, M.; Campbell, J.; Byers, H. L.; Hooper, C.; Rijsdijk, F.; Tabrizi, S. J.; Banner, S.; et al. Proteome-based plasma biomarkers for Alzheimer's disease. *Brain* **2006**, *129* (11), 3042–3050.

(158) Güntert, A.; Campbell, J.; Saleem, M.; O'Brien, D. P.; Thompson, A. J.; Byers, H. L.; Ward, M. A.; Lovestone, S. Plasma gelsolin is decreased and correlates with rate of decline in Alzheimer's disease. *Journal of Alzheimer's Disease* **2010**, *21* (2), 585–596.

(159) Thambisetty, M.; Simmons, A.; Hye, A.; Campbell, J.; Westman, E.; Zhang, Y.; Wahlund, L. O.; Kinsey, A.; Causevic, M.; Killick, R.; et al. Plasma biomarkers of brain atrophy in Alzheimer's disease. *PLoS ONE* **2011**, *6* (12), 1–7.

(160) Zubarev, R. A. The challenge of the proteome dynamic range and its implications for in-depth proteomics. *Proteomics* **2013**, *13* (5), 723–726.

(161) Picotti, P.; Bodenmiller, B.; Mueller, L. N.; Domon, B.; Aebersold, R. Full Dynamic Range Proteome Analysis of S. cerevisiae by Targeted Proteomics. *Cell* **2009**, *138* (4), 795–806.

(162) Anderson, N. L.; Anderson, N. G. The human plasma proteome: History, character, and diagnostic prospects. *Molecular & Cellular Proteomics* **2002**, *1* (11), 845–867.

(163) Pieper, R.; Su, Q.; Gatlin, C. L.; Huang, S. T.; Anderson, N. L.; Steiner, S. Multi-component immunoaffinity subtraction chromatography: An innovative step towards a comprehensive survey of the human plasma proteome. *Proteomics* **2003**, *3* (4), 422–432.

(164) Jin, W.; Dai, J.; Li, S.; Xia, Q.; Zou, H.; Zeng, R. Human plasma proteome analysis by multidimensional chromatography prefractionation and linear ion trap mass spectrometry identification. *Journal of Proteome Research* **2005**, *4* (2), 613–619.

(165) Faca, V.; Pitteri, S. J.; Newcomb, L.; Glukhova, V.; Phanstiel, D.; Krasnoselsky, A.; Zhang, Q.; Struthers, J.; Wang, H.; Eng, J.; et al. Contribution of protein fractionation to depth of analysis of the serum and plasma proteomes. *Journal of Proteome Research* **2007**, *6* (9), 3558–3565.

(166) Hortin, G. L.; Sviridov, D.; Anderson, N. L. High-abundance polypeptides of the human plasma proteome comprising the top 4 logs of polypeptide abundance. *Clinical Chemistry* **2008**, *54* (10), 1608–1616.

(167) Mitchell, P. Proteomics retrenches. *Nature Biotechnology* **2010**, *28* (7), 665–670.

(168) Dayon, L.; Kussmann, M. Proteomics of human plasma: A critical comparison of analytical workflows in terms of effort, throughput and outcome. *EuPA Open Proteomics* **2013**, *1*, 8–16.

(169) Shi, T.; Su, D.; Liu, T.; Tang, K.; Camp, D. G.; Qian, W.-J.; Smith, R. D. Advancing the sensitivity of selected reaction monitoring-based targeted quantitative proteomics. *Proteomics* **2012**, *12* (8), 1074–1092.

(170) Joska, J. A.; Westgarth-Taylor, J.; Myer, L.; Hoare, J.; Thomas, K. G. F.; Combrinck, M.; Paul, R. H.; Stein, D. J.; Flisher, A. J. Characterization of HIV-Associated Neurocognitive Disorders among individuals starting antiretroviral therapy in South Africa. *AIDS and Behavior* **2011**, *15* (6), 1197–1203.

(171) Joska, J. A.; Combrinck, M.; Valcour, V. G.; Hoare, J.; Leisegang, F.; Mahne, A. C.; Myer, L.; Stein, D. J. Association between apolipoprotein E4 genotype and human immunodeficiency virus-associated dementia in younger adults starting antiretroviral therapy in South Africa. *Journal of Neurovirology* **2010**, *16* (5), 377–383.

(172) Gallagher, S. R. One-Dimensional SDS Gel Electrophoresis of Proteins. *Current Protocols in Molecular Biology* **1999**.

(173) Laemmli, U. K. Cleavage of structural proteins during the assembly of the head of bacteriophage T4. *Nature* **1970**, *227*, 680–685.

(174) Hardy, E.; Castellanos-Serra, L. R. “Reverse-staining” of biomolecules in electrophoresis gels: Analytical and micropreparative applications. *Analytical Biochemistry* **2004**, *328* (1), 1–13.

(175) Smit, S. Trypsin Digest Protocol for MS Sample Preparation. *Personal Communication* **2013**.

(176) Kussmann, M.; Nordhoff, E.; Rahbek-Nielsen, H.; Haebel, S.; Rossel-Larsen, M.; Jakobsen, L.; Gobom, J.; Mirgorodskaya, E.; Kroll-Kristensen, A.; Palm, L.; et al. Matrix-assisted laser desorption/ionization mass spectrometry sample preparation techniques designed for various peptide and protein analytes. *Journal of Mass Spectrometry* **1997**, *32* (6), 593–601.

(177) Thermo Scientific. Pierce C18 Spin Columns https://www.lifetechnologies.com/order/catalog/product/89870 (accessed Sep 10, 2013).

(178) Pirmoradian, M.; Budamgunta, H.; Chingin, K.; Zhang, B.; Astorga-Wells, J.; Zubarev, R. A. Rapid and deep human proteome analysis by single-dimension shotgun proteomics. *Molecular & Cellular Proteomics* **2013**, *12* (11), 3330–3338.

(179) Omenn, G. S.; States, D. J.; Adamski, M.; Blackwell, T. W.; Menon, R.; Hermjakob, H.; Apweiler, R.; Haab, B. B.; Simpson, R. J.; Eddes, J. S.; et al. Overview of the HUPO Plasma Proteome Project: Results from the pilot phase with 35 collaborating laboratories and multiple analytical groups, generating a core dataset of 3020 proteins and a publicly-available database. *Proteomics* **2005**, *5* (13), 3226–3245.

(180) Jones, K. A.; Kim, P. D.; Patel, B. B.; Kelsen, S. G.; Braverman, A.; Swinton, D. J.; Gafken, P. R.; Jones, L. A.; Lane, W. S.; Neveu, J. M.; et al. Immunodepletion plasma proteomics by TripleTOF 5600 and Orbitrap Elite/LTQ-Orbitrap Velos/Q Exactive mass spectrometers. *Journal of Proteome Research* **2013**, *12*, 4351–4365.

(181) Boichenko, A. P.; Govorukhina, N.; Klip, H. G.; van der Zee, A. G. J.; Güzel, C.; Luider, T. M.; Bischoff, R. A Panel of Regulated Proteins in Serum from Patients with Cervical Intraepithelial Neoplasia and Cervical Cancer. *Journal of Proteome Research* **2014**, *13*, 4995–5007.

(182) Schroeder, T.; Nicklay, J.; Peterman, S.; Xuan, Y. How to Best Utilize your QE/QE Plus for Maximum Peptides IDs and for Peptide Quantitation. *Technical Note* **2014**.

(183) Wiśniewski, J. R.; Zougman, A.; Nagaraj, N.; Mann, M. Universal sample preparation method for proteome analysis. *Nature Methods* **2009**, *6* (5), 359–362.

(184) Morelle, W.; Canis, K.; Chirat, F.; Faid, V.; Michalski, J. C. The use of mass spectrometry for the proteomic analysis of glycosylation. *Proteomics* **2006**, *6* (14), 3993–4015.

(185) Promega. Sequencing Grade Modified Trypsin https://www.promega.sg/~/media/Files/Resources/Protocols/Product Information Sheets/N/Sequencing Grade Modified Trypsin Frozen Protocol.pdf (accessed Sep 28, 2011).

(186) Todd, J. F. J.; Waldren, R. M.; Mather, R. E. The quadrupole ion store (quistor) part IX. space-charge and ion stability. a theoretical background and experimental results. *International Journal of Mass Spectrometry and Ion Physics* **1980**, *34* (3-4), 325–349.

(187) Michalski, A.; Damoc, E.; Hauschild, J.-P.; Lange, O.; Wieghaus, A.; Makarov, A.; Nagaraj, N.; Cox, J.; Mann, M.; Horning, S. Mass Spectrometry-based Proteomics Using Q Exactive, a High-performance Benchtop Quadrupole Orbitrap Mass Spectrometer. *Molecular & Cellular Proteomics* **2011**, *10* (9), M111.011015.

(188) Perry, R. H.; Cooks, R. G.; Noll, R. J. Orbitrap mass spectrometry: Instrumentation, ion motion and applications. *Mass Spectrometry Reviews* **2008**, *27* (December 2007), 661–699.

(189) Picotti, P.; Aebersold, R. Selected reaction monitoring–based proteomics: workflows, potential, pitfalls and future directions. *Nature Methods* **2012**, *9* (6), 555–566.

(190) Addona, T. A.; Abbatiello, S. E.; Schilling, B.; Skates, S. J.; Mani, D. R.; Bunk, D. M.; Spiegelman, C. H.; Zimmerman, L. J.; Ham, A. L.; Keshishian, H.; et al. Multi-site assessment of the precision and reproducibility of multiple reaction monitoring-based measurements of proteins in plasma. *Nature Biotechnology* **2009**, *27* (7), 633–641.

(191) Sedmak, J. J.; Grossberg, S. E. A rapid, sensitive, and versatile assay for protein using Coomassie brilliant blue G250. *Analytical Biochemistry* **1977**, *79* (1–2), 544–552.

(192) Moore, S.; Stein, W. Photometric ninhydrin method for use in the chromatography of amino acids. *The Journal of Biological Chemistry* **1948**, *176* (1), 367–388.

(193) Boja, E. S.; Rodriguez, H. Mass spectrometry-based targeted quantitative proteomics: Achieving sensitive and reproducible detection of proteins. *Proteomics* **2012**, *12* (8), 1093–1110.

(194) Brun, V.; Dupuis, A.; Adrait, A.; Marcellin, M.; Thomas, D.; Court, M.; Vandenesch, F.; Garin, J. Isotope-labeled protein standards: toward absolute quantitative proteomics. *Molecular & Cellular Proteomics* **2007**, *6* (12), 2139–2149.

(195) Ferguson, R. E.; Carroll, H. P.; Harris, A.; Maher, E. R.; Selby, P. J.; Banks, R. E. Housekeeping proteins: A preliminary study illustrating some limitations as useful references in protein expression studies. *Proteomics* **2005**, *5* (2), 566–571.

(196) R Core Team. *R: A Language and Environment for Statistical Computing*; R Foundation for Statistical Computing: Vienna, Austria, 2008.

(197) Raux, M.; Finkielsztejn, L.; Salmon-Céron, D.; Bouchez, H.; Excler, J. L.; Dulioust, E.; Grouin, J. M.; Sicard, D.; Blondeau, C. IgG subclass distribution in serum and various mucosal fluids of HIV type 1-infected subjects. *AIDS Research and Human Retroviruses* **2000**, *16* (6), 583–594.

(198) Nirula, A.; Glaser, S. M.; Kalled, S. L.; Taylor, F. R. What is IgG4? A review of the biology of a unique immunoglobulin subtype. *Current Opinion in Rheumatology* **2011**, *23* (1), 119–124.

(199) Bereman, M. S.; Maclean, B.; Tomazela, D. M.; Liebler, D. C.; Maccoss, M. J. The development of selected reaction monitoring methods for targeted proteomics via empirical refinement. *Proteomics* **2012**, *12* (8), 1134–1141.

(200) Zhang, H.; Liu, Q.; Zimmerman, L. J.; Ham, A.-J. L.; Slebos, R. J. C.; Rahman, J.; Kikuchi, T.; Massion, P. P.; Carbone, D. P.; Billheimer, D.; et al. Methods for peptide and protein quantitation by liquid chromatography-multiple reaction monitoring mass spectrometry. *Molecular & Cellular Proteomics* **2011**, *10* (6), M110.006593.

(201) Van Belle, G.; Martin, D. C. Sample Size as a Function of Coefficient of Variation and Ratio of Means. *The American Statistician* **1993**, *47* (3), 165–167.

(202) Wickham, H. Reshaping Data with the reshape Package. *Journal of Statistical Software* **2007**, *21* (12), 1–20.

(203) Wickham, H. The Split-Apply-Combine Strategy for Data Analysis. *Journal of Statistical Software* **2011**, *40* (1), 1–29.

(204) Wickham, H. *ggplot2: Elegant Graphics For Data Analysis*, 1st ed.; Springer-Verlag: New York, 2009.

(205) Shapiro, S. S.; Wilk, M. B. An Analysis of Variance Test for Normality (Complete Samples). *Biometrika* **1965**, *52* (3/4), 591–611.

(206) Welch, B. L. The generalisation of student's problems when several different population variances are involved. *Biometrika* **1947**, *34* (1-2), 28–35.

(207) Student. The probable error of a mean. *Biometrika* **1908**, *6* (1), 1–25.

(208) Zimmerman, D. W. A note on preliminary tests of equality of variances. *The British Journal of Mathematical and Statistical Psychology* **2004**, *57* (Pt 1), 173–181.

(209) Wilcoxon, F. Individual comparisons of grouped data by ranking methods. *Biometrics Bulletin* **1946**, *1* (6), 80–83.

(210) Holm, S. A Simple Sequentially Rejective Multiple Test Procedure on JSTOR. *Scandinavian Journal of Statistics* **1979**, *6*, 65–70.

(211) Rice, W. R. Analyzing Tables of Statistical Tests. *Evolution* **1989**, *43* (1), 223.

(212) Glukhova, V. A.; Tomazela, D. M.; Findlay, G. D.; Monnat, R. J.; MacCoss, M. J. Rapid Assessment of RNAi-mediated Protein Depletion by Selected Reaction Monitoring Mass Spectrometry. *Journal of Proteome Research* **2013**, *12* (7), 3246–3254.

(213) Cohen, J. *Statistical Power Analysis for the Behavioral Sciences*, 2nd ed.; L. Erlbaum Associates: New Jersey, 1988.

(214) WHO. *Global Tuberculosis Report 2014*; World Health Organization: Geneva, 2014.

(215) Barrett, A. J.; Starkey, P. M. The interaction of alpha 2-macroglobulin with proteinases. Characteristics and specificity of the reaction, and a hypothesis concerning its molecular mechanism. *The Biochemical Journal* **1973**, *133* (4), 709–724.

(216) Kristensen, T.; Moestrup, S. K.; Gliemann, J.; Bendtsen, L.; Sand, O.; Sottrup-Jensen, L. Evidence that the newly cloned low-density-lipoprotein receptor related protein (LRP) is the α2-macroglobulin receptor. *FEBS Letters* **1990**, *276* (1-2), 151–155.

(217) Davidsen, O.; Christensen, E. I.; Gliemann, J. The plasma clearance of human α2-macroglobulin-trypsin complex in the rat is mainly accounted for by uptake into hepatocytes. *Biochimica et Biophysica Acta (BBA) - Molecular Cell Research* **1985**, *846* (1), 85–92.

(218) Narita, M.; Holtzman, D. M.; Schwartz, a L.; Bu, G. Alpha2-macroglobulin complexes with and mediates the endocytosis of beta-amyloid peptide via cell surface low-density lipoprotein receptor-related protein. *Journal of Neurochemistry* **1997**, *69* (5), 1904–1911.

(219) Qiu, W. Q.; Borth, W.; Ye, Z.; Haass, C.; Teplow, D. B.; Selkoe, D. J. Degradation of amyloid β-protein by a serine protease-α2-macroglobulin complex. *Journal of Biological Chemistry* **1996**, *271* (14), 8443–8451.

(220) Bauer, J.; Strauss, S.; Schreiter-Gasser, U.; Ganter, U.; Schlegel, P.; Witt, I.; Yolk, B.; Berger, M. Interleukin-6 and α-2-macroglobulin indicate an acute-phase state in Alzheimer's disease cortices. *FEBS Letters* **1991**, *285* (1), 111–114.

(221) Fabrizi, C.; Businaro, R.; Lauro, G. M.; Fumagalli, L. Role of alpha2-macroglobulin in regulating amyloid beta-protein neurotoxicity: protective or detrimental factor? *Journal of Neurochemistry* **2001**, *78* (2), 406–412.

(222) Liu, Y.; Jones, M.; Hingtgen, C. M.; Bu, G.; Laribee, N.; Tanzi, R. E.; Moir, R. D.; Nath, A.; He, J. J. Uptake of HIV-1 tat protein mediated by low-density lipoprotein receptor-related protein disrupts the neuronal metabolic balance of the receptor ligands. *Nature Medicine* **2000**, *6* (12), 1380–1387.

(223) Jones, S. E.; Jomary, C. Clusterin. *The International Journal of Biochemistry & Cell Biology* **2002**, *34* (5), 427–431.

(224) Humphreys, D. T.; Carver, J. a.; Easterbrook-Smith, S. B.; Wilson, M. R. Clusterin has chaperone-like activity similar to that of small heat shock proteins. *Journal of Biological Chemistry* **1999**, *274* (11), 6875–6881.

(225) Poon, S.; Easterbrook-Smith, S. B.; Rybchyn, M. S.; Carver, J. A.; Wilson, M. R. Clusterin is an ATP - Independent chaperone with very broad substrate specificity that stabilizes

stressed proteins in a folding-competent state. *Biochemistry* **2000**, *39* (51), 15953–15960.

(226) Torres-Muñoz, J. E.; Redondo, M.; Czeisler, C.; Roberts, B.; Tacoronte, N.; Petito, C. K. Upregulation of glial clusterin in brains of patients with AIDs. *Brain Research* **2001**, *888* (2), 297–301.

(227) Holmberg, C. G.; Laurell, C. . Investigations in Serum Copper. II. Isolation of the Copper Containing Protein, and a Description of some of its Properties. *Acta Chemica Scandinavica* **1948**, *2*, 550–556.

(228) Osaki, S.; Johnson, D. A.; Frieden, E. The possible significance of the ferrous oxidase activity of ceruloplasmin in normal human serum. *Journal of Biological Chemistry* **1966**, *241* (12), 2746–2751.

(229) Harris, Z. L.; Takahashi, Y.; Miyajima, H.; Serizawa, M.; MacGillivray, R. T.; Gitlin, J. D. Aceruloplasminemia: molecular characterization of this disorder of iron metabolism. *Proceedings of the National Academy of Sciences of the United States of America* **1995**, *92* (7), 2539–2543.

(230) Osaki, S.; Johnson, D. A.; Frieden, E. The mobilization of iron from the perfused mammalian liver by a serum copper enzyme, ferroxidase I. *Journal of Biological Chemistry* **1971**, *246* (9), 3018–3023.

(231) Markowitz, H.; Gubler, C. J.; Mahoney, J. P.; Cartwright, G. E.; Wintrobe, M. M. Studies on copper metabolism. XIV. Copper, ceruloplasmin and oxidase activity in sera of normal human subjects, pregnant women, and patients with infection, hepatolenticular degeneration and the nephrotic syndrome. *The Journal of Clinical Investigation* **1955**, *34* (10), 1498–1508.

(232) Goldstein, I. M.; Kaplan, H. B.; Edelson, H. S.; Weissmann, G. Ceruloplasmin: an acute phase reactant that scavenges oxygen-derived free radicals. *Annals of the New York Academy of Sciences* **1982**, *389*, 368–379.

(233) Gabay, C.; Kushner, I. Acute-phase proteins and other systemic responses to inflammation. *The New England Journal of Medicine* **1999**, *340* (6), 448–454.

(234) Kessler, H.; Pajonk, F. G.; Meisser, P.; Schneider-Axmann, T.; Hoffmann, K. H.; Supprian, T.; Herrmann, W.; Obeid, R.; Multhaup, G.; Falkai, P.; et al. Cerebrospinal fluid diagnostic markers correlate with lower plasma copper and ceruloplasmin in patients with Alzheimer's disease. *Journal of Neural Transmission* **2006**, *113* (11), 1763–1769.

(235) Boswell, D. R.; Bathurst, I. C. Molecular physiology and pathology of α1-antitrypsin. *Biochemical Education* **1985**, *13* (3), 98–104.

(236) Beatty, K.; Bieth, J.; Travis, J. Kinetics of association of serine proteinases with native and oxidized alpha-1-proteinase inhibitor and alpha-1-antichymotrypsin. *The Journal of Biological Chemistry* **1980**, *255* (9), 3931–3934.

(237) Tilg, H.; Vannier, E.; Vachino, G.; Dinarello, C. A.; Mier, J. W. Antiinflammatory properties of hepatic acute phase proteins: preferential induction of interleukin 1 (IL-1) receptor antagonist over IL-1 beta synthesis by human peripheral blood mononuclear cells. *The Journal of Experimental Medicine* **1993**, *178* (5), 1629–1636.

(238) Johnson, D.; Travis, J. The oxidative inactivation of human alpha-1-proteinase inhibitor. Further evidence for methionine at the reactive center. *The Journal of Biological Chemistry* **1979**, *254* (10), 4022–4026.

(239) Clark, R. A.; Stone, P. J.; El Hag, A.; Calore, J. D.; Franzblau, C. Myeloperoxidase-catalyzed inactivation of alpha 1-protease inhibitor by human neutrophils. *The Journal of Biological Chemistry* **1981**, *256* (7), 3348–3353.

(240) Nielsen, H. M.; Minthon, L.; Londos, E.; Blennow, K.; Miranda, E.; Perez, J.; Crowther, D. C.; Lomas, D. A.; Janciauskiene, S. M. Plasma and CSF serpins in Alzheimer disease and dementia with Lewy bodies. *Neurology* **2007**, *69* (16), 1569–1579.

(241) Sun, Y.-X.; Minthon, L.; Wallmark, A.; Warkentin, S.; Blennow, K.; Janciauskiene, S. Inflammatory markers in matched plasma and cerebrospinal fluid from patients with Alzheimer's disease. *Dementia and Geriatric Cognitive Disorders* **2003**, *16* (3), 136–144.

(242) Shapiro, L.; Pott, G. B.; Ralston, a H. Alpha-1-antitrypsin inhibits human immunodeficiency virus type 1. *The FASEB Journal* **2001**, *15* (1), 115–122.

(243) Cordelier, P.; Zern, M. A.; Strayer, D. S. HIV-1 proprotein processing as a target for gene therapy. *Gene Therapy* **2003**, *10* (6), 467–477.

(244) Bryan, C. L.; Beard, K. S.; Pott, G. B.; Rahkola, J.; Gardner, E. M.; Janoff, E. N.; Shapiro, L. HIV infection is associated with reduced serum alpha-1-antitrypsin concentrations. *Clinical and Investigative Medicine* **2010**, *33* (6), 384–389.

(245) Ferreira, T. C. d. S.; Sampaio, E. P.; Argañaraz, G. A.; Gondim, M. V. P.; Shapiro, L.; Argañaraz, E. R. Increased prevalence of the alpha-1-antitrypsin (A1AT) deficiency-related S gene in patients infected with human immunodeficiency virus type 1. *Journal of Medical Virology* **2014**, *86* (1), 23–29.

(246) Fournier, T.; Medjoubi-N, N.; Porquet, D. Alpha-1-acid glycoprotein. *Biochimica et Biophysica Acta* **2000**, *1482* (1), 157–171.

(247) Kremer, J. M.; Wilting, J.; Janssen, L. H. Drug binding to human alpha-1-acid glycoprotein in health and disease. *Pharmacological Reviews* **1988**, *40* (1), 1–47.

(248) Oie, S.; Jacobson, M. A.; Abrams, D. I. Alpha 1-acid glycoprotein levels in AIDS patients before and after short-term treatment with zidovudine (ZDV). *Journal of Acquired Immune Deficiency Syndromes* **1993**, *6* (5), 531–533.

(249) Yin, H. L.; Stossel, T. P. Control of cytoplasmic actin gel–sol transformation by gelsolin, a calcium-dependent regulatory protein. *Nature* **1979**, *281* (5732), 583–586.

(250) Yin, H. L.; Zaner, K. S.; Stossel, T. P. Ca2+ control of actin gelation. Interaction of gelsolin with actin filaments and regulation of actin gelation. *The Journal of biological chemistry* **1980**, *255* (19), 9494–9500.

(251) Cunningham, C.; Stossel, T.; Kwiatkowski, D. Enhanced motility in NIH 3T3 fibroblasts that overexpress gelsolin. *Science* **1991**, *251* (4998), 1233–1236.

(252) Ohtsu, M.; Sakai, N.; Fujita, H.; Kashiwagi, M.; Gasa, S.; Shimizu, S.; Eguchi, Y.; Tsujimoto, Y.; Sakiyama, Y.; Kobayashi, K.; et al. Inhibition of apoptosis by the actin-regulatory protein gelsolin. *The EMBO journal* **1997**, *16* (15), 4650–4656.

(253) Harris, H. E.; Weeds, A. G. Plasma gelsolin caps and severs actin filaments. *FEBS Letters* **1984**, *177* (2), 184–188.

(254) Harris, H. E.; Weeds, A. G. Plasma actin depolymerizing factor has both calcium-dependent and calcium-independent effects on actin. *Biochemistry* **1983**, *22* (11), 2728–2741.

(255) Janmey, P. A.; Chaponnier, C.; Lind, S. E.; Zaner, K. S.; Stossel, T. P.; Yin, H. L. Interactions of gelsolin and gelsolin-actin complexes with actin. Effects of calcium on actin nucleation, filament severing, and end blocking. *Biochemistry* **1985**, *24* (14), 3714–3723.

(256) Yin, H. L.; Stossel, T. P. Purification and structural properties of gelsolin, a Ca2+-activated regulatory protein of macrophages. *The Journal of Biological Chemistry* **1980**, *255* (19), 9490–9493.

(257) Janmey, P. A.; Stossel, T. P. Modulation of gelsolin function by phosphatidylinositol 4,5-bisphosphate. *Nature* **1987**, *325* (6102), 362–364.

(258) Janmey, P. A.; Iida, K.; Yin, H. L.; Stossel, T. P. Polyphosphoinositide micelles and polyphosphoinositide-containing vesicles dissociate endogenous gelsolin-actin complexes and promote actin assembly from the fast-growing end of actin filaments blocked by gelsolin. *The Journal of Biological Chemistry* **1987**, *262* (25), 12228–12236.

(259) Haddad, J. G.; Harper, K. D.; Guoth, M.; Pietra, G. G.; Sanger, J. W. Angiopathic consequences of saturating the plasma scavenger system for actin. *Proceedings of the National Academy of Sciences of the United States of America* **1990**, *87* (4), 1381–1385.

(260) Lind, S. E.; Smith, D. B.; Janmey, P. A.; Stossel, T. P. Role of plasma gelsolin and the vitamin D-binding protein in clearing actin from the circulation. *The Journal of Clinical Investigation* **1986**, *78* (3), 736–742.

(261) Harris, D. A.; Schwartz, J. H. Characterization of brevin, a serum protein that shortens actin filaments. *Proceedings of the National Academy of Sciences of the United States of America* **1981**, *78* (11), 6798–6802.

(262) Yin, H. L.; Kwiatkowski, D. J.; Mole, J. E.; Cole, F. S. Structure and biosynthesis of cytoplasmic and secreted variants of gelsolin. *The Journal of Biological Chemistry* **1984**, *259* (8), 5271–5276.

(263) Antequera, D.; Vargas, T.; Ugalde, C.; Spuch, C.; Molina, J. A.; Ferrer, I.; Bermejo-Pareja, F.; Carro, E. Cytoplasmic gelsolin increases mitochondrial activity and reduces Abeta burden in a mouse model of Alzheimer's disease. *Neurobiology of disease* **2009**, *36* (1), 42–50.

(264) Qiao, H.; Koya, R. C.; Nakagawa, K.; Tanaka, H.; Fujita, H.; Takimoto, M.; Kuzumaki, N. Inhibition of Alzheimer's amyloid-beta peptide-induced reduction of mitochondrial membrane potential and neurotoxicity by gelsolin. *Neurobiology of aging* **2005**, *26* (6), 849–855.

(265) Chauhan, V.; Ji, L.; Chauhan, A. Anti-amyloidogenic, anti-oxidant and anti-apoptotic role of gelsolin in Alzheimer's disease. *Biogerontology* **2008**, *9* (6), 381–389.

(266) Ray, I.; Chauhan, A.; Wegiel, J.; Chauhan, V. P. S. Gelsolin inhibits the fibrillization of amyloid beta-protein, and also defibrillizes its preformed fibrils. *Brain Research* **2000**, *853* (2), 344–351.

(267) Furukawa, K.; Smith-Swintosky, V. L.; Mattson, M. P. Evidence that actin depolymerization protects hippocampal neurons against excitotoxicity by stabilizing [Ca2+]i. *Experimental neurology* **1995**, *133* (2), 153–163.

(268) Furukawa, K.; Fu, W.; Li, Y.; Witke, W.; Kwiatkowski, D. J.; Mattson, M. P. The Actin-Severing Protein Gelsolin Modulates Calcium Channel and NMDA Receptor Activities and Vulnerability to Excitotoxicity in Hippocampal Neurons. *J. Neurosci.* **1997**, *17* (21), 8178–8186.

(269) Jiang, Z.-G.; Piggee, C.; Heyes, M. .; Murphy, C.; Quearry, B.; Bauer, M.; Zheng, J.; Gendelman, H. .; Markey, S. . Glutamate is a mediator of neurotoxicity in secretions of activated HIV-1-infected macrophages. *Journal of Neuroimmunology* **2001**, *117* (1-2), 97–107.

(270) Liu, H.; Liu, J.; Liang, S.; Xiong, H. Plasma gelsolin protects HIV-1 gp120-Induced neuronal injury via voltage-gated K(+) channel Kv2.1. *Molecular and Cellular Neurosciences* **2013**, *57*, 73–82.

(271) Osborn, T. M.; Verdrengh, M.; Stossel, T. P.; Tarkowski, A.; Bokarewa, M. Decreased levels of the gelsolin plasma isoform in patients with rheumatoid arthritis. *Arthritis research & therapy* **2008**, *10* (5), R117.

(272) Kulakowska, A.; Drozdowski, W.; Sadzynski, A.; Bucki, R.; Janmey, P. A. Gelsolin concentration in cerebrospinal fluid from patients with multiple sclerosis and other neurological disorders. *European Journal of Neurology* **2008**, *15* (6), 584–588.

(273) Pepys, M. B.; Butler, P. J. G. Serum amyloid P component is the major calcium-dependent specific DNA binding protein of the serum. *Biochemical and Biophysical Research Communications* **1987**, *148* (1), 308–313.

(274) Breathnach, S. M.; Kofler, H.; Sepp, N.; Ashworth, J.; Woodrow, D.; Pepys, M. B.; Hintner, H. Serum amyloid P component binds to cell nuclei in vitro and to in vivo deposits of extracellular chromatin in systemic lupus erythematosus. *The Journal of experimental medicine* **1989**, *170* (4), 1433–1438.

(275) Bickerstaff, M. C.; Botto, M.; Hutchinson, W. L.; Herbert, J.; Tennent, G. a; Bybee, a; Mitchell, D. a; Cook, H. T.; Butler, P. J.; Walport, M. J.; et al. Serum amyloid P component controls chromatin degradation and prevents antinuclear autoimmunity. *Nature medicine* **1999**, *5* (6), 694–697.

(276) Hawkins, P. .; Lavender, J. .; Myers, M. .; Pepys, M. . Diagnostic radionuclide imaging of amyloid: biological targeting by circulating human serum amyloid P component. *The Lancet* **1988**, *331* (8600), 1413–1418.

(277) Hawkins, P. N.; Lavender, J. P.; Pepys, M. B. Evaluation of systemic amyloidosis by scintigraphy with 123I-labeled serum amyloid P component. *The New England Journal of Medicine* **1990**, *323* (8), 508–513.

(278) Tennent, G. A.; Lovat, L. B.; Pepys, M. B. Serum amyloid P component prevents proteolysis of the amyloid fibrils of Alzheimer disease and systemic amyloidosis. *Proceedings of the National Academy of Sciences of the United States of America* **1995**, *92* (10), 4299–4303.

(279) Ghiso, J.; Frangione, B. Amyloidosis and Alzheimer's disease. *Advanced Drug Delivery Reviews* **2002**, *54* (12), 1539–1551.

(280) Duong, T.; Pommier, E. C.; Scheibel, A. B. Immunodetection of the amyloid P component in Alzheimer's disease. *Acta Neuropathologica* **1989**, *78* (4), 429–437.

(281) Kalaria, R. N.; Grahovac, I. Serum amyloid P immunoreactivity in hippocampal tangles, plaques and vessels: implications for leakage across the blood-brain barrier in Alzheimer's disease. *Brain Research* **1990**, *516* (2), 349–353.

(282) Rempel, H. C.; Pulliam, L. HIV-1 Tat inhibits neprilysin and elevates amyloid beta. *AIDS* **2005**, *19*, 127–135.

(283) Eichner, J. E. Apolipoprotein E Polymorphism and Cardiovascular Disease: A HuGE Review. *American Journal of Epidemiology* **2002**, *155* (6), 487–495.

(284) Mahley, R. W.; Innerarity, T. L.; Rall, S. C.; Weisgraber, K. H. Plasma lipoproteins: apolipoprotein structure and function. *Journal of lipid research* **1984**, *25* (12), 1277–1294.

(285) Innerarity, T. L.; Mahley, R. W. Enhanced binding by cultured human fibroblasts of apo-E-containing lipoproteins as compared with low density lipoproteins. *Biochemistry* **1978**, *17* (8), 1440–1447.

(286) Zannis, V. I.; Breslow, J. L.; Utermann, G.; Mahley, R. W.; Weisgraber, K. H.; Havel, R. J.; Goldstein, J. L.; Brown, M. S.; Schonfeld, G.; Hazzard, W. R.; et al. Proposed nomenclature of apoE isoproteins, apoE genotypes, and phenotypes. *Journal of Lipid Research* **1982**, *23* (6), 911–914.

(287) Zannis, V. I.; Breslow, J. L. Human very low density lipoprotein apolipoprotein E isoprotein polymorphism is explained by genetic variation and posttranslational modification. *Biochemistry* **1981**, *20* (4), 1033–1041.

(288) Weintraub, M. S.; Eisenberg, S.; Breslow, J. L. Dietary fat clearance in normal subjects is regulated by genetic variation in apolipoprotein E. *The Journal of Clinical Investigation* **1987**, *80* (6), 1571–1577.

(289) Levine, A. J.; Service, S.; Miller, E. N.; Reynolds, S. M.; Singer, E. J.; Shapshak, P.; Martin, E. M.; Sacktor, N.; Becker, J. T.; Jacobson, L. P.; et al. Genome-wide association study of neurocognitive impairment and dementia in HIV-infected adults. *American Journal of Medical Genetics. Part B, Neuropsychiatric Genetics* **2012**, *159B* (6), 669–683.

(290) Corder, E. H.; Robertson, K.; Lannfelt, L.; Bogdanovic, N.; Eggertsen, G.; Wilkins, J.; Hall, C. HIV-infected subjects with the E4 allele for APOE have excess dementia and peripheral neuropathy. *Nature Medicine* **1998**, *4* (10), 1182–1184.

(291) Valcour, V.; Shikuma, C.; Shiramizu, B.; Watters, M.; Poff, P.; Selnes, O. A.; Grove, J.; Liu, Y.; Abdul-Majid, K. B.; Gartner, S.; et al. Age, apolipoprotein E4, and the risk of HIV dementia: The Hawaii Aging with HIV Cohort. *Journal of Neuroimmunology* **2004**, *157* (1-2 SPEC. ISS.), 197–202.

(292) Strittmatter, W. J.; Saunders, A. M.; Schmechel, D.; Pericak-Vance, M.; Enghild, J.; Salvesen, G. S.; Roses, A. D. Apolipoprotein E: high-avidity binding to beta-amyloid and increased frequency of type 4 allele in late-onset familial Alzheimer disease. *Proceedings of the National Academy of Sciences of the United States of America* **1993**, *90* (5), 1977–1981.

(293) Smit, M.; de Knijff, P.; Rosseneu, M.; Bury, J.; Klasen, E.; Frants, R.; Havekes, L. Apolipoprotein E polymorphism in The Netherlands and its effect on plasma lipid and apolipoprotein levels. *Human Genetics* **1988**, *80* (3), 287–292.

(294) Fielding, C. J.; Shore, V. G.; Fielding, P. E. A protein cofactor of lecithin:Cholesterol acyltransferase. *Biochemical and Biophysical Research Communications* **1972**, *46* (4), 1493–1498.

(295) Glomset, J. A. The plasma lecithins:cholesterol acyltransferase reaction. *Journal of Lipid Research* **1968**, *9* (2), 155–167.

(296) Soutar, A. K.; Garner, C. W.; Baker, H. N.; Sparrow, J. T.; Jackson, R. L.; Gotto, A. M.; Smith, L. C. Effect of the human plasma apolipoproteins and phosphatidylcholine acyl donor on the activity of lecithin. Cholesterol acyltransferase. *Biochemistry* **1975**, *14* (14), 3057–3064.

(297) Baza Caraciolo, B.; Pérez de Oteyza, C.; Carrió Montiel, D.; Carrió Montiel, J. C.; Salguero Aparicio, M.; Del Romero Guerrero, J. Lipid profile in untreated HIV positive patients. HIV infection: cardiovascular risk factor?. *Anales de Medicina Interna* **2007**, *24* (4), 160–167.

(298) Malavazi, I.; Abrão, E. P.; Mikawa, A. Y.; Landgraf, V. O.; da Costa, P. I. Abnormalities in apolipoprotein and lipid levels in an HIV-infected Brazilian population under different treatment profiles: the relevance of apolipoprotein E genotypes and immunological status. *Clinical Chemistry and Laboratory Medicine* **2004**, *42* (5), 525–532.

(299) Asztalos, B. F.; Schaefer, E. J.; Horvath, K. V; Cox, C. E.; Skinner, S.; Gerrior, J.; Gorbach, S. L.; Wanke, C. Protease inhibitor-based HAART, HDL, and CHD-risk in HIV-infected patients. *Atherosclerosis* **2006**, *184* (1), 72–77.

(300) Negredo, E.; Ribalta, J.; Paredes, R.; Ferré, R.; Sirera, G.; Ruiz, L.; Salazar, J.; Reiss, P.; Masana, L.; Clotet, B. Reversal of atherogenic lipoprotein profile in HIV-1 infected patients with lipodystrophy after replacing protease inhibitors by nevirapine. *AIDS* **2002**, *16* (10), 1383–1389.

(301) Van der Valk, M.; Kastelein, J. J.; Murphy, R. L.; van Leth, F.; Katlama, C.; Horban, A.; Glesby, M.; Behrens, G.; Clotet, B.; Stellato, R. K.; et al. Nevirapine-containing antiretroviral therapy in HIV-1 infected patients results in an anti-atherogenic lipid profile. *AIDS* **2001**, *15* (18), 2407–2414.

(302) Franssen, R.; Sankatsing, R. R.; Hassink, E.; Hutten, B.; Ackermans, M. T.; Brinkman, K.; Oesterholt, R.; Arenas-Pinto, A.; Storfer, S. P.; Kastelein, J. J.; et al. Nevirapine increases high-density lipoprotein cholesterol concentration by stimulation of apolipoprotein A-I production. *Arteriosclerosis, Thrombosis, and Vascular Biology* **2009**, *29* (9), 1336–1341.

(303) Janeway, C. A.; Travers, P.; Walport, M.; Shlomchik, M. J. *Immunobiology: The Immune System in Health and Disease*, 5th ed.; Garland Science: New York, 2001.

(304) Roitt, I. M.; Brostoff, J.; Male, D. K. *Immunology*, 6th ed.; Mosby: Edinburgh, 2001.

(305) Lian, H.; Yang, L.; Cole, A.; Sun, L.; Chiang, A. C.-A.; Fowler, S. W.; Shim, D. J.; Rodriguez-Rivera, J.; Taglialatela, G.; Jankowsky, J. L.; et al. NFκB-Activated Astroglial Release of Complement C3 Compromises Neuronal Morphology and Function Associated with Alzheimer's Disease. *Neuron* **2015**, *85* (1), 101–115.

(306) McGeer, P. L.; Akiyama, H.; Itagaki, S.; McGeer, E. G. Activation of the classical complement pathway in brain tissue of Alzheimer patients. *Neuroscience Letters* **1989**, *107* (1–3), 341–346.

(307) Eikelenboom, P.; Hack, C. E.; Rozemuller, J. M.; Stam, F. C. Complement activation in amyloid plaques in Alzheimer's dementia. *Virchows Archiv B Cell Pathology Including Molecular Pathology* **1988**, *56* (1), 259–262.

(308) Schmitz, J.; Zimmer, J. P.; Kluxen, B.; Aries, S.; Bogel, M.; Gigli, I.; Schmitz, H. Antibody-dependent complement-mediated cytotoxicity in sera from patients with HIV-1 infection is controlled by CD55 and CD59. *Journal of Clinical Investigation* **1995**, *96* (3), 1520–1526.

(309) Saifuddin, M.; Parker, C. J.; Peeples, M. E.; Gorny, M. K.; Zolla-Pazner, S.; Ghassemi, M.; Rooney, I. A.; Atkinson, J. P.; Spear, G. T. Role of virion-associated glycosylphosphatidylinositol-linked proteins CD55 and CD59 in complement resistance of cell line-derived and primary isolates of HIV-1. *The Journal of Experimental Medicine* **1995**, *182* (2), 501–509.

(310) Stoiber, H.; Pintér, C.; Siccardi, A. G.; Clivio, A.; Dierich, M. P. Efficient destruction of human immunodeficiency virus in human serum by inhibiting the protective action of complement factor H and decay accelerating factor (DAF, CD55). *The Journal of Experimental Medicine* **1996**, *183* (1), 307–310.

(311) Soelder, B. M.; Reisinger, E. C.; Koefler, D.; Bitterlich, G.; Wachter, H.; Dierich, M. P. Complement receptors: another port of entry for HIV. *Lancet* **1989**, *2* (8657), 271–272.

(312) Robinson, W. E.; Montefiori, D. C.; Mitchell, W. M. Antibody-dependent enhancement of human immunodeficiency virus type 1 infection. *The Lancet* **1988**, *331* (8589), 790–794.

(313) Speth, C.; Stöckl, G.; Mohsenipour, I.; Würzner, R.; Stoiber, H.; Lass-Flörl, C.; Dierich, M. P. Human immunodeficiency virus type 1 induces expression of complement factors in human astrocytes. *Journal of Virology* **2001**, *75* (6), 2604–2615.

(314) Speth, C.; Schabetsberger, T.; Mohsenipour, I.; Stöckl, G.; Würzner, R.; Stoiber, H.; Lass-Flörl, C.; Dierich, M. P. Mechanism of human immunodeficiency virus-induced complement expression in astrocytes and neurons. *Journal of Virology* **2002**, *76* (7), 3179–3188.

(315) Jongen, P. J. H.; Doesburg, W. H.; Ibrahim-Stappers, J. L. M.; Lemmens, W. A. J. G.; Hommes, O. R.; Lamers, K. J. B. Cerebrospinal fluid C3 and C4 indexes in immunological disorders of the central nervous system. *Acta Neurologica Scandinavica* **2000**, *101* (2), 116–121.

Chapter 8
Appendix A: Sample Preparation

TABLE 8.1: TABLE OF SERUM BATCHING AND DILUTIONS FOR MASS SPECTROMETRY ANALYSIS (FINAL CONCENTRATION: 1.53 µG/µL)

Batch	Group	Samples	Concentration (µg/µl)	23 µg in 15 µl (1.53 µg/µl)	Volume of Diluent (23 µg)
BATCH 1	N	J061	116	7	493
	N	J200	100	8	492
	N	J0223	100	8	492
	M	J0179	105	7	493
	M	J027	120	6	494
	M	J0209	101	8	492
	H	J010	77	10	490
	H	J0149	91	8	492
	H	J0104	68	11	489
BATCH 2	N	J087	72	11	489
	N	J204	100	8	492
	N	J031	73	10	490
	M	J056	91	8	492
	M	J0193	73	10	490
	M	J0146	85	9	491
	H	J0229	108	7	493
	H	J0166	73	11	489
	H	J030	131	6	494
BATCH 3	N	J032	80	10	490
	N	J0213	69	11	489
	N	J0231	131	6	494
	M	J0156	122	6	494
	M	J040	90	9	491
	M	J0125	78	10	490
	H	J025	73	11	489
	H	J206	97	8	492

Batch	Group	Samples	Concentration (µg/µl)	23 µg in 15 µl (1.53 µg/µl)	Volume of Diluent (23 µg)
	H	J0126	120	6	494
BATCH 4	N	J180	83	9	491
	N	J0203	70	11	489
	N	J067	92	8	492
	M	J0137	95	8	492
	M	J0214	104	7	493
	M	J063	105	7	493
	H	J0148	96	8	492
	H	J038	126	6	494
	H	J0130	84	9	491
BATCH 5	N	J009	89	9	491
	N	J081	96	8	492
	N	J059	127	6	494
	M	J020	77	10	490
	M	J0136	86	9	491
	M	J029	90	8	492
	H	J004	74	10	490
	H	J097	132	6	494
	H	J0172	80	10	490
BATCH 6	N	J0224	98	8	492
	N	J142	92	8	492
	N	J0260	81	9	491
	M	J043	72	11	489
	M	J0167	89	9	491
	M	J003	110	7	493
	H	J0147	87	9	491
	H	J050	112	7	493
	H	J0236	87	9	491
BATCH 7	N	J026	91	8	492
	N	J0135	86	9	491
	N	J035	81	9	491
	M	J0152	98	8	492
	M	J079	131	6	494
	M	J0201	106	7	493
	H	J005	94	8	492

Batch	Group	Samples	Concentration (µg/µl)	23 µg in 15 µl (1.53 µg/µl)	Volume of Diluent (23 µg)
	H	J225	108	7	493
	H	J0198	77	10	490
BATCH 8	N	J068	82	9	491
	N	J237	95	8	492
	N	J0215	87	9	491
	M	J0183	86	9	491
	M	J047	104	7	493
	M	J074	94	8	492
	H	J016	90	9	491
	H	J0132	102	7	493
	H	J024	84	9	491
BATCH 9	N	J0176	92	8	492
	N	J0233	95	8	492
	N	J0210	87	9	491
	N	J0239	126	6	494
	M	J0207	99	8	492
	M	J036	90	8	492
	H	J0106	90	8	492
	H	J202	106	7	493
	H	J216	117	7	493

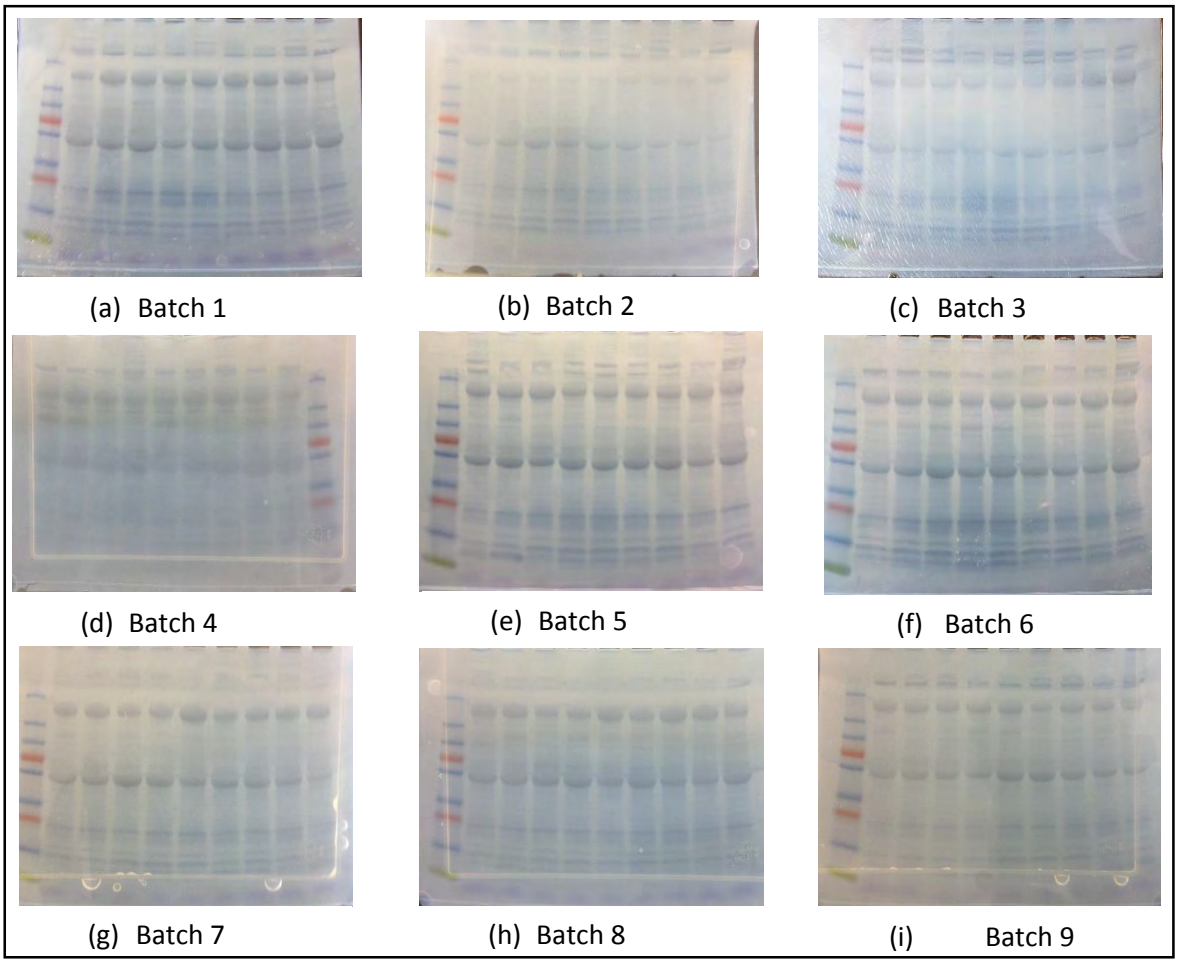

FIGURE 8.1: FIGURE SHOWING IMAGES OF SDS-PAGE GELS STAINED WITH ZINC-IMIDAZOLE REVERSIBLE STAIN. GEL PHOTOGRAPHED AGAINST A DARK BACKGROUND. CLEAR PROTEIN BANDS APPEAR DARK.

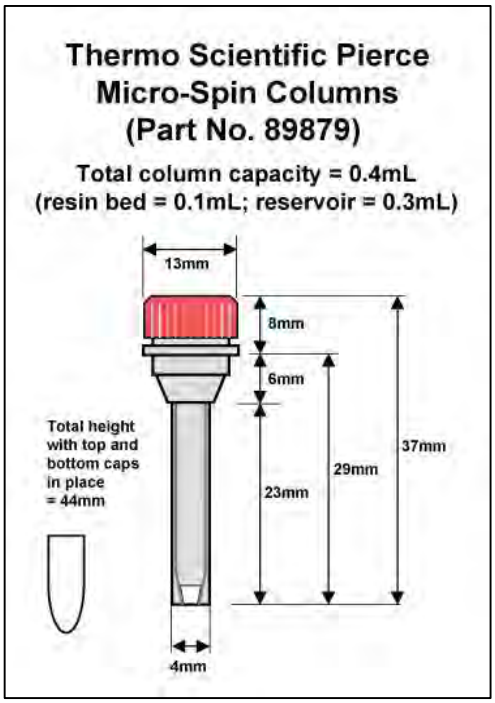

FIGURE 8.2: SCHEMATIC OF THERMO-PIERCE SPIN COLUMN FOR C18-BASED SAMPLE CLEAN-UP

Chapter 9
Appendix B: Optimisation A

TABLE 9.1: MAXQUANT SETTINGS FOR SHOTGUN PROTEOMIC ANALYSIS OF POOLED SAMPLES

Group-specific parameters								
Variable Mods	Oxidation (M)				Acetyl (Protein N-term)			
Multiplicity	1							
Enzyme	Trypsin/P							
First search ppm	20							
Main search ppm	6							
Max number of modifications per peptide	5							
Max. missed cleavages	2							
Max. charge	7							
Individual peptide mass tolerances	yes							
Type	Standard							
MS/MS Settings								
Mass Analyser	***MS/MS tolerance***	***Unit***	***Top peaks per 100 Da***	***De-isotoping***	***Higher charge***	***Water loss***	***Ammonia loss***	***Dependent loss***
FTMS	20	ppm	10	yes	yes	yes	yes	yes
ITMS	0.5	Da	6	no	yes	yes	yes	yes
TOF	0.1	Da	10	yes	yes	yes	yes	yes
Unknown	0.5	Da	6	no	yes	yes	yes	yes
Sequences								
Include contaminants	yes							

FASTA file	Reverse	
Special Aas	KR	
I=L	yes	
Fixed modifications		
Fixed Mods	Carbamidomethyl (C)	
Identification		
Peptide FDR	0.01	
Protein FDR	0.01	
Site FDR	0.01	
Apply site FDR separately	yes	
Max. peptide PEP	1	
Min. peptide length	7	
Min. peptides	1	
Min. score	0	
Min. razor + unique peptides	1	
Filter labelled amino acids	no	
Min. unique peptides	no	
Second peptides	yes	
Protein Quantitation		
Use only unmodified peptides and…	Oxidation (M)	Acetyl (Protein N-term)
Use razor and unique peptides	yes	
Discard unmodified counterpart peptides	yes	
Min. ratio count	2	
Site quantitation		
Mode	Use least modified peptides	
Use for occupancies	Normalised ratios	
Miscellaneous		
Re-quantify	yes	
Keep low-scoring versions of identified peptides	No	

Match between runs	no
Label-free quantitation	yes
LFQ min. ratio count	2
Fast LFQ	yes
iBAQ	yes
Log fit	yes

TABLE 9.2: TABLE OF DISCOVERY PROTEIN IDS FROM POOLED ANALYSIS. LEADING PROTEINS OF EACH GROUP ARE SHOWN FOR SIMPLICITY. PEP: POSTERIOR ERROR PROBABILITY

#	Protein ID	Protein name	Peptides	Sequence coverage [%]	PEP
1	P43652	Afamin	2	3.5	0.00018149
2	P02763	Alpha-1-acid glycoprotein 1	2	10.9	5.59E-15
3	G3V5I3	Alpha-1-antichymotrypsin	9	23.4	4.65E-268
4	P01009	Alpha-1-antitrypsin	18	47.8	0
5	P04217	Alpha-1B-glycoprotein	7	18	2.66E-37
6	C9JV77	Alpha-2-HS-glycoprotein	2	4.6	1.21E-08
7	P01023	Alpha-2-macroglobulin	58	51.8	0
8	P01019	Angiotensinogen	5	14.6	7.75E-50
9	P01008	Antithrombin-III	4	10.3	7.02E-42
10	P02647	Apolipoprotein A-I	12	48.3	0
11	P02652	Apolipoprotein A-II	3	39	2.15E-27
12	P06727	Apolipoprotein A-IV	9	26.5	1.01E-29
13	P04114	Apolipoprotein B-100	127	34.1	0
14	B0YIW2	Apolipoprotein C-III	1	13.7	4.50E-06
15	P02649	Apolipoprotein E	7	27.8	0
16	O14791-2	Apolipoprotein L1	2	5.6	3.08E-06
17	P08519	Apolipoprotein(a)	2	8.6	2.71E-07
18	O75882	Attractin	3	2.9	3.86E-06
19	P02749	Beta-2-glycoprotein 1	5	22.3	6.55E-49
20	Q9Y2P5	Bile acyl-CoA synthetase	1	2.6	0.043381
21	P04003	C4b-binding protein alpha chain	10	19.1	2.61E-38
22	Q9H257	Caspase recruitment domain-containing protein 9	1	2.2	0.0017862
23	O43866	CD5 antigen-like	6	21.6	6.77E-114
24	P00450	Ceruloplasmin	22	24.7	0
25	P10909-2	Clusterin	7	19.4	8.77E-61
26	P00748	Coagulation factor XII	3	5.7	7.31E-06
27	P02747	Complement C1q subcomponent subunit C	4	21.2	2.92E-33
28	P00736	Complement C1r subcomponent	4	8.1	2.73E-15
29	P09871	Complement C1s subcomponent	2	4.2	0.00036161
30	P01024	Complement C3	75	49.2	0
31	P0C0L4	Complement C4-A	45	32.9	0
32	P0C0L5	Complement C4-B	43	30.4	0
33	P01031	Complement C5	20	13.5	3.97E-79
34	P13671	Complement component C6	6	8.2	3.33E-90
35	P10643	Complement component C7	3	4.9	3.97E-37
36	P07357	Complement component C8 alpha chain	2	5.8	9.02E-09
37	P07360	Complement component C8 gamma chain	1	7.4	0.0013995

#	Protein ID	Protein name	Peptides	Sequence coverage [%]	PEP
38	P02748	Complement component C9	8	15.9	1.19E-18
39	B4E1Z4	Complement factor B	21	18.4	1.60E-89
40	P08603	Complement factor H	21	24.1	6.41E-130
41	E7ETH0	Complement factor I	3	6.1	1.40E-05
42	P08185	Corticosteroid-binding globulin	3	8.4	1.88E-05
43	P81605-2	Dermcidin	2	18.2	6.23E-05
44	O75150	E3 ubiquitin-protein ligase BRE1B	1	1.1	0.00015515
45	Q99814	Endothelial PAS domain-containing protein 1	1	1.8	0.014815
46	Q8IWU5	Extracellular sulfatase Sulf-2	1	1.7	0.037666
47	C9JC84	Fibrinogen gamma chain	1	2.6	0.0018074
48	P02751	Fibronectin	29	17.9	1.07E-262
49	Q08380	Galectin-3-binding protein	2	4.6	7.29E-06
50	P06396	Gelsolin	10	19.1	3.50E-48
51	P00738	Haptoglobin	24	47	0
52	P00739-2	Haptoglobin-related protein	16	27	2.09E-188
53	P68871	Hemoglobin subunit beta	5	40.1	1.93E-11
54	P02790	Hemopexin	9	26	1.05E-149
55	P05546	Heparin cofactor 2	7	14.8	6.68E-18
56	P04196	Histidine-rich glycoprotein	4	10.1	8.43E-17
57	P01876	Ig alpha-1 chain C region	10	39.4	0
58	P01877	Ig alpha-2 chain C region	7	27.9	7.41E-250
59	P01880-2	Ig delta chain C region	3	8.4	2.43E-08
60	P01857	Ig gamma-1 chain C region	15	54.8	0
61	P01859	Ig gamma-2 chain C region	11	39.3	7.01E-246
62	P01860	Ig gamma-3 chain C region	13	45.9	0
63	P01861	Ig gamma-4 chain C region	10	40.7	0
64	P01743	Ig heavy chain V-I region HG3	2	22.2	1.47E-38
65	P06326	Ig heavy chain V-I region Mot	1	9.6	0
66	P06331	Ig heavy chain V-II region ARH-77	2	17.1	7.80E-129
67	P01825	Ig heavy chain V-II region NEWM	2	24.8	5.08E-130
68	P04438	Ig heavy chain V-II region SESS	1	4.8	2.05E-07
69	P01824	Ig heavy chain V-II region WAH	3	22.5	2.00E-05
70	P01766	Ig heavy chain V-III region BRO	2	25	3.31E-232
71	P01773	Ig heavy chain V-III region BUR	1	9.2	0.00026232
72	P01767	Ig heavy chain V-III region BUT	2	26.1	1.95E-85
73	P01781	Ig heavy chain V-III region GAL	4	40.5	1.11E-24
74	P80419	Ig heavy chain V-III region GAR	1	16.1	0.00048591
75	P01771	Ig heavy chain V-III region HIL	1	9.1	9.41E-05
76	P01780	Ig heavy chain V-III region JON	2	16.5	3.82E-05

#	Protein ID	Protein name	Peptides	Sequence coverage [%]	PEP
77	P01772	Ig heavy chain V-III region KOL	1	12.7	3.07E-07
78	P01765	Ig heavy chain V-III region TIL	2	26.1	5.48E-145
79	P01764	Ig heavy chain V-III region VH26	2	18.8	6.61E-17
80	P01834	Ig kappa chain C region	6	80.2	0
81	P01594	Ig kappa chain V-I region AU	2	31.5	9.49E-85
82	P04430	Ig kappa chain V-I region BAN	1	16.7	2.13E-40
83	P01597	Ig kappa chain V-I region DEE	2	10.2	1.38E-06
84	P01598	Ig kappa chain V-I region EU	3	31.5	1.79E-117
85	P01601	Ig kappa chain V-I region HK101	1	13.7	2.54E-20
86	P01602	Ig kappa chain V-I region HK102	3	29.1	2.04E-78
87	P01604	Ig kappa chain V-I region Kue	1	10.2	0.00021108
88	P01613	Ig kappa chain V-I region Ni	2	30.4	5.37E-78
89	P01608	Ig kappa chain V-I region Roy	2	24.1	1.22E-80
90	P01609	Ig kappa chain V-I region Scw	3	42.6	2.88E-88
91	P01610	Ig kappa chain V-I region WEA	2	30.6	6.55E-115
92	P01611	Ig kappa chain V-I region Wes	2	31.5	1.57E-43
93	P06309	Ig kappa chain V-II region GM607	2	31.6	1.06E-62
94	P01619	Ig kappa chain V-III region B6	2	21.3	9.20E-09
95	P04207	Ig kappa chain V-III region CLL	4	36.4	3.72E-20
96	P04206	Ig kappa chain V-III region GOL	5	63.3	0
97	P18135	Ig kappa chain V-III region HAH	5	41.9	3.63E-178
98	P06311	Ig kappa chain V-III region IARC/BL41	2	24.2	2.82E-63
99	P01621	Ig kappa chain V-III region NG9	5	54	1.13E-31
100	P01620	Ig kappa chain V-III region SIE	6	66.1	0
101	P04433	Ig kappa chain V-III region VG	3	27	9.72E-29
102	P01623	Ig kappa chain V-III region WOL	5	60.6	0
103	P06313	Ig kappa chain V-IV region JI	4	27.1	5.03E-42
104	P01625	Ig kappa chain V-IV region Len	4	36.8	1.42E-101
105	P04211	Ig lambda chain V region 4A	2	15.4	0.00078687
106	P06316	Ig lambda chain V-I region BL2	1	6.2	5.02E-11
107	P01701	Ig lambda chain V-I region NEW	3	34.2	4.41E-10
108	P01703	Ig lambda chain V-I region NEWM	1	16.5	2.82E-05
109	P01699	Ig lambda chain V-I region VOR	2	23.4	2.01E-09
110	P04208	Ig lambda chain V-I region WAH	2	27.5	8.69E-32
111	P80748	Ig lambda chain V-III region LOI	3	37.8	0
112	P01714	Ig lambda chain V-III region SH	2	25	7.50E-56
113	P01717	Ig lambda chain V-IV region Hil	1	17.8	1.47E-55
114	P06319	Ig lambda chain V-VI region EB4	1	15.3	1.58E-20
115	P0CG05	Ig lambda-2 chain C regions	5	74.5	0

#	Protein ID	Protein name	Peptides	Sequence coverage [%]	PEP
116	P01871-2	Ig mu chain C region	16	36.6	0
117	P01591	Immunoglobulin J chain	4	26.4	5.34E-18
118	B9A064	Immunoglobulin lambda-like polypeptide 5	5	36	0
119	P35858-2	Insulin-like growth factor-binding protein complex acid labile subunit	3	7	2.37E-06
120	P19827	Inter-alpha-trypsin inhibitor heavy chain H1	10	14.5	1.26E-47
121	P19823	Inter-alpha-trypsin inhibitor heavy chain H2	14	18.2	2.61E-122
122	Q06033	Inter-alpha-trypsin inhibitor heavy chain H3	2	2.8	2.62E-07
123	B7ZKJ8	Inter-alpha-trypsin inhibitor heavy chain H4	14	17.2	0
124	CON__Q15323	Keratin, type I cuticular Ha1	5	11.3	6.43E-18
125	CON__Q14525	Keratin, type I cuticular Ha3-II	5	10.6	2.33E-15
126	CON__P13645	Keratin, type I cytoskeletal 10	21	35.8	0
127	CON__P02533	Keratin, type I cytoskeletal 14	12	30.5	2.76E-39
128	CON__P08779	Keratin, type I cytoskeletal 16	12	27.7	1.76E-45
129	CON__P35527	Keratin, type I cytoskeletal 9	21	50.4	0
130	CON__Q9NSB4	Keratin, type II cuticular Hb2	1	1.9	3.28E-07
131	CON__P78385	Keratin, type II cuticular Hb3	3	5.5	7.06E-12
132	CON__P04264	Keratin, type II cytoskeletal 1	27	44.1	0
133	CON__P35908	Keratin, type II cytoskeletal 2 epidermal	16	28.8	0
134	CON__P13647	Keratin, type II cytoskeletal 5	12	21.2	1.89E-65
135	CON__P02538	Keratin, type II cytoskeletal 6A	13	24.5	4.14E-67
136	P04259	Keratin, type II cytoskeletal 6B	13	24.5	1.38E-84
137	CON__O95678	Keratin, type II cytoskeletal 75	5	8.7	1.80E-31
138	P01042	Kininogen-1	5	10.6	3.81E-17
139	P02750	Leucine-rich alpha-2-glycoprotein	2	8.1	2.30E-05
140	P51884	Lumican	3	10.1	6.42E-05
141	Q685J3	Mucin-17	1	0.2	7.94E-17
142	P20916	Myelin-associated glycoprotein	1	1.9	0.025319
143	Q96PD5-2	N-acetylmuramoyl-L-alanine amidase	3	6.6	1.85E-07
144	P80108	Phosphatidylinositol-glycan-specific phospholipase D	1	1.8	0.00070946
145	H0YAC1	Plasma kallikrein	2	2.9	1.99E-05
146	B4E1F0	Plasma protease C1 inhibitor	8	18.2	3.07E-59
147	P00747	Plasminogen	13	20.9	2.28E-36
148	P20742	Pregnancy zone protein	10	9.4	3.96E-132
149	P02760	Protein AMBP	8	27.6	3.88E-23
150	P60903	Protein S100-A10	2	18.6	0.0005562
151	Q16384	Protein SSX1	1	8	0.025058
152	P00734	Prothrombin	6	10.1	3.63E-23

#	Protein ID	Protein name	Peptides	Sequence coverage [%]	PEP
153	P02787	Serotransferrin	32	46.8	0
154	CON__P02768-1	Serum albumin	37	63.1	0
155	P02743	Serum amyloid P-component	5	23.8	2.00E-13
156	P27169	Serum paraoxonase/arylesterase 1	5	23.4	4.25E-20
157	P61009	Signal peptidase complex subunit 3	1	3.9	0.038591
158	Q17RD7	Synaptotagmin-16	1	2.5	0.023998
159	P24821	Tenascin	1	0.8	1.65E-06
160	Q6N022	Teneurin-4	1	0.4	6.91E-05
161	P02766	Transthyretin	4	47.6	3.78E-144
162	E7EQ64	Trypsin-1	1	7.7	0.00059298
163	D6RF35	Vitamin D-binding protein	7	25.4	9.87E-25
164	P07225	Vitamin K-dependent protein S	2	2.4	0.0017815
165	P04004	Vitronectin	5	12.8	7.17E-23
166	P04275	von Willebrand factor	5	2.3	1.33E-09
167	C9JEE0		1	3.9	0.00017252
168	CON__REFSEQ:XP_986630		5	10.9	6.35E-19
169	CON__P00761		5	31.6	0
170	CON__P02662		2	11.1	0.00017217
171	CON__P02769		21	35.7	0
172	E9PQP7		1	2.2	0.032163
173	REV__CON__Q6IFZ6		1	2.1	0.0013335
174	S4R394		1	13.8	7.15E-06
175	S4R460		1	8.7	1.42E-07

TABLE 9.3: TABLE OF RAW PEPTIDE DATA FOR CANDIDATE BIOMARKERS. LEADING PROTEINS OF EACH GROUP ARE USED FOR SIMPLICITY.

Proteins	Sequence	Missed cleavages	Unique (Groups)	Unique (Proteins)	Charge	PEP	HAD 1	HAD 2	HAD 3	MNI 1	MNI 2	MNI 3	POS 1	POS 2	POS 3
A1AG	TEDTIFLR	0	no	no	2	4.28E-13	1.73E+07	1.18E+07	0	9.07E+06	0	0	8.90E+06	0	0
A1AG	EQLGEFYEALDCLR	0	yes	yes	2	0.013071	0	5.60E+06	0	0	0	0	0	0	0
A1AT	TLNQPDSQLQLTTGNGLFLSEGLK	0	yes	no	2,3	4.61E-188	4.99E+07	6.70E+07	6.50E+06	5.57E+07	1.37E+07	1.64E+06	2.85E+07	1.28E+07	1.81E+06
A1AT	VFSNGADLSGVTEEAPLK	0	yes	no	2,3	1.54E-111	2.69E+08	1.73E+08	2.51E+07	2.66E+08	0	0	2.26E+08	1.17E+08	0
A1AT	DTEEEDFHVDQVTTVK	0	yes	no	2,3	1.59E-107	1.71E+07	4.20E+07	9.17E+06	1.05E+08	5.27E+06	2.59E+06	3.51E+07	4.18E+07	9.81E+06
A1AT	AVLTIDEK	0	yes	yes	2	1.03E-67	1.93E+08	0	0	0	0	7.96E+07	1.49E+08	1.29E+08	0
A1AT	LQHLENELTHDIITK	0	yes	no	2,3,4	1.25E-61	7.74E+07	2.19E+08	3.06E+06	1.89E+08	3.32E+07	0	1.53E+08	1.66E+07	0
A1AT	LYHSEAFTVNFGDTEEAK	0	yes	no	2,3	5.25E-31	1.23E+07	5.11E+07	0	1.92E+07	2.94E+06	0	1.52E+07	2.75E+06	0
A1AT	LYHSEAFTVNFGDTEEAKK	1	yes	no	2,3,4	1.09E-16	0	7.50E+07	0	4.24E+07	0	0	4.01E+07	0	0
A1AT	LSITGTYDLK	0	yes	no	2	1.21E-15	2.56E+08	2.49E+08	9.02E+06	2.48E+08	1.93E+07	8.25E+06	1.72E+08	1.29E+08	0
A1AT	SASLHLPK	0	yes	no	2	2.46E-09	3.27E+07	1.21E+07	5.14E+06	2.50E+07	5.56E+06	8.10E+06	1.88E+07	1.09E+07	5.52E+06

Proteins	Sequence	Missed cleavages	Unique (Groups)	Unique (Proteins)	Charge	PEP	HAD 1	HAD 2	HAD 3	MNI 1	MNI 2	MNI 3	POS 1	POS 2	POS 3
A1AT	FLENEDRR	1	yes	no	2,3	1.21E-08	9.63E+06	6.08E+06	0	2.68E+07	0	1.57E+07	2.16E+07	1.43E+07	0
A1AT	ITPNLAEFAFSLYR	0	yes	no	2,3	6.61E-06	1.81E+07	5.58E+06	1.23E+06	6.46E+07	2.57E+06	0	2.25E+07	4.46E+06	0
A1AT	QINDYVEK	0	yes	no	2	8.86E-05	1.05E+08	6.60E+07	4.56E+07	9.94E+07	6.00E+07	7.14E+07	8.84E+07	6.98E+07	4.12E+06
A1AT	SVLGQLGITK	0	yes	no	2	0.000359	3.57E+08	2.20E+08	1.77E+07	2.73E+08	2.24E+07	1.76E+07	2.21E+08	1.40E+08	2.75E+07
A1AT	DTVFALVNYIFFK	0	yes	no	2	0.000665	0	0	0	0	0	0	1.75E+06	0	0
A1AT	LSSWVLLMK	0	yes	no	2	0.003533	0	9.05E+06	0	6.26E+06	0	0	3.94E+06	1.71E+06	0
A1AT	GKWERPFEVK	2	yes	no	2	0.011852	0	0	0	0	0	0	0	0	0
A1AT	FLENEDR	0	yes	no	2	0.037749	2.60E+07	9.73E+06	0	0	1.23E+07	1.58E+07	1.37E+07	0	0
A1AT	LGMFNIQHCK	0	yes	no	3	0.042353	2.80E+06	0	0	0	0	0	0	0	0
A2M	TEVSSNHVLIYLDK	0	yes	yes	2,3	0	4.77E+07	1.72E+08	5.62E+06	2.17E+08	1.65E+07	2.52E+06	8.59E+07	2.80E+07	0
A2M	VYDYYETDEFAIAEYNAPCSK	0	yes	yes	2,3	2.54E-180	1.24E+07	3.84E+07	3.32E+06	4.72E+07	6.67E+06	2.66E+06	1.53E+07	1.90E+07	2.48E+06
A2M	VTAAPQSVCALR	0	yes	yes	2	4.60E-172	1.55E+08	8.70E+07	1.99E+07	2.41E+08	1.17E+07	2.88E+07	1.19E+08	1.22E+08	1.19E+07

Proteins	Sequence	Missed cleavages	Unique (Groups)	Unique (Proteins)	Charge	PEP	HAD 1	HAD 2	HAD 3	MNI 1	MNI 2	MNI 3	POS 1	POS 2	POS 3
A2M	QFSFPLSSEPFQGSYK	0	yes	yes	2,3	1.64E-145	4.06E+07	9.02E+07	2.57E+07	7.58E+07	2.85E+07	1.89E+07	2.83E+06	3.82E+06	1.80E+07
A2M	LHTEAQIQEEGTVVELTGR	0	yes	yes	2,3	2.89E-132	3.67E+07	1.45E+08	0	6.11E+07	9.65E+05	4.20E+06	2.70E+07	2.32E+07	0
A2M	NEDSLVFVQTDK	0	yes	no	2	8.08E-124	1.52E+08	1.49E+08	1.92E+07	2.81E+08	2.52E+07	2.02E+07	1.24E+08	1.34E+08	2.43E+07
A2M	HNVYINGITYTPVSSTNEK	0	yes	yes	2,3	1.02E-82	2.48E+07	4.40E+07	1.47E+06	4.61E+07	3.35E+06	0	2.40E+07	2.38E+07	0
A2M	AAQVTIQSSGTFSSK	0	yes	yes	2	5.71E-75	2.96E+07	7.15E+06	1.51E+07	7.34E+07	1.07E+07	1.43E+07	3.59E+07	4.94E+07	3.87E+06
A2M	YNILPEKEEFPFALGVQTLPQT CDEPK	1	yes	yes	3	1.63E-57	9.29E+06	2.03E+07	2.36E+06	2.30E+07	8.35E+06	0	4.88E+06	5.35E+06	0
A2M	AIGYLNTGYQR	0	yes	yes	2	7.04E-52	1.84E+08	1.77E+08	2.37E+07	3.15E+08	2.08E+07	2.85E+07	1.23E+08	2.05E+08	3.11E+07
A2M	FSGQLNSHGCFYQQVK	0	yes	yes	2,3	7.94E-49	2.01E+07	2.80E+07	0	6.17E+07	3.28E+06	0	3.20E+07	9.21E+06	0
A2M	DTVIKPLLVEPEGLEK	1	yes	yes	2,3	1.64E-47	7.26E+07	1.71E+08	3.15E+07	1.15E+08	2.60E+07	1.39E+07	6.93E+07	6.28E+07	3.86E+07
A2M	IAQWQSFQLEGGLK	0	yes	yes	2	2.91E-47	7.03E+06	1.02E+08	1.13E+07	7.44E+07	1.70E+07	7.64E+06	2.22E+07	2.24E+07	6.04E+06
A2M	VTGEGCVYLQTSLK	0	yes	yes	2	4.44E-47	8.02E+06	1.91E+07	0	1.96E+07	2.92E+06	1.04E+06	9.07E+06	9.76E+06	1.37E+06

Proteins	Sequence	Missed cleavages	Unique (Groups)	Unique (Proteins)	Charge	PEP	HAD 1	HAD 2	HAD 3	MNI 1	MNI 2	MNI 3	POS 1	POS 2	POS 3
A2M	VSVQLEASPAFLAVPVEK	0	yes	no	2,3	3.59E-41	2.11E+07	1.46E+08	1.70E+07	4.52E+07	1.75E+07	1.45E+07	1.28E+07	1.98E+07	1.13E+07
A2M	GHFSISIPVK	0	yes	no	2,3	3.52E-40	2.74E+07	6.49E+07	6.37E+06	9.20E+07	1.54E+07	3.69E+06	3.71E+07	2.52E+07	1.40E+06
A2M	YDVENCLANK	0	yes	yes	2	6.88E-39	1.28E+08	8.89E+07	1.60E+07	1.88E+08	1.40E+07	2.64E+07	8.30E+07	1.03E+08	0
A2M	ALLAYAFALAGNQDK	0	yes	yes	2,3	1.90E-36	7.09E+06	1.37E+07	0	2.97E+07	2.59E+06	7.72E+05	1.15E+07	4.01E+06	0
A2M	HYDGSYSTFGER	0	yes	yes	2,3	9.62E-36	2.20E+07	4.88E+07	5.47E+06	3.43E+07	0	2.51E+06	2.61E+07	4.71E+07	1.62E+06
A2M	ETTFNSLLCPSGGEVSEELSLK	0	yes	yes	2,3	7.53E-34	4.56E+06	0	0	1.25E+07	2.17E+06	0	0	0	0
A2M	QQNAQGGFSSTQDTVVALHALSK	0	yes	yes	2,3	5.75E-30	4.28E+06	5.54E+07	7.27E+06	7.65E+07	1.00E+07	5.86E+06	3.38E+07	1.60E+07	6.71E+06
A2M	VDLSFSPSQSLPASHAHLR	0	yes	yes	2,3,4	2.18E-27	0	7.25E+07	0	8.16E+07	9.70E+06	0	3.09E+07	0	0
A2M	TEHPFTVEEFVLPK	0	yes	yes	2,3	5.52E-27	5.57E+07	1.19E+08	2.14E+07	1.33E+08	4.86E+07	1.68E+07	4.78E+07	2.19E+07	7.74E+06
A2M	LVHVEEPHTETVR	0	yes	yes	2,3,4	9.84E-27	9.01E+07	7.63E+07	5.22E+06	1.71E+08	1.85E+07	2.52E+06	7.15E+07	6.15E+07	0
A2M	FEVQVTVPK	0	yes	yes	2	4.32E-22	8.18E+07	1.01E+08	1.06E+07	1.77E+08	1.33E+07	6.15E+06	5.96E+07	7.32E+07	7.17E+06

Proteins	Sequence	Missed cleavages	Unique (Groups)	Unique (Proteins)	Charge	PEP	HAD 1	HAD 2	HAD 3	MNI 1	MNI 2	MNI 3	POS 1	POS 2	POS 3
A2M	FQVDNNNR	0	yes	yes	2	1.93E-19	1.56E+07	9.50E+06	1.37E+07	2.66E+07	1.29E+07	1.43E+07	9.87E+06	1.51E+07	0
A2M	TGTHGLLVK	0	yes	no	2,3	3.03E-15	3.19E+07	1.80E+07	5.69E+06	5.14E+07	4.26E+06	1.20E+07	1.99E+07	2.74E+07	2.74E+06
A2M	YSDASDCHGEDSQAFCEK	0	yes	yes	2,3	8.84E-14	1.24E+07	8.62E+06	0	2.72E+07	0	2.39E+06	9.70E+06	1.51E+07	0
A2M	EEFPFALGVQTLPQTCDEPK	0	yes	yes	2	1.93E-11	3.37E+06	3.60E+06	1.42E+06	5.26E+06	2.79E+06	1.10E+06	0	2.74E+06	2.18E+06
A2M	QTVSWAVTPK	0	yes	no	2	1.74E-10	9.14E+07	7.26E+07	1.67E+07	1.49E+08	1.42E+07	1.66E+07	5.76E+07	8.78E+07	0
A2M	LLIYAVLPTGDVIGDSAK	0	yes	yes	2,3	3.50E-10	1.87E+07	8.60E+07	1.35E+07	6.46E+07	2.19E+07	7.84E+06	1.78E+07	1.51E+07	3.04E+06
A2M	SIYKPGQTVK	1	yes	no	2	1.50E-09	1.70E+07	1.09E+07	6.81E+06	3.43E+07	5.47E+06	8.01E+06	1.28E+07	1.89E+07	6.34E+06
A2M	LPPNVVEESAR	0	yes	no	2	8.16E-06	1.07E+08	8.60E+07	3.32E+07	1.71E+08	2.96E+07	3.29E+07	7.96E+07	1.35E+08	2.49E+07
A2M	AVDQSVLLMKPDAELSASSVYNLLPEK	1	yes	yes	3	3.31E-05	0	2.84E+06	0	4.24E+06	0	0	0	0	0
A2M	SSSNEEVMFLTVQVK	0	yes	no	2	3.65E-05	2.45E+06	2.59E+06	0	9.05E+06	0	0	2.18E+06	0	0
A2M	NALFCLESAWK	0	yes	yes	2	3.93E-05	7.20E+06	2.38E+07	1.74E+06	1.60E+07	5.15E+06	0	6.13E+06	0	0

Proteins	Sequence	Missed cleavages	Unique (Groups)	Unique (Proteins)	Charge	PEP	HAD 1	HAD 2	HAD 3	MNI 1	MNI 2	MNI 3	POS 1	POS 2	POS 3
A2M	QGIPFFGQVR	0	yes	yes	2	5.78E-05	3.57E+07	4.27E+07	9.77E+06	9.69E+07	1.12E+07	8.62E+06	3.14E+07	1.46E+07	4.17E+06
A2M	DLKPAIVK	1	yes	no	2	0.000103	4.97E+07	4.08E+07	0	9.23E+07	0	2.77E+07	3.22E+07	5.47E+07	1.86E+07
A2M	PVPGHVTVSICR	0	yes	yes	2,3	0.000155	1.71E+07	3.16E+07	0	8.16E+07	4.24E+06	0	4.12E+07	1.36E+07	0
A2M	SASNMAIVDVK	0	yes	yes	2	0.000159	1.61E+06	0	1.90E+06	0	0	4.35E+06	0	4.01E+06	0
A2M	PLLVEPEGLEK	0	yes	no	2	0.000229	4.62E+06	4.74E+06	0	1.11E+07	0	0	3.84E+06	3.73E+06	0
A2M	VGFYESDVMGR	0	yes	yes	2	0.000373	1.04E+07	0	0	2.32E+07	0	0	7.19E+06	4.85E+06	0
A2M	SLFTDLEAENDVLHCVAFAVPK	0	yes	no	2,3	0.001512	0	0	0	1.07E+07	0	0	0	0	0
A2M	SDIAPVAR	0	yes	no	2	0.006611	2.62E+07	1.63E+07	2.21E+07	4.67E+07	2.26E+07	2.36E+07	1.85E+07	2.86E+07	0
A2M	SLNEEAVK	0	yes	yes	2	0.007352	0	0	0	0	0	1.75E+07	0	2.07E+07	0
A2M	GPTQEFK	0	yes	no	2	0.013773	0	0	0	0	0	0	3.60E+06	0	0
A2M	KDTVIKPLLVEPEGLEK	2	yes	yes	3	0.019333	0	0	0	0	5.64E+06	0	0	0	0

Proteins	Sequence	Missed cleavages	Unique (Groups)	Unique (Proteins)	Charge	PEP	HAD 1	HAD 2	HAD 3	MNI 1	MNI 2	MNI 3	POS 1	POS 2	POS 3
A2M	VVSMDENFHPLNELIPLVYIQDPK	0	yes	yes	3	0.02955	0	0	0	1.93E+06	0	0	0	0	0
A2M	VSNQTLSLFFTVLQDVPVR	0	yes	yes	3	0.0313	0	0	0	1.29E+06	0	0	0	0	0
A2M	DMYSFLEDMGLK	0	yes	yes	2	0.036487	0	0	0	7.11E+05	0	0	0	0	0
A2M	GEAFTLK	0	yes	no	2	0.038312	0	0	2.69E+07	0	0	0	0	4.58E+07	9.17E+06
A2M	EQAPHCICANGR	0	yes	no	3	0.043784	3.38E+06	0	0	0	0	0	0	0	0
A2M	SLNEEAVKK	1	yes	yes	2	0.047426	0	0	0	2.98E+06	0	0	0	0	0
APOA-I	DYVSQFEGSALGK	0	yes	yes	2	7.99E-185	1.05E+08	8.32E+07	0	1.32E+08	0	0	1.19E+08	7.47E+07	0
APOA-I	LLDNWDSVTSTFSK	0	yes	no	2	8.52E-74	2.87E+07	7.32E+07	1.07E+07	4.28E+07	1.09E+07	1.35E+07	3.26E+07	1.57E+07	1.02E+07
APOA-I	EQLGPVTQEFWDNLEK	0	yes	no	2	3.04E-68	1.55E+07	0	4.42E+06	1.81E+07	6.89E+06	6.61E+06	1.08E+07	5.13E+06	2.73E+06
APOA-I	VSFLSALEEYTK	0	yes	no	2	4.38E-47	3.39E+07	7.55E+07	6.93E+06	6.20E+07	1.00E+07	6.29E+06	3.89E+07	1.22E+07	2.55E+06
APOA-I	DLATVYVDVLK	0	yes	yes	2	2.96E-14	1.68E+07	4.96E+07	8.27E+06	5.74E+07	0	6.75E+06	2.51E+07	1.12E+07	2.80E+06

Proteins	Sequence	Missed cleavages	Unique (Groups)	Unique (Proteins)	Charge	PEP	HAD 1	HAD 2	HAD 3	MNI 1	MNI 2	MNI 3	POS 1	POS 2	POS 3
APOA-I	ATEHLSTLSEK	0	yes	no	2,3	2.66E-13	3.38E+07	1.95E+07	1.06E+07	3.75E+07	5.74E+06	1.29E+07	2.62E+07	1.44E+07	7.13E+06
APOA-I	AKPALEDLR	1	yes	no	2,3	1.40E-09	5.03E+07	1.52E+07	0	2.29E+07	0	0	1.83E+07	1.71E+07	0
APOA-I	THLAPYSDELR	0	yes	no	2,3	1.59E-08	1.33E+08	9.15E+07	4.73E+06	1.36E+08	3.43E+06	6.16E+06	5.63E+07	0	8.31E+06
APOA-I	QGLLPVLESFK	0	yes	no	2	0.000402	2.83E+07	3.74E+07	1.53E+07	4.28E+07	1.69E+07	1.49E+07	2.69E+07	9.27E+06	0
APOA-I	VQPYLDDFQK	0	yes	no	2	0.000966	1.16E+08	8.47E+07	8.08E+06	1.06E+08	0	9.30E+06	1.02E+08	6.06E+07	1.83E+07
APOA-I	LSPLGEEMR	0	yes	no	2	0.020836	8.14E+06	0	0	0	0	0	0	0	0
APOA-I	VKDLATVYVDVLK	1	yes	yes	3	0.05691	0	0	0	6.07E+06	0	0	0	0	0
ApoE	LEEQAQQIR	0	yes	yes	2	0	0	0	0	0	0	0	0	0	0
ApoE	SELEEQLTPVAEETR	0	yes	no	2	4.25E-19	1.05E+07	2.83E+06	0	7.17E+06	0	0	5.59E+06	3.98E+06	0
ApoE	VQAAVGTSAAPVPSDNH	0	yes	yes	2	0.000696	0	0	0	0	0	0	4.13E+06	0	0
ApoE	AATVGSLAGQPLQER	0	yes	no	2	0.001296	1.04E+07	5.92E+06	0	6.99E+06	8.87E+05	0	6.59E+06	6.45E+06	0
ApoE	VEQAVETEPEPELR	0	yes	no	2	0.020221	0	0	0	0	0	0	0	0	0
ApoE	LGPLVEQGR	0	yes	no	2	0.020788	0	0	0	0	0	0	0	0	0

Proteins	Sequence	Missed cleavages	Unique (Groups)	Unique (Proteins)	Charge	PEP	HAD 1	HAD 2	HAD 3	MNI 1	MNI 2	MNI 3	POS 1	POS 2	POS 3
ApoE	LAVYQAGAR	0	yes	no	2	0.027538	4.61E+06	0	0	0	0	0	0	0	0
CERU	VNKDDEEFIESNK	1	yes	no	2,3	2.00E-122	6.21E+07	3.79E+07	0	4.70E+07	0	0	4.45E+07	5.34E+07	0
CERU	NNEGTYYSPNYNPQSR	0	yes	no	2	1.62E-61	2.42E+07	1.39E+07	4.02E+06	1.74E+07	6.17E+06	6.77E+06	2.46E+07	1.60E+07	2.19E+06
CERU	DIASGLIGPLIICK	0	yes	no	2,3	2.51E-48	2.46E+07	4.04E+07	1.39E+07	2.46E+07	1.43E+07	1.46E+07	1.77E+07	1.30E+07	9.40E+06
CERU	ALYLQYTDETFR	0	yes	no	2	2.07E-36	1.45E+07	6.81E+07	2.73E+06	3.47E+07	4.07E+06	2.62E+06	3.38E+07	1.10E+07	0
CERU	SGAGTEDSACIPWAYYSTVDQVK	0	yes	no	2,3	4.32E-35	9.09E+06	1.19E+07	2.15E+06	1.12E+07	2.73E+06	3.28E+06	8.75E+06	5.61E+06	2.96E+06
CERU	EYTDASFTNR	0	yes	no	2	3.12E-29	6.26E+07	4.66E+07	2.20E+07	5.28E+07	2.57E+07	4.17E+07	6.41E+07	5.22E+07	3.30E+06
CERU	LISVDTEHSNIYLQNGPDR	0	yes	no	2,3	5.17E-27	6.16E+06	2.62E+07	0	2.39E+07	0	0	2.90E+07	7.61E+06	0
CERU	GAYPLSIEPIGVR	0	yes	no	2	3.51E-26	5.08E+07	5.18E+07	9.49E+06	6.05E+07	1.09E+07	1.12E+07	6.92E+07	2.70E+07	1.50E+07
CERU	EVGPTNADPVCLAK	0	yes	no	2	6.20E-26	7.80E+07	6.12E+07	2.17E+07	6.45E+07	1.09E+07	2.22E+07	7.10E+07	6.37E+07	6.59E+06
CERU	DLYSGLIGPLIVCR	0	yes	no	2,3	1.53E-19	1.40E+07	2.23E+07	4.67E+06	1.61E+07	8.22E+06	3.43E+06	1.18E+07	4.73E+06	1.50E+06

Proteins	Sequence	Missed cleavages	Unique (Groups)	Unique (Proteins)	Charge	PEP	HAD 1	HAD 2	HAD 3	MNI 1	MNI 2	MNI 3	POS 1	POS 2	POS 3
CERU	DDEEFIESNK	0	yes	no	2	4.86E-11	0	0	0	0	1.07E+06	0	0	0	0
CERU	SVPPSASHVAPTETFTYEWTVPK	0	yes	no	2,3	1.26E-06	0	1.61E+07	0	0	0	0	3.54E+06	0	0
CERU	QSEDSTFYLGER	0	yes	no	2	1.97E-05	4.25E+07	3.54E+07	1.59E+06	3.69E+07	2.01E+06	2.05E+06	4.05E+07	3.75E+07	8.92E+05
CERU	TTIEKPVWLGFLGPIIK	1	yes	no	2,3	0.001087	0	8.83E+06	0	6.66E+06	0	0	5.26E+06	0	0
CERU	RQSEDSTFYLGER	1	yes	no	3	0.008378	0	0	0	0	0	0	0	0	0
CERU	DIFTGLIGPMK	0	yes	no	2	0.009039	0	3.46E+06	0	0	0	0	0	0	0
CERU	QYTDSTFR	0	yes	no	2	0.010863	2.47E+07	1.69E+07	1.36E+07	2.44E+07	1.69E+07	2.48E+07	2.24E+07	2.29E+07	0
CERU	AEEEHLGILGPQLHADVGDK	0	yes	no	3,4	0.015779	0	2.93E+06	0	4.79E+06	0	0	3.41E+06	0	0
CERU	AGLQAFFQVQECNK	0	yes	no	2	0.018401	0	0	0	2.17E+06	0	0	2.51E+06	0	0
CERU	GEFYIGSK	0	yes	no	2	0.024898	2.01E+07	0	0	0	0	0	0	0	0
CERU	KAEEEHLGILGPQLHADVGDK	1	yes	no	3	0.037227	0	0	0	0	0	0	2.82E+06	0	0
CERU	PVWLGFLGPIIK	0	yes	no	2	0.046533	0	0	0	1.46E+06	0	0	0	0	0

Proteins	Sequence	Missed cleavages	Unique (Groups)	Unique (Proteins)	Charge	PEP	HAD 1	HAD 2	HAD 3	MNI 1	MNI 2	MNI 3	POS 1	POS 2	POS 3
CLU	ASSIIDELFQDR	0	yes	no	2	2.65E-26	5.99E+06	2.16E+07	2.98E+06	1.48E+07	5.04E+06	2.64E+06	6.16E+06	3.43E+06	0
CLU	LFDSDPITVTVPVEVSR	0	yes	no	2	8.44E-12	0	1.48E+07	0	8.71E+06	1.86E+06	0	3.72E+06	0	0
CLU	EILSVDCSTNNPSQAK	0	yes	no	2	2.34E-09	7.29E+06	4.62E+06	0	1.18E+07	0	0	5.87E+06	0	0
CLU	VTTVASHTSDSDVPSGVTEVVVK	0	yes	no	3	7.60E-07	7.22E+06	7.48E+06	0	1.86E+07	0	0	1.54E+07	4.75E+06	2.19E+06
CLU	EIQNAVNGVK	0	yes	no	2	0.0002	2.72E+06	0	0	4.74E+06	2.87E+06	2.85E+06	3.03E+06	2.96E+06	0
CLU	IDSLLENDR	0	yes	no	2	0.001805	1.52E+07	1.08E+07	4.19E+06	1.95E+07	5.59E+06	7.77E+06	1.51E+07	1.07E+07	0
CLU	TLLSNLEEAK	0	yes	no	2	0.006125	1.00E+07	8.72E+06	1.55E+06	0	0	0	0	0	2.15E+06
C3	APSTWLTAYVVK	0	yes	yes	2	0	9.09E+06	6.82E+07	0	3.12E+07	0	0	2.09E+07	2.35E+07	0
C3	GVFVLNK	0	no	no	1,2	0	2.39E+07	3.02E+07	7.54E+06	5.33E+07	1.23E+07	7.79E+06	3.46E+07	7.24E+07	0
C3	VPVAVQGEDTVQSLTQGDGVAK	0	yes	yes	2,3	1.02E-285	1.88E+07	1.06E+08	0	1.06E+08	3.21E+07	0	1.12E+08	4.64E+07	4.10E+07
C3	DYAGVFSDAGLTFTSSSGQQTAQR	0	yes	yes	2,3	1.15E-145	1.62E+07	3.98E+07	4.85E+06	2.70E+07	6.73E+06	5.37E+06	1.97E+07	2.58E+07	2.86E+06

Proteins	Sequence	Missed cleavages	Unique (Groups)	Unique (Proteins)	Charge	PEP	HAD 1	HAD 2	HAD 3	MNI 1	MNI 2	MNI 3	POS 1	POS 2	POS 3
C3	AYYENSPQQVFSTEFEVK	0	yes	yes	2	3.44E-94	0	3.26E+07	7.74E+06	2.17E+07	1.33E+07	8.60E+06	1.58E+07	2.16E+07	1.01E+07
C3	CAEENCFIQK	0	yes	yes	2	1.37E-91	1.75E+07	1.47E+07	8.22E+06	3.24E+07	1.27E+07	1.27E+07	2.91E+07	2.60E+07	3.60E+06
C3	SGSDEVQVGQQR	0	yes	no	2	2.07E-89	1.09E+07	1.06E+07	1.21E+07	1.92E+07	2.30E+07	1.92E+07	2.05E+07	2.35E+07	2.21E+06
C3	SNLDEDIIAEENIVSR	0	yes	yes	2,3	5.71E-76	3.43E+07	1.10E+08	1.26E+07	8.53E+07	2.58E+07	3.13E+06	6.94E+07	6.50E+07	1.88E+07
C3	QELSEAEQATR	0	yes	yes	2	3.98E-61	1.68E+07	1.50E+07	1.05E+07	2.22E+07	2.22E+07	1.90E+07	2.62E+07	2.93E+07	0
C3	DICEEQVNSLPGSITK	0	yes	no	2	6.06E-57	1.02E+07	9.30E+06	2.00E+06	2.19E+07	4.45E+06	2.06E+06	1.44E+07	1.90E+07	0
C3	SEETKENEGFTVTAEGK	1	yes	no	2,3	5.43E-50	1.05E+07	0	0	2.04E+07	0	0	2.89E+07	3.09E+07	6.05E+06
C3	VHQYFNVELIQPGAVK	0	yes	no	2,3	2.45E-48	5.41E+06	7.06E+07	2.54E+06	5.18E+07	2.03E+07	0	3.83E+07	1.24E+07	0
C3	TIYTPGSTVLYR	0	no	no	2	2.06E-47	1.12E+08	1.54E+08	0	1.66E+08	2.16E+07	1.34E+07	1.64E+08	1.87E+08	2.70E+07
C3	EDIPPADLSDQVPDTESETR	0	yes	yes	2	9.42E-36	4.16E+06	6.76E+06	2.65E+06	6.90E+06	7.88E+06	4.03E+06	5.46E+06	1.11E+07	5.35E+06
C3	IPIEDGSGEVVLSR	0	yes	yes	2,3	1.39E-35	1.01E+08	1.18E+08	1.15E+07	1.56E+08	2.38E+07	1.21E+07	1.46E+08	1.72E+08	2.20E+07

Proteins	Sequence	Missed cleavages	Unique (Groups)	Unique (Proteins)	Charge	PEP	HAD 1	HAD 2	HAD 3	MNI 1	MNI 2	MNI 3	POS 1	POS 2	POS 3
C3	TGLQEVEVK	0	yes	yes	2	1.22E-33	8.35E+07	8.54E+07	4.67E+07	1.21E+08	7.68E+07	7.88E+07	1.23E+08	1.41E+08	8.86E+06
C3	GYTQQLAFR	0	no	no	2	2.70E-30	5.52E+07	6.92E+07	6.03E+06	8.22E+07	1.12E+07	9.25E+06	8.59E+07	9.96E+07	1.21E+07
C3	KGYTQQLAFR	1	no	no	3	7.00E-30	0	5.27E+06	0	6.43E+06	1.21E+06	0	7.72E+06	8.82E+06	0
C3	VELLHNPAFCSLATTK	0	yes	yes	2,3	6.91E-28	1.04E+07	4.51E+07	0	4.00E+07	1.43E+07	0	3.54E+07	1.70E+07	1.80E+06
C3	LVAYYTLIGASGQR	0	yes	yes	2,3	4.68E-26	1.23E+07	8.29E+07	3.07E+06	8.30E+07	1.28E+07	2.74E+06	7.89E+07	3.77E+07	0
C3	VFLDCCNYITELR	0	yes	yes	2	7.73E-26	9.06E+06	2.41E+07	0	1.36E+07	5.38E+06	1.55E+06	9.63E+06	8.11E+06	1.38E+06
C3	VYAYYNLEESCTR	0	yes	yes	2	1.62E-24	2.92E+07	0	1.02E+06	5.66E+07	0	1.60E+06	4.59E+07	4.24E+07	1.03E+06
C3	GLEVTITAR	0	yes	yes	2	3.64E-24	0	4.52E+07	0	3.93E+07	0	0	3.05E+07	0	0
C3	IHWESASLLR	0	yes	no	2,3	1.50E-22	1.12E+07	1.78E+07	0	4.30E+07	5.43E+06	0	1.77E+07	1.22E+07	0
C3	EVVADSVWVDVK	0	no	no	2	1.00E-21	2.56E+07	5.62E+07	0	6.27E+07	0	2.32E+06	4.10E+07	4.66E+07	2.78E+06
C3	VTIKPAPETEK	1	yes	yes	2,3	2.00E-18	2.20E+07	1.83E+07	1.24E+07	3.93E+07	2.42E+07	2.44E+07	4.18E+07	5.21E+07	1.20E+07

Proteins	Sequence	Missed cleavages	Unique (Groups)	Unique (Proteins)	Charge	PEP	HAD 1	HAD 2	HAD 3	MNI 1	MNI 2	MNI 3	POS 1	POS 2	POS 3
C3	KQELSEAEQATR	1	yes	yes	2,3	4.63E-18	5.20E+06	1.11E+07	0	2.15E+07	6.00E+06	1.30E+07	2.09E+07	2.58E+07	0
C3	VLLDGVQNPR	0	yes	yes	2	2.21E-15	6.68E+07	6.69E+07	1.37E+07	9.15E+07	2.62E+07	1.76E+07	9.29E+07	1.10E+08	1.45E+07
C3	SDDKVTLEER	1	yes	no	2,3	3.78E-15	5.76E+06	0	4.56E+06	1.65E+07	8.45E+06	1.28E+07	1.31E+07	1.89E+07	0
C3	HQQTVTIPPK	0	yes	yes	2,3	3.83E-15	6.17E+06	5.61E+06	2.99E+06	1.48E+07	7.80E+06	6.02E+06	1.64E+07	2.59E+07	0
C3	FVTVQATFGTQVVEK	0	yes	no	2	1.27E-14	4.33E+06	2.23E+07	0	1.42E+07	4.48E+06	0	1.28E+07	9.77E+06	0
C3	FYYIYNEK	0	yes	yes	2	4.83E-13	4.68E+07	5.91E+07	3.64E+06	7.35E+07	8.87E+06	2.34E+06	7.85E+07	8.34E+07	3.90E+06
C3	EPGQDLVVLPLSITTDFIPSFR	0	yes	yes	2,3	7.97E-13	4.04E+06	1.46E+07	0	1.05E+07	1.16E+06	0	7.72E+06	0	0
C3	EYVLPSFEVIVEPTEK	0	yes	yes	2	3.70E-10	1.65E+07	5.60E+07	6.88E+06	2.35E+07	2.09E+07	6.56E+06	1.54E+07	1.72E+07	2.88E+06
C3	ADIGCTPGSGK	0	yes	yes	2	2.37E-09	5.84E+06	5.68E+06	7.42E+06	9.61E+06	1.31E+07	9.98E+06	1.06E+07	1.50E+07	1.32E+06
C3	LSINTHPSQKPLSITVR	1	yes	yes	3,4	4.66E-09	0	4.16E+07	0	4.24E+07	5.34E+06	0	4.41E+07	0	0
C3	ENEGFTVTAEGK	0	yes	no	2	2.06E-08	4.45E+07	4.09E+07	1.50E+07	4.17E+07	2.78E+07	2.99E+07	5.97E+07	6.91E+07	3.81E+06

Proteins	Sequence	Missed cleavages	Unique (Groups)	Unique (Proteins)	Charge	PEP	HAD 1	HAD 2	HAD 3	MNI 1	MNI 2	MNI 3	POS 1	POS 2	POS 3
C3	EALKLEEK	1	yes	no	2,3	1.00E-07	0	0	0	5.08E+06	0	4.32E+06	4.02E+06	2.73E+06	0
C3	DFDFVPPVVR	0	yes	yes	2	2.47E-07	4.83E+07	1.48E+08	2.49E+07	1.21E+08	4.60E+07	2.47E+07	9.34E+07	8.50E+07	3.38E+07
C3	SEFPESWLWNVEDLKEPPK	1	yes	yes	3	8.75E-07	2.49E+06	4.31E+06	0	5.05E+06	0	0	3.13E+06	0	0
C3	SGIPIVTSPYQIHFTK	0	yes	yes	2,3	1.43E-06	8.41E+06	5.63E+07	7.19E+06	3.23E+07	3.15E+07	7.87E+06	2.91E+07	1.17E+07	3.74E+06
C3	ILLQGTPVAQMTEDAVDAER	0	yes	yes	2	2.69E-06	0	0	0	4.06E+06	0	0	2.24E+06	0	3.38E+06
C3	ISLPESLK	0	yes	yes	2	3.51E-06	9.52E+07	9.99E+07	0	1.19E+08	0	0	1.14E+08	1.66E+08	2.31E+07
C3	VSHSEDDCLAFK	0	yes	no	2,3	3.03E-05	5.11E+06	4.03E+06	0	2.53E+07	0	0	2.08E+07	1.90E+07	3.91E+06
C3	TVMVNIENPEGIPVK	0	yes	yes	2	3.71E-05	4.09E+06	0	0	7.22E+06	0	0	8.80E+06	6.29E+06	2.07E+06
C3	TELRPGETLNVNFLLR	1	yes	yes	3	4.09E-05	4.03E+06	0	0	6.83E+06	0	0	0	0	0
C3	DSCVGSLVVK	0	yes	yes	2	6.19E-05	7.11E+07	6.55E+07	2.37E+07	8.23E+07	4.24E+07	3.65E+07	8.95E+07	9.80E+07	7.39E+06
C3	RIPIEDGSGEVVLSR	1	yes	yes	3	0.000131	0	3.34E+06	0	3.34E+06	0	0	0	3.02E+06	0

Proteins	Sequence	Missed cleavages	Unique (Groups)	Unique (Proteins)	Charge	PEP	HAD 1	HAD 2	HAD 3	MNI 1	MNI 2	MNI 3	POS 1	POS 2	POS 3
C3	KVEGTAFVIFGIQDGEQR	1	yes	yes	2,3	0.000327	0	1.19E+07	0	6.64E+06	0	0	6.10E+06	0	0
C3	QPSSAFAAFVK	0	yes	yes	2	0.000371	2.90E+07	3.27E+07	0	4.76E+07	7.39E+06	0	4.81E+07	4.81E+07	9.38E+06
C3	AAVYHHFISDGVR	0	yes	yes	2,3,4	0.000645	1.39E+06	1.36E+07	0	3.03E+07	0	0	3.59E+07	4.97E+06	0
C3	SSLSVPYVIVPLK	0	yes	yes	2	0.000735	2.39E+07	1.20E+08	2.30E+07	3.81E+07	4.55E+07	2.32E+07	3.86E+07	3.58E+07	3.94E+07
C3	NTLIIYLDK	0	no	no	2	0.000927	3.45E+07	4.58E+07	1.49E+06	8.43E+07	5.63E+06	0	5.35E+07	3.99E+07	0
C3	RQGALELIK	1	yes	yes	3	0.001155	0	0	0	0	0	0	2.30E+06	0	0
C3	VEGTAFVIFGIQDGEQR	0	yes	yes	2	0.001238	0	4.22E+06	0	2.20E+06	0	0	8.42E+05	0	0
C3	ACEPGVDYVYK	0	no	no	2	0.001645	7.26E+07	6.91E+07	9.50E+06	9.22E+07	3.03E+07	1.35E+07	9.29E+07	1.27E+08	6.98E+06
C3	SYTVAIAGYALAQMGR	0	yes	no	2	0.001897	0	1.86E+06	0	0	0	0	0	0	0
C3	FISLGEACK	0	yes	yes	2	0.002504	2.35E+07	1.65E+07	0	4.58E+07	2.12E+06	0	4.49E+07	2.87E+07	5.44E+06
C3	YYTYLIMNK	0	yes	yes	2	0.002989	9.48E+06	6.70E+06	0	1.71E+07	0	0	1.18E+07	9.80E+06	0

Proteins	Sequence	Missed cleavages	Unique (Groups)	Unique (Proteins)	Charge	PEP	HAD 1	HAD 2	HAD 3	MNI 1	MNI 2	MNI 3	POS 1	POS 2	POS 3
C3	KVLLDGVQNPR	1	yes	yes	2	0.004021	4.65E+06	0	0	6.23E+06	0	0	5.15E+06	5.89E+06	0
C3	LPYSVVR	0	no	no	2	0.005779	0	0	0	0	0	0	1.15E+08	1.34E+08	1.44E+07
C3	VQLSNDFDEYIMAIEQTIK	0	yes	no	2	0.007734	0	0	0	9.95E+05	0	0	0	0	0
C3	NTMILEICTR	0	yes	no	2	0.008338	0	0	0	4.56E+06	0	0	0	0	0
C3	LSINTHPSQK	0	yes	yes	2,3	0.008726	0	0	0	0	0	0	1.36E+06	2.84E+06	0
C3	AGDFLEANYMNLQR	0	yes	no	2	0.010457	3.00E+06	0	0	5.52E+06	0	0	0	0	0
C3	ISLPESLKR	1	yes	yes	3	0.01151	6.51E+06	0	0	6.89E+06	0	0	8.52E+06	0	0
C3	QGALELIK	0	yes	yes	2	0.012758	0	0	0	8.11E+07	0	0	8.09E+07	7.93E+07	0
C3	IFTVNHK	0	yes	yes	2	0.012853	3.06E+06	0	0	0	0	2.50E+06	4.73E+06	5.40E+06	0
C3	VVPEGIR	0	yes	yes	2	0.022027	6.33E+06	0	5.88E+06	1.13E+07	1.10E+07	0	9.73E+06	1.30E+07	0
C3	LMNIFLK	0	yes	yes	2	0.022874	6.64E+06	0	0	1.27E+07	0	0	1.06E+07	9.62E+06	0

Proteins	Sequence	Missed cleavages	Unique (Groups)	Unique (Proteins)	Charge	PEP	HAD 1	HAD 2	HAD 3	MNI 1	MNI 2	MNI 3	POS 1	POS 2	POS 3
C3	IWDVVEK	0	no	no	2	0.032481	6.14E+07	0	0	0	0	0	0	8.35E+07	0
C3	LVLSSEK	0	yes	no	2	0.033095	7.53E+06	0	9.11E+06	0	0	1.09E+07	1.51E+07	1.75E+07	0
C3	SEFPESWLWNVEDLK	0	yes	yes	2	0.051115	0	0	0	0	1.62E+06	0	0	0	0
C3	VVLVAVDK	0	yes	yes	2	0.056084	0	0	0	0	0	0	0	0	5.23E+06
C3	NEQVEIR	0	no	no	2	0.061346	0	0	0	0	0	1.62E+07	0	0	0
C4-A	PVAFSVVPTAAAAVSLK	0	yes	no	2,3	2.47E-50	1.85E+06	2.08E+07	2.09E+06	5.25E+06	2.66E+06	3.02E+06	4.99E+06	3.11E+06	1.46E+06
C4-A	LQETSNWLLSQQQADGSFQDPCPVLDR	0	yes	no	3	7.10E-08	0	4.85E+06	0	0	0	0	0	0	0
C4-A	DSSTWLTAFVLK	0	yes	no	2	0.020117	0	3.15E+06	0	3.50E+06	2.62E+06	0	3.66E+06	0	0
C4-B	VLSLAQEQVGGSPEK	0	no	no	2	6.66E-175	6.75E+07	7.22E+07	1.50E+07	7.51E+07	4.78E+06	1.02E+07	6.58E+07	7.39E+07	0
C4-B	VTASDPLDTLGSEGALSPGGVASLLR	0	no	no	2,3	4.29E-106	1.72E+07	4.68E+07	7.58E+06	1.84E+07	4.58E+06	1.16E+07	9.88E+06	1.09E+07	9.75E+06
C4-B	LLATLCSAEVCQCAEGK	0	no	no	2,3	2.97E-66	1.90E+07	3.48E+07	2.92E+06	4.33E+07	3.46E+06	1.64E+06	2.98E+07	3.22E+07	4.40E+06

Proteins	Sequence	Missed cleavages	Unique (Groups)	Unique (Proteins)	Charge	PEP	HAD 1	HAD 2	HAD 3	MNI 1	MNI 2	MNI 3	POS 1	POS 2	POS 3
C4-B	TTNIQGINLLFSSR	0	no	no	2	1.75E-60	2.78E+06	4.51E+07	6.00E+06	1.26E+07	5.29E+06	3.74E+06	8.64E+06	7.81E+06	1.30E+06
C4-B	ALEILQEEDLIDEDDIPVR	0	no	no	2	1.31E-44	0	0	2.77E+06	0	0	0	0	6.79E+06	0
C4-B	DHAVDLIQK	0	no	no	2	5.73E-40	2.02E+07	1.93E+07	8.44E+06	2.50E+07	5.26E+06	8.70E+06	2.00E+07	2.09E+07	3.68E+06
C4-B	EELVYELNPLDHR	0	no	no	2,3	1.31E-35	6.72E+06	2.92E+07	2.77E+06	1.82E+07	6.74E+06	0	1.35E+07	3.62E+06	0
C4-B	STQDTVIALDALSAYWIASHTTEER	0	no	no	2,3	7.49E-27	0	4.61E+06	0	1.29E+07	0	0	1.02E+07	0	0
C4-B	GHLFLQTDQPIYNPGQR	0	no	no	2,3	1.99E-22	0	4.79E+06	0	1.17E+07	0	0	1.66E+06	0	0
C4-B	AACAQLNDFLQEYGTQGCQV	0	no	no	2	6.00E-22	7.42E+06	8.54E+06	6.26E+06	1.17E+07	5.12E+06	6.14E+06	6.06E+06	1.01E+07	0
C4-B	QGSFQGGFR	0	no	no	2	2.49E-15	1.54E+07	1.16E+07	8.41E+06	1.89E+07	5.55E+06	9.53E+06	1.54E+07	1.61E+07	0
C4-B	DFALLSLQVPLK	0	no	no	2	2.64E-13	8.41E+06	2.19E+07	5.30E+06	1.10E+07	6.02E+06	2.12E+06	8.27E+06	4.31E+06	6.71E+05
C4-B	VGDTLNLNLR	0	no	no	2	1.71E-11	0	6.24E+07	0	8.45E+07	5.08E+06	0	4.76E+07	3.43E+07	4.53E+06
C4-B	CSVFYGAPSK	0	no	no	2	2.17E-07	6.38E+06	0	2.07E+06	0	1.97E+06	2.56E+06	9.29E+06	6.81E+06	0

Proteins	Sequence	Missed cleavages	Unique (Groups)	Unique (Proteins)	Charge	PEP	HAD 1	HAD 2	HAD 3	MNI 1	MNI 2	MNI 3	POS 1	POS 2	POS 3
C4-B	SCGLHQLLR	0	no	no	2,3	2.55E-06	1.03E+07	9.07E+06	0	3.15E+07	0	0	1.24E+07	0	0
C4-B	AEFQDALEK	0	no	no	2	3.09E-06	3.29E+07	3.10E+07	1.42E+07	3.99E+07	9.99E+06	1.62E+07	3.04E+07	3.79E+07	0
C4-B	PVQGVAYVR	0	no	no	2	3.35E-06	8.55E+06	1.03E+07	3.37E+06	2.02E+07	3.26E+06	2.94E+06	1.16E+07	1.35E+07	0
C4-B	HLVPGAPFLLQALVR	0	no	no	3	1.74E-05	5.92E+05	5.06E+06	0	2.28E+06	0	0	8.86E+05	0	0
C4-B	GPEVQLVAHSPWLK	0	no	no	2,3	4.71E-05	0	1.56E+07	0	6.13E+06	0	0	7.44E+06	0	0
C4-B	LGQYASPTAK	0	no	no	2	0.000324	6.94E+06	6.72E+06	8.09E+06	1.28E+07	6.17E+06	7.39E+06	7.26E+06	8.87E+06	0
C4-B	GLQDEDGYR	0	no	no	2	0.000327	5.76E+06	6.06E+06	5.74E+06	1.08E+07	4.66E+06	5.67E+06	6.01E+06	8.42E+06	0
C4-B	VDFTLSSER	0	no	no	2	0.000359	2.85E+07	3.24E+07	6.00E+06	3.53E+07	0	0	2.68E+07	2.87E+07	0
C4-B	KADGSYAAWLSR	1	no	no	3	0.000379	0	0	0	0	0	0	0	0	0
C4-B	TEQWSTLPPETK	0	no	no	2	0.00054	7.50E+06	0	0	0	0	0	6.02E+06	6.88E+06	0
C4-B	GSFEFPVGDAVSK	0	no	no	2	0.000868	2.62E+07	2.62E+07	0	3.57E+07	0	0	2.68E+07	3.04E+07	0
C4-B	LTVAAPPSGGPGFLSIERPDSRPPR	2	no	no	4	0.001097	0	9.92E+06	0	0	0	0	0	0	0

Proteins	Sequence	Missed cleavages	Unique (Groups)	Unique (Proteins)	Charge	PEP	HAD 1	HAD 2	HAD 3	MNI 1	MNI 2	MNI 3	POS 1	POS 2	POS 3
C4-B	ITQVLHFTK	0	no	no	2,3	0.001421	1.20E+07	1.37E+07	0	2.10E+07	0	0	1.94E+07	1.35E+07	0
C4-B	GLCVATPVQLR	0	no	no	2	0.001456	0	0	0	0	0	0	2.51E+07	2.45E+07	2.57E+06
C4-B	FGLLDEDGKK	1	no	no	2,3	0.002211	7.34E+06	8.50E+06	0	8.20E+06	0	0	2.24E+07	0	0
C4-B	YVLPNFEVK	0	no	no	2	0.002692	0	0	3.44E+06	0	2.71E+06	2.30E+06	2.27E+07	1.68E+07	0
C4-B	ASAGLLGAHAAAITAYALTLTK	0	no	no	3	0.003771	0	1.86E+06	0	0	0	0	4.48E+06	0	0
C4-B	LELSVDGAK	0	no	no	1,2	0.00404	1.93E+07	1.91E+07	0	3.49E+07	0	0	1.68E+07	2.00E+07	0
C4-B	FGLLDEDGK	0	no	no	2	0.005188	9.85E+06	0	0	1.71E+07	0	0	0	0	0
C4-B	VDVQAGACEGK	0	no	no	2	0.0083	0	0	3.23E+06	4.80E+06	2.56E+06	0	3.67E+06	4.58E+06	0
C4-B	VEYGFQVK	0	no	no	2	0.011353	2.02E+07	2.62E+07	0	3.11E+07	0	0	1.97E+07	0	0
C4-B	LTVAAPPSGGPGFLSIER	0	no	no	2	0.013815	0	9.91E+06	0	9.59E+06	0	0	0	0	0
C4-B	LVNGQSHISLSK	0	no	no	2,3	0.017968	0	5.58E+06	0	2.62E+06	0	0	6.04E+06	4.71E+06	0

Proteins	Sequence	Missed cleavages	Unique (Groups)	Unique (Proteins)	Charge	PEP	HAD 1	HAD 2	HAD 3	MNI 1	MNI 2	MNI 3	POS 1	POS 2	POS 3
C4-B	LNMGITDLQGLR	0	no	no	2	0.019475	0	0	0	6.36E+06	0	0	1.75E+06	0	0
C4-B	SHALQLNNR	0	no	no	2,3	0.029639	1.03E+06	0	0	4.64E+06	0	0	1.35E+06	0	0
C4-B	EPFLSCCQFAESLR	0	no	no	2	0.031572	0	0	0	2.17E+06	0	0	0	0	0
C4-B	FACYYPR	0	no	no	2	0.054082	0	0	0	0	0	0	1.09E+07	1.29E+07	0
C4-B	GLEEELQFSLGSK	0	no	no	2	0.058066	0	0	0	3.96E+06	0	0	0	0	0
C4-B	GSSTWLTAFVLK	0	yes	no	2	0.058978	0	0	0	0	0	0	4.25E+06	0	0
CFH	LGYVTADGETSGSITCGK	0	yes	yes	2	1.66E-40	7.43E+06	1.25E+07	0	1.29E+07	3.35E+06	1.69E+06	1.29E+07	1.13E+07	0
CFH	AGEQVTYTCATYYK	0	yes	yes	2	1.33E-26	1.21E+07	2.34E+07	0	2.19E+07	2.93E+06	1.12E+06	1.96E+07	2.33E+07	7.34E+05
CFH	VSVLCQENYLIQEGEEITCK	0	yes	yes	2,3	1.58E-15	2.83E+06	1.33E+07	2.97E+06	1.25E+07	3.05E+06	3.30E+06	9.27E+06	6.16E+06	1.29E+06
CFH	AVYTCNEGYQLLGEINYR	0	yes	no	2	1.49E-06	0	1.02E+07	0	3.54E+06	2.08E+06	0	2.20E+06	2.79E+06	0
CFH	SSIDIENGFISESQYTYALK	0	yes	yes	2	1.94E-06	0	2.80E+06	0	2.88E+06	0	0	0	1.16E+06	0

Proteins	Sequence	Missed cleavages	Unique (Groups)	Unique (Proteins)	Charge	PEP	HAD 1	HAD 2	HAD 3	MNI 1	MNI 2	MNI 3	POS 1	POS 2	POS 3
CFH	LSYTCEGGFR	0	yes	yes	2	9.26E-05	2.20E+07	2.16E+07	0	2.48E+07	4.80E+06	0	2.34E+07	2.53E+07	2.10E+06
CFH	SSNLIILEEHLK	0	yes	yes	2,3	0.000662	0	0	0	1.58E+07	0	0	1.65E+07	0	0
CFH	EQVQSCGPPPELLNGNVK	0	yes	yes	2	0.00172	8.15E+05	7.63E+05	0	1.71E+06	0	0	1.20E+06	1.31E+06	0
CFH	WSSPPQCEGLPCK	0	yes	yes	2	0.002179	4.04E+06	6.20E+06	0	5.28E+06	0	0	5.00E+06	7.18E+06	0
CFH	CFEGFGIDGPAIAK	0	yes	yes	2	0.003203	4.76E+06	8.66E+06	1.26E+06	2.54E+06	2.98E+06	3.77E+06	9.18E+06	1.56E+06	0
CFH	IDVHLVPDR	0	yes	yes	2	0.003643	7.37E+06	8.93E+06	0	8.12E+06	0	0	0	0	0
CFH	NTEILTGSWSDQTYPEGTQAIYK	0	yes	no	2	0.004231	0	0	0	1.76E+06	0	0	0	0	0
CFH	DTSCVNPPTVQNAYIVSR	0	yes	yes	2	0.004345	0	0	0	1.58E+06	0	0	0	0	0
CFH	SCDNPYIPNGDYSPLR	0	yes	no	2	0.005497	2.14E+06	0	0	2.37E+06	0	0	2.12E+06	0	0
CFH	KGEWVALNPLR	1	yes	no	3	0.005629	0	6.66E+06	0	0	0	0	0	0	0
CFH	SIDVACHPGYALPK	0	yes	no	3	0.011134	9.48E+06	0	0	0	0	0	1.21E+07	8.42E+06	0
CFH	TGESVEFVCK	0	yes	yes	2	0.013467	0	0	0	0	0	0	0	0	0

Proteins	Sequence	Missed cleavages	Unique (Groups)	Unique (Proteins)	Charge	PEP	HAD 1	HAD 2	HAD 3	MNI 1	MNI 2	MNI 3	POS 1	POS 2	POS 3
CFH	WQSIPLCVEK	0	yes	yes	2	0.030882	7.14E+06	0	0	0	0	0	9.51E+06	1.22E+07	0
CFH	FVCNSGYK	0	yes	no	2	0.049407	0	0	0	0	0	2.98E+06	0	0	0
GSN	TPSAAYLWVGTGASEAEK	0	yes	no	2	4.20E-16	0	5.43E+06	0	5.78E+06	0	0	5.17E+06	0	0
GSN	QTQVSVLPEGGETPLFK	0	yes	no	2	3.62E-08	2.62E+06	6.26E+06	0	8.74E+06	2.76E+06	1.48E+06	6.08E+06	1.96E+06	1.99E+06
GSN	EVQGFESATFLGYFK	0	yes	no	2	7.65E-07	1.50E+06	5.17E+06	0	4.19E+06	1.64E+06	0	3.03E+06	9.55E+05	0
GSN	AQPVQVAEGSEPDGFWEALGGK	0	yes	no	2	1.78E-06	0	1.88E+06	0	1.87E+06	0	0	0	0	0
GSN	AGALNSNDAFVLK	0	yes	no	2	0.000408	0	1.11E+07	0	1.35E+07	0	0	1.23E+07	7.21E+06	0
GSN	HVVPNEVVVQR	0	yes	no	2,3	0.000929	2.87E+06	9.48E+06	0	4.78E+06	0	0	4.68E+06	2.97E+06	0
GSN	PALPAGTEDTAK	0	yes	no	2	0.007971	0	1.03E+06	0	3.18E+06	0	0	3.45E+06	0	0
GSN	DPDQTDGLGLSYLSSHIANVER	0	yes	no	3	0.033608	0	3.62E+06	0	0	0	0	0	0	0
GSN	EPGLQIWR	0	yes	no	2	0.037589	0	0	0	4.82E+06	0	0	0	0	0

Proteins	Sequence	Missed cleavages	Unique (Groups)	Unique (Proteins)	Charge	PEP	HAD 1	HAD 2	HAD 3	MNI 1	MNI 2	MNI 3	POS 1	POS 2	POS 3
GSN	SEDCFILDHGK	0	yes	no	3	0.044182	0	0	0	5.05E+06	0	0	3.44E+06	0	0
SAP	IVLGQEQDSYGGK	0	yes	yes	2	0.00064	0	9.38E+06	0	7.40E+06	0	0	0	8.68E+06	0
SAP	AYSLFSYNTQGR	0	yes	yes	2	0.001124	7.95E+06	1.02E+07	0	0	0	0	3.48E+06	9.08E+06	0
SAP	QGYFVEAQPK	0	yes	yes	2	0.005256	8.02E+06	6.10E+06	0	5.57E+06	0	0	2.09E+06	0	0
SAP	VGEYSLYIGR	0	yes	yes	2	0.005256	0	0	0	6.48E+06	0	0	0	4.80E+06	0
SAP	DNELLVYK	0	yes	yes	2	0.010095	4.69E+06	0	0	4.09E+06	0	0	2.25E+06	2.61E+06	0

A1AG: Alpha-1-acid Glycoprotein 1, Alpha-1-antitrypsin, A2M: Alpha-2-macroglobulin, APOA-I: Apolipoprotein A-I, ApoE: Apolipoprotein E, CERU: Ceruloplasmin, CLU: Clusterin, C3: Complement C3, C4-A: Complement C4-A, C4-B: Complement C4-B, CFH: Complement Factor H, GSN: Gelsolin, SAP: Serum Amyloid P, PEP: Posterior Error Probability, HAD: HIV Associated Dementia, MNI: Minor Neurocognitive Impairment, POS: HIV Positive Control.

Chapter 10
Appendix C: Final High Throughput PRM Assay

TABLE 10.1: RAW PRM PEPTIDE DATA AVERAGED TO GIVE REPRESENTATIVE PROTEIN VALUES

Patient	Group	sp|P01023|A2MG	sp|P08603|CFAH	sp|P02649|APOE	sp|P10909|CLUS	sp|P06396|GELS	sp|P02743|SAMP	sp|P02763|A1AG1	sp|P01009|A1AT	sp|P02647|APOA1	sp|P00450|CERU	sp|P0C0L4/5|CO4	sp|P01024|CO3	sp|P01861|IGHG4
1	Control	71415240	7782003.5	3005355.5	28342590	1976906	5459729	16087954	162214952	24498716	14719187	13581328	109646488	364794112
2	Control	52129109	4385080	2571627	11731742.5	1791102.5	974658.5	2978098	43001348	20283971.5	8391309	8885475	51170122	125390672
3	Control	127857096	28001535.5	4515216.5	34542406	2969473.5	3281467.5	8087178	370852104	120183592	68558466	21229840	175824432	69829224
4	Control	31038437	4951136.5	2378897.5	16315096	1228586.5	1580298.5	2673960	53969152	18746663.5	9124818.5	4577692	34658233	107740912
5	Control	76752152	11372512.5	19642228.5	21359258	2677493.5	3787371.5	10446998	128273852	83526428	19062201.5	12107538.5	108438652	116419552
6	Control	139099216	24346128	6209569.5	33012315	7868341	4913925	7974155	339105928	90043424	28399462.5	25744344.5	120121712	278351744
7	Control	118268156	8251494.5	3051418	16911857.5	4446138	2812805.5	3846511	121708816	63961296	15666995	14109685	78038792	187938144
8	Control	40971485	4671514.5	2527727.5	3833214.5	1140821	426361.5	3482209	52822860.5	29146965	20133176	8785312.5	48358052	83294096
9	Control	186723108	7429973	3024476.5	17131421	5917342.5	2435026.5	4185877	121318896	76642656	16167725.5	10149872	86233520	460260288
10	Control	30600575	5264585.5	331081	2228899.5	333533	219455	266995	17813551	5434796.5	6770917.5	3502921.5	30999221	47338588
11	Control	62875034	13070363	3778758	29855144	4477281	2120263	9786252	207387764	61891420	24773361.5	20581086	101192244	322006336
12	Control	47720084	5397422	847515	8501861.5	1395505.5	1792274	6061244	113427948	10308760.5	6641527	7040750	31753697	187952416
13	Control	74276900	8980958.5	1435482.5	14394037	4419215	2374187	4171083	102854760	43535230	14837424	16652011	79516444	303216544
14	Control	15808946.5	2359398	665491	5844688.5	551203.5	410623.5	1500618	30298256	16610541	4211243	1910304	16860396	78688216
15	Control	120247584	6759115	3223988	6852747.5	1953956.5	1023690.5	2439245	66121876	73446776	20474389	25649003	99313522	408156736

Patient	Group	sp|P01023|A2MG	sp|P08603|CFAH	sp|P02649|APOE	sp|P10909|CLUS	sp|P06396|GELS	sp|P02743|SAMP	sp|P02763|A1AG1	sp|P01009|A1AT	sp|P02647|APOA1	sp|P00450|CERU	sp|P0C0L4/5|CO4	sp|P01024|CO3	sp|P01861|IGHG4
16	MNI	88291824	7620870	1493390.5	21169530	4758269	2006419	4286864	116800936	37773016	16185603.5	14379728	76327432	155389136
17	MNI	53544132	7337609	2441690	17908449	2083936.5	1867961.5	7952100	93523060	45873736	10045208.5	6324152	68423628	179910640
18	MNI	47672056	5488237.5	3112809.5	15978493	2512214	978790.5	3519266	100915548	41580204	11176691.5	4321570.5	51875911	102396912
19	MNI	69228184	3664150	2016456.5	4579725	1269919.5	644324	1090137	56661637	47418528	13862198	10593164	48490256	252821088
20	MNI	20262673.5	2635658	1773659	4464641.5	286336	680871.5	2744753	18835456.5	35002434	8966417.5	4308796.5	24933156	340503168
21	MNI	117708460	10168868.5	5709580.5	11839329	3874366.5	4234713	11342191	152095680	46896716	13967214	29646386	111102890	398986560
22	MNI	66804868	6769401	6102588.5	13057389.5	3934892.5	1247721.5	4046640	58185862	25832714	10464291.5	3839362	43134483	133165632
23	MNI	134680188	15959997	5195610	32392362	3120948	4343323	6229029	450204768	113495916	66014988	17803499	114117580	101900992
24	MNI	29963433.5	3579147	700875	4001824	186940.5	150254.5	479414	14531012	2021808	4829164	3734617	27716160	130550624
25	MNI	48911861.5	4139702	3501762.5	4306121	1215172	283623.5	2120573	30138193.5	33004678	11815181	15534560	43292248	128076048
26	MNI	38714812	4423493	1361706	9242173	1100106.5	2141258.5	2282136	52862528	24472652	7156103.5	23468479	47997062	152971296
27	MNI	68494746	9211729	3979955.5	12957829	3992021.5	2302753.5	6065798	132553744	40494978	16038148.5	8426071	76753120	177657616
28	MNI	143961544	13548344.5	3667905	10435447.5	7924100	2941204.5	9171624	201714520	94025928	19669716	20893720	82611320	256112528
29	MNI	25386745	1507772	513909.5	10822541.5	377264	348190.5	1324898	24678678	10351605.5	3760096.5	1436296.5	14426151	86584272
30	MNI	91805160	9049173	4337352.5	16458916	5421910	1004962	6038602	98058144	34488036	10753532.5	8883311.5	98318448	235977520
31	MNI	189187896	12475102	5610050	37524168	6397663	2902836.5	5342622	241858456	87412308	20016506	9543129.5	93353770	295328448
32	MNI	60121362	2140080	1408479.5	4146871.5	1799490	966303.5	3755979	51346934	13057015	5100867	11669926	25850538	151998000
33	MNI	34436701	6400458	3344146.5	6731984.5	4120149	686112	3049857	79989896	46082434	20858918	6681812.5	38925167	62998372
34	MNI	57967822	3870003	3438583.5	14764470	2263790.5	1041401	4597926	45204798	39410417	6011602	3149905.5	38055560	226230304
35	HAD	51663995	1218220.5	1478444.5	2855886.5	838789.5	260533.5	2258124	16502588.5	20741299	8248530	15473913	33093102	59543972
36	HAD	101879098	6695897	4453699	11954896	2152749.5	1080419	8107634	85693580	81421648	21496135.5	9649306	54215179	169055216
37	HAD	36286189	4408163	4281051	7784639	2055526.5	1884295	6796799	39666368	28578644	7183159	5119908	26851710	145633104
38	HAD	69952882	3490371.5	3068845	5637284	1101445	1292262	3222662	170576264	45031175	22465446	19926566.5	61244850	175132496
39	HAD	45795688.5	3946849.5	4500845.5	3610073.5	584933	614984	10875511	88743229	23511536.5	23452458	9237182.5	37613059	377994240

Patient	Group	sp|P01023|A2MG	sp|P08603|CFAH	sp|P02649|APOE	sp|P10909|CLUS	sp|P06396|GELS	sp|P02743|SAMP	sp|P02763|A1AG1	sp|P01009|A1AT	sp|P02647|APOA1	sp|P00450|CERU	sp|P0C0L4/5|CO4	sp|P01024|CO3	sp|P01861|IGHG4
40	HAD	16993130	639493	113651	2850656.5	41431.5	213251	442980	3442754	1227566	1190016	930737.5	9153840	127574400
41	HAD	84107122	9717010	3382701.5	45512672	3402831.5	1827378.5	6276358	168346184	29069894	14899599	10115792	93675354	473510720
42	HAD	40185817	3730220	1445284	10911724	2762519.5	715564.5	3155959	79287800	21648663	10030367	6061592.5	24861771	25087292
43	HAD	102602756	5067124	3221815	6991871.5	1318362.5	1831027	6590752	80696956	74732576	8380369	23423117	63255314	110797592
44	HAD	13831621.5	4323035.5	3587371.5	5616585.5	2249925.5	539033.5	2699763	60205885	23157904	16165624.5	6651118.5	28448224	127471664
45	HAD	10962366	2313828.5	1027276	6401974	431793	701535	1689882	33528150	25229709	4511380	2005976.5	12960586	76192208
46	HAD	15875901.5	1599381	468258.5	885080.5	154803	94207	1534472	7519493	2607760.5	2886735	4680470	18593668.5	27886574
47	HAD	50184458	2659655.5	2895260	3757791	757118.5	644755	3883461	37076222.5	30419750	11278870	11749858.5	27163198	191662496
48	HAD	24527972	2421385.5	124044.5	2327620	110601	19655	799932	8191831.5	2494018	2657487.5	4448834.5	13065813	47137068
49	HAD	68607036	4866749	4876377	14879189	1889519	2793653	6083366	85035396	46753664	23337234	12760288	53114288	140024896
50	HAD	125255456	23605346	12722663.5	18609392	9971867	2964539	22348520	569511504	64718892	55524336	51808254	180579332	529726080
51	HAD	112982948	8172602.5	4178825	14764597	2210517.5	2976913	2991793	180976224	73767740	31658604	23077656	109146452	252886208
52	HAD	20710982	4625799.5	3244832	6972436	1722401	3072159	3354974	58307678	34587680	6116484	7215073	18505733	65128100
53	HAD	35989406	1892619.5	1255688	3001321	1476131	529710.5	2475604	41195249	20810329	3769935	2541726.5	14668839.5	74167632
54	HAD	52099989	8334503	2756482.5	6530325	2129374	1173244.5	2303642	69593258	42438433	28433389	18772659	81470712	171216880
55	HAD	89279406	10465974	4766587.5	23714767	5879800	6488826.5	14747374	172278784	64634224	17661993	21735459	90282218	185202192

A2MG: Alpha-2-macroglobulin, CFAH: Complement factor H, APOE: Apolipoprotein E, CLUS: Clusterin, GELS: Gelsolin, SAMP: Serum Amyloid P, A1AG1: Alpha-1-acid glycoprotein 1, A1AT: Alpha-1antitrypsin, APOA1: Apolipoprotein A-I, CERU: Ceruloplasmin, CO4: Complement C component 4, CO3: Complement component 3, IGHG4: IgG_4 (Peptide STSESTAALGC[+57.0]LV)